The Thesis Committee for Maria Christina Burton
Certifies that this is the approved version of the following thesis:

Assessment of Automated Technologies in Texas for Pavement Distress Identification, Texture, and Cross Slope Measurement

APPROVED BY
SUPERVISING COMMITTEE:

Supervisor:

Jorge A. Prozzi

Andre d.F. Smit

Assessment of Automated Technologies in Texas for Pavement Distress Identification, Texture, and Cross Slope Measurement

by

Maria Christina Burton, B.S.C.E., M.S.C.E.

Thesis

Presented to the Faculty of the Graduate School of

The University of Texas at Austin

in Partial Fulfillment

of the Requirements

for the Degree of

Master of Science in Engineering

The University of Texas at Austin

May 2014

Abstract

Assessment of Automated Technologies in Texas for Pavement Distress Identification, Texture, and Cross Slope Measurement

Maria Christina Burton, M.S.E.

The University of Texas at Austin, 2014

Supervisor: Jorge A. Prozzi

Automated technologies can be beneficial for collecting data on the condition of pavements. As opposed to a traditional manual survey of the road, automated data collection can provide a safer alternative that is objective, repeatable, and consistent, while traveling at highway speeds. Though the automated method is preferred, it still needs to be reliable enough to accurately model the current pavement performance. The Texas Department of Transportation (TxDOT) initiated a project to allow an independent assessment of the accuracy and repeatability of new automated distress data measurements. In this study, 20 550-ft. pavement sections were tested with automated data collection technologies. The sections were located in Austin and Waco Districts. The accuracy and repeatability was evaluated for cracking and other distress measurements, cross slope measurements, and texture measurements. Known manual methods were used as a reference, and a 3D system developed by TxDOT was compared with three systems of other vendors (Dynatest, Fugro, and Waylink-OSU). With the data provided for the

texture and cross slope, an additional investigation was done to evaluate hydroplaning potential. This thesis reports in the latter investigation.

Table of Contents

List of Tables

List of Figures

Chapter 1: Introduction

1.1.MOTIVATION FOR PROJECT

In order to effectively manage the condition of a roadway network, the pavement must be monitored and its condition reported regularly. Based on the severity of the pavement distresses, maintenance repairs, rehabilitation, or reconstruction can be scheduled. Pavement condition data can be collected manually or by driving a vehicle equipped with an automated data collection system.

Manual data collection depends on human judgment and, as a result, is subjective. It is also tedious, time consuming, and the results can vary depending on the individual making the evaluation. Automated pavement data collection systems can provide pavement distress data that is objective, repeatable, and consistent. The technology is efficient, as data are collected and stored while the vehicle is traveling at highway speeds. The automated method is also a safer alternative, as the rater does not need to step outside the vehicle and walk alongside the traffic. Automated systems allow agencies to assess road performance at both network and project levels. Though the automated method is preferred, it still needs to be reliable enough to accurately model the current pavement performance. Current technology is not ready yet.

The Texas Department of Transportation (TxDOT) has developed a state-of-the-art 3D system for rut measurements, and is currently improving its automated system for measuring and quantifying roadway cracking. As the accuracy of the system improves, this will impact TxDOT's Pavement Management Information System (PMIS), which is

used to monitor statewide pavement condition, evaluate the effectiveness of pavement maintenance and rehabilitation treatments, and report progress towards the annual statewide pavement condition goal (90 percent of lane miles in "good" or better condition). Before fully adopting these automated systems, TxDOT initiated a project to allow an independent assessment of the accuracy and repeatability of the new automated distress data measurements. The project involved evaluating TxDOT's automated data collection system and comparing it to similar systems from a variety of vendors to identify the best system for use in Texas. The project had two phases. Phase 1 evaluated the rut measurements, and Phase 2 evaluated automated distress data measurements (cracking, failures, punchouts, etc.), cross slope measurements, texture measurements, and crack map images. This thesis presents results from Phase 2 of the project.

1.1.1. Phase 1

In Phase 1, 26 550-ft. pavement sections were tested, including those with hot-mix asphalt, cement concrete and surface treatments representing different pavement textures. The test sections were located in the Austin District. The accuracy and repeatability of rut measurements using a 6-ft straight edge was compared to that of the TxDOT system and four other vendor systems, i.e. Applus, Dynatest, Pathways, and Roadware.

1.1.2. Phase 2

In Phase 2, 20 550-ft. pavement sections were tested. The sections were located in TxDOT's Austin and Waco Districts. The accuracy and repeatability was evaluated for cracking and other distress measurements, cross slope measurements, and texture

measurements. Known manual methods were used as a reference, and the TxDOT system was compared with three other vendor systems: Dynatest, Fugro, and Waylink-OSU.

1.2.OBJECTIVES

The purpose of this study was to analyze and compare automated data collection technologies for use in Texas. The effectiveness of these technologies for measuring pavement surface distresses, texture, and cross slope was compared to manual measurement procedures. With the data provided for the texture and cross slope, an additional investigation was done to evaluate hydroplaning potential. The objectives of this study include:

1. Identify pavement test sections.
2. Collect data from manual methods (to serve as a reference) and automated methods (TxDOT, Dynatest, Fugro, and Waylink-OSU). The data collected include:
    a. Distress identification (cracks, patches, failures, etc.)
    b. Texture (mean profile depth)
    c. Cross slope
    d. Crack map images
3. Evaluate efficiency of automated methods when compared to reference.
4. Evaluate hydroplaning potential with cross slope data.
5. Provide recommendations on effective methods for use in Texas.

1.3.ORGANIZATION OF THESIS

This thesis is divided into five chapters. The first chapter introduces the topic of automated data collection and reasons for the project. The second chapter reviews literature on previous studies on automated data collection and current practices in the U.S. and other countries. The third chapter describes the experimental methods used in this study, including selection of pavement test sections and data collection procedures. The fourth chapter analyzes the effectiveness of the automated data compared to the manually collected reference data and evaluates the hydroplaning potential using data provided. The fifth chapter concludes the study with recommendations and implications regarding the tested automated technologies.

Chapter 2: Literature Review

2.1. BACKGROUND

2.1.1. Manual Surveys

Some agencies still use manual pavement condition surveys (Timm & McQueen, 2004; Haas et al., 1994). One manual method is a "walking survey," where a rater who is trained to rate distresses, walks along the roadway and fills out a pavement condition form, describing the severity and extent of each distress observed on the pavement. Another manual method is a "windshield survey," where a rater rates the pavement condition through the windshield of their vehicle while driving along the road or on the shoulder. Walking surveys provide a more precise description of the pavement condition; however, they cannot be produced for the entire network due to the excessive time walking surveys take. Windshield surveys take less time to conduct and can be produced for the entire network; however, the quality of the data is compromised. To collect detailed pavement distress data while also covering a higher percentage of the network, random samples can be selected for walking surveys, and the remaining surveys can be conducted via windshield.

2.1.2. Automated Techniques

The idea of automating pavement data collection is not new. In 1985, a study in Canada conceived the feasibility of the idea of using an "expert distress data analysis (EDDA) system" rather than depend directly on human judgment (Haas et al., 1985). The study describes an automated data collection system prototype, which involves: (1) acquiring images of the pavement surface with a video camera mounted on a vehicle, (2) digitizing

the images into computer readable form by converting them into an array of numbers (pixels), and (3) processing and analyzing the images using appropriate algorithms. Features, such as cracks, are located after identifying horizontal and vertical "edges" between road surface regions and are quantified as vectors. IF-THEN rules are used to interpret results; for example, if the cracks are transverse to the length, then they are identified as shrinkage cracks. The study found that the edge vector classification algorithm was successful in identifying types of cracking and that the EDDA system is feasible for full operation.

A 2004 report by the National Cooperative Highway Research Program (NCHRP) documented efforts in practice and research on network-level automated pavement data collection (NCHRP, 2004). Information was gathered from 43 state highway agencies, 2 FHWA offices, 10 Canadian provinces or territories, and Transport Canada, as well as literature from North American and European references. It was found that essentially all North American highway agencies were collecting pavement condition data through some type of automated means, some of which use vendors to collect some of the automated data. Some methods of collection are semi-automated, where a rater identifies distresses by reviewing the images from an automated collection. Fully-automated methods require minimal to no human intervention to identify distresses.

Some types of digital pavement imaging used include: area scanning (uses a two-dimensional array of pixels in a sequence of snapshots for a defined pavement area), line scanning (uses a single line of sensor pixels to build a two-dimensional image), and

three-dimensional laser imaging (establishes a three-dimensional surface) (NCHRP, 2004). Figure 2.1 shows a schematic of line scanning.

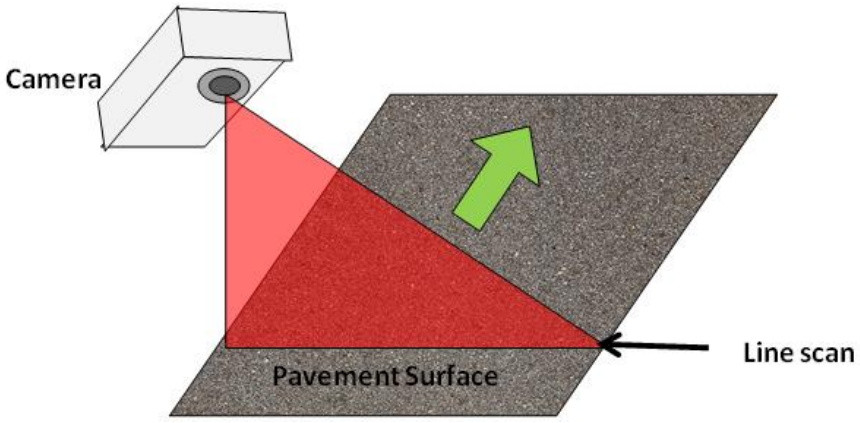

Figure 2.1: Schematic of digital pavement imaging using line scanning.

Most of the network-level roughness monitoring vehicles in the U.S. and Canada are equipped with accelerometers and at least one of three types of sensors to measure the longitudinal profile of the pavement roughness: lasers, acoustic, or infrared (NCHRP, 2004). Generally, rut-depth measurements are also collected using the same laser or acoustic technologies as those used to measure roughness.

2.1.2.1. 3D Surface Data

Because 2D laser images of the pavement surface exclude some of the surface distress characteristics in the third dimension, researchers have been trying to improve technology for 3D images (Wang, 2011). Some of the techniques to collect 3D surface data include: the photogrammetric principle (matches a pair of 2D images with common points to generate a 3D image, but requires high illumination of the surface); Light Detection and

Ranging or LIDAR, which has been used for geo-reference terrain features (collects laser scan data with a scanning mirror that rotates transverse to the direction of motion, but the laser beam becomes a distorted ellipsoidal shape during the scanning); and a laser line based technique that has been widely used for objects on conveyor belts (illuminates the surface with a line laser, shoots 2D images with an area camera, and combines sequential images to form a 3D image). Figures 2.2, 2.3, and 2.4 illustrate these techniques.

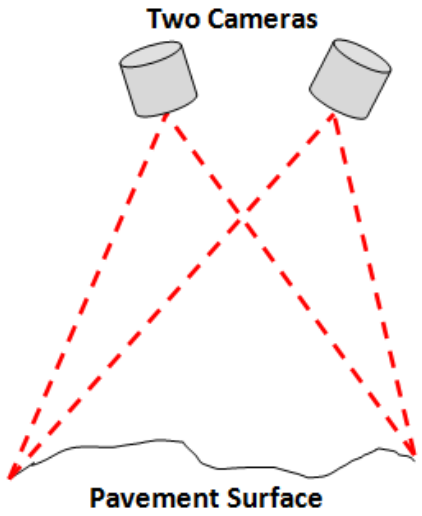

Figure 2.2: Photogrammetric principle

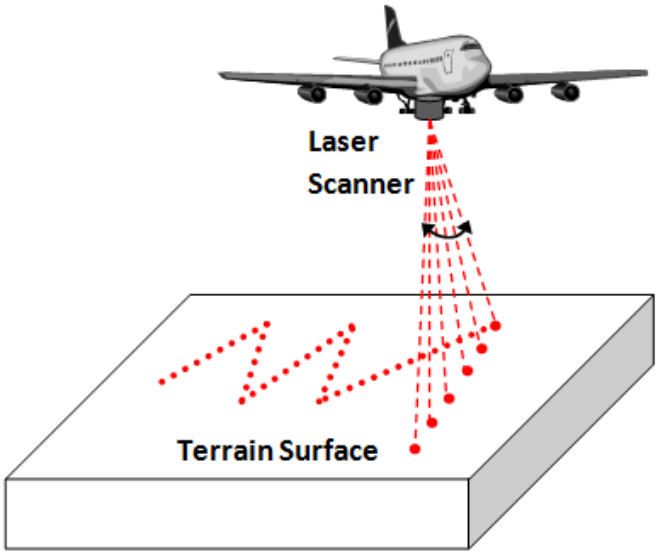

Figure 2.3: LIDAR technology mounted on an aircraft

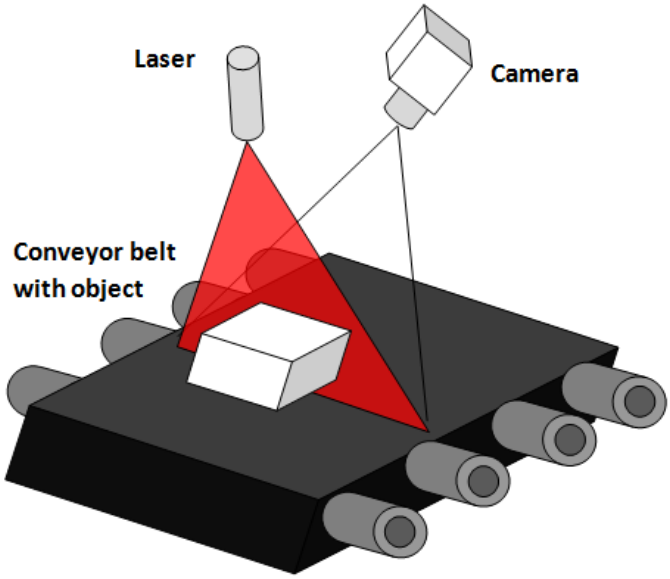

Figure 2.4: Laser line based technique

In 2011, a study in Arkansas produced a prototype, "PaveVision3D," equipment that, based on the authors claim, could obtain 3D pavement surface models at true one mm resolution with complete lane coverage (Wang, 2011). The prototype consisted of a vehicular platform with laser based sensors (using a laser line method and integrating a 2D laser imaging subsystem) to capture the 3D representation of the pavement surface. The prototype was able to clearly show surface defects with 2D and 3D laser images of pavements. Basic algorithms were also developed for measuring rutting and cracking distresses.

2.1.2.2. Post-processing Tool

The AASHTOWare Pavement ME Design software is useful for predicting pavement distress conditions; however, it needs to be calibrated with local data before it can produce accurate results. Because the calibration process can be time consuming, using pavement distress data for calibration from automated collection methods is preferred over manual methods. Automated data collection methods are faster, but they have difficulties with recognizing cracks that fit the Long Term Pavement Performance (LTPP) cracking protocol, which the protocol is also used by AASHTOWare. A study in 2012 in Arkansas presented implementation of a post-processing tool that would modify the cracking interpretations of an existing surveying software, Automated Distress Analyzer (ADA) (Byram et al., 2013). Typically, the ADA software would have difficulty identifying cracking patterns (e.g. falsely classifying alligator cracking as an assortment of longitudinal and transverse cracks). With the new tool, a wheelpath protocol was incorporated, where wheelpath boundaries were used to establish a means

of defining cracks (longitudinal and alligator) that meet LTPP definitions. Results showed that the post-processing tool had the ability to replicate AASHTOWare distress predictions better than a surveying method with human intervention, as well as ADA before processing with the new tool.

2.1.3. Case Studies

2.1.3.1. Oregon & Washington

Many transportation agencies use defined indexes to rate pavement condition. Data are collected manually or with automated technology and are then used to calculate the defined index for pavement condition. A 1998 study evaluated several automated and manual (walking and driving) methods for collecting pavement distress data in Washington and Oregon (Smith et al., 1998). Using automated and manual data, the Pavement Structural Condition (PSC) index used in Washington and the Pavement Condition Index (PCI) used in Oregon were calculated and compared to indexes based on detailed distress surveys. The results showed that some of the automated method vendors were closer to the ground truth data than manual methods; however, there was no consistent pattern where any vendor was consistently better than the others for both PSC and PCI values. Some errors in values for both vendor and manual methods were believed to be related to not using standard distress type and severity definitions. Identifying and quantifying weathering and raveling was difficult for automated vendors, and these distress types showed considerable variation among manual inspections.

In 2005, the Oregon Department of Transportation (ODOT) conducted a study for evaluating automated data collection equipment for Oregon's highways (Mullis et al.,

2005). Four vendors were evaluated based on their system's performance in measuring pavement condition, measuring road roughness, and video logging. The pavement condition was compared to a walking survey by experienced ODOT personnel (the reference "ground truth"), and it was also compared to a survey made by three rating crews that ODOT typically used to measure pavement condition. The rating crews were found to have pavement condition rating values closer to the reference ground truth than the automated equipment. The study suggests that the quality of data from automated equipment might be improved if ODOT could change the way the distresses are defined or measured or if ODOT followed some protocols proven to improve automated data quality.

2.1.3.2. Alabama

In 2004, a study in Alabama compared manual and automated pavement condition surveys (Timm & McQueen, 2004). The study gathered information about the data collection systems of 27 states through survey questionnaires and evaluated the accuracy of the automated data collected in Alabama compared to manual data. A few states have successfully incorporated a fully automated data collection process into their pavement management systems (PMS). Some of the problems faced by the states that used manual surveys were the amount of time the surveys took, the lack of consistency in raters, and distinguishing load related distresses from non-load related distresses. With respect to automated data collection, some states found the quality of the data to suffer, the amount of storage required to save the data to be a problem, and the collection and analysis of crack data to be a challenge. When comparing automated data collected in Alabama with

manual data, no systematic error was found between the data types; however, the vendor was found to report greater average outside wheel path rutting, underreport alligator 1 cracking, and over report alligator 3 cracking. For Alabama, cracking data are the most difficult distress type to detect and classify, and its accuracy is important, as it causes the greatest amount of sensitivity in Alabama's Pavement Condition Rating (PCR) equations.

2.1.3.3. California

A study in California evaluated the effect of different distress data collection methods to determine the pavement condition index (PCI) (Chang-Albitres et al., 2007). One issue that can be seen is that data from automated technologies do not necessarily produce the same condition index that is produced from manual data. Differences in the pavement condition index can lead to major differences in treatment recommendations and funding needs. It is important to research and identify these differences before agencies transition from manual to automated data collection.

Researchers in 2007 investigated the impact on network-level analysis by comparing pavement distress data collected by semi-automated methods versus the manual collection method (Smith & Chang-Albitres, 2007). The study involved four vendors, which collected semi-automated data from the entire pavement network of two California cities. The Metropolitan Transportation Commission (MTC) StreetSaver® pavement management software was used to calculate the Pavement Condition Index (PCI) from the given distress data, budget needs for a 20-year period based on the PCI values calculated, and scenario analyses (calculating pavement condition before, after, and long-term after applying treatment) with the PCI data for an annual budget. The

study found two vendors (Adhara and IMS) to have the smallest total PCI differences from manual surveys, both with budget needs calculated less than 30% different from manual surveys. The other two vendors (Stantec and Fugro) had more sections with differences of 20 PCI points or more from manual surveys, with budget needs calculated varying from 11% different to 48% different from manual surveys. The scenario analysis results were consistent with the PCI analysis.

A 2014 study documented use of a new pavement management system in California, PaveM, which includes sensor and distress data for pavements from automated pavement data collection (Lea et al., 2014). The study focused on combining the sensor and distress measurements of jointed concrete pavements into condition variables, which a decision tree could use to determine treatments for network management. Statistical performance models were developed to predict the future condition. It was found that current data collection protocols made simplifications to the reported data, which made aggregation of the data more difficult (e.g. reporting that the "majority" of cracks were of a certain type, rather than reporting the lengths of the crack types). The study suggested that data might be reported in more detail than required in the future. It was realized that there is a large amount of work involved in dealing with the data from the automated systems, and this should not be underestimated when budgeting for a new pavement management system.

2.1.3.4. Canada

In Canada, a 2008 study compared automated data collection technology with traditional survey methods for its accuracy, as use of the new technology will minimize road crew

exposure (increase safety) as well as increase productivity (Huber et al., 2008). Hardware components on the automated data collection vehicle used in the study included digital cameras, 2D laser scanners, and internal navigation systems. The study focused on data elements relating to cross slope, ditch slopes/depths, lane widths, and drainage models. The mobile laser scanning methodology that the automated vehicle used was proven successful in controlled tests measuring cross slope: 1) fabricated ramps to simulate cross slopes, and 2) field testing using manual method of using two six-foot levels that spanned one lane of the road. The laser scanning had accuracy within 0.5% compared to the traditional manual method.

2.1.3.5. Georgia

A 2011 study in Georgia evaluated the performance of rut depth measurement using 3D continuous transverse profile data collected in the laboratory and also in the field (Tsai et al., 2011). The study used a commercially available 3D continuous laser profiling system, the Laser Crack Measurement System (LCMS), which can collect 3D continuous pavement transverse profiles at highway speed. Laboratory test results on eleven simulated rut profiles (using a curved wood board and a curved metal bar) showed that rut depth measurement error can be less than one mm, and the standard deviation ranged from 0.07 mm to 0.34 mm. Field test results on ten field-collected rut profiles showed that rut depth measurement error ranged from 0.8 mm to 2.3 mm. Overall, the study found the 3D continuous laser profiling technology to be more accurate in rut depth measurement than the traditionally used point-based rut bar systems.

2.1.3.6. Michigan

Sampling can reduce time and costs in data collection; however, the results may not be an accurate representation of the entire pavement condition. A 2013 study in Michigan investigated the impacts of continuous data collection compared to sampling on the accuracy of pavement management decisions (Dean & Baladi, 2013). Continuously collected pavement distress data was used from 109 miles of pavement from Colorado, Louisiana, Michigan, and Washington. Transverse and longitudinal cracking data were analyzed to determine the effects of sample size, investigating sample sizes of 10, 20, 30, 40, 50, and 60 percent. The results showed that data sampling error is a function of sample size and the uniformity or variability of the distress data (increasing the sample size reduces the differences between sampled and continuous data). The study suggested that the states that use ten percent sample size could be misallocating pavement treatment funds, which outweigh the savings incurred by sampling. Increasing the sample size reduces the differences between the sampled and the continuous data; however, the results showed that at 60 percent sampling, the error could be as high was ten times the continuous data.

A 2014 study in Michigan researched the potential of using data from automated data collection to assess pavement condition and performance and improve Michigan Department of Transportation's transportation asset management practices (Dennis et al., 2014). Research reports and pilot projects were reviewed to determine feasible methods to implement automated data into pavement condition monitoring programs. The study focused on data collected by sensors installed on consumer-available vehicles and smartphones. It concluded that within three to five years of standardizing methods for

data collection, processing, and management, consumer-available data could be used in addition to the employment of crowdsourcing (collecting data from privately owned vehicles operated by the general public; e.g. collecting data from smartphones). With existing technologies, the study projected that acute distress events, rough ride events, and slippery pavement events might be obtained within 3-5 years; faulting, event-based ride quality index, and single-vehicle pseudo-IRI might be obtained within 5-10 years; deflection under non-standard load, rutting, cracking, composite distress indexes, crowdsourced pseudo-IRI, and pavement markings and roadside assets might be obtained within 10+ years; and standardized deflectometer data, standardized friction coefficient, and subjective pavement ratings are unlikely to be obtained.

2.1.3.7. Texas

The data used in this thesis come from a larger project, of which the first part thereof produced a paper discussing the rut-depth accuracy of different automated systems in Texas (Sergios et al., 2013). The initial rut-depth study involved automated data collection technologies provided by vendors different from those in this thesis, as the availability of the different vendors changed over time. The road sections were also different, as the initial study measured sections with varying rut-depths. This thesis measured sections with varying texture, cross slope, cracking, and other distresses. The rut-depth study analyzed rut-depth values obtained from five different optical continuous automated systems (CAS) and from calculations simulating the use of discrete automated systems (DAS) with different configurations. DAS, the first automated systems, collect a small number of coordinates per transverse profile. CAS, the newest available systems,

generally collect more than 1,000 coordinates per transverse profile, which essentially is a continuous profile.

The rut-depth study performed the following: CAS measurements were compared to manual measurements for accuracy; DAS accuracy was assessed based on the effects of the number of sensors and width of measurement; and the impact of rut-depth accuracy at network level was analyzed for both CAS and DAS (Sergios et al., 2013). It was found that most DAS measurements underestimated manual measurements. DAS measurements with an increasing number of sensors became more accurate when the coverage was increased. CAS underestimated the percentage of sections needing rehabilitation by 7-8% when compared to manual measurements. Five-points DAS missed 28% of sections needing rehabilitation.

2.1.4. Technology Selection

After an agency compares various automated technologies, the next step is to select the most appropriate technology for the given pavement management system. In 2012, a study in Canada presented a framework for evaluating and selecting appropriate automated data collection technologies for pavement management systems (Alyami et al., 2012). The framework involves a Multi Criteria Decision Making (MCDM) computational approach to aid in the technology selection. Steps in the framework include: (1) identifying Key Performance Measures or KPM (the important physical attributes to be monitored and evaluated – e.g. roughness, rutting, cracking, skid resistance); (2) identifying available automated data collection technologies; (3) identifying selection criteria and level of importance (e.g. accuracy, repeatability,

collection speed, cost – rating each from highly important to medium importance); (4) evaluating automated data collection technologies against selection criteria-computational approach; (5) short listing automated data collection technologies (listing the top three with the highest final scores for each KPM); and (6) optimization and final selection. The computational approach involves tabulating and comparing overall scores for each alternative after applying "weights" for selection criteria according to level of importance. After applying data from an example case study, the process showed that it was easier for evaluation and decision making, and selections can be mathematically justified using this process.

2.1.5. Quality Assurance

When an agency adopts a manual or an automated method for pavement data collection, it needs to be ensured that the produced data adequately represents the true condition of the pavement. It is important to ensure accuracy and repeatability of the results. The Federal Highway Administration (FHWA) has a guide for ensuring quality management in pavement condition data collection at network-level (Pierce et al., 2013). The guide provides information on implementing a quality management program, incorporating quality management practices, and showing examples using data from different state DOTs. Some of the quality management techniques discussed include: ensuring testing equipment is calibrated and testing methods are accepted prior to data collection; providing training for respective personnel on data collection, rating, and data reduction; testing control sites as a reference; having a lead rater check the ratings of random

samples to ensure the ratings are being conducted accurately; and conducting checks on formatting, missing data, or other errors after the data has been reduced and processed.

In Indiana, researchers had also investigated the topic of quality assurance of pavement condition data (Ong et al., 2010). For agencies who hire contractors to collect pavement condition data, it is important to assure the quality of the data independently. The quality control protocols that the contractors follow themselves may not always match industry standards. The study focused on establishing quality control procedures for receiving data delivered by contractors. They found that network level International Roughness Index (IRI) was the same as project level IRI, with less than 5% error, and that an error of ± 20% was found between network and project level Pavement Condition Rating (PCR). The study recommended that contractors follow a quality control plan for all phases of the data collection process (pre-project, data collection, and post-processing). Quality assurance procedures for the agency hiring the contractor to follow include: certifying the data collection vehicle before data collection, quality assurance tests on selected sections of a test road, and quality assurance checks for completeness and error before importing data into the pavement management database.

2.2. CROSS SLOPE

One of the features this thesis looks into is the cross slope data. Cross slope is an important feature to maintain safety on roads. They reduce puddles that contribute to hydroplaning by allowing rain water on the surface to drain down the sides of the road into a ditch or gutter drainage system (Figure 2.5). By reducing the water on the surface,

this can also prevent water from penetrating and weakening the top and base layers of the road. On horizontal curves, proper cross slopes (superelevation) reduce centrifugal forces that push vehicles to the outside of the lane when cornering (Figure 2.6).

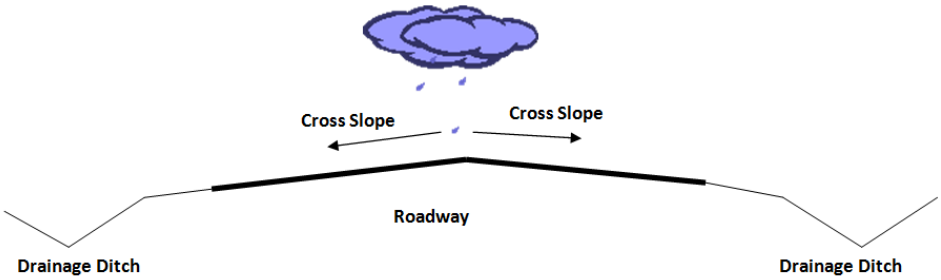

Figure 2.5: Proper cross slope on roadway for storm water drainage

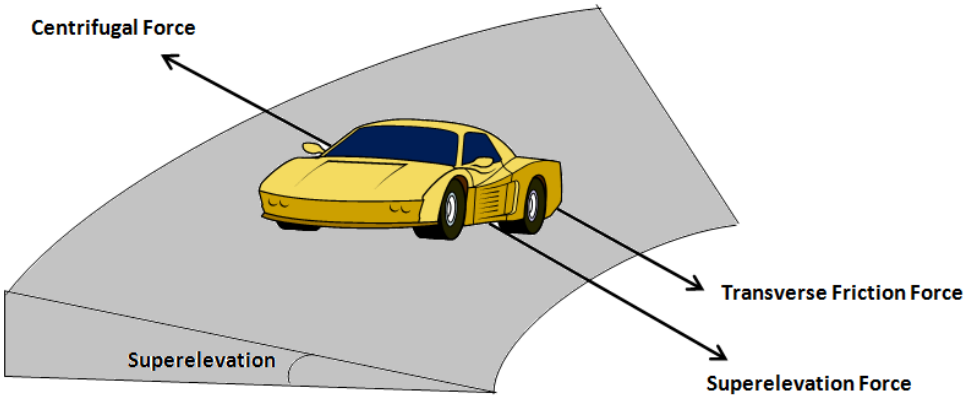

Figure 2.6: Superelevation on horizontal curve to counteract centrifugal forces

Table 2.1 shows the AASHO recommended guidelines for cross slope given the surface type (Gallaway et al., 1971). The surface type describes the ability of a surface to retain its shape and dimensions, to drain, and to retain adequate skid resistance (AASHTO,

2001). A high surface type pavement retains its shape, does not ravel at the edges if placed on a stable subgrade, and its smoothness and proper cross slope design enable drivers to maintain travel in the correct path. A low surface type pavement tends to ravel, which reduces the effective width and makes it more difficult for the driver to maintain travel in the correct path.

Table 2.1: AASHO Guidelines for rural highway pavement cross slopes (Gallaway et al., 1971).

Surface Type	Range in Rate of Cross Slope			
	in/ft	Ratio	ft/ft	Percent
High	1/8 - 1/4	1:96 - 1:48	0.010 - 0.020	1.0 - 2.0
Intermediate	3/16 - 3/8	1:72 - 1:36	0.015 - 0.030	1.5 - 3.0
Low	1/4 - 1/2	1:48 - 1:24	0.020 - 0.040	2.0 - 4.0

2.2.1. Automated Cross Slope Measurement

Cross slope can be measured with automated equipment, but not all automated techniques can measure the cross slope accurately. A 2007 study in Italy compared two different methods to measure the road cross slope using a Mobile Mapping System (MMS), which is an automated data collection vehicle that collects roadway geometric data such as cross-slopes, grades of vertical curves, and radii of curvature of horizontal curves (Bolzon et al., 2007). The first method implemented an algorithm that computes the cross slope value from the INS (Inertial Navigation System) data, modeling of the dynamics of the travelling vehicle. The second method implemented a single axis laser scanner synchronized with the INS/DGPS system (INS/Differential Global Positioning System). The methods were compared with cross slope obtained from manual measurement using

a total station. The results showed that cross slopes from the first method provided "*excellent accuracy and fair precision*." Data collected on old pavements were more variable compared to new pavements. Comparison of the second laser scanning method against the first INS method yielded a positive differences mean value, greater than the manual total station method versus the first INS method.

A 2003 study in Iowa investigated the use of LIDAR technology to collect road grade and cross slope data for large-scale inventories (Souleyrette et al., 2003). The LIDAR data points created a three-dimensional surface model, from which grades and cross slopes were extracted and evaluated in terms of accuracy using regression. Grades and cross slopes from LIDAR data were compared to grades and cross slopes collected using an automated level. Results showed that the grade could be estimated within 1%, but the cross slope could not practically be estimated using a LIDAR derived surface model.

2.2.2. Hydroplaning

Sometimes the cross slope can be disturbed when rutting appears and water becomes held within the ruts, preventing it from draining down the sides as it normally would. Hydroplaning occurs when a rolling tire is separated from the roadway surface by a layer of fluid. When examining the safety of highways during wet pavement conditions, there are two types of hydroplaning of concern: viscous hydroplaning (caused by a thin film of water due to insufficient pavement microtexture) and dynamic hydroplaning (caused by a thick layer of water) (Mounce & Bartoskewitz, 1993). Viscous hydroplaning is influenced by the viscosity of the fluid, tire condition, and the pavement surface quality,

with the worst scenario having bald tires and a smooth pavement surface (polished surface). Dynamic hydroplaning is caused by thick water layers that drive a wedge between a moving tire and the pavement surface, resulting in uplift forces (fluid inertial forces dominate). Under the worst-condition scenario (bald tires and smooth pavement surfaces), water depths as little as 0.76mm (0.03 inch) can cause dynamic hydroplaning (Mounce & Bartoskewitz, 1993; Yeager, 1974). Hydroplaning can be avoided if the vehicle travels at a low enough speed.

Research published by Gallaway and Rose (1971) and expanded by Gallaway, et al. (1979) reported findings related to the pavement and geometric design to reduce hydroplaning (Glennon, 2006). It was recommended that the cross slope should be a minimum of 1.5%, and that most pavements (wider ones) should have cross slopes of 2.0%.

A Texas study in 1993 reviewed the phenomena of hydroplaning and its relation to causing accidents (Mounce & Bartoskewitz, 1993). Factors that can reduce hydroplaning include not only responsibilities from the driver (maintaining the condition and inflation pressure of tires and slowing down on wet roadways) but also proper highway design (providing adequate pavement texture and cross slope). A longer drainage path length (the distance water travels before draining off the pavement surface) could contribute to increasing hydroplaning and can be reduced with appropriate cross slope and pavement texture. Gallaway et al. (1982) found that a cross slope of 2.5% can facilitate adequate surface drainage and reduce hydroplaning for common rainfall intensities (Mounce & Bartoskewiz, 1993). It is recommended to have a pavement texture

depth of 1.52mm (0.06 in) or greater for roadways with high operating speeds to provide adequate drainage and reduce hydroplaning for common rainfall rates (Mounce & Bartoskewiz, 1993; Gallaway et al., 1982). For roadways with low operating speeds, lower texture depths can be tolerated; however, when rain storms are of high intensity, texture alone cannot prevent flooding on the pavement surface.

A 1983 American Society for Testing and Materials (ASTM) study conducted simulation, laboratory, and full-scale tests on tire hydroplaning, skid resistance, and other tire-pavement interactions (Balmer & Gallaway, 1983). Factors that influence hydroplaning and vehicle control include: pavement cross slope, texture, rut depth, pavement wear, surface drainage, drainage-path length, precipitation intensity and duration, tire inflation, tread-pattern depth, tire construction, and vehicle traveling speed. For a pavement that is smooth and low tire-tread pattern depth (1.6 mm or smaller), 1.8 mm (0.07 in.) water depth could cause hydroplaning. Figure 2.7 shows that: (1) hydroplaning increases as the water depth increases, and (2) hydroplaning increases as tire-tread pattern depth decreases (Balmer & Gallaway, 1983). The worst-condition scenarios to cause hydroplaning are: bald tires, smooth pavement surfaces, thick water layers, low tire pressures, and vehicles traveling at high speeds. The following were some conclusions of the study: (1) a pavement cross slope of 2.5% will facilitate surface drainage and reduce hydroplaning; (2) a pavement texture depth of 1.5 mm (0.06 in.) or greater will help reduce hydroplaning; (3) pavement maintenance or resurfacing is needed for rut depths exceeding 6 mm (0.24 in.) on pavement cross slopes of 2.5% (less

rut depth is tolerated for smaller cross slopes); and (4) traveling speed should be reduced below 50 mph on wet pavement to decrease occurrence of dynamic hydroplaning.

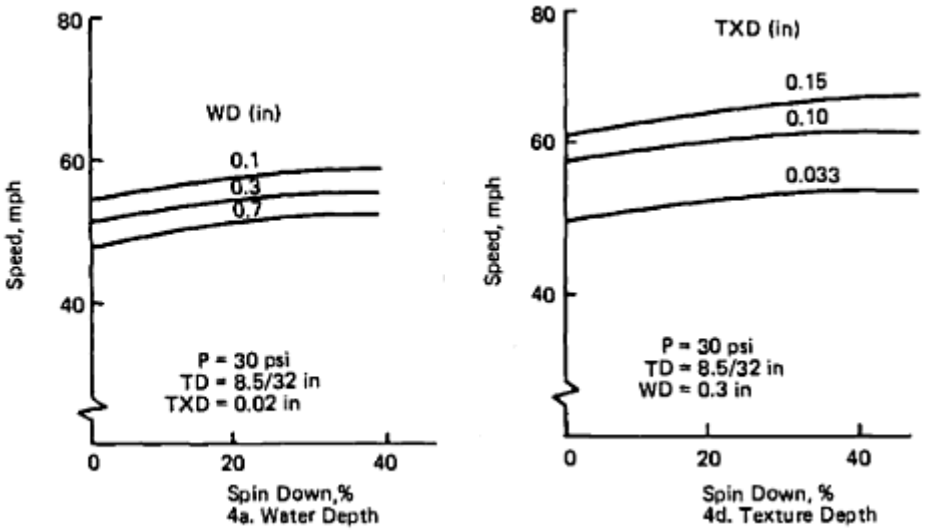

a. **b.**

Figure 2.7: Influence a) water depth and b) texture depth on hydroplaning speed (Balmer & Gallaway, 1983).

2.2.2.1. Cross Slope Specifications in Texas

In TxDOT's Hydraulic Design Manual, the following is noted regarding transverse slopes in Texas (TxDOT, 2011):

"*For TxDOT projects, a recommended minimum transverse slope for tangent roadway sections is 2%. The recommended maximum transverse slopes for a tangent roadway section is 4%.*"

With regards to reducing hydroplaning in Texas, TxDOT's Hydraulic Design Manual recommends a minimum cross slope of 2% (TxDOT, 2011).

2.2.2.2. Drainage Path Length

The drainage path length (the maximum distance that water travels before it leaves the pavement) can be calculated from Equation 1 (Mraz & Nazef, 2007; Glennon, 2006).

$$L_F^2 = W_C^2\left[1+\left(\frac{S_G}{S_C}\right)^2\right] \quad [1]$$

Where:
L_F = drainage path length
W_C = pavement drainage width
S_C = cross slope
S_G = longitudinal grade

The drainage path length increases with a steeper longitudinal grade and decreases with a steeper cross slope. The drainage path length also increases with a wider pavement width. To further explain, when water is traveling in the longitudinal direction, it can travel as far as the road extends, which is miles in length, so a steeper grade will encourage it to travel farther longitudinally. When water is traveling in the transverse direction, the width of the road only extends so far, so a steeper cross slope may encourage it to travel farther transversely but it will also leave the pavement faster. A lower cross slope will give the water more time to travel longitudinally before draining off the sides. A wider road will give the water more time to travel transversely before leaving the pavement, so the water travels farther with a wider pavement width.

A 1971 study in Texas developed an equation relating cross slope, rainfall intensity, surface texture, and drainage length to water depth (Gallaway et al., 1971).

After testing various surface types and rainfall intensities, the best fit of the data was determined using multiple regression analysis. Equation 2 was obtained from the study.

$$D = 3.38 \times 10^{-3} \left(\frac{1}{T}\right)^{-.11} (L)^{.43} (I)^{.59} \left(\frac{1}{S}\right)^{.42} - T \qquad [2]$$

Where:
D = average water depth above top of texture (in)
T = average texture depth (in)
L = drainage-path length (ft)
I = rainfall intensity (in/hr)
S = cross slope (ft/ft)

A 2007 study presented the capabilities of Florida Department of Transportation's (FDOT) automated pavement data collection equipment, the Multi-Purpose Survey Vehicle (MPSV), in collecting pavement features such as cross-slope, longitudinal grade, and rutting, and using this information to compute surface drainage paths (Mraz & Nazef, 2007). The MPSV includes an automated analysis tool that identifies areas with cross-slope and longitudinal grade deficiencies using pavement geometry data. Data are collected at highway speeds, and the technology of the vehicle and cross-slope analysis tool both were found to provide an effective, practical, and cost effective way to identify areas on the roadway prone to surface runoff or hydroplaning.

2.2.3. Roll Vibration

Besides hydroplaning, there are other problems that can occur when the cross slope is not adequate. A 2008 study in Sweden investigated the dangers of inadequate cross slopes on

icy roads (Granlund, 2008). The study found that heavy vehicles on frost damaged roads experienced high rates of roll-related lateral vibration (Figure 2.8), which was caused by large changes in cross slope due to pavement edge local deformation. A new index, Rut Bottom Cross Slope (RBCS) was defined to reflect this kind of damage, which is the slope between the left and right truck wheel track bottom. An automated data collection vehicle (laser/inertial Profilograph) was used to collect cross slope data. In identifying areas with undesired Rut Bottom Cross Slope Variance (RBCSV) which could cause truck roll vibration, the study was able to show potential "black ice" skid accident sections in need of edge repair.

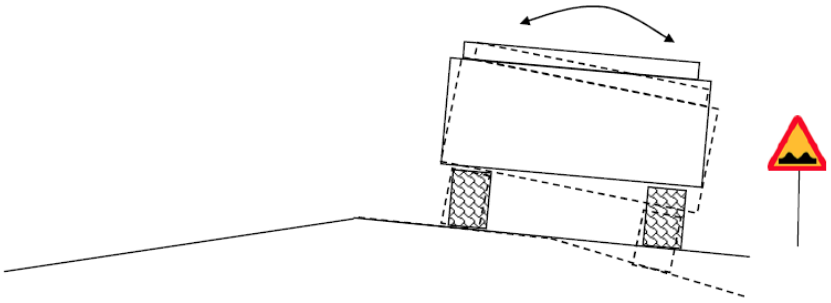

Figure 2.8: Pavement edge deformations (Granlund, 2008)

2.3. CRITICAL RUT DEPTH

When analyzing the data collected from automated technologies, it is important to note the rejection thresholds in order to identify failures in the roadway. Though the rut depth was not a parameter being reported and compared in this study, it is an important parameter in pavement management and can be estimated from the transverse cross slope profile (cross slope reported every transverse foot). Table 2.2 shows rut depth thresholds for different highway agencies (Fwa et al., 2012).

Table 2.2: Rut Severity Classification by Highway Agencies (Fwa et al., 2012).

Highway Agency	**Low**	**Medium**	**High**
Pavement Condition Index (PCI) *(Shahin 1994)*	0.25-0.5 in. (6.3-12.7 mm)	0.5-1 in. (12.7-25.4 mm)	>1 in. (>25.4 mm)
PASER Manual, Asphalt Roads *(Walker et al. 2002)*	0-0.5 in. (0-12.7 mm)	>1 in. (>25.4 mm)	>2 in. (>50.8 mm)
Washington State DOT *(WsDOT 1999)*	0.25-0.5 in. 6.3-12.7 mm	0.5-0.75 in. 12.7-19.1 mm)	>0.75 in. (>19.1 mm)
Ohio DOT *(OhDOT 2006)*	0.125-0.375 in. (3.2-9.5 mm)	0.375-0.75 in. (9.5-19.1 mm)	>0.75 in. (>19.1 mm)
Massachusetts Highway Dept. *(CMMPO 2006)*	0.25-0.5 in. (6.3-12.7 mm)	0.5-1.5 in. (12.7-38.1 mm)	>1.5 in. (>38.1 mm)
Ministry of Transportation and Infrastructure, British Columbia *(MTI BC 2009)*	3-10 mm	10-20 mm	>20 mm
California DOT *(Caltrans 2006)*	Schedule corrections when rut depth >1 in. (>25.4 mm)		

Note: 1 in. = 25.4 mm

Table 2.3 was found on Teede Tehnokeskus website (Teede Tehnokeskus, n.d.). The table shows their limit values for rut depth to ensure road safety. Rut depths of 10-20 mm are advised to be eliminated within 1 to 3 years, as rain water can accumulate in the ruts. Ruts with depths of 20-30 mm are advised to be eliminated when possible, as the accumulated water in the ruts can cause hydroplaning. Rut depths greater than 30 mm can affect traffic safety in both wet and dry conditions.

Table 2.3: Limit values of rut depth (Teede Tehnokeskus, n.d.).

Pavement Condition	**Traffic safety and impact on the road user**	**Rut depth limits (mm)**
Very good	Pavement has no ruts.	< 5
Good	No ruts can be observed in the pavement and there is no impact on road users.	5 -10
Fair	Ruts in the pavement can be observed. When it rains water accumulates in the ruts. Road users start to search for best trajectory. Ruts should be eliminated within 1 to 3 years.	10 - 20
Poor	Ruts can clearly be seen in the pavement, driving speed as well as trajectory are influenced. When it rains, a lot of water accumulates in ruts and aquaplaning may occur. Ruts should be eliminated.	20 - 30
Very poor	Ruts can clearly be seen in the pavement, driving speed as well as trajectory and traffic safety are influenced. Ruts affect traffic safety both in rain and in dry conditions. Ruts should be eliminated immediately.	> 30

A 2012 study in Singapore presented an analytical procedure to assess rutting severity based on analysis of vehicle skidding and hydroplaning (Fwa et al., 2012). For worst case scenarios, where a rut with a given rut depth is filled with water, finite element simulation was used to model and compute (1) the speed at which a typical passenger car will hydroplane and (2) the braking distance required for a car traveling at a known speed. The study demonstrated that, due to either hydroplaning risk or safety requirement of braking distance, the severity classification of a rut depends on the rut depth and the pavement surface friction. The influence of pavement surface friction type (static friction μ_0) on hydroplaning speed is negligible; however, the influence of friction on skid

resistance, which affects braking distance, is significant. As rut depth increases, the potential to hydroplane increases (hydroplaning speed reduces) and the braking distance increases.

The critical rut depth is reached when either hydroplaning occurs or the required braking distance exceeds the design braking distance, whichever occurs first (Fwa et al., 2012). The critical rut depth depends on the speed and skid number, SN_0, (which is equal to 100 μ_0). The hatched areas in Figure 2.9 represent when hydroplaning will occur, and the gray area represents when the required braking distance exceeds the design braking distance based on AASHTO guidelines.

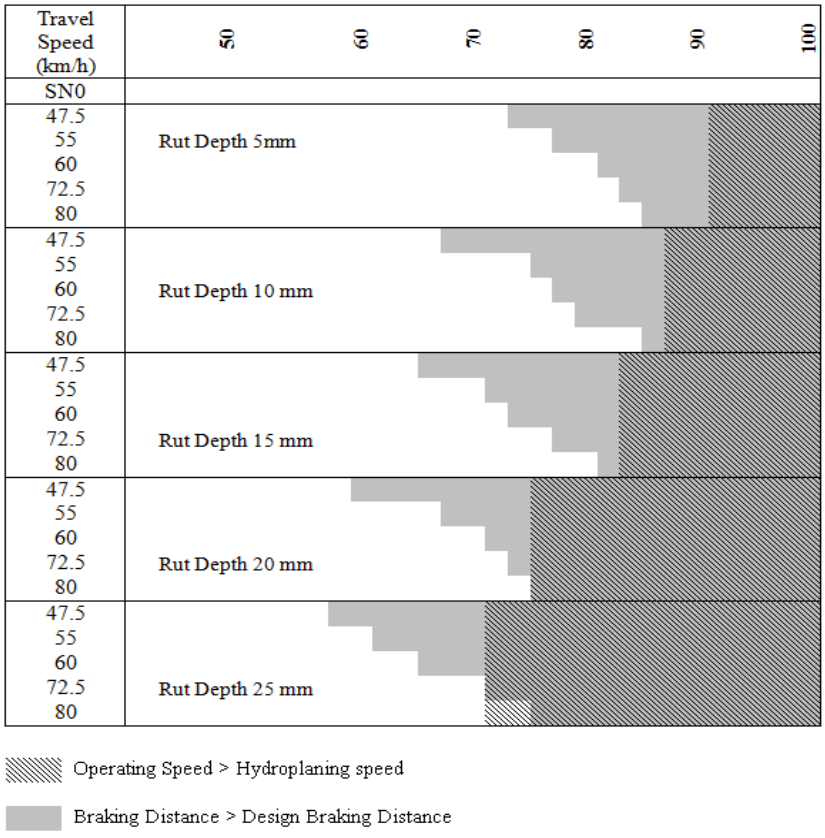

Figure 2.9: Governing Criterion for Safety Assessment at Different Rut Depths (Fwa et al., 2012).

2.3.1. Rut Depth Specifications in Texas

With regards to rutting in Texas, rut depths are categorized into three severity categories: shallow (0.25-0.49 in.), deep (0.50-0.99 in.), and severe (1.00-1.99 in.) (TxDOT, 2011). Rutting 2.0 in. or greater is defined as a failure.

With regards to reducing hydroplaning in Texas, TxDOT's Hydraulic Design Manual states, "*a wheel path depression in excess of about 0.2 in. (5 mm) has potential for causing conditions that may lead to hydroplaning*." (TxDOT, 2011).

2.4. FRICTION DEMAND

2.4.1. Wet Weather Accident Reduction

The texture of the pavement surface is another characteristic that can be measured by automated technologies, and determining a road's friction requirement can involve multiple variables. In Texas, the Wet Weather Accident Reduction Program (WWARP) provides tools for engineers to identify existing pavement friction and to specify new pavement surfaces that meet friction demand (TxDOT, 2006). Phases of the program include: wet weather accident analysis, aggregate selection, and skid testing. There are four climatic regions in Texas (Figure 2.10), and the frictional demand is different for pavement surfaces in these regions.

Table 2.4 shows how to determine the overall frictional demand of the roadway, given various characteristics of the roadway. For example, a high cross slope will drain well, have a high available friction and a low microtexture is needed by the aggregate. If

the design life is high however, low friction will available by the end of the design life and the microtexture demand will be high on the aggregate.

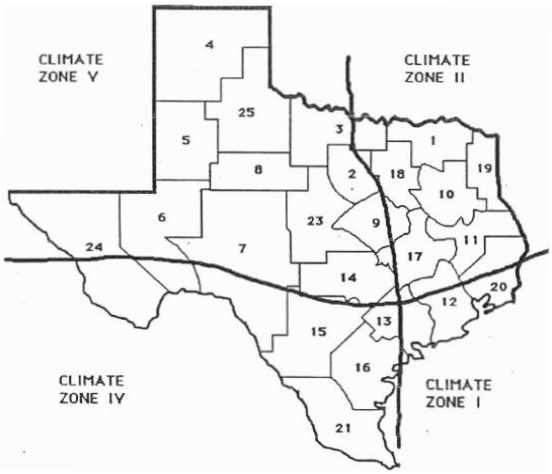

Figure 2.10: Climatic Regions in Texas (TxDOT, 2006).

Table 2.4: Selection Guidelines for Bituminous Surface Aggregate Classification (SAC) (TxDOT, 2006).

Demand for Friction	**Low**	**Moderate**	**High**
Rain Fall (in./yr.)	≤ 20	> 20 ≤ 40	> 40
Traffic (ADT)	≤ 5000	> 5,000 ≤ 15,000	> 15,000
Posted Speed (mph)	≤ 35	> 35 ≤ 60	> 60
Trucks (%)	≤ 8	> 8 ≤ 15	> 15
Vertical Grade (%)	≤ 2	> 2 ≤ 5	> 5
Horizontal Curve	≤ 3°	> 3° ≤ 7°	> 7°
Driveways (per mi.)	≤ 5	> 5 ≤ 10	> 10
Intersecting Rdwys (ADT)	≤ 500	> 500 ≤ 750	> 750
Available Friction	**Low**	**Moderate**	**High**
Cross Slope (in./ft.)	≤ 1/4	1/4 - 3/8	3/8 - 1/2
Surface Design Life (yrs.)	> 7	> 3 ≤ 7	≤ 3
Macro Texture of proposed surface	Fine (Examples: Microsurface, Type "F" HMAC)	Medium (Examples: HMAC Type "C" & "D," CMHB, SuperPave, SMA)	Coarse (Examples: Seal Coat, PFC, OGFC)

2.4.2. Texture Specifications in Texas

Different texture specifications are required for different scenarios. The following texture requirements were noted in the TxDOT standard specifications for construction and maintenance on Texas roadways (TxDOT, 2004):

- "*When an overlay on the planed pavement is not required, provide a minimum texture depth of not less than 0.05 in. (1.27 mm) (p. 421).*"

- "*When the plans call for a concrete overlay to be placed on the slab (new construction) or on prestressed concrete box beams or other precast elements, give a carpet drag, burlap drag, or broom finish to all concrete surfaces to be overlaid. Saw-grooving is not required in this case. Provide an average texture depth for the finish of approximately 0.035 in. (.889 mm) with no individual test falling below 0.020 in. (.508 mm), unless otherwise shown on the plans, when tested in accordance with Tex-436-A (p. 520).*"

- "*When the plans require an asphalt seal, with or without overlay, on the slab (new construction), on prestressed concrete box beams, or on other precast elements, give all concrete surfaces to be covered a lightly textured broom or carpet drag finish. Provide an average texture depth of approximately 0.025 in. (.635 mm) when tested in accordance with Tex-436-A (p. 520).*"

A specification that TxDOT used for a diamond grinding project in Fort Worth, Texas is shown in Table 2.5 (Buddhavarapu et al., 2013). The contractor had to grind until a mean texture depth (MTD) of 1.2 mm was achieved for concrete pavement containing limestone aggregate.

Table 2.5: Grinding Specification for a project in Fort Worth, Texas (Buddhavarapu et al., 2013).

Dimensional Limits/Aggregate Type	**Limestone**	**Gravel**
Blade segment thickness (minimum)	0.120"	0.120"
Blade segment thickness (maximum)	0.125"	0.130"
Land-width between grooves*	0.110" to 0.120"	0.090" to 0.110"
Minimum texture depth **	1.2 mm	1.0 mm

* Based on an average of a minimum of five measurements per lane mile of pavement ground.
** Based on an average of a minimum of five sand patch measurements per lane mile.

With regards to reducing hydroplaning with texture in Texas, TxDOT's Hydraulic Design Manual states, "*Studies have indicated that a permeable surface course or a high macrotexture surface course has the highest potential for reducing hydroplaning problems*" (TxDOT, 2011).

A rough pavement texture can have advantages and disadvantages (TxDOT, 2011). Some advantages are that a rough texture can minimize hydroplaning to some extent, and a very rough texture can benefit inlet interception. Some disadvantages are that a very rough pavement texture can cause a wider spread of water in the gutter and inhibit runoff from the pavement. If longitudinal grooving is applied to the pavement, it can help remove small amounts of water, but TxDOT discourages this, as it tends to impede runoff from moving toward the curb and gutter.

2.4.3. Mean Texture Depth vs. Mean Profile Depth

The texture data in this thesis was reported as the mean profile depth (MPD); however, texture can be measured in different ways. The macrotexture of a pavement can be described in terms of mean texture depth (MTD), obtained through a volumetric method, or MPD, obtained through processing profiles. A study in Italy estimated the MTD from MPD measurements using stationary and mobile profilometers (Losa et al., 2007). MPD values were calculated from profiles collected by the profilometers on asphalt concrete pavement, and they were calculated using alternatives 1 and 2 of the International Organization for Standardization (ISO) 13473-1. The surface texture direction (parallel, perpendicular and at 45° to the direction of traffic) was incorporated into the evaluation by taking the mean of the three different measurement directions. When taking the mean of the different surface texture directions, the estimated texture depth was found to be:

- $ETD = 0.92MPD_{mean} + 0.15$ (alternative 1)
- $ETD = 0.90MPD_{mean} + 0.17$ (alternative 2)

When only considering the direction parallel with forward moving traffic, the estimated texture depth given the MPD from stationary measurement was found to be:

- $ETD = 0.85MPD_{longitudinal} + 0.19$ (alternative 1)
- $ETD = 0.83MPD_{longitudinal} + 0.21$ (alternative 2)

When only considering the direction parallel with forward moving traffic, the estimated texture depth given the MPD from mobile measurement was found to be:

- $ETD = 0.82MPD_{mobile} + 0.20$ (alternative 1)

  Where, ETD and MPD are in mm.

The standard ISO 13473-1 (1997), which also considered only the direction parallel with forward moving traffic, is known to be: ETD = 0.8MPD + 0.2.

The results of the study show that obtaining the profile along different directions provides an MPD that estimates the texture depth (ETD) better than obtaining the profile in only one direction. When measuring in the forward moving direction, relationships from both stationary and mobile measurements were found to be similar to the ISO 13473-1 standard.

A study in Portugal also analyzed different test methods used for macrotexture depth evaluation on asphalt pavements (Freitas et al., 2008). The methods analyzed included the volumetric patch method and two methods using high speed profilometers to obtain surface profiles. The texture indicators analyzed included the MTD – estimated from the volumetric patch method, MPD – calculated by dividing the measured profile into segments, and sensor measured texture depth (SMTD) – calculated as the standard deviation of the sensor-measured profile amplitudes. As noted with the previous study, the MTD can be estimated with the MPD using the ISO 13473-1 equation. The following were the best correlations found from the study:

- Dense asphalt: MTD = 0.7MPD + 0.2; $R^2 = 0.8$
- Dense asphalt: MTD = 1.0SMTD + 0.3; $R^2 = 0.7$
- Dense asphalt and open texture asphalt: SMTD = 0.6MPD; $R^2 = 0.9$

The results showed that the study found a good correlation between the MPD and SMTD in the range of 0.6 to 1.1 mm for texture depths.

2.5. VEHICLE SPEED

Because rainfall intensities can reach high levels in Texas, the potential for hydroplaning cannot be completely eliminated by just adjusting the cross slope and texture in the design of the pavement. In addition to rainfall intensity, vehicle speed is also a primary factor in hydroplaning. In areas prone to hydroplaning, wet weather warning signs should be placed to warn the driver of the danger (TxDOT, 2011). The speed limit could be reduced for wet conditions.

TxDOT's Hydraulic Design Manual has an empirical equation (equations 3 in English units and 4 in metric units) for estimating the vehicle speed at which hydroplaning occurs (TxDOT, 2011):

English:

$$V = SD^{0.04} P^{0.3} (TD + 1)^{0.06} A \quad [3]$$

Metric:

$$V = 0.9143 SD^{0.04} P^{0.3} (TD + 0.794)^{0.06} A \quad [4]$$

Where:

V = vehicle speed at which hydroplaning occurs (mph or km/h)

SD = $[W_d\text{-}W_w/W_d]*100$ = spindown percent (10% spindown is used as an indicator of hydroplaning)

W_d = rotational velocity of a rolling wheel on a dry surface

W_w = rotational velocity of a wheel after spinning down due to contact with a flooded pavement

P = tire pressure (psi or kPa), use 24 psi or 165 kPa for design

TD = tire tread depth (in. or mm), use 2/32-in. or 0.5 mm for design

WD = water depth, in. or mm

TXD = pavement texture depth (in. or mm), use 0.02 in. or 0.5 mm for design

A = For English measurement, the greater of:

$$\left[10.409/WD^{0.06}\right]+3.507 \; or \; \left\{\left[28.952/WD^{0.06}\right]-7.817\right\}*TXD^{0.14}$$

For metric, the greater of:

$$\left[12.639/WD^{0.06}\right]+3.50 \; or \; \left\{\left[22.351/WD^{0.06}\right]-4.97\right\}*TXD^{0.14}$$

NOTE: This equation is limited to vehicle speeds of less than 55 mph (90 km/h) (TxDOT, 2011).

2.6. SUMMARY

The literature review conducted for this thesis was comprehensive, covering various aspects of automated data collection. The first part of the literature review was an overview of the background of automated data collection, including a review of automated techniques and how they compare to manual methods, case studies, and how transportation agencies select appropriate technologies and assure quality results. The next part of the literature review focused on parameters investigated in this study (cross slope, critical rut depth, friction demand, and vehicle speed). Based on the literature review for each of these parameters, the thresholds for hydroplaning prevention, as well as typical design values, were used to compare with the data reported in this study.

Chapter 3: Experimental Methods

3.1. SELECTION OF TEST SECTIONS

Before the pavement test sections could be determined, the critical variables that affect automated distress measurements needed to be identified. The most important variables considered for the selection of test sections were:

1. Pavement type:
    a. Flexible (hot-mix asphalt (HMA) and surface treatments)
    b. Rigid (JCP, CRCP)
2. Pavement condition:
    a. Type of distress (from LTPP and PMIS protocols)
    b. Severity of distress (low, medium, high)
3. Characteristics of the road:
    a. Surface texture (fine, coarse)
    b. Lane width (narrow, wide)

Secondary variables considered for the selection of test sections were:

4. Pavement condition (additional):
    a. Combination of distresses
    b. Presence of sealed cracks
5. Characteristics of the road (additional):
    a. Presence of horizontal curve
    b. Presence of vertical curve
    c. Presence of shoulders

d. Variation in pavement cross slope

6. Facility type (IH, US, SH, FM/RM)
7. Other anomalies considered were: lighting/shades and environmental conditions, flushing, lane-shoulder separation, transitions from light to dark pavement surface coloration, extensive patching, variable edge conditions including vegetation and edge drop offs.

When selecting the test sections, various degrees of the following distresses were considered: longitudinal, transverse and alligator cracking, failures (as defined in TxDOT's Rater's Manual), spalled cracks and punch-outs. This study included flexible pavements (HMA and surface treatments), and rigid pavements, jointed concrete pavements (JCP), and continuously reinforced concrete pavement CRCP). Twenty sections were tested, which included 15 flexible pavements and 5 rigid pavements (2 JCP and 3 CRCP). The 20 sections surveyed during this phase were not the same as those sections surveyed during Phase 1.Table 3.1 shows the number of test sections for each surface type in the study.

Table 3.1: Distribution of Test Sections According to Surface Type

Type of Pavement		**Number of Test Sections**
Flexible	HMA	7
	Surface Treatments	7
	PFC	1
Rigid	JCP	2
	CRCP	3
Total		20

Figure 3.1 shows the locations of all 20 sections plotted in Google Maps. The sections are located in or near Austin or Waco, Texas. Figures 3.2 and 3.3 show the locations in closer view for the sections in the Austin and Waco areas respectively. Table 3.2 summarizes each of the sections and the order in which data were collected. Auto DC # is the order in which the automatic data collection vehicles collected the data. Manual DC # is the order in which the reference data was collected manually.

Figure 3.1: All sections marked in Google Maps

Figure 3.2: Close up on Austin locations (Auto DC #'s labeled in yellow)

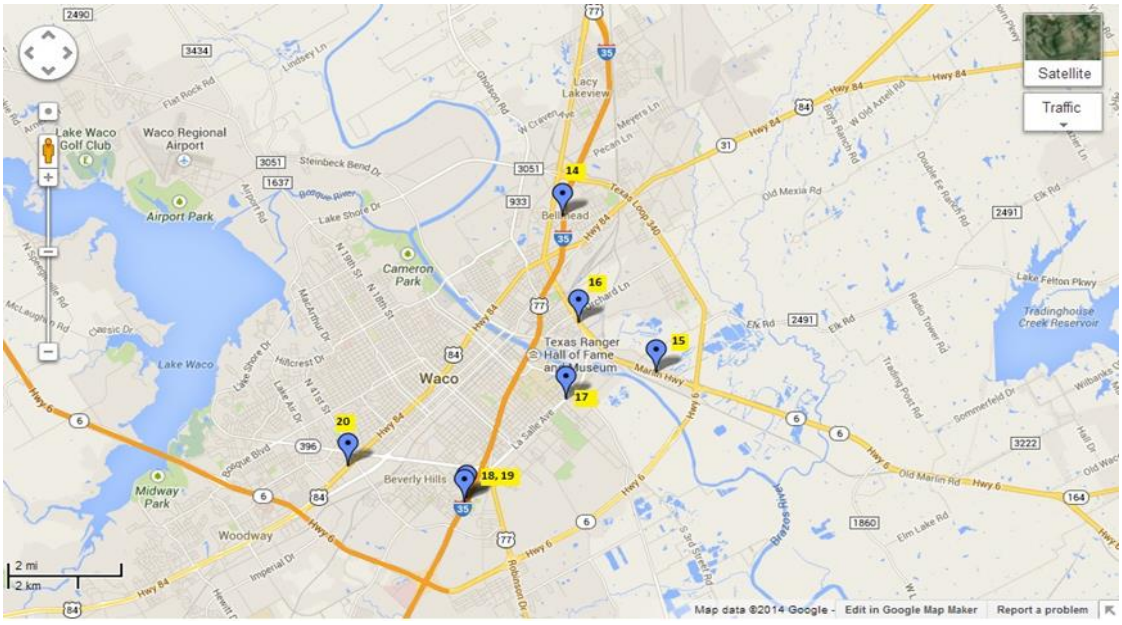

Figure 3.3: Close up on Waco locations (Auto DC #'s labeled in yellow)

Table 3.2: Data collection order

Auto DC #	Manual DC #	Name	Direction	speed limit	Location	Type	Inner Stripe	Outer Stripe
1	12	FM973-1	NB	60	Austin	HMA	Solid	Solid
2	13	FM3177-1	SB	60	Austin	HMA	Dashed	Solid
3	2	FM696-1	EB[1]	65	Austin	ST	Solid	Solid
4	4	FM696-3	EB[1]	65	Austin	HMA	Solid	Solid
5	5	FM696-4	WB[1]	65	Austin	HMA	Solid	Solid
6	3	FM696-2	WB[1]	65	Austin	ST	Solid	Solid
7	6	FM696-5	WB	65	Austin	HMA	Solid	Solid
8	1	FM619-1	NB	65	Austin	ST	Solid	None
9	7	FM112-1	EB	35	Austin	ST	Solid	None
10	8	FM1331-1	WB[1]	65	Austin	ST	Dashed	Solid
11	9	FM1331-2	EB[1]	65	Austin	ST	Dashed	Solid
12	10	FM1063-1	SB	65	Austin	ST	Solid	None
13	11	US79-1	WB	70	Austin	PFC	Dashed	Solid
14	20	IH35-3	SB	40	Waco	CRCP	Dashed	Curb
15	15	Spur484-1	EB	60	Waco	HMA	Dashed	Solid
16	16	US77-1	EB	40	Waco	JCP	Dashed	Joint
17	14	La_Salle-1	SB	40	Waco	HMA	Dashed	Solid
18	18	IH35-1	SB[3]	50	Waco	CRCP[2]	Dashed	Curb
19	19	IH35-2	SB[3]	50	Waco	CRCP	Dashed	Curb
20	17	US84-1	NB	50	Waco	JCP	Dashed	Curb

[1] Side-by-side section [2] CRCP with asphalt patch/overlay [3] contiguous sections

Each section was visited and marked with white tape, with an arrow and lines marking the beginning of the section and lines marking the end of the section. Each subsection was marked with spray paint, with numbered crosses marking every 50 feet, dashes marking every 25 feet, and dots marking every 5 feet (total section = 550 feet). Figure 3.4 shows the schematic of the section markings.

Figure 3.4: Schematic of section and subsection markings (beginning of section shown)

3.2. DESCRIPTION OF INDIVIDUAL SECTIONS

The following are descriptions of each individual section:

- **AutoDC1_FM973-1:**
  This section is the first to have data collection by automated technologies, located in the Austin area on FM 973 (coordinates: -97.638672, 30.214649). It is an HMA pavement with a speed limit of 60 mph.

- **AutoDC2_FM3177-1:**
  This section is the second to have data collection by automated technologies, located in Austin area on Decker Lane, near Highway 290 (coordinates: -97.601555, 30.333504). It is an HMA pavement with a speed limit of 60 mph.

- **AutoDC3_FM696-1:**
  This section is the third to have data collection by automated technologies, located in Austin area on FM 696 (coordinates: -97.197021, 30.381105). It is a surface treated pavement with a speed limit of 65 mph.

- **AutoDC4_FM696-3:**
  This section is the fourth to have data collection by automated technologies, located in Austin area on FM 696 (coordinates: -97.112907, 30.404057). It is an HMA pavement with a speed limit of 65 mph.

- **AutoDC5_FM696-4:**
  This section is the fifth to have data collection by automated technologies, located in Austin area on FM 696 (coordinates: -97.111603, 30.405031). It is an HMA pavement with a speed limit of 65 mph.

- **AutoDC6_FM696-2:**
  This section is the sixth to have data collection by automated technologies, located in Austin area on FM 696 (coordinates: -97.195511, 30.381889). It is a surface treated pavement with a speed limit of 65 mph.

- **AutoDC7_FM696-5:**
  This section is the seventh to have data collection by automated technologies, located in Austin area on FM 696 (coordinates: -97.264336, 30.366222). It is an HMA pavement with a speed limit of 65 mph.

- **AutoDC8_FM619-1:**
  This section is the eighth to have data collection by automated technologies, located in Austin area on FM 619 (coordinates: -97.260216, 30.427958). It is a surface treated pavement with a speed limit of 65 mph.

- **AutoDC9_FM112-1:**
  This section is the ninth to have data collection by automated technologies, located in Austin area on FM 112, Walnut St. (coordinates: -97.395889,30.564747). It is a surface treated pavement with a speed limit of 35 mph.

- **AutoDC10_FM1331-1:**
  This section is the tenth to have data collection by automated technologies, located in Austin area on FM 1331 (coordinates: -97.305000, 30.677795). It is a surface treated pavement with a speed limit of 65 mph.

- **AutoDC11_FM1331-2:**
  This section is the eleventh to have data collection by automated technologies, located in Austin area on FM 1331 (coordinates: -97.306343, 30.677818). It is a surface treated pavement with a speed limit of 65 mph.
- **AutoDC12_FM1063-1:**
  This section is the twelth to have data collection by automated technologies, located in Austin area on FM 1063 (coordinates: -97.285370, 30.645325). It is a surface treated pavement with a speed limit of 65 mph.
- **AutoDC13_US79-1:**
  This section is the thirteenth to have data collection by automated technologies, located in Austin area on US 79 (coordinates: -97.285011, 30.593393). It is a PFC pavement with a speed limit of 70 mph.
- **AutoDC14_IH35-3:**
  This section is the fourteenth to have data collection by automated technologies, located in Waco area on the frontage road alongside IH-35 (coordinates: -97.109703, 31.593853). It is a CRCP pavement with a speed limit of 40 mph.
- **AutoDC15_Spur484-1:**
  This section is the fifteenth to have data collection by automated technologies, located in Waco area on Marlin Hwy, Spur 484 (coordinates: -97.081589, 31.550722). It is an HMA pavement with a speed limit of 60 mph.
- **AutoDC16_US77-1:**
  This section is the sixteenth to have data collection by automated technologies, located in Waco area on S Loop Dr., alongside US-77 (coordinates: -97.104897, 31.564384). It is a JCP pavement with a speed limit of 40 mph.

- **AutoDC17_La_Salle-1:**
  This section is the seventeenth to have data collection by automated technologies, located in Waco area on State Loop 491, La Salle Ave. (coordinates: -97.108971, 31.543566). It is an HMA pavement with a speed limit of 40 mph.

- **AutoDC18_IH35-1:**
  This section is the eighteenth to have data collection by automated technologies, located in Waco area on the frontage road alongside IH-35 (coordinates: -97.138550, 31.516293). It is a CRCP pavement with a speed limit of 50 mph.

- **AutoDC19_IH35-2:**
  This section is the nineteenth to have data collection by automated technologies, located in Waco area on the frontage road alongside IH-35 (coordinates: -97.139343, 31.514938). It is a CRCP pavement with a speed limit of 50 mph.

- **AutoDC20_US84-1:**
  This section is the twentieth to have data collection by automated technologies, located in Waco area on US-84, W Waco Dr. (coordinates: -97.174248, 31.524954). It is a JCP pavement with a speed limit of 50 mph.

Figure 3.5: Auto DC Section 1

Figure 3.6: Auto DC Section 2

Figure 3.7: Auto DC Section 3

Figure 3.8: Auto DC Section 4

Figure 3.9: Auto DC Section 5

Figure 3.10: Auto DC Section 6

Figure 3.11: Auto DC Section 7

Figure 3.12: Auto DC Section 8

Figure 3.13: Auto DC Section 9

Figure 3.14: Auto DC Section 10

Figure 3.15: Auto DC Section 11

Figure 3.16: Auto DC Section 12

Figure 3.17: Auto DC Section 13

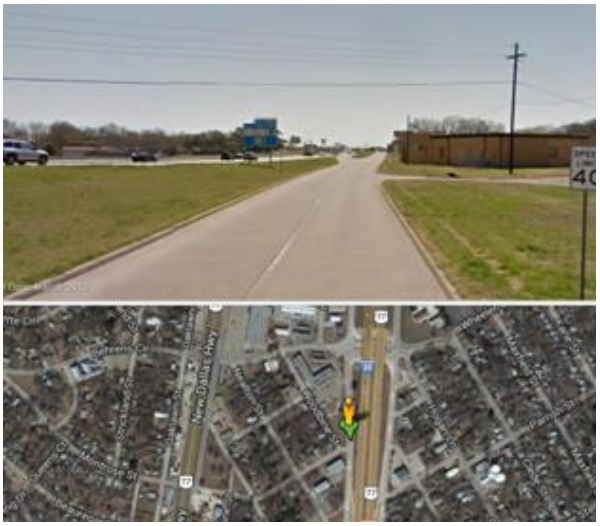

Figure 3.18: Auto DC Section 14

Figure 3.19: Auto DC Section 15

Figure 3.20: Auto DC Section 16

Figure 3.21: Auto DC Section 17

Figure 3.22: Auto DC Section 18

Figure 3.23: Auto DC Section 19

Figure 3.24: Auto DC Section 20

3.3. DATA COLLECTION

Data collection was divided into two main parts: 1) manual measurements to establish the benchmark reference or "true" distress level and 2) automated or dynamic measurements at highway speeds. During the dynamic measurements, each section was measured three times to determine the repeatability of the technology and to quantify the standard error of the measurement associated with each technology in the field. At the same time, by establishing a reference benchmark for each distress, the bias of each technology could be determined.

The sections were selected to start at a specific reference marker number (RMN) for ease of location. All sections were 550 feet in length. Traffic control was used for each section: once during the initial survey for the determination of the reference distress and once (after all vendors had collected automated distress information) for collection of the reference crack maps.

3.3.1. Distress Identification and Cross Slope

First, manual distress measurements were performed to establish the reference value of the various distress types. These measurements (for distresses and cross slope of each section) were carried out by Fugro with the help of LTPP certified and experienced technicians. Distresses were identified visually during a walk-through at each section, and the cross slope was measured using a dipstick. During this assessment the focus was on the quantification of longitudinal, transverse and alligator cracking, failures, spalled cracks and punchouts. The reference distress identification was performed following two protocols:

1. Visual Distress Assessment as described in the latest TxDOT Pavement Management Information System (PMIS) Rater's Manual (TxDOT, 2009),
2. Manual Distress Assessment as described in LTPP's Distress Identification Manual (Miller & Bellinger, 2003).

3.3.2. Reference Texture

The reference texture was obtained manually using a Circular Track Meter (CTM), shown in Figure 3.25. The CTM was placed at two locations (inner and outer wheelpaths) at each subsection of 50 feet (Figure 3.26), and texture data were recorded 3 times for each location.

Figure 3.25: Circular Track Meter (CTM)

Figure 3.26: CTM testing location

3.3.3. Automated Data Collection

After the manual distress assessments were conducted following TxDOT and LTPP procedures, the vendors were given the detailed location of the sections and were contracted to conduct their automated surveys. Automated data collection service providers were selected to represent all promising technologies that are commercially

available at the time of the survey. The following list of vendors performed the data collection and reported distress measurements on each of these sections:

1. Dynatest
2. Fugro
3. Waylink – OSU

Each vendor was to report the following types of data:

- Distresses from the Long-Term Pavement Performance Program (LTPP) protocol on each 50 ft. subsection. TxDOT follows PMIS protocol.
- Texture: Mean Profile Depth (MPD) in mm every 50 ft. for at least the outer wheel path
- Cross slope in mm/mm every longitudinal 50 ft. For each 50 ft. subsection, the cross slope is reported every transverse one foot.
- Digital crack maps of each section

Vendors were asked to report data within 3 different time frames:

- Fully Automated with no manual post-processing (immediately after data collection run)
- Semi Automated with minimum manual post-processing (within 2 business days)
- Semi Automated with higher manual post-processing (4 weeks after data collection)

Figure 3.27 shows pictures of the automatic data collection vehicle for TxDOT. Figure 3.28 shows pictures of the vehicle for one of the vendors, Dynatest. Figures 3.29 and 3.30 show Fugro and Waylink-OSU's vehicles respectively.

Figure 3.27: TxDOT van

Figure 3.28: Dynatest van –back and inside

Figure 3.29: Fugro van

Figure 3.30: Waylink-OSU van

3.3.4. Crack Maps

When all vendors completed their automated surveys, the research team returned to the sections and marked (painted) all cracks and distresses of interest using a color coding system to differentiate the levels of distress such as low (L), moderate (M) and high (H). Although TxDOT does not record severity, LTPP does. For example, longitudinal and transverse cracks are classified as low severity if they are narrower than 6 mm, moderate if they are between 6 and 19 mm and high if they are wider than 19 mm.

Cracks were marked with 3 chalk colors depending on crack widths (red < 3mm, blue 3-6mm, green >6mm). Each Team member had a ruler marked in millimeters to check crack widths when necessary. Figures 3.31-3.33 show the crack coloring process.

Figure 3.31: Marking section with colored chalk (FM 1063)

Due to coarse aggregate patterns, “phantom” cracks (lines formed by aggregate edges, cracked aggregate, flushed asphalt, etc.) had to be closely examined and left unmarked. An example of a phantom crack (outlined in white) is shown in Figure 3.34. Phantom cracks can also be created by loss of aggregates which roughly form a line and create the illusion of a crack (Figure 3.35).

Sealed cracks also exhibited open cracks of various widths (Figure 3.36).

Figure 3.32: Crack marked in green (FM 1331)

Figure 3.33: Phantom cracks marked in white (FM 1063)

Figure 3.34: Phantom cracks created by loss of aggregates (FM 1063)

Figure 3.35: Cracks within sealed cracks (FM 1331).

During the coloring process, the area was secured with traffic control, which included cones, flaggers on each end of the section, and a pilot car (Figure 3.37).

Once the cracks were marked with different colors, the sections were photographed and the images were digitized to obtain a true crack map of each section. The 10 consecutive pictures taken at each test sub-section were stitched using the panoramic image stitcher software Microsoft Image Composite Editor (ICE), obtaining a unique digital image per sub-section. A custom image processing algorithm was developed by the research team using MATLAB to detect the location of each red, blue

and green line, and the images of these lines drawn by chalk were highlighted darker on the computer. Figures 3.38, 3.39, and 3.40 show the installation of the camera mounting system, laptop computer connection to the digital camera, and the vehicle with the camera mounted and ready for crack map image collection.

Figure 3.36: Traffic control, pilot car, and flaggers

Figure 3.37: Installing the digital camera on the mounting system

Figure 3.38: Computer used to operate digital camera

Figure 3.39: Vehicle ready for taking crack map pictures

RESULTS AND ANALYSIS

Chapter 4: Texture

4.1. GENERAL RESULTS

4.1.1. All texture profiles

The results for all texture given from each vendor (Fugro and Waylink-OSU given every 5-ft., Dynatest given every 10-ft., and Reference and TxDOT given every 50-ft.), with units of mean profile depth (MPD) in mm, are shown in Appendix A. Below each texture graph in Appendix A is an image close-up of the respective section.

4.1.2. Average texture every subsection

The results for the texture for each 50-ft subsection, with units of MPD in mm, are shown in Appendix B (inner wheelpath) and Appendix C (outer wheelpath).

Appendix B and C also show the error results (error = reference – vendor). Table 4.1 shows a summary of the average texture error for all sections. The following observations are noted:

- In most sections, the texture reported by Dynatest and Fugro were close with the Reference, with values close to 0.5 or 1.0 mm.
- Waylink-OSU texture readings were slightly higher in magnitude, with values close to 1.5 or 2.0 mm (sometimes higher).
- TxDOT readings were also usually higher in magnitude, usually 1.5 mm or higher (sometimes 3 or 4mm). TxDOT is represented in the graphs as a single straight line because the reading was reported as an average value for the entire 550 ft.

section. In many of the sections, the TxDOT average texture graph-line is close to the Waylink-OSU line in magnitude.

- Waylink-OSU and Fugro reported values for both wheelpaths.
- Though Waylink-OSU is reported at higher magnitudes, in many of the sections the texture graph-line follows a similar trend in shape as the reference, Dynatest, and Fugro.

Table 4.1: Summary of texture average error for all sections

	***Inner* wheelpath (IWP) - MPD Average Error (mm)**		***Outer* wheelpath (IWP) - MPD Average Error (mm)**			
	Vendors		Vendors			
Section	Fugro	Waylink-OSU	Dynatest	Fugro	Waylink-OSU	TxDOT
AutoDC1_FM973-1	0.00	-1.55	0.02	-0.14	-1.73	-1.26
AutoDC2_FM3177-1	0.13	-1.13	0.47	0.38	-0.77	-0.79
AutoDC3_FM696-1	0.21	-1.45	0.45	0.47	-0.98	-3.31
AutoDC4_FM696-3	0.01	-1.18	0.04	0.06	-0.95	-2.56
AutoDC5_FM696-4	-0.01	-1.54	0.01	-0.02	-1.12	-1.54
AutoDC6_FM696-2	0.03	-1.67	0.04	0.09	-1.53	-0.48
AutoDC7_FM696-5	0.32	-0.98	0.36	0.37	-0.82	-1.76
AutoDC8_FM619-1	0.52	-0.98	0.73	0.75	-1.14	-2.38
AutoDC9_FM112-1	0.35	-0.95	0.19	0.37	-0.65	-2.09
AutoDC10_FM1331-1	0.33	-2.38	0.63	0.54	-9.51	-2.00
AutoDC11_FM1331-2	0.55	-1.32	0.45	0.56	-1.98	-1.94
AutoDC12_FM1063-1	0.62	-1.30	0.52	0.53	-1.08	-1.59
AutoDC13_US79-1	0.04	-3.16	0.50	0.12	-2.07	-2.75
AutoDC14_IH35-3	0.06	-0.98	-0.07	0.05	-0.61	-1.32
AutoDC15_Spur484-1	0.27	-1.86	0.22	0.28	-1.09	-2.02
AutoDC16_US77-1	0.28	-1.41	0.01	0.27	-0.43	-0.81
AutoDC17_La_Salle-1	-0.17	-1.32	0.10	-0.06	-1.05	0.48
AutoDC18_IH35-1	0.05	-1.38	0.04	0.23	-0.87	-1.22
AutoDC19_IH35-2	0.01	-1.13	-0.08	-0.01	-0.93	-1.15
AutoDC20_US84-1	0.01	-1.31	-0.12	-0.07	-1.14	-1.20
Average	**0.18**	**-1.45**	**0.23**	**0.24**	**-1.52**	**-1.59**

RESULTS AND ANALYSIS

Chapter 5: Cross Slope

5.1. GENERAL RESULTS

5.1.1. Average cross-slope every subsection

The results for the cross slope measurements (both automated and the manual reference) for each 50-ft subsection, with units in percent, are shown in Appendix D. Based on a preliminary review of the data, the results were adjusted when it appeared that the vendors used different sign conventions to report slope values when compared to the reference data. An example of this is shown in Figure 5.1. In Appendix D, the table for each section shows the error results every 50 feet (error = reference – vendor) of the cross slopes after they have been adjusted to correct sign direction.

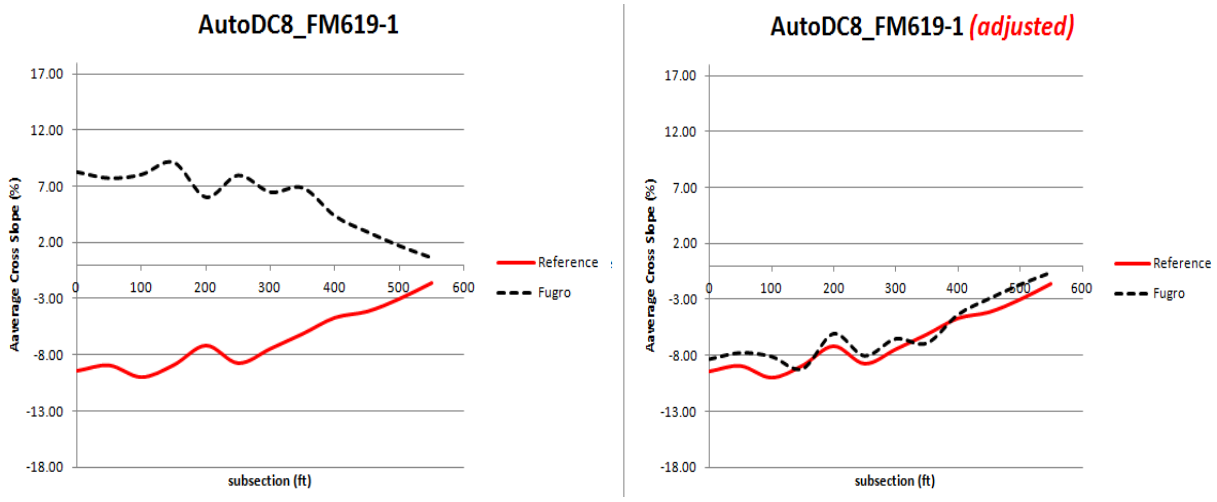

Figure 5.1: Adjusted cross slope values after correction.

5.1.2. Average cross-slope for each entire section

TxDOT reported the average cross slope of the entire 550-ft. section for each section, calculated with three different algorithms: AASHTO pp69, 2 point, and line fitting algorithm. The results for the average cross slope error for each entire 550-ft section from all vendors, with units in percent, are shown in Table 5.1.

Table 5.1: Average automated cross slope error for entire 550-ft section

Section	***Adjusted* Cross Slope - Average Error (percent)**						**Std. Dev. (percent)**		
	Vendors			TxDOT			Vendors		
	Dynatest	Fugro	Waylink-OSU	pp69 algorithm	2 point algorithm	line fitting algorithm	Dynatest	Fugro	Waylink-OSU
AutoDC1_FM973-1	3.09	-0.89	-0.05	2.25	0.85	0.80	0.09	0.23	1.10
AutoDC2_FM3177-1	3.30	-0.90	-0.52	1.58	0.17	0.16	0.14	0.44	0.72
AutoDC3_FM696-1	3.44	-1.48	-2.30	1.24	0.34	0.64	0.66	2.53	1.03
AutoDC4_FM696-3	3.29	-0.87	-0.88	1.03	-0.37	-0.43	0.15	0.60	0.95
AutoDC5_FM696-4	0.22	-0.79	-2.75	0.84	-0.41	-0.45	0.23	0.52	0.61
AutoDC6_FM696-2	0.17	-0.92	-1.73	0.43	-0.92	-0.67	0.27	1.24	0.89
AutoDC7_FM696-5	0.15	-0.78	-0.55	1.85	0.60	0.72	0.17	0.65	0.50
AutoDC8_FM619-1	0.45	-0.82	-5.91	-5.74	-5.87	-5.93	0.37	0.73	3.13
AutoDC9_FM112-1	-0.16	-1.38	-1.87	1.10	-0.30	-0.58	0.45	1.12	0.72
AutoDC10_FM1331-1	0.34	-0.49	-1.24	1.96	0.83	1.00	0.65	1.15	0.62
AutoDC11_FM1331-2	0.19	-0.73	-1.95	2.18	1.49	1.81	0.20	1.00	0.72
AutoDC12_FM1063-1	-0.02	-1.01	-1.01	2.32	1.22	1.27	0.32	0.85	0.58
AutoDC13_US79-1	0.25	-0.86	-1.58	1.67	0.67	0.58	0.16	0.69	0.62
AutoDC14_IH35-3	0.17	-0.92	-0.12	-0.24	-1.27	-0.63	0.26	0.44	1.81
AutoDC15_Spur484-1	0.02	-0.99	-2.54	0.67	-0.50	-0.62	0.06	0.23	0.20
AutoDC16_US77-1	0.03	-1.05	-1.58	0.67	-0.45	-0.54	0.13	0.29	0.45
AutoDC17_La_Salle-1	0.09	-1.08	-1.06	0.86	-0.40	-0.46	0.12	0.27	0.32
AutoDC18_IH35-1	-0.22	-1.60	-2.75	0.54	-0.47	-0.53	0.26	0.70	0.70
AutoDC19_IH35-2	0.06	-1.23	-2.52	0.04	-0.94	-0.75	0.22	0.67	1.11
AutoDC20_US84-1	0.16	-1.07	-1.46	0.68	-0.46	-0.87	0.28	0.27	0.19
Average	**0.75**	**-0.99**	**-1.72**	**0.80**	**-0.31**	**-0.27**	**0.26**	**0.73**	**0.85**

The following observations were made regarding the cross slope graphs:

- In most of the sections (18 out of 20), Dynatest follows a closely similar trend to the graph-line shape of the reference (See Figure 5.2). Of the ones that were

different, they were only slightly different in graph-line shape. The Dynatest data did not have to be corrected in sign to match the reference.

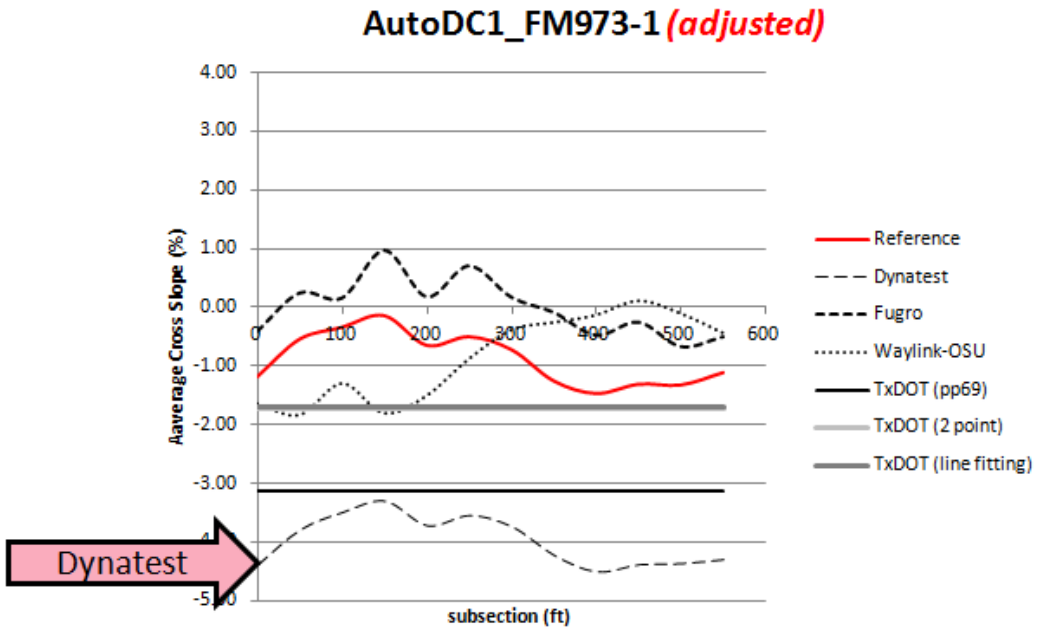

Figure 5.2: Example showing Dynatest data

- Sometimes Fugro-Roadware (12 out of 20 sections) follows a similar or partially similar shape to the reference graph-line and many times has to be flipped in sign to match (see Figure 5.3).

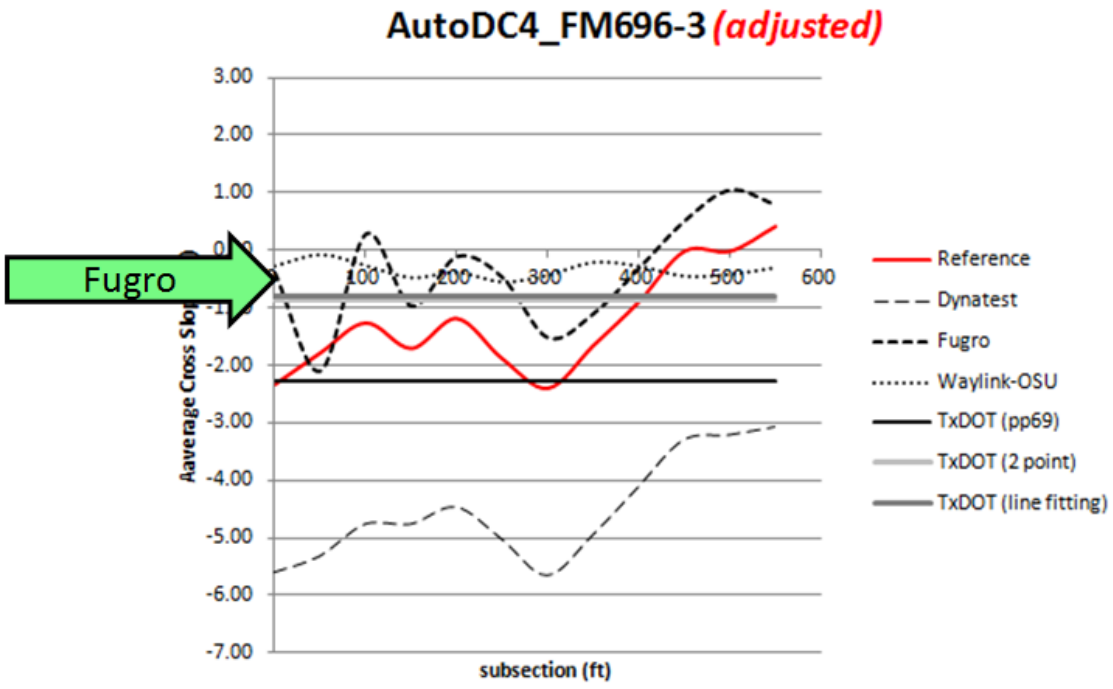

Figure 5.3: Example showing Fugro data

- Sometimes Waylink-OSU (5 out of 20 sections) follows a similar or partially similar shape graph-line as the reference, though it is often higher or lower in magnitude (see Figure 5.4). For some of the sections the Waylink-OSU line had to get flipped in sign.

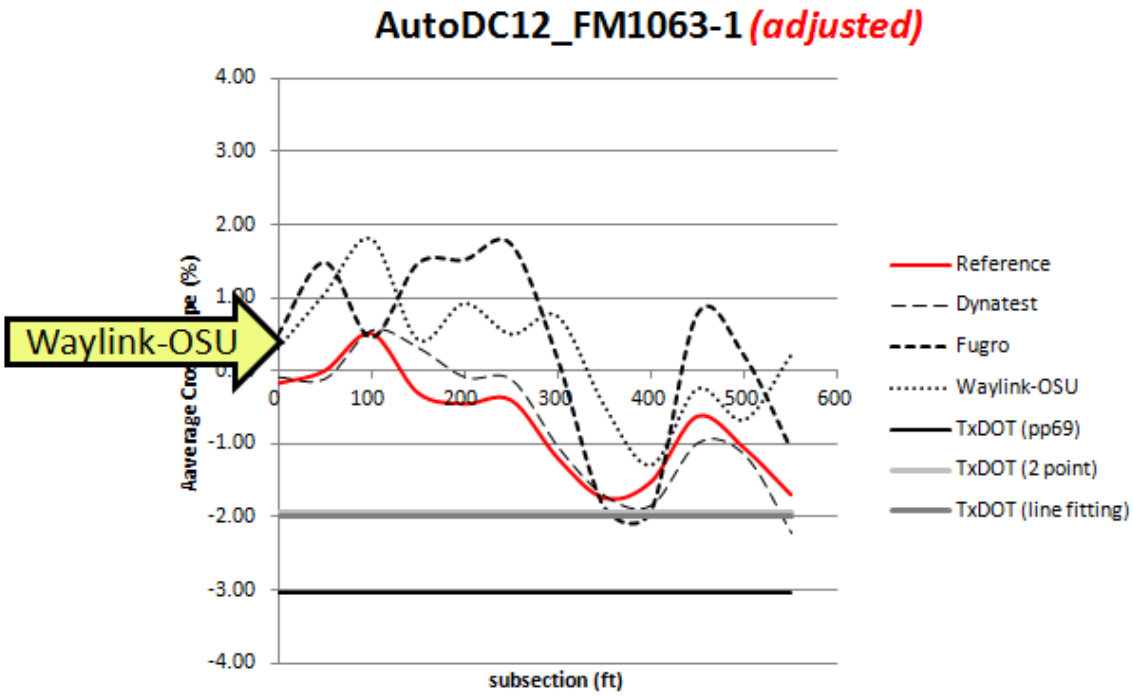

Figure 5.4: Example showing Waylink-OSU data

- Sometimes Waylink-OSU cross slope magnitude is closer to Fugro magnitude, though many times Fugro is closer to the reference in magnitude (after being flipped in sign). Dynatest and the reference are usually closer in magnitude. An example of these characteristics is shown in Figure 5.5.

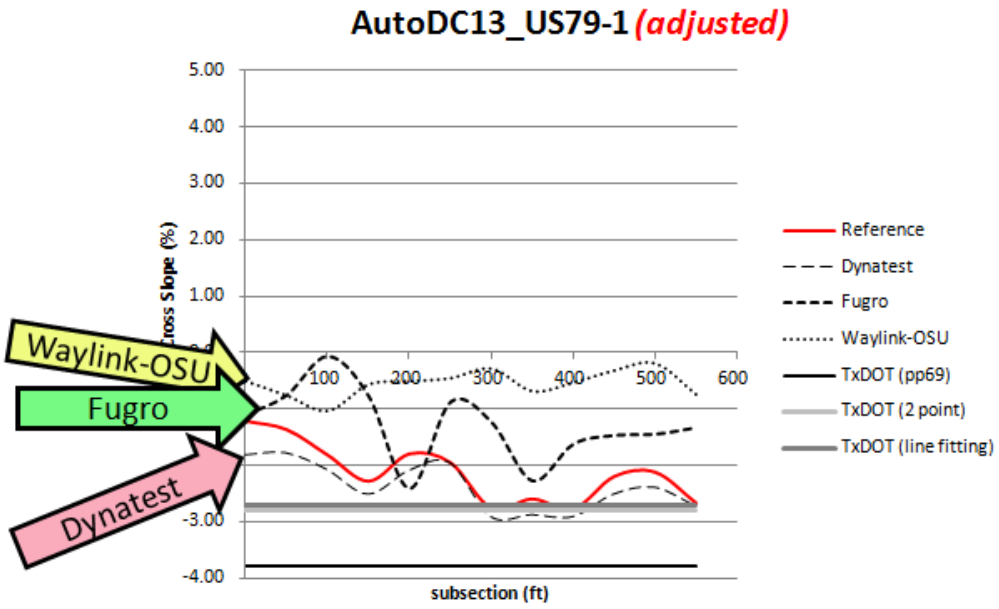

Figure 5.5: Example showing all vendors.

- The TxDOT average cross slope readings are often close to the other vendors and reference readings, but sometimes needs to be flipped in sign. The pp69 algorithm graph-line is often farther from the reference (higher in magnitude) than the other two algorithms, 2 point and line fitting (see figure 5.6).

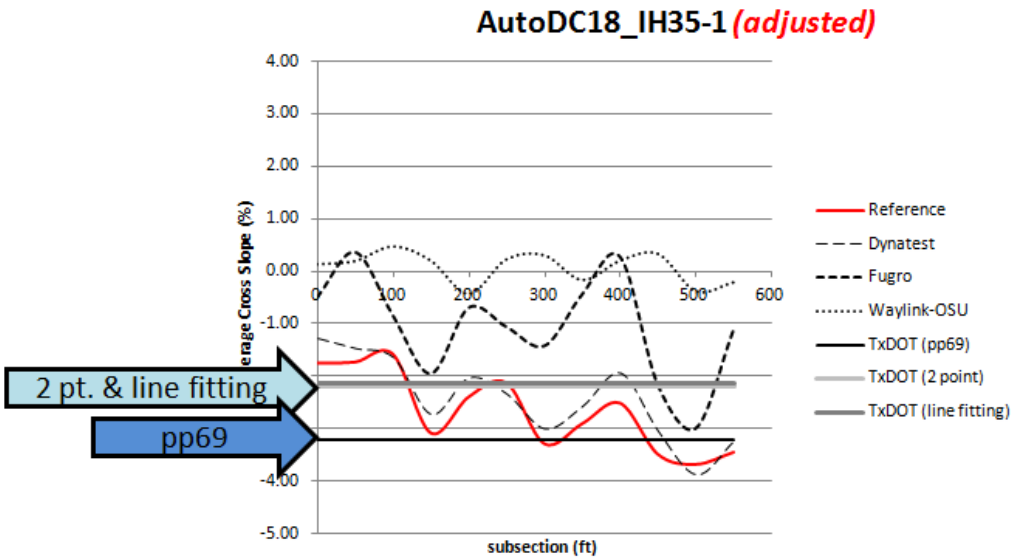

Figure 5.6: Example showing TxDOT data.

5.1.3. Cross-slope every transverse foot of every subsection

Fugro and Waylink-OSU reported cross slope values for each one-foot transverse segment of each 50-foot longitudinal subsection of each section (each section length = 550 longitudinal feet). The transverse cross slope profiles were obtained from the given data and graphed (height vs. transverse feet), starting with the first cross slope at zero feet in height. The results for the cross slope for every transverse foot of every 50-ft subsection, with units in percent, are shown in Appendix E. The following observations are noted regarding the graphs of the transverse cross slope profiles:

- The reference profiles typically show that the pavement slopes downward towards the outer edge (increasing transverse feet toward the right side of graph). This is expected for pavements to drain rainfall.

- Fugro profiles typically do not follow the same trend as the reference. Fugro profiles show significant jumps, typically with a sharp decrease in height at the beginning (toward the inner edge of the pavement) and then leveling out or following with milder jumps after that. An example of such profiles is shown in Figure 5.7, which shows four consecutive profiles in a section with a significant jump at the same location from profile to profile. The sharp decrease at one location may be caused by a flaw in the equipment on that side, and this will affect further calculations if these data are used. The jumps were not seen in the same location in all profiles, so these jumps were not treated as outliers and were kept for the analysis of this thesis. Figure 5.8 shows four consecutive profiles in a section where there is no consistent location of a jump from profile to profile.
- Waylink-OSU profiles typically do not show much sloping when compared to the reference. Waylink-OSU profiles mostly remain near zero-feet in height, with very minor increases and decreases. The profiles typically do not follow the same trend as the reference. As with the Fugro profiles, some of the Waylink-OSU profiles were seen to have significant jumps, though not as many profiles as Fugro.

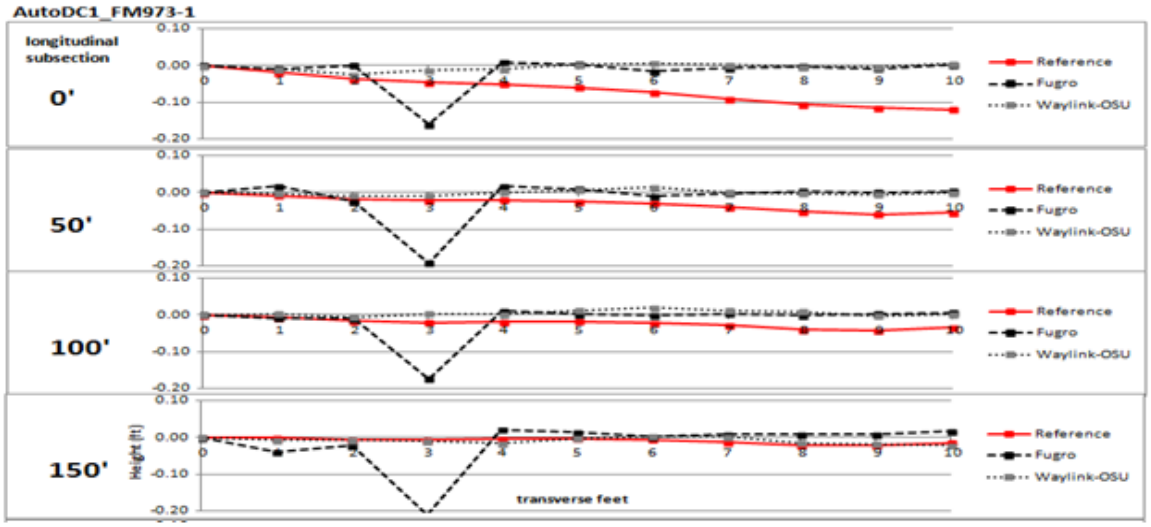

Figure 5.7: Four consecutive transverse cross slope profiles for section AutoDC1_FM973-1

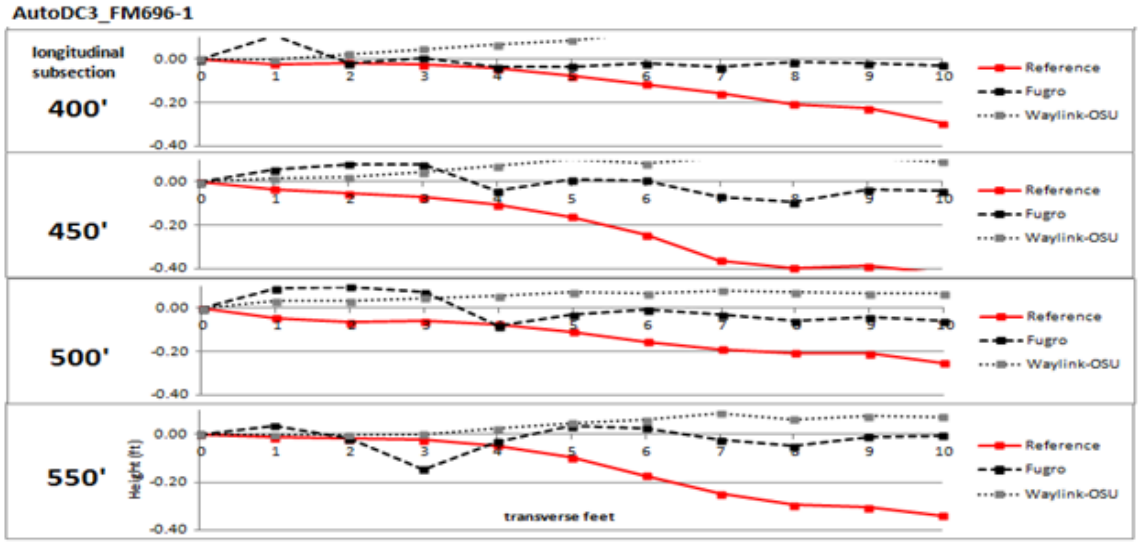

Figure 5.8: Consecutive transverse cross slope profiles for section AutoDC3_FM696-1

5.2. HYDROPLANING ANALYSIS

5.2.1. Potential Ponding

Water collected in ruts or depressions in the roadway can lead to hydroplaning if they are deep enough. The cross slope profiles given from the automated data collection could be used to identify potential areas of ponding.

5.2.1.1. Calculate Ruts

Cross slope data given for each transverse-foot were used to draw the cross slope profile for each 50-ft subsection. From each profile, surface depressions were identified. The depth, width, and area of potential water that could collect in each surface depression were calculated.

Figure 5.9 shows an exaggerated example to illustrate different types of surface depressions that can collect water. The shaded regions indicate the maximum amount of water that could collect within each depression before spilling out of the depression. The depressions labeled “Rut 1” and “Rut 4” are examples of depressions where the water rises to the exact same height on each side. In cases like “Rut 3” and “Rut 5,” the water rises to a maximum height at the lower side of the depression and the respective locations at points B and C have to be calculated where the water stops on the opposite side. “Rut 2” represents a scenario where there are two (or more) smaller ruts within a larger rut, and the maximum height the water reaches is at the lower side of the larger rut. The location (point A) where the water stops on the opposite side of the larger rut has to be calculated.

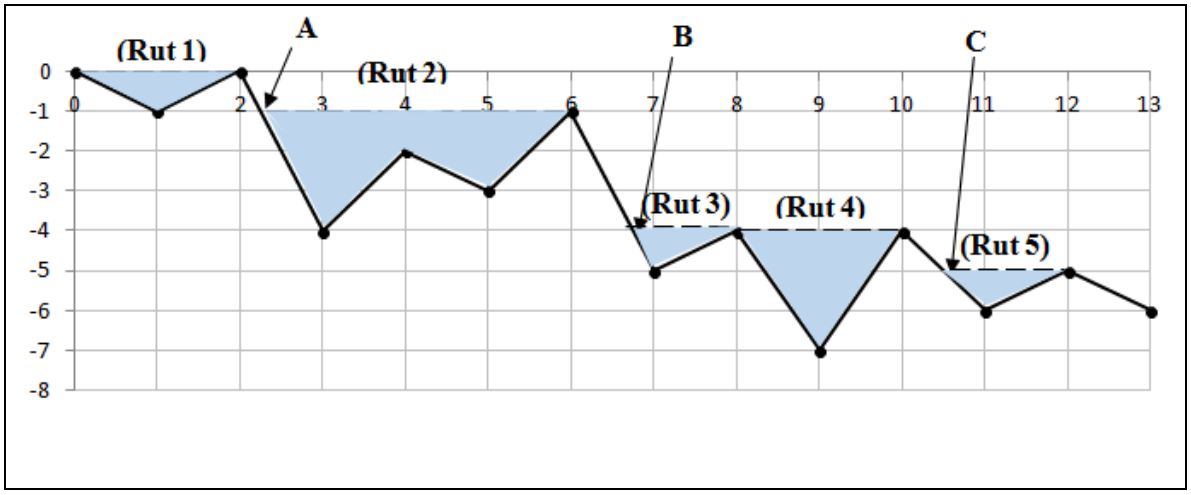

Figure 5.9: Example illustrating surface depressions that can collect water

An algorithm was used to identify peaks and valleys in the cross-slope profiles and was then used to calculate the depth of water ponding. The parameters of area, depth, and width of water were calculated in Microsoft Excel using IF, AND, and OR statements. Some of the steps to these calculations included the following:

1. Identify negative (-), positive (+), and zero (0) slope areas.
2. Identify areas that change from (-) to (+) slope.
3. Identify point where water reaches maximum (to draw a horizontal line across)
4. Calculate area, depth and width of water
    a. Area of water: subtract area under corresponding curve from area under horizontal water line
    b. Depth of water (find deepest part): calculate vertical distance from water line to minimum point in the water area
    c. Width of water: calculate horizontal distance between water line points

After the area, depth, and width of water were calculated for each surface depression in each cross slope profile, the summary data from the reference in Appendix F (total number of surface depressions, cumulative area of all water, maximum depth, and maximum width) were calculated. Tables 5.2, 5.3, and 5.4 summarizes data for each entire section (the overall maximum of: total number of surface depressions, cumulative area of all water, maximum depth, and maximum width) collected from the Reference, Fugro, and Waylink-OSU respectively.

Table 5.2: Summary data of potential water in surface depressions collected by Reference.

Section	Maximum Within Section			
	Total Number of Puddles/Ruts	**Cumulative Area of All Water (in^3)**	**Maximum Depth (in)**	**Maximum Width (ft)**
AutoDC1_FM973-1	2	3.16	0.091	3.61
AutoDC2_FM3177-1	2	10.25	0.472	4.32
AutoDC3_FM696-1	2	5.88	0.364	2.03
AutoDC4_FM696-3	2	9.06	0.197	8.27
AutoDC5_FM696-4	0	0.00	0.000	0.00
AutoDC6_FM696-2	2	6.48	0.262	3.80
AutoDC7_FM696-5	2	17.97	0.472	4.59
AutoDC8_FM619-1	1	0.15	0.024	1.06
AutoDC9_FM112-1	2	23.44	0.819	6.00
AutoDC10_FM1331-1	1	10.82	0.508	3.88
AutoDC11_FM1331-2	2	11.59	0.537	2.95
AutoDC12_FM1063-1	2	5.22	0.285	2.67
AutoDC13_US79-1	0	0.00	0.000	0.00
AutoDC14_IH35-3	1	1.33	0.069	3.11
AutoDC15_Spur484-1	0	0.00	0.000	0.00
AutoDC16_US77-1	0	0.00	0.000	0.00
AutoDC17_La_Salle-1	2	0.51	0.057	1.61
AutoDC18_IH35-1	0	0.00	0.000	0.00
AutoDC19_IH35-2	0	0.00	0.000	0.00
AutoDC20_US84-1	0	0.00	0.000	0.00

Table 5.3: Summary data of potential water in surface depressions collected by Fugro.

Section	Maximum Within Section			
	Total Number of Puddles/Ruts	Cumulative Area of All Water (in^3)	Maximum Depth (in)	Maximum Width (ft)
AutoDC1_FM973-1	3	44.40	2.773	9.88
AutoDC2_FM3177-1	2	76.43	1.433	9.41
AutoDC3_FM696-1	3	89.53	2.935	7.97
AutoDC4_FM696-3	3	41.46	2.753	9.91
AutoDC5_FM696-4	3	33.37	0.785	8.31
AutoDC6_FM696-2	3	68.61	4.460	7.81
AutoDC7_FM696-5	4	65.07	3.278	9.47
AutoDC8_FM619-1	3	48.07	2.188	7.17
AutoDC9_FM112-1	4	64.04	2.781	9.98
AutoDC10_FM1331-1	2	201.42	2.719	9.73
AutoDC11_FM1331-2	2	198.01	3.232	9.69
AutoDC12_FM1063-1	4	90.38	3.201	6.73
AutoDC13_US79-1	2	140.96	2.442	9.51
AutoDC14_IH35-3	5	32.56	2.475	3.97
AutoDC15_Spur484-1	2	162.40	2.738	9.56
AutoDC16_US77-1	3	72.92	1.334	9.47
AutoDC17_La_Salle-1	3	43.45	0.730	9.27
AutoDC18_IH35-1	4	42.43	3.087	9.95
AutoDC19_IH35-2	4	29.23	1.861	9.93
AutoDC20_US84-1	3	2.32	0.208	2.47

Table 5.4: Summary data of potential water in surface depressions collected by Waylink-OSU.

Section	Maximum Within Section			
	Total Number of Puddles/Ruts	Cumulative Area of All Water (in^3)	Maximum Depth (in)	Maximum Width (ft)
AutoDC1_FM973-1	3	14.37	0.300	5.91
AutoDC2_FM3177-1	4	49.02	1.940	9.73
AutoDC3_FM696-1	2	18.14	0.760	3.87
AutoDC4_FM696-3	4	14.72	0.286	8.73
AutoDC5_FM696-4	4	18.56	0.390	10.60
AutoDC6_FM696-2	3	27.90	0.770	6.69
AutoDC7_FM696-5	3	45.95	1.240	11.16
AutoDC8_FM619-1	3	39.93	1.914	4.89
AutoDC9_FM112-1	4	46.90	1.053	6.91
AutoDC10_FM1331-1	4	23.63	0.954	5.43
AutoDC11_FM1331-2	3	29.81	0.680	6.54
AutoDC12_FM1063-1	3	29.19	0.798	5.91
AutoDC13_US79-1	5	35.17	0.835	10.76
AutoDC14_IH35-3	4	60.49	4.524	11.99
AutoDC15_Spur484-1	4	20.32	0.556	10.94
AutoDC16_US77-1	3	20.14	0.222	10.76
AutoDC17_La_Salle-1	3	19.67	0.524	8.94
AutoDC18_IH35-1	2	21.05	0.287	11.06
AutoDC19_IH35-2	3	21.51	0.264	10.71
AutoDC20_US84-1	3	18.85	0.459	11.18

The following observations are noted regarding potential water calculations:

- The reference data showed 0-2 puddles in each cross slope profile.
    - Cumulative area of all water per cross slope profile ranged from 0 to23.4 in^3.
    - Maximum depth of water per cross slope profile ranged from 0 to 0.82 in.
    - Maximum width of water per cross slope profile ranged from 0 to 8.27 ft.
- The Fugro data showed 2-5 puddles in each cross slope profile. In comparison to the reference, the profiles measured by Fugro can collect water at deeper and wider depths. The Fugro profiles can cumulatively collect significantly more water than the reference; however, it is noted that the significant jumps seen in the profiles affect the results largely and makes the values unrealistic.
    - Cumulative area of all water per cross slope profile ranged from 2.3 to 201.4 in^3.
    - Maximum depth of water per cross slope profile ranged from 0.21 to 4.46 in.
    - Maximum width of water per cross slope profile ranged from 2.47 to 9.98 ft.
- The Waylink-OSU data showed 2-5 puddles in each cross slope profile. In comparison to the reference, Waylink-OSU profiles can also collect water at deeper and wider depths, but cumulatively, Waylink-OSU profiles cannot collect as much water as Fugro profiles. It is noted that these values are also unrealistic due to the significant jumps seen in some of the profiles.

- Cumulative area of all water per cross slope profile ranged from 14.4 to 60.5 in^3.
- Maximum depth of water per cross slope profile ranged from 0.22 to 4.52 in.
- Maximum width of water per cross slope profile ranged from 3.87 to 11.99 ft.

5.2.1.2. Compare with Known Thresholds

The data obtained for potential ponding in each transverse profile was compared to minimum and maximum thresholds determined by previous research studies that indicate occurrence of hydroplaning.

5.2.1.2.1. Water Depth

As noted in the literature review, the rut depth categories in Texas are (TxDOT, 2011):

- Shallow (0.25-0.49 in.). Possible hydroplaning can occur for smooth pavements and bald tires (Mounce & Bartoskewitz, 1993; Yeager, 1974; Balmer & Gallaway, 1983; TxDOT, 2011).
- Deep (0.50-0.99 in.). Possible hydroplaning can occur (Teede Technokeskus, n.d.).
- Severe (1.00-1.99 in.). Hydroplaning can occur (Teede Technokeskus, n.d.).
- Rutting 2.0 in. or greater is a failure. Hydroplaning can occur (Teede Technokeskus, n.d.).

Based on these thresholds, the question "*Can hydroplaning occur? (yes or no)*" is asked for each profile. Table 5.5 summarizes if hydroplaning could occur with regards to water depth per section. It is noted that these thresholds apply to high operating speeds, and not all sections have high speed limits. Speed is discussed in a further section.

Table 5.5: Summary if hydroplaning will occur with regards to water depth per section.

Section	**Hydroplaning could occur? Yes or No (note: these apply to high operating speeds)**											
	Texas: Shallow rut depth? *Possible Hydroplaning for smooth pavements, bald tires*			**Texas: Deep rut depth? *Possible hydroplaning***			**Texas: Severe rut depth? *Hydroplaning***			**Texas: Rut depth = Failure? *Hydroplaning***		
	Reference	**Fugro**	**Waylink-OSU**	**Reference**	**Fugro**	**Waylink-OSU**	**Reference**	**Fugro**	**Waylink-OSU**	**Reference**	**Fugro**	**Waylink-OSU**
AutoDC1_FM973-1	no	no	yes	no	no	no	no	yes	no	no	yes	no
AutoDC2_FM3177-1	yes	yes	yes	no	yes	yes	no	yes	yes	no	no	no
AutoDC3_FM696-1	yes	no	yes	no	yes	yes	no	yes	no	no	yes	no
AutoDC4_FM696-3	no	yes	yes	no	yes	no	no	yes	no	no	yes	no
AutoDC5_FM696-4	no	yes	yes	no	yes	no	no	no	no	no	no	no
AutoDC6_FM696-2	yes	yes	yes	no	yes	yes	no	yes	no	no	yes	no
AutoDC7_FM696-5	yes	no	yes	no	no	yes	no	yes	yes	no	yes	no
AutoDC8_FM619-1	no	yes	yes	no	yes	yes	no	yes	yes	no	yes	no
AutoDC9_FM112-1	no	yes	yes	yes	yes	yes	no	yes	yes	no	yes	no
AutoDC10_FM1331-1	yes	no	yes	yes	yes	yes	no	yes	no	no	yes	no
AutoDC11_FM1331-2	no	yes	yes	yes	yes	yes	no	yes	no	no	yes	no
AutoDC12_FM1063-1	yes	yes	yes	no	yes	yes	no	yes	no	no	yes	no
AutoDC13_US79-1	no	no	yes	no	yes	yes	no	yes	no	no	yes	no
AutoDC14_IH35-3	no	yes	yes	no	yes	no	no	no	no	no	yes	yes
AutoDC15_Spur484-1	no	no	yes	no	no	yes	no	yes	no	no	yes	no
AutoDC16_US77-1	no	yes	no	no	yes	no	no	yes	no	no	no	no
AutoDC17_La_Salle-1	no	yes	yes	no	yes	yes	no	no	no	no	no	no
AutoDC18_IH35-1	no	yes	yes	no	yes	no	no	yes	no	no	yes	no
AutoDC19_IH35-2	no	no	yes	no	yes	no	no	yes	no	no	no	no
AutoDC20_US84-1	no	no	yes	no	no	no	no	no	no	no	no	no

The results show the following:

- Shallow rut depth hydroplaning can occur
    - Reference: 30% of sections
    - Fugro: 60% of sections
    - Waylink-OSU: 95% of sections
- Deep rut depth hydroplaning can occur
    - Reference: 15% of sections
    - Fugro: 80% of sections
    - Waylink-OSU: 60% of sections
- Severe rut depth hydroplaning can occur
    - Reference: 0% of sections
    - Fugro: 80% of sections
    - Waylink-OSU: 20% of sections
- Rut depth failure – hydroplaning can occur
    - Reference: 0% of sections
    - Fugro: 70% of sections
    - Waylink-OSU: 5% of sections

It is noted that the results for Fugro and Waylink-OSU are heavily affected by the significant jumps seen in the cross slope profiles.

5.2.1.2.2. Texture

Several relationships were found in the literature to convert MPD into an estimated texture depth; however, these relationships may vary depending on the direction the texture was measured and type of pavement measured. In this thesis, these relationships found by other research are noted but are not used.

With regards to hydroplaning thresholds, it has been noted that texture depth less than 1.5 mm is not adequate enough to reduce hydroplaning on high speed roadways (Mounce & Bartoskewiz, 1993; Gallaway et al., 1982; Balmer & Gallaway, 1983). Typical texture for pavement design has been noted to be at least 0.5 mm (sometimes higher) (TxDOT, 2011; TxDOT, 2004; Buddhavarapu et al., 2013). Based on these thresholds, the question "*Can hydroplaning occur? (yes or no)*" is asked for each profile. Table 5.6 summarizes if hydroplaning will occur with regards to texture per section. The table also shows if the texture is at least typical for design in Texas.

Table 5.6: Summary if hydroplaning will occur with regards to texture per section.

Section	Hydroplaning could occur? Yes or No (note: these apply to high operating speeds)					
	Texture NOT adequate to reduce hydroplaning? (<1.5 mm)			Texas: Texture NOT typical for design? (<.5 mm)		
	Reference	Fugro	Waylink-OSU	Reference	Fugro	Waylink-OSU
AutoDC1_FM973-1	yes	yes	no	yes	no	no
AutoDC2_FM3177-1	yes	yes	no	yes	yes	no
AutoDC3_FM696-1	yes	yes	no	no	yes	no
AutoDC4_FM696-3	yes	yes	yes	yes	yes	no
AutoDC5_FM696-4	yes	yes	yes	yes	yes	no
AutoDC6_FM696-2	yes	yes	no	no	no	no
AutoDC7_FM696-5	yes	yes	no	no	no	no
AutoDC8_FM619-1	yes	yes	no	no	no	no
AutoDC9_FM112-1	yes	yes	yes	no	no	no
AutoDC10_FM1331-1	yes	yes	no	no	no	no
AutoDC11_FM1331-2	yes	yes	no	no	no	no
AutoDC12_FM1063-1	yes	yes	no	no	no	no
AutoDC13_US79-1	yes	yes	no	no	no	no
AutoDC14_IH35-3	yes	yes	yes	yes	yes	no
AutoDC15_Spur484-1	yes	yes	no	no	no	no
AutoDC16_US77-1	yes	yes	yes	no	yes	no
AutoDC17_La_Salle-1	yes	yes	yes	yes	yes	no
AutoDC18_IH35-1	yes	yes	yes	yes	yes	no
AutoDC19_IH35-2	yes	yes	yes	yes	yes	no
AutoDC20_US84-1	yes	yes	yes	yes	yes	no

The results show the following:

- Low texture depth hydroplaning can occur
    - Reference: 100% of sections
    - Fugro: 100% of sections
    - Waylink-OSU: 45% of sections
- Low texture in general
    - Reference: 45% of sections
    - Fugro: 50% of sections
    - Waylink-OSU: 0% of sections

5.2.1.2.3. Cross slope

It has been noted that cross slope less than 1.5% is not adequate enough to reduce hydroplaning (Glennon, 2006; Gallaway and Rose, 1971; Gallaway, et al., 1979; Mounce & Bartoskewiz, 1993; Gallaway et al., 1982; Balmer & Gallaway, 1983; TxDOT, 2011). The combination of a rut depth greater than 0.24 inches and cross slope less than 2.5% was noted to indicate that pavement maintenance was needed (Balmer & Gallaway, 1983). Based on these thresholds, the question "*Can hydroplaning occur? (yes or no)*" is asked for each profile. Table 5.7 summarizes if hydroplaning will occur with regards to cross slope per section.

Table 5.7: Summary if hydroplaning will occur with regards to cross slope per section.

Section	Hydroplaning could occur? Yes or No (note: these apply to high operating speeds)					
	Cross slope NOT adequate to reduce hydroplaning? (<1.5 %)			Large rut depth & small cross slope = maintenance required? (rut depth>.24in) (cross slope<=2.5%)		
	Reference	Fugro	Waylink-OSU	Reference	Fugro	Waylink-OSU
AutoDC1_FM973-1	yes	yes	yes	no	yes	yes
AutoDC2_FM3177-1	yes	yes	yes	yes	yes	yes
AutoDC3_FM696-1	no	yes	yes	yes	yes	yes
AutoDC4_FM696-3	yes	yes	yes	no	yes	yes
AutoDC5_FM696-4	no	yes	yes	no	yes	yes
AutoDC6_FM696-2	yes	yes	yes	yes	yes	yes
AutoDC7_FM696-5	yes	yes	yes	yes	yes	yes
AutoDC8_FM619-1	no	yes	yes	no	yes	yes
AutoDC9_FM112-1	yes	yes	yes	yes	yes	yes
AutoDC10_FM1331-1	yes	yes	yes	yes	yes	yes
AutoDC11_FM1331-2	yes	yes	yes	yes	yes	yes
AutoDC12_FM1063-1	yes	yes	yes	yes	yes	yes
AutoDC13_US79-1	yes	yes	yes	no	yes	yes
AutoDC14_IH35-3	yes	yes	yes	no	yes	yes
AutoDC15_Spur484-1	no	yes	yes	no	yes	yes
AutoDC16_US77-1	yes	yes	yes	no	yes	no
AutoDC17_La_Salle-1	yes	yes	yes	no	yes	yes
AutoDC18_IH35-1	no	yes	yes	no	yes	yes
AutoDC19_IH35-2	yes	yes	yes	no	yes	yes
AutoDC20_US84-1	yes	yes	yes	no	no	yes

The results show the following:

- Low cross slope hydroplaning can occur
    - Reference: 75% of sections
    - Fugro: 100% of sections
    - Waylink-OSU: 100% of sections
- Maintenance required (large rut depth and small cross slope)
    - Reference: 40% of sections
    - Fugro: 95% of sections
    - Waylink-OSU: 95% of sections

5.2.1.2.4. Speed

Because these thresholds only apply to roadways with high operating speeds, the speed at which hydroplaning could occur was calculated and compared to the actual speed limit of the roadway. The hydroplaning speed was calculated using TxDOT's Hydraulic Design Manual Equation 3 mentioned previously in the literature review (TxDOT, 2011).

The posted speed limit for each section was compared to the calculated value for the speed at which hydroplaning will occur. Table 5.8 summarizes if hydroplaning will be a problem with regards to average speed per section.

Table 5.8: Summary if hydroplaning will be a problem with regards to average speed per section.

		Note: This equation is limited to speeds less than 55 mph		
Section	**Speed limit (mph)**	**Texas: Vehicle speed for hydroplaning (mph)** ***Average***		
		Reference	**Fugro**	**Waylink-OSU**
AutoDC1_FM973-1	60	47	39	49
AutoDC2_FM3177-1	60	44	41	43
AutoDC3_FM696-1	65	48	39	50
AutoDC4_FM696-3	65	47	40	46
AutoDC5_FM696-4	65		42	47
AutoDC6_FM696-2	65	47	39	49
AutoDC7_FM696-5	65	48	39	45
AutoDC8_FM619-1	65	54	40	46
AutoDC9_FM112-1	35	50	39	44
AutoDC10_FM1331-1	65	47	40	52
AutoDC11_FM1331-2	65	50	39	48
AutoDC12_FM1063-1	65	49	39	49
AutoDC13_US79-1	70		39	51
AutoDC14_IH35-3	40	45	40	39
AutoDC15_Spur484-1	60		39	48
AutoDC16_US77-1	40		41	49
AutoDC17_La_Salle-1	40	46	43	45
AutoDC18_IH35-1	50		41	50
AutoDC19_IH35-2	50		41	48
AutoDC20_US84-1	50		47	47

The results show the following:

- Hydroplaning can occur within speed limit (occurs at speed under speed limit or within 5 mph above speed limit)
    - Reference: 85% of sections (based on 13 sections which hydroplaning can occur)
    - Fugro: 100% of sections (based on 20 sections which hydroplaning can occur)
    - Waylink-OSU: 85% of sections (based on 20 sections which hydroplaning can occur)

It is noted that the results for Fugro and Waylink-OSU are affected by the significant jumps seen in the cross slope profiles, which the cross slope profiles are used to estimate the water depth, and the water depth is a parameter used in the equation to calculate the hydroplaning speed.

Table 5.9 shows the overall results when the reference, Fugro, and Waylink-OSU are compared with each other in regards to the hydroplaning analysis. The vendors are compared as to how many of their answers match the answers of the reference. If the cross slope values are too far from the ground truth, the results will be too different from the manual (reference) procedure, and hence, wrong decisions will be made for pavement management.

Table 5.9: Overall comparison in regards to hydroplaning analysis.

Hydroplaning could occur? Yes or No							
Number of sections/subsections same as reference					**TOTAL**		
WATER DEPTH							
Vendor	Texas: Shallow rut depth? *Possible Hydroplaning for smooth pavements, bald tires* (.25-.49 in)	Texas: Deep rut depth? *Possible hydroplaning* (.5-.99 in)	Texas: Severe rut depth? *Hydroplaning* (1-1.99 in)	Texas: Rut depth = Failure? *Hydroplaning* (>=2 in)	Vendor	Total number same as reference	% Total same as reference
Fugro	206	194	163	192	Fugro	***1361***	***63.01***
Waylink -OSU	163	204	232	231			
TEXTURE							
	Texture NOT adequate to reduce hydroplaning?: (<1.5 mm)		Texas: Texture NOT typical for design? (<.5 mm)				
Fugro	216		186				
Waylink -OSU	68		168				
CROSS SLOPE							
	Cross slope NOT adequate to reduce hydroplaning?: (<1.5 %)		Large rut depth & small cross slope = maintenance required? (rut depth>.24in) (cross slope<=2.5%)		Waylink -OSU	***1273***	***58.94***
Fugro	138		65				
Waylink -OSU	86		117				
SPEED							
	Texas: Vehicle speed for hydroplaning (mph)						
Fugro	1						
Waylink -OSU	4						

In total, it was found that 63% of the Fugro data tested for hydroplaning potential agreed with the reference, and 59% of the Waylink-OSU data agreed with the reference. Again, it is noted that the Fugro and Waylink-OSU results are affected by the jumps seen in the cross slope profiles, giving unrealistic values.

5.2.2. Drainage Path

The cross slope profiles given from the automated data collection could also be used to estimate potential drainage path lengths, which could lead to surface runoff large enough to cause hydroplaning. The drainage path length was calculated using Equation 1 noted previously in the literature review (Mraz & Nazef, 2007; Glennon, 2006). Because data on the longitudinal grade was not provided, the sensitivity of the drainage path length was calculated with varying longitudinal grades.

Appendix G shows the results for drainage path lengths using reference data. The results show that in general, as the cross slope increases (becomes more positive or more flat in the transverse direction), the drainage path length increases. As the longitudinal grade increases (becomes more steep in longitudinal direction), the drainage path length increases. Because the road can extend longitudinally to a far distance, a steeper longitudinal grade encourages the water to travel further. The cross-slope extends only a short distance transversely, so a steeper cross slope will only encourage the water to leave the pavement faster. A flatter cross-slope will allow the water to travel farther in other directions before leaving the pavement transversely. Pavement widths ranged from 10 feet to 12 feet.

RESULTS AND ANALYSIS

Chapter 6: Distress Identification – PMIS

6.1. GENERAL RESULTS

For the distress measurements, TxDOT is compared to the reference, which was measured following the TxDOT Pavement Management Information System (PMIS) Rater's Manual (TxDOT, 2009). The PMIS distress identification for the reference measurements was conducted manually by having experienced raters walk through and identify the extent and severity of distresses for each section. TxDOT collected data at highway speeds and reported a summary of the distress statistics for each section. Tables 6.1, 6.2, and 6.3 show the summary of the reference (labeled as PMIS) and TxDOT distress data for flexible pavement sections, JCP sections, and CRCP sections respectively. Bar charts of the PMIS compared with TxDOT results are shown in Appendix H.

For the flexible pavement sections (labeled "flexible pavement" in Appendix H bar charts), possible distresses reported were:

- Alligator cracking (%of total area rated)
- Longitudinal cracking (ft)
- Transverse cracking (count)
- Patching (% of total area rated)

- Raveling (rating code: 0 = *none* = 0% area, 1 = *low* = 1%-10% area, 2 = *medium* = 11%-50% area, 3 = *high* = > 50% area)
- Failures (count)

For the JCP sections (labeled “JCP” in Appendix H bar charts), possible distresses reported were:

- Alligator cracking (%of total area rated)
- Longitudinal cracking (ft)
- Transverse cracking (count)
- Failed joints & cracks (count)
- Failures (count)
- Apparent joint spacing (ft)

For the CRCP sections (labeled “CRCP” in Appendix H bar charts), possible distresses reported were:

- Alligator cracking (%of total area rated)
- Longitudinal cracking (ft)
- Transverse cracking (count)
- Patching (%of total area rated)
- Block (% of total area rated)
- Spalled cracks (count)

- Concrete patches (count)
- Average crack spacing (ft)
- Punchouts (count)

Some observations are noted:

- TxDOT only reported three different types of distresses for all sections: alligator cracking, longitudinal cracking, and transverse cracking. This may be due to the capabilities of the current set-up of the equipment. Enhancements are in the process of being made so that the equipment can read other distresses. These same three distress types were reported for concrete pavements as well because of this issue. The alligator cracking reading may not be calibrated in the current set-up, as all the readings were 0 for that particular distress, even though alligator cracking was recorded in the reference sections.
- Sometimes values for transverse or longitudinal cracking are close between PMIS and TxDOT data. Many times, the transverse or longitudinal cracking was higher for TxDOT readings, but this may be because TxDOT reported cracking for both sealed and non-sealed cracks. PMIS data were reported as a total value (without sealed and non-sealed cracks distinguished); however, PMIS may have counted less sealed cracks than TxDOT for some sections. In these cases, if only the TxDOT non-sealed cracks are counted, the TxDOT value will be closer to the PMIS value.

- The fact that TxDOT readings consider only the transverse and longitudinal cracking readings take away from the other distress categories the readings could potentially have been in. For example, in JCP, joints may be reported as transverse cracks in the TxDOT data.

Table 6.1: Summary of PMIS vs. TxDOT distress data for flexible pavement sections

Ratings – Flexible Pavement																
	Alligator (% alligator) cracking area		**Longitudinal (feet per 100 ft. station)**				**Transverse (# per 100 ft. station)**				**Patching (% patching area)**		**Raveling (raveling rating code)**		**Failures (# for entire section)**	
Section	PMIS	TXDOT	PMIS	TXDOT (non-sealed)	TXDOT (sealed)	TXDOT (non-sealed + sealed)	PMIS	TXDOT (non-sealed)	TXDOT (sealed)	TXDOT (non-sealed + sealed)	PMIS	TXDOT	PMIS	TXDOT	PMIS	TXDOT
AutoDC1_FM973-1	**1**	**0**	**205**	66	157	**223**	**5**	34	5	**39**	**0**	**0**	**0**	**0**	**0**	**0**
AutoDC2_FM3177-1	**20**	**0**	**48**	36	201	**237**	**2**	44	3	**47**	**57**	**0**	**0**	**0**	**0**	**0**
AutoDC3_FM696-1	**39**	**0**	**79**	20	125	**145**	**0**	4	1	**5**	**0**	**0**	**0**	**0**	**0**	**0**
AutoDC4_FM696-3	**17**	**0**	**37**	3	31	**34**	**0**	1	0	**1**	**0**	**0**	**0**	**0**	**0**	**0**
AutoDC5_FM696-4	**7**	**0**	**35**	8	82	**90**	**0**	1	0	**1**	**0**	**0**	**0**	**0**	**0**	**0**
AutoDC6_FM696-2	**22**	**0**	**82**	35	171	**207**	**0**	7	3	**10**	**0**	**0**	**1**	**0**	**0**	**0**
AutoDC7_FM696-5	**0**	**0**	**2**	8	23	**30**	**0**	5	2	**7**	**42**	**0**	**0**	**0**	**0**	**0**
AutoDC8_FM619-1	**63**	**0**	**42**	50	241	**291**	**0**	10	5	**15**	**67**	**0**	**1**	**0**	**0**	**0**
AutoDC9_FM112-1	**69**	**0**	**95**	106	363	**468**	**0**	5	9	**14**	**5**	**0**	**0**	**0**	**0**	**0**
AutoDC10_FM1331-1	**15**	**0**	**86**	49	130	**179**	**0**	3	2	**5**	**0**	**0**	**0**	**0**	**4**	**0**
AutoDC11_FM1331-2	**15**	**0**	**126**	33	121	**155**	**0**	5	5	**10**	**0**	**0**	**0**	**0**	**0**	**0**
AutoDC12_FM1063-1	**7**	**0**	**57**	13	60	**73**	**0**	7	3	**10**	**47**	**0**	**0**	**0**	**0**	**0**
AutoDC13_US79-1	**0**	**0**	**4**	13	10	**24**	**0**	8	3	**11**	**0**	**0**	**0**	**0**	**0**	**0**
AutoDC15_Spur484-1	**0**	**0**	**55**	2	28	**29**	**1**	1	0	**1**	**0**	**0**	**0**	**0**	**0**	**0**
AutoDC17_La_Salle-1	**0**	**0**	**161**	10	92	**102**	**7**	6	5	**11**	**0**	**0**	**0**	**0**	**0**	**0**

Table 6.2: Summary of PMIS vs. TxDOT distress data for JCP sections

Ratings - JCP																
	Alligator (% alligator) cracking area		Longitudinal (feet per 100 ft. station)				Transverse (# per 100 ft. station)				Failed Joints & Cracks (# for entire section)		Failures (# for entire section)		Apparent Joint Spacing (feet, average from two 200' areas)	
Section	PMIS	TXDOT	PMIS	TXDOT (non-sealed)	TXDOT (sealed)	TXDOT (non-sealed + sealed)	PMIS	TXDOT (non-sealed)	TXDOT (sealed)	TXDOT (non-sealed + sealed)	PMIS	TXDOT	PMIS	TXDOT	PMIS	TXDOT
AutoDC16_US77-1	**0**	**0**	**0**	49	54	**103**	**0**	11	7	**18**	**10**	**0**	**4**	**0**	**15**	**0**
AutoDC20_US84-1	**0**	**0**	**0**	22	15	**37**	**0**	3	1	**5**	**9**	**0**	**0**	**0**	**60**	**0**

Table 6.3: Summary of PMIS vs. TxDOT distress data for CRCP sections

Ratings - CRCP																				
	Alligator (% alligator) cracking area		Longitudinal (feet per 100 ft. station)				Transverse (# per 100 ft. station)				Patching (% patching area)		Block (% of lane's total surface area)		Spalled Cracks (# for entire section)		Concrete Patches (# for entire section)		Average Crack Spacing (feet, average from two 200' areas)		Punch-outs (# for entire section)	
Section	PMIS	TXDOT	PMIS	TXDOT (non-sealed)	TXDOT (sealed)	TXDOT (non-sealed + sealed)	PMIS	TXDOT (non-sealed)	TXDOT (sealed)	TXDOT (non-sealed + sealed)	PMIS	TXDOT	PMIS	TXDOT	PMIS	TXDOT	PMIS	TXDOT	PMIS	TXDOT	PMIS	TXDOT
AutoDC14_IH35-3	**0**	**0**	**0**	3	15	**19**	**0**	2	0	**2**	**0**	**0**	**0**	**0**	**1**	**0**	**4**	**0**	**5**	**0**	**0**	**0**
AutoDC18_IH35-1	**28**	**0**	**127**	34	31	**65**	**3**	3	1	**4**	**2**	**0**	**3**	**0**	**2**	**0**	**7**	**0**	**3**	**0**	**1**	**0**
AutoDC19_IH35-2	**0**	**0**	**0**	86	51	**137**	**0**	15	9	**23**	**0**	**0**	**0**	**0**	**4**	**0**	**12**	**0**	**6**	**0**	**2**	**0**

RESULTS AND ANALYSIS

Chapter 7: Other Results

The remaining results of this project were analyzed separately by the research team and are fully documented in the project technical report (Serigos et al., 2014). This chapter presents a summary of the remaining results of the project, which include distress identification measurements from Dynatest, Fugro, and Waylink-OSU, and crack map images.

7.1. DISTRESS IDENTIFICATION – LTPP

For the distress measurements of the participating vendors, Dynatest, Fugro, and Waylink-OSU were compared to the reference, which was measured following the Long-Term Pavement Performance Program (LTPP) Protocol (Miller & Bellinger, 2003). This protocol is different from TxDOT measurements, which followed the PMIS protocol outlined in the previous chapter.

The LTPP distress identification was conducted manually for the reference reading by having experienced raters walk through the sections and identify the extent and severity of distresses every 50 ft. Each vendor collected data at highway speeds and reported a summary of the distress statistics for the eleven 50-ft. subsections per section. Distress statistics were reported for the three pavement types: flexible pavements, jointed concrete pavements (JCP), and continuously reinforced concrete pavements (CRCP).

7.1.1. Asphalt Concrete Pavements

Figure 7.1, adapted from (Serigos et al., 2014), shows the LTPP distress identification flexible pavement results for Section AutoDC8_FM619-1.

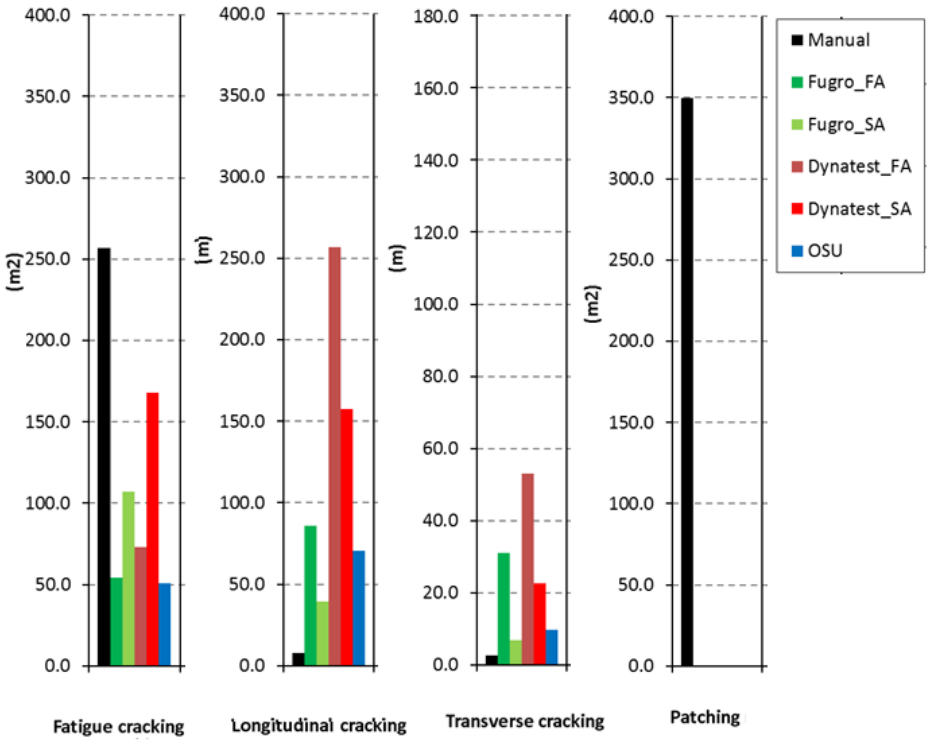

Figure 7.1: LTPP distress identification for Section AutoDC8_FM619-1. Adapted from (Serigos et al., 2014)

The following observations were noted regarding the flexible pavement sections:

- Fatigue cracking:
    - Both Dynatest and Fugro tended to increase the reported fatigue cracking area after manual intervention. This could be related to the hardware that both vendors used, which was developed by the same manufacturer (both used INO LCMS sensors).

- Waylink-OSU typically reported lower values for fatigue cracking than the other vendors.

- Longitudinal cracking:
  - The reference reported significantly lower values than the vendors for most of the flexible pavement test sections.

- Transverse Cracking:
    - Fugro after manual intervention and Waylink-OSU reported similar or values close to the reference.

- Edge cracking:
  - Fugro after manual intervention reported values similar or close to the reference for several sections
  - Dynatest reported values similar or close to the reference for one section. Waylink-OSU did not report edge cracking for any section.

- Patching:
  - Waylink-OSU and Fugro after manual intervention always reported less number and area of patches than the reference.
  - Dynatest did not report the number of patches and Fugro only reported them after manual intervention.

7.1.2. Jointed Concrete Pavements

Table 7.1 shows the LTPP distress identification results for the JCP sections, AutoDC16_US77-1 (S16) and AutoDC20_US84-1 (S17). The following observations were noted:

- Longitudinal cracking:
    - After manual intervention, the reported longitudinal cracking was reduced for Dynatest and Fugro. This could suggest that manual intervention might also introduce errors to the crack maps.
    - Waylink-OSU values were significantly larger than the rest.
- Transverse Cracking:
    - No clear pattern was observed among the different vendors and the reference. There was an inconsistency in some of the distress counts reported by Fugro after manual intervention.

Table 7.1: Comparison of LTPP Distresses on JCP sections (Serigos et al., 2014)

		Longitudinal_m	Transverse_#	Transverse_m	Spalling_of_Long_Joints_m	Spalling_of_Trans_Joints_#	Spalling_of_Trans_Joints_m	Patching_#	Patching_m2	Map_Cracking__
S16	**Manual**	**22.5**	**0.0**	**0.0**	**23.5**	**21.0**	**33.4**	**13.0**	**20.0**	**0.0**
	Fugro_fully_autom	25.6	25.0	16.3	0.0	0.0	0.0	0.0	0.0	0.0
	Fugro_semi_autom	21.1	0.0	12.0	7.2	19.0	66.3	20.0	31.9	2.0
	Dynatest_fully_autom	54.9	5.0	1.3	0.0	0.0	0.0	0.0	30.2	0.0
	Dynatest_semi_autom	47.5	0.0	0.0	15.8	0.0	46.7	0.0	30.1	0.0
	OSU	992.5	4.0	15.3	10.0	29.0	15.8	9.0	10.1	0.0
S17	**Manual**	**1.3**	**28.0**	**94.2**	**0.0**	**9.0**	**18.5**	**0.0**	**0.0**	**12.0**
	Fugro_fully_autom	44.1	52.0	43.2	0.0	0.0	0.0	0.0	0.0	0.0
	Fugro_semi_autom	5.6	0.0	45.5	154.9	9.0	33.9	0.0	0.0	0.0
	Dynatest_fully_autom	93.8	22.0	32.5	0.0	0.0	0.0	0.0	0.0	0.0
	Dynatest_semi_autom	0.7	26.0	65.1	106.4	0.0	25.7	0.0	0.0	0.0
	OSU	157.3	46.0	45.7	3.6	8.0	7.8	0.0	0.0	0.0

7.1.3. Continuously Reinforced Concrete Pavements

Table 7.2 shows the LTPP distress identification results for the CRCP sections, AutoDC18_IH35-1 (S18), AutoDC19_IH35-2 (S19), and AutoDC14_IH35-3 (S20). The following observations were noted:

- Longitudinal cracking:
    - No clear pattern was observed among the different vendors and the reference.

- After manual intervention, the number and extent of transverse cracks significantly increased for Fugro and Dynatest.

Table 7.2: Comparison of LTPP Distresses on CRCP sections (Serigos et al., 2014)

		Longitudinal_m	Transverse_#	Transverse_m	Patching_#	Patching_m2	Punchouts_#	Spalling_of_Long_Joints_m	Longitudinal_Joint_Seal_Damage__	Longitudinal_Joint_Seal_Damage__m
S18	**Manual**	**90.7**	**90.0**	**304.7**	**8.0**	**3.2**	**0.0**	**0.0**	**5.0**	**74.5**
	Fugro_fully_ autom	149.3	38.0	21.2	0.0	0.0	0.0	0.0	0.0	0.0
	Fugro_semi_ autom	63.6	55.0	155.0	12.0	334.4	4.0	63.2	1.0	36.2
	Dynatest_fully_ autom	183.6	77.0	87.3	16.0	12.1	0.0	0.0	0.0	0.0
	Dynatest_semi_ autom	55.2	81.0	138.2	0.0	5.2	8.0	57.7	0.0	0.0
	OSU	103.7	67.0	114.1	8.0	2.5	22.0	60.4	0.0	0.0
S19	**Manual**	**148.2**	**148.0**	**532.0**	**17.0**	**45.8**	**0.0**	**0.5**	**11.0**	**167.8**
	Fugro_fully_ autom	64.6	50.0	28.2	0.0	0.0	0.0	0.0	0.0	0.0
	Fugro_semi_ autom	80.8	151.0	459.0	20.0	49.2	7.0	7.0	0.0	0.0
	Dynatest_fully_ autom	74.5	97.0	188.7	21.0	14.7	0.0	0.0	0.0	0.0
	Dynatest_semi_ autom	59.0	158.0	338.1	0.0	20.0	11.0	68.6	0.0	0.0
	OSU	66.6	124.0	153.7	9.0	2.5	1.0	4.6	0.0	0.0
S20	**Manual**	**91.4**	**126.0**	**457.1**	**4.0**	**1.0**	**0.0**	**0.0**	**0.0**	**0.0**
	Fugro_fully_ autom	27.2	11.0	10.4	0.0	0.0	0.0	0.0	0.0	0.0
	Fugro_semi_ autom	53.6	127.0	444.6	0.0	1.3	0.0	0.0	0.0	0.0
	Dynatest_fully_ autom	37.0	142.0	347.6	3.0	1.2	0.0	0.0	0.0	0.0
	Dynatest_semi_ autom	81.3	172.0	452.5	0.0	1.6	11.0	0.0	0.0	0.0
	OSU	44.7	274.0	296.4	0.0	0.0	14.0	5.1	0.0	0.0

7.2. CRACK MAPS

Each participant produced images that outlined a map of the cracks on the pavement (crack maps). A qualitative comparison was performed for these crack map images against the reference. Detection of cracks and their respective crack widths were done manually for the reference measurements and collected at highway speeds by the vendors. The crack maps were collected at three 50’ subsections per section on ten test sections (30 50-ft. crack maps in total). The ten test sections selected for the collection of crack maps included flexible pavement, JCP and CRCP.

As an example, Figure 7.2, adapted from (Serigos et al., 2014), shows crack maps reported for Section AutoDC2_FM3177-1, station 150 ft. to 200 ft., which is a flexible pavement. The color convention for the reference crack maps are: the red lines represent the crack less than 3 mm wide, the blue lines represent cracks 3 mm – 6 mm wide, and the green lines represent cracks greater than 6 mm wide. The crack maps manually drawn in the field by LTPP raters were also included to the comparison. In developing the crack maps for the reference, the research team only identified cracks and crack severity, whereas the vendors and manual LTPP rater were identifying all types of distresses.

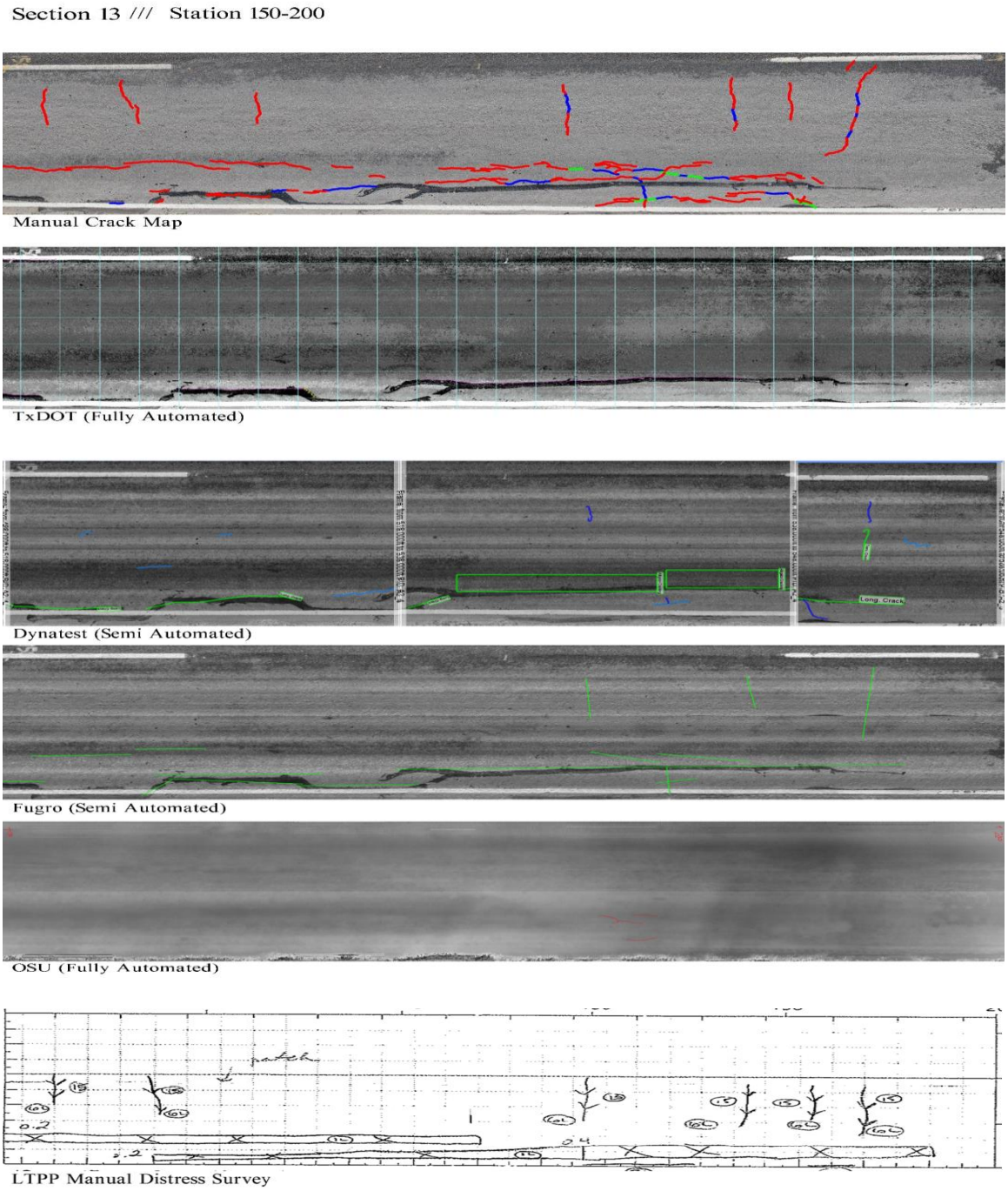

Figure 7.2: Crack maps for Section AutoDC2_FM3177-1 (Serigos et al., 2014)

The following observations were noted regarding the crack maps developed:

- LTPP Manual Distress Survey:
    - There is an overall good match between the cracks reported by the LTPP Manual raters and the reference; however, there are instances found that even trained raters have missed identification of distresses. These differences might be due to:
        - The number of people and time spent searching for distresses
        - Lighting conditions
        - Interpreting phantom cracks as actual cracks or vice-versa
        - Different criteria between LTPP protocol and the research team's interpretation of distress extent and severity
- Dynatest:
    - Significant improvement after manual intervention
    - Many of the cracks less than 3 mm wide did not get identified
    - Sealed cracks were identified as shown in the reference before manual intervention
    - Some false positive cracks were identified, which might actually be indentations in the pavement surface caused by overweight vehicles. Other false positives include a vegetation area being classified as sealed and joints being identified as cracks
    - Some failure cracks were reported as sealed cracks but were corrected after manual intervention.

- Fugro:
    - Crack maps improved after manual intervention. False positives were removed and missed cracks and patches were identified
    - Much of the cracks less than 3 mm wide (fine cracks) did not get identified
    - Sealed cracks were not identified before manual intervention, but many of them were reported as unsealed cracks after manual intervention.
    - Cracks on PFC surface section were identified similar to the reference, but few false positives were introduced after manual intervention.
    - Transverse and longitudinal joints were falsely identified as cracks before manual intervention but corrected after manual intervention

- Waylink-OSU:
    - There were very few false positives observed in the PFC section, but a large number of cracks did not get identified in some sections
    - Crack widths were identified similar to reference on asphalt sections, much of the cracks less than 3mm did not get identified in rigid pavements
    - Transverse and longitudinal joints on rigid pavements were not misidentified as cracks. Cracks nearby the joint were identified similar to the reference.
    - There was no classification of sealed cracks.

- TxDOT:
    - There was no categorization of crack widths or other types of distresses.
    - A large number of unsealed cracks were not identified. Sealed cracks were identified better than unsealed cracks.
    - A large number of failure longitudinal cracks were either not identified or falsely identified as sealed cracks.
    - False positives were observed on drop-off and rumble stripes. Very few false positives were observed on PFC surface
    - A large number of cracks were not identified on rigid pavements. Transverse and longitudinal joints were falsely identified as cracks

Chapter 8: Conclusions and Recommendations

8.1. SUMMARY FINDINGS

8.1.1. Texture

The texture was reported as the Mean Profile Depth (MPD) in mm, every 50 feet for each wheel path. In most sections, Dynatest and Fugro were close to the reference measurements, whereas Waylink-OSU and TxDOT's reported average reading were usually higher in magnitude. Waylink-OSU followed a similar trend in shape as the reference.

8.1.2. Cross-Slope

- General Results:

  The cross slope was reported every 50 feet, and values were compared with units in percent. In most sections, Dynatest follows very close to the reference in the graph-line shape and is usually close in magnitude. Sometimes Fugro follows a similar shape to the reference, and sometimes Waylink-OSU follows a similar shape to the reference, though Waylink-OSU is often higher or lower in magnitude. TxDOT's average cross slope readings were often close to the reference and the other vendors, though readings with the pp69 algorithm were often farther from the reference than the other two algorithms.

- Hydroplaning Analysis:

  As an additional analysis, the hydroplaning potential was determined from given texture and transverse cross slope profiles from two vendors (Fugro and Waylink-OSU). The results were determined for each profile if hydroplaning will occur

given the maximum water depth (calculated from the transverse cross slope profile), texture, cross slope, or the speed limit on the section. It was found that 63% of the Fugro data tested for hydroplaning potential agreed with the reference, and 59% of the Waylink-OSU data agreed with the reference. It is noted that the Fugro and Waylink-OSU results were affected by the significant jumps seen in the cross slope profiles, giving unrealistic values. This could be an issue with the equipment.

8.1.3. Distress Identification - PMIS

TxDOT distress readings were compared with the reference, which used the TxDOT Pavement Management Information System (PMIS) Rater's Manual. Only longitudinal cracking and transverse cracking could be reported using TxDOT's current set-up, whether the section was flexible pavement, JPCP or CRCP. In many sections where TxDOT values were significantly higher than the reference, values became closer after TxDOT's sealed crack counts were removed, counting only non-sealed cracks.

8.1.4. Other Results

The remaining results of this project include distress identification with the other vendors and crack maps. The vendors, Dynatest, Fugro, and Waylink-OSU, distress readings were compared with the reference, which used the Long-Term Pavement Performance Program (LTPP) protocol. Crack map images were developed manually and used as reference, collected at highway speeds from the vendors, and also developed manually by LTPP raters. None of the vendors perfectly matched the reference in identifying distresses both quantitatively and qualitatively on the crack maps. The vendors reported

results before and after manual intervention. Oftentimes, values reported after manual intervention showed significant improvement in identifying distresses similar to the reference. Sometimes manual intervention can introduce errors. In the crack maps, sometimes distresses were overlooked or misinterpreted by LTPP raters.

8.2. RECOMMENDATIONS

8.2.1. Texture

For texture measurements, Dynatest and Fugro provided results close to the reference in magnitude with minor errors. This was not the case for Waylink-OSU and TxDOT, who should update or calibrate their algorithms to match the reference measurements. Note that TxDOT texture was evaluated with average values per entire section, and values reported every 50 feet would have led to a more precise comparison.

8.2.2. Cross Slope

For cross slope measurements, Dynatest provided results closest to the reference in graph-line shape and magnitude, though there were some sections where the magnitude was slightly off. Fugro can deliver results fairly close to the reference in magnitude sometimes at certain portions of the graph-line, though the overall graph-line shape is not always close to the reference. Waylink-OSU can deliver sometimes in a similar graph-line shape to the reference, though often the magnitude is higher or lower than the reference. Out of the TxDOT algorithms used, pp69 algorithm is not the algorithm that should be used if one wants to be closest to the reference; however, TxDOT cross slope

was evaluated with average values for the entire section, so a precise comparison could not be done. All vendors had situations where cross slope was reported in reverse direction from the reference. All of these issues should be corrected before any of the systems can be used to measure cross slope.

It should be noted that hydroplaning cannot be prevented completely from pavement design alone. High intensity rain storms and flash floods cannot be avoided and often the best solution is to require lower speeds. It could be recommended to lower the speed limit for the sections that were found to induce hydroplaning at speeds s significantly lower than the current posted speed limit.

8.2.3. Distress Identification - PMIS

TxDOT still needs to update their automated system to include more distresses. The difference between the number of sealed cracks and the number of non-sealed cracks should be investigated and compared against the reference. In particular, the number of sealed cracks reported by TxDOT often cause the entire crack count to be significantly higher than the reference. The reason for this should be determined in order to correct the problem.

8.2.4. Other Results

All vendors were able to identify distresses similar to the reference to some extent; however, there is still a significant amount of manual intervention needed before the automated data can accurately match the manual reference data. This should be considered when selecting and integrating any automated technology into a pavement management system.

8.3. IMPLICATIONS

Using automated data collection technologies has many advantages. When compared to the traditional, manual survey method, automated technologies should be objective, repeatable, consistent, and safer. Automated technologies can be used for network level data collection. The basic data collection can be used to update inventory in pavement systems. These data can be further used to analyze the safety of roadways. Given the cross slope, longitudinal grade, and rutting measured with automated equipment, surface drainage paths can be computed and areas can be identified that are prone to surface runoff or hydroplaning. If more cross slope profiles were collected, the sequence of profiles could be connected (interpolated) longitudinally, and the areas of the ponded water could be connected in three dimensions to provide the total volume of ponded water. Data from automated technologies can also be used to identify hazardous areas when friction is low (high curvature and lack of cross slope increase side friction demand), but also keep friction low enough to reduce ride vibration and limit truck roll.

Appendix A. Texture Graphs

Note: Images of pavement sections Auto DC 5, 6, 8, 9, 10, 14, 15, 16, 17, and 18 are from Google Maps.

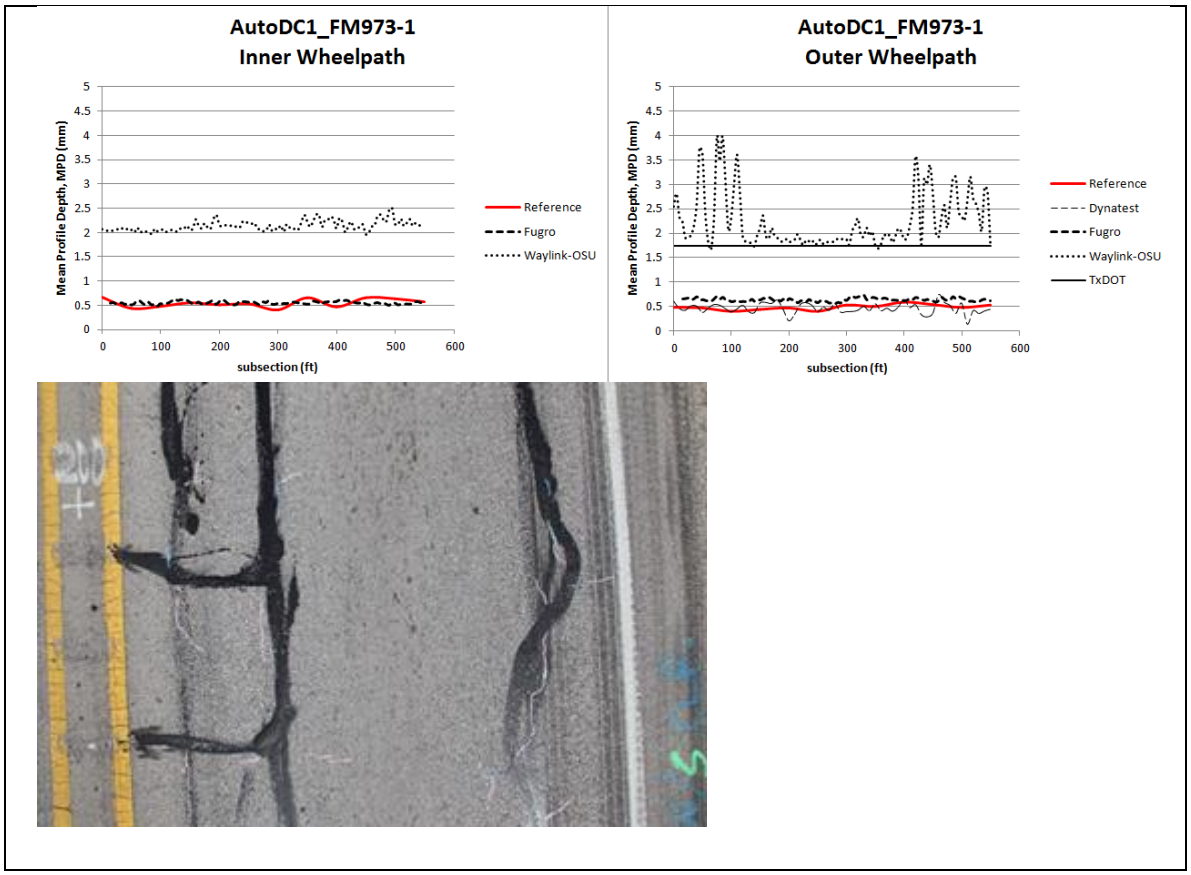

Figure A1: Inner and outer wheelpath texture graphs for AutoDC1_FM973-1 with image close-up of the pavement section

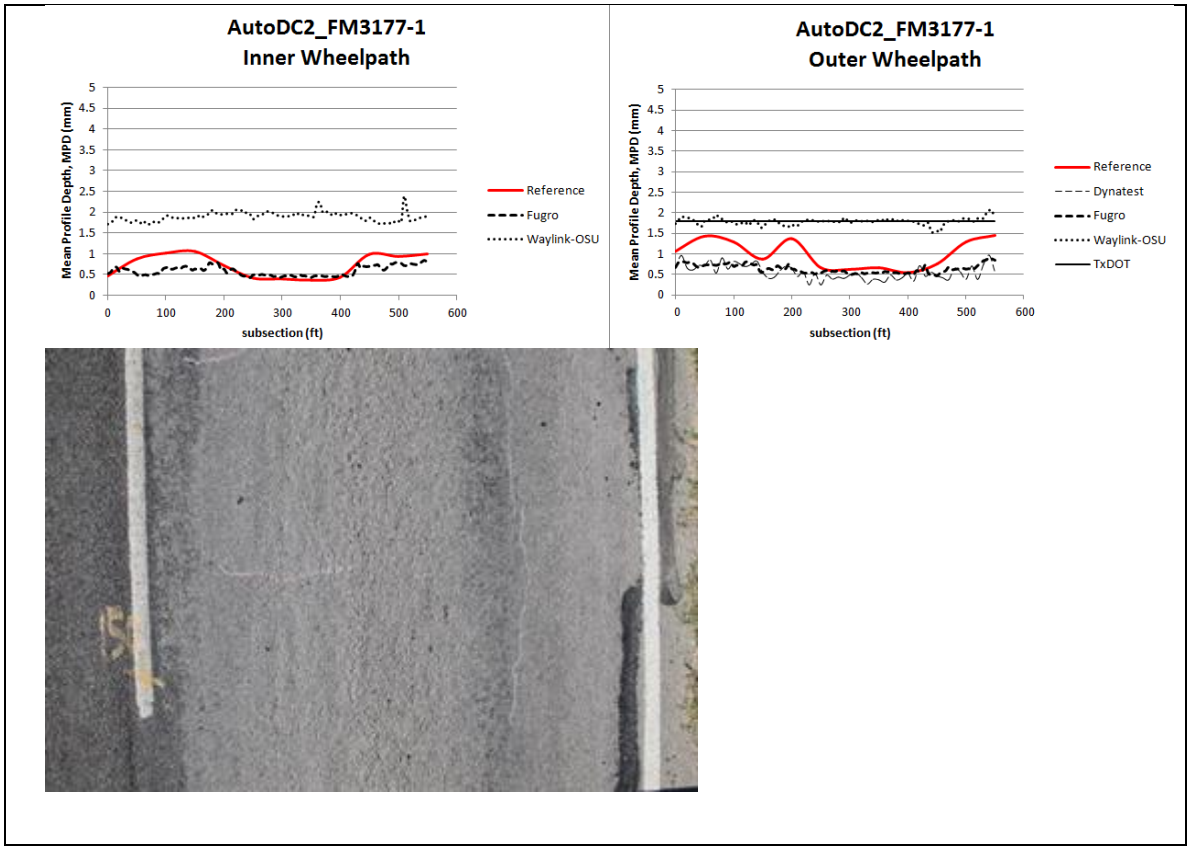

Figure A2: Inner and outer wheelpath texture graphs for AutoDC2_FM3177-1 with image close-up of the pavement section

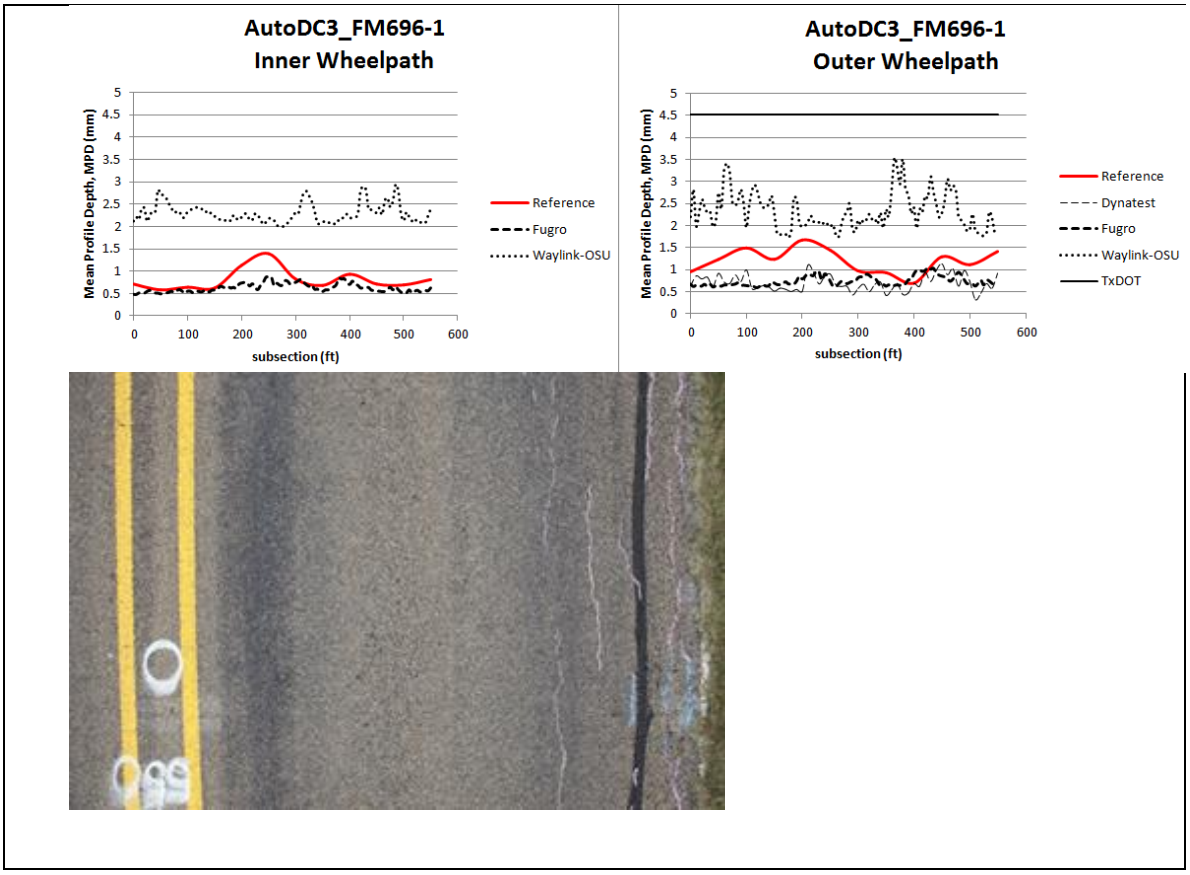

Figure A3: Inner and outer wheelpath texture graphs for AutoDC3_FM696-1 with image close-up of the pavement section

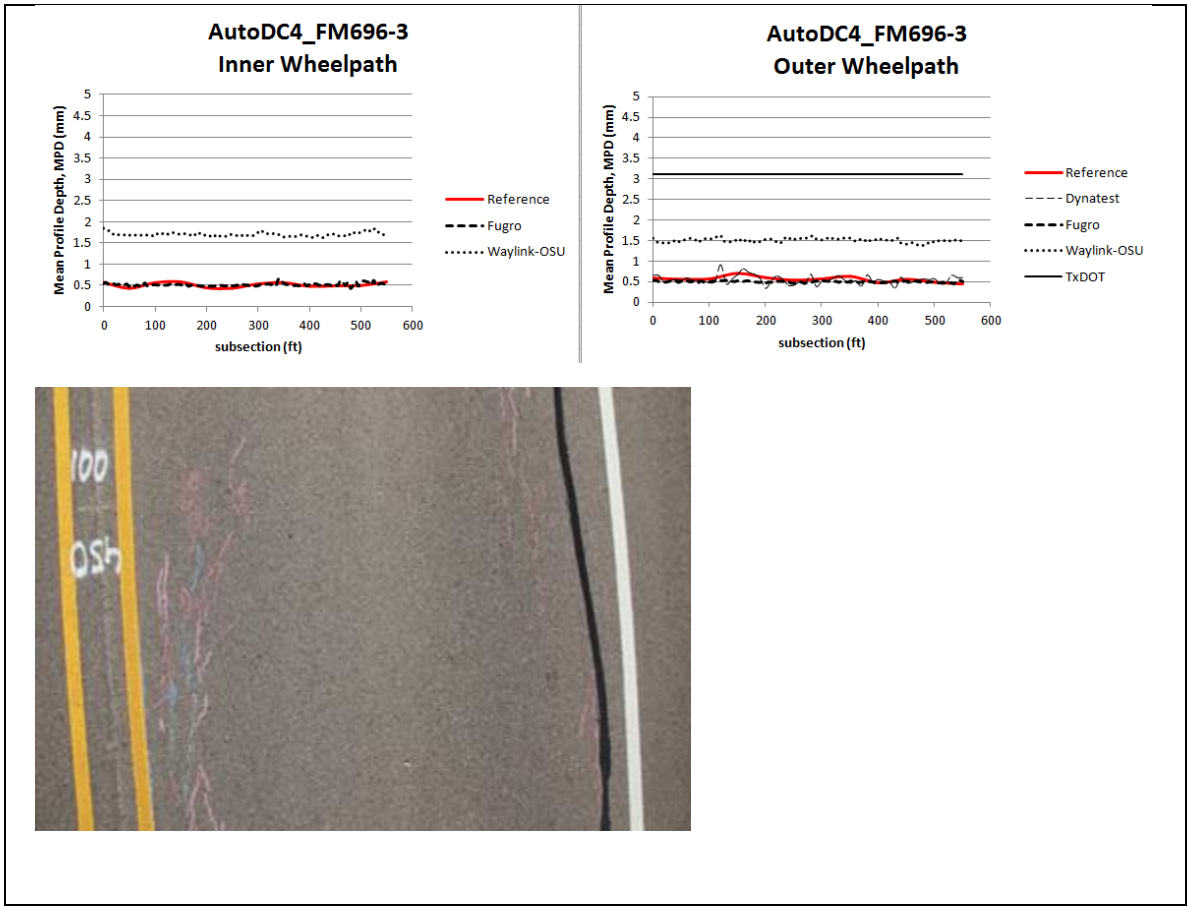

Figure A4: Inner and outer wheelpath texture graphs for AutoDC4_FM696-3 with image close-up of the pavement section

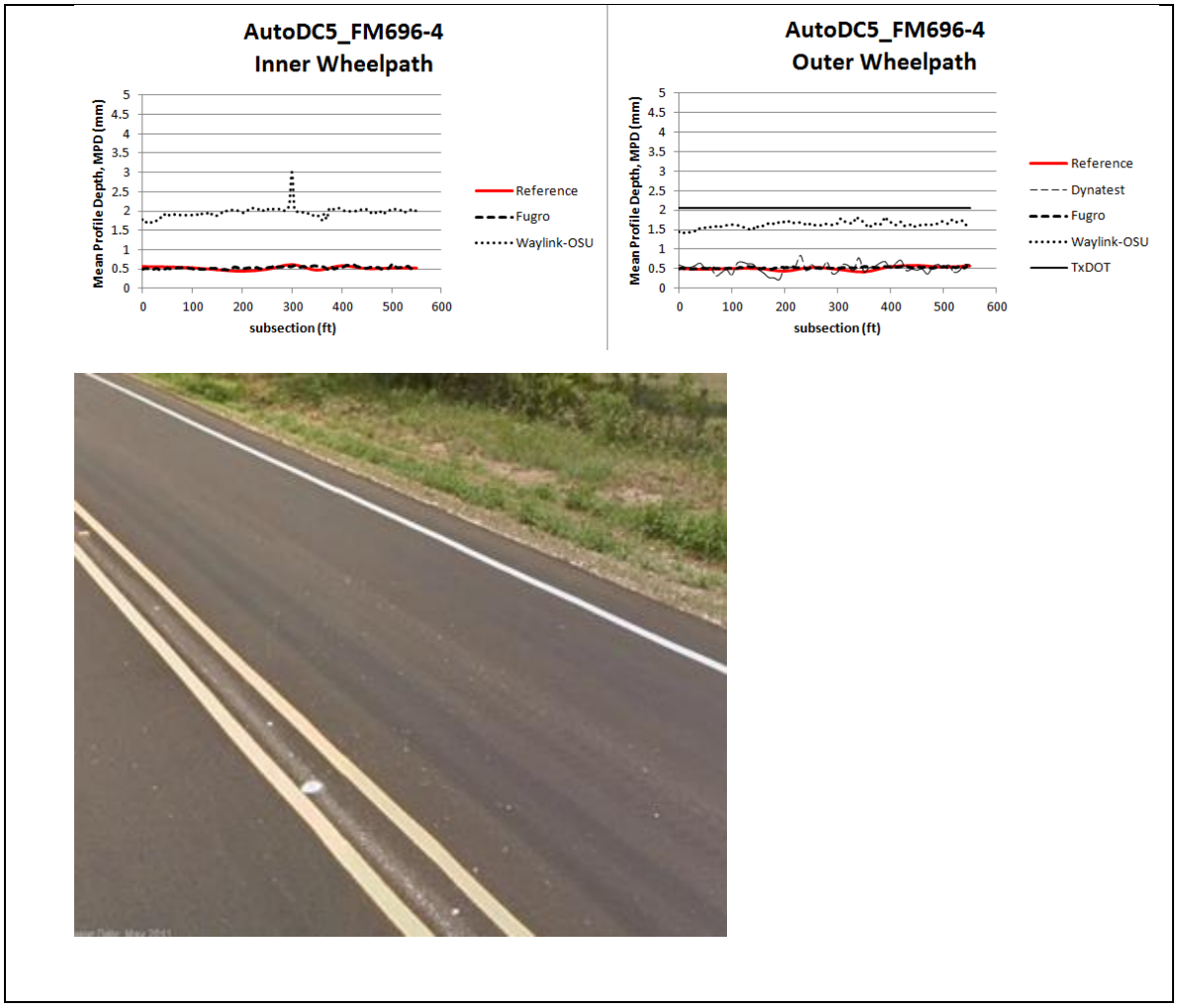

Figure A5: Inner and outer wheelpath texture graphs for AutoDC5_FM696-4 with image close-up of the pavement section

Figure A6: Inner and outer wheelpath texture graphs for AutoDC6_FM696-2 with image close-up of the pavement section

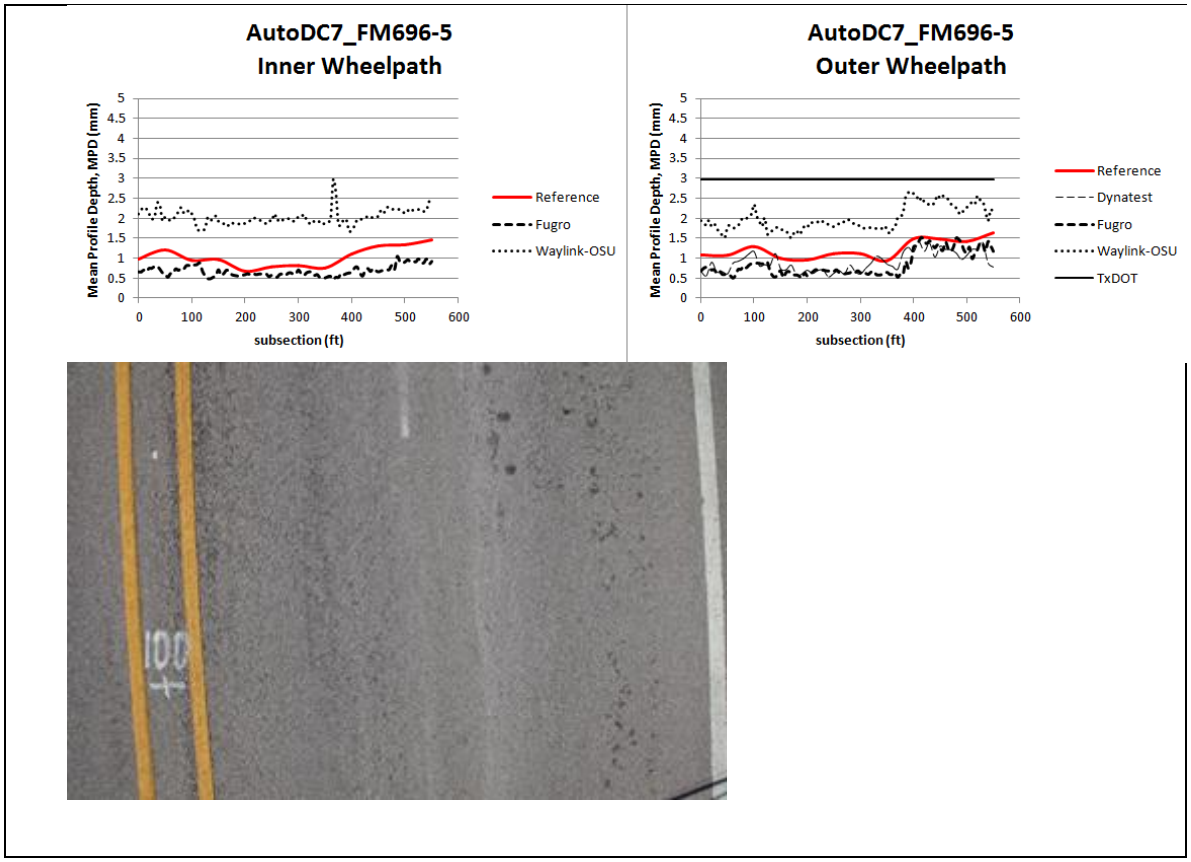

Figure A7: Inner and outer wheelpath texture graphs for AutoDC7_FM696-5 with image close-up of the pavement section

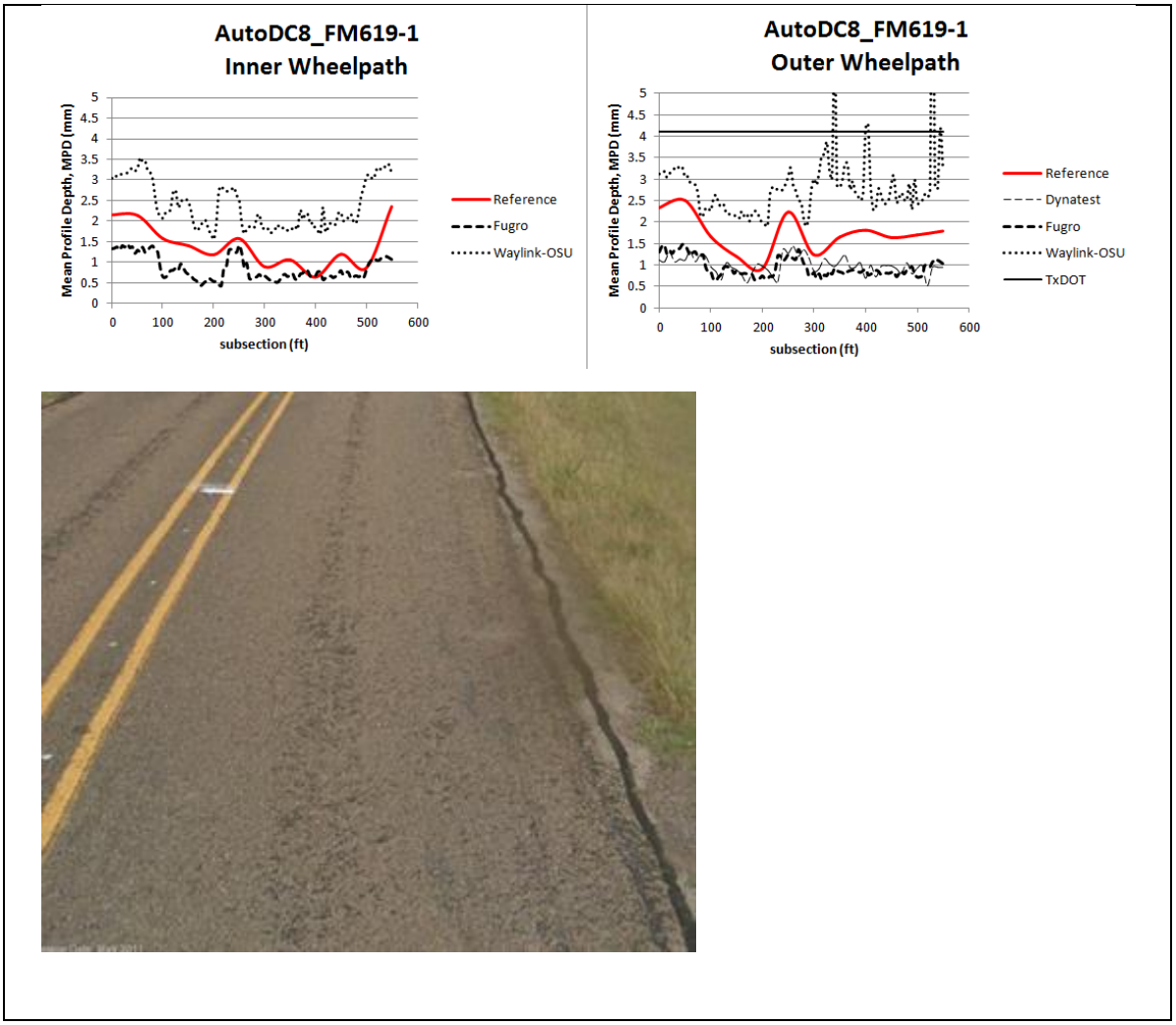

Figure A8: Inner and outer wheelpath texture graphs for AutoDC8_FM619-1 with image close-up of the pavement section

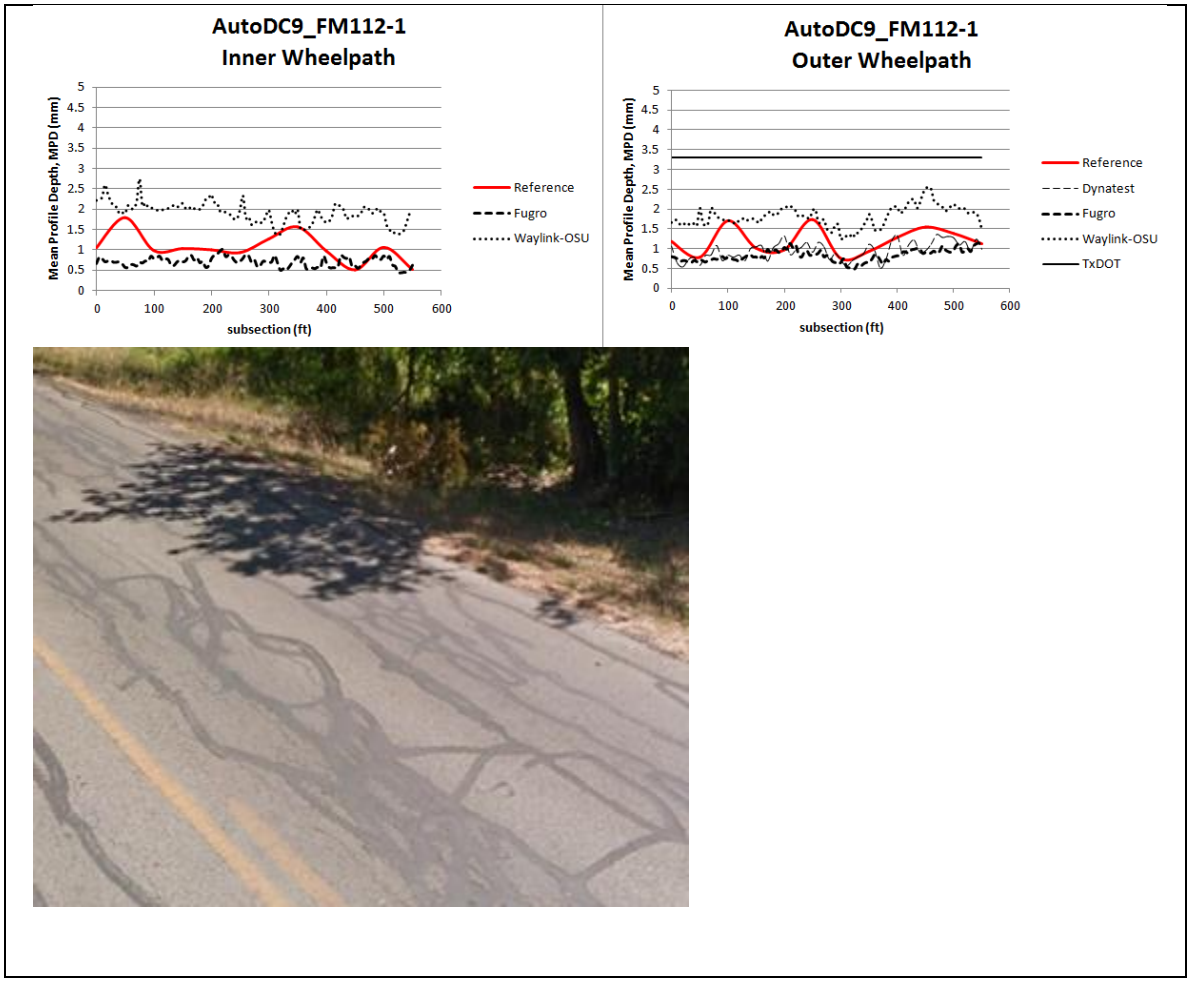

Figure A9: Inner and outer wheelpath texture graphs for AutoDC9_FM112-1 with image close-up of the pavement section

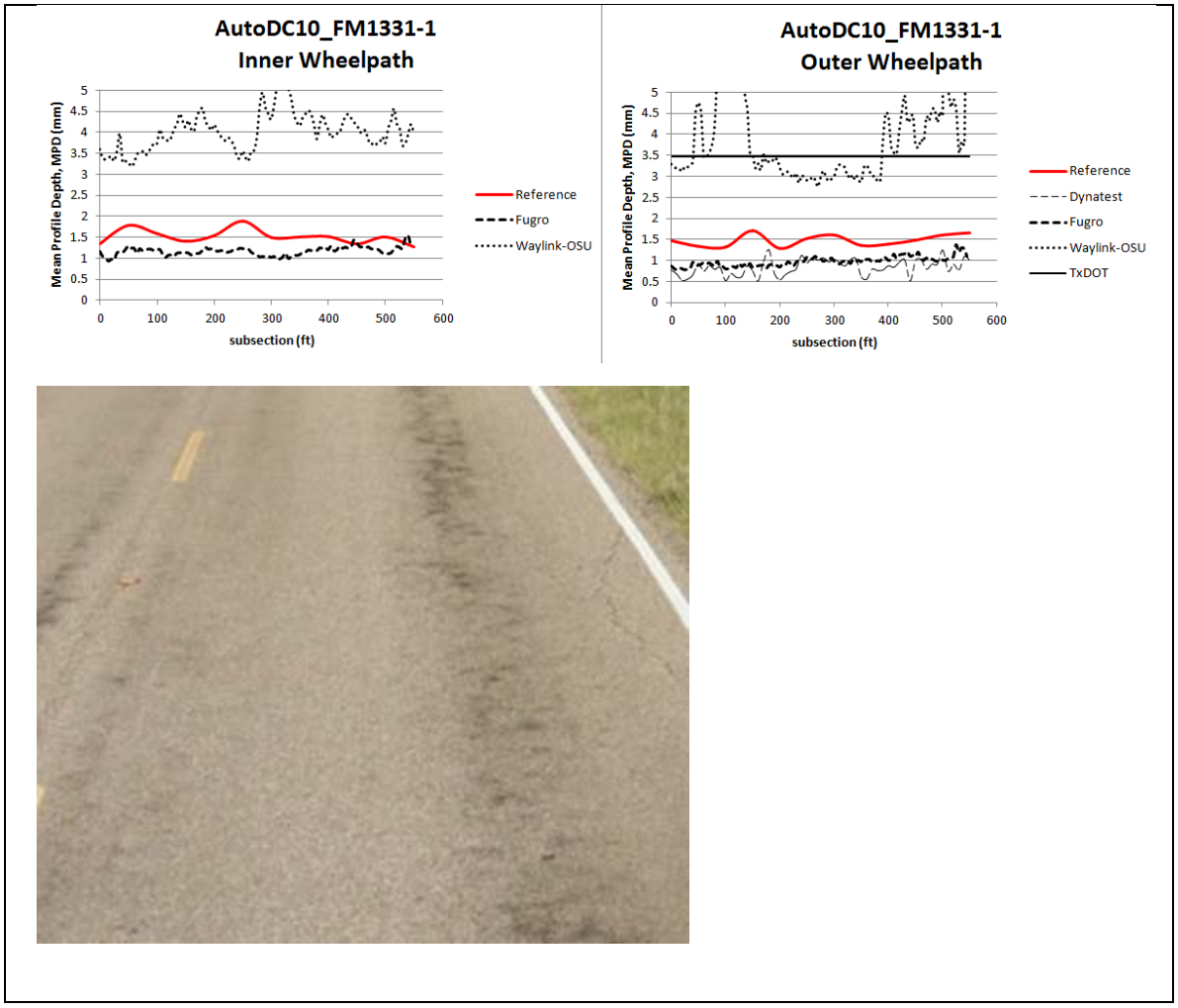

Figure A10: Inner and outer wheelpath texture graphs for AutoDC10_FM1331-1 with image close-up of the pavement section

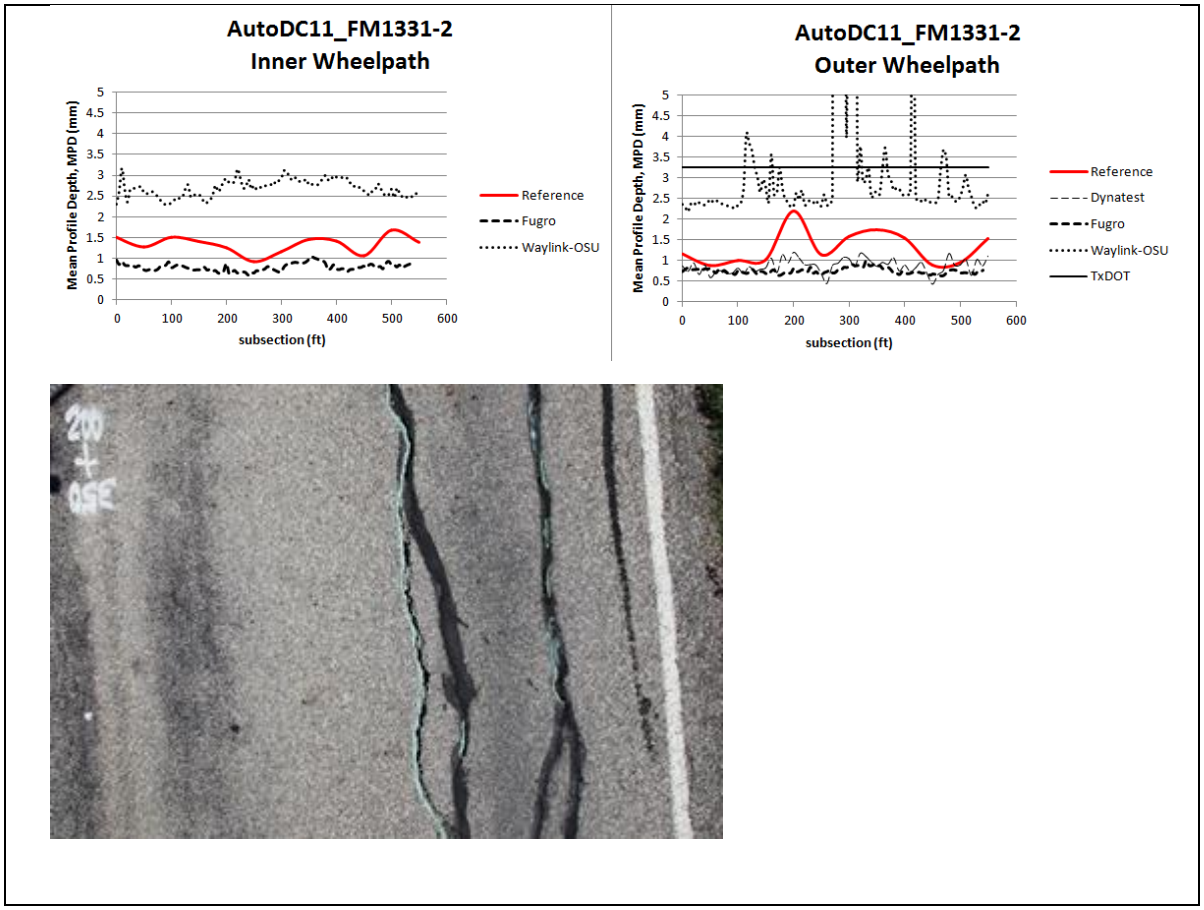

Figure A11: Inner and outer wheelpath texture graphs for AutoDC11_FM1331-2 with image close-up of the pavement section

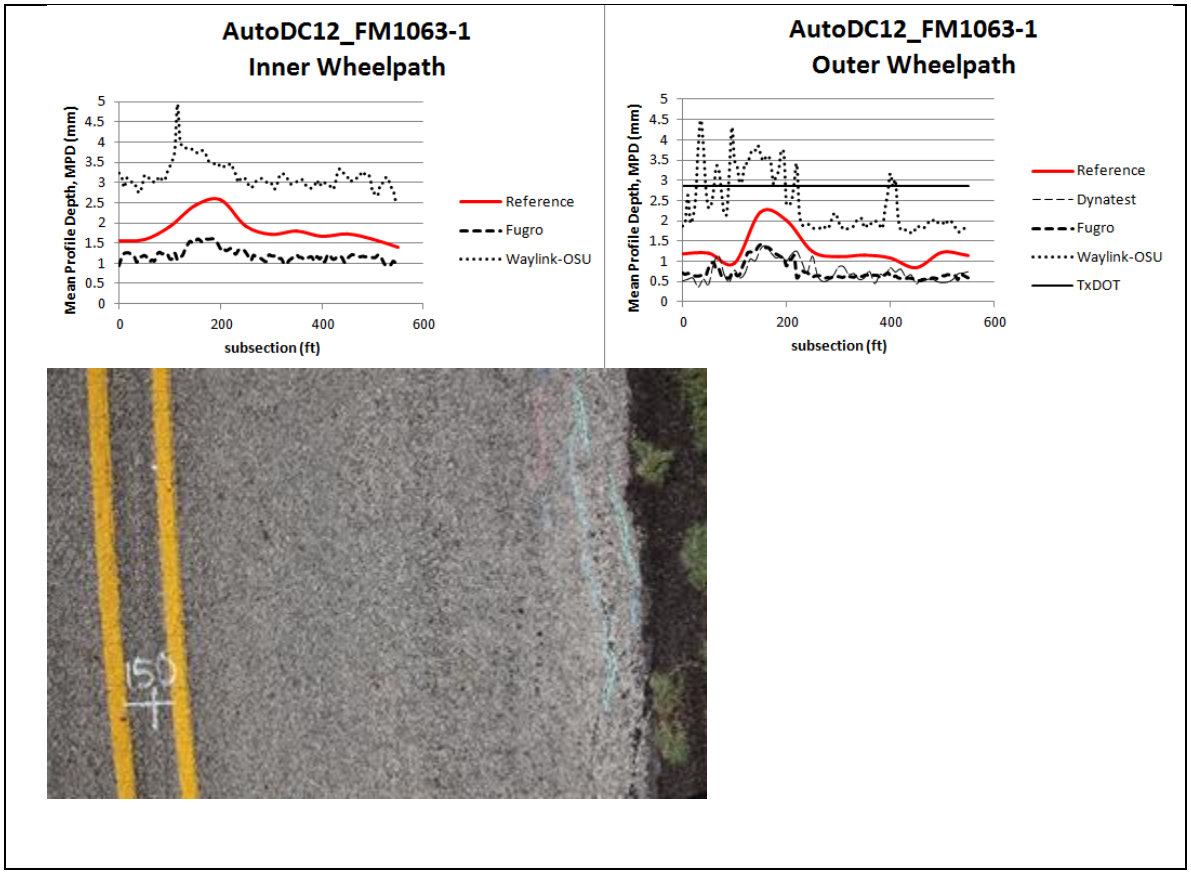

Figure A12: Inner and outer wheelpath texture graphs for AutoDC12_FM1063-1 with image close-up of the pavement section

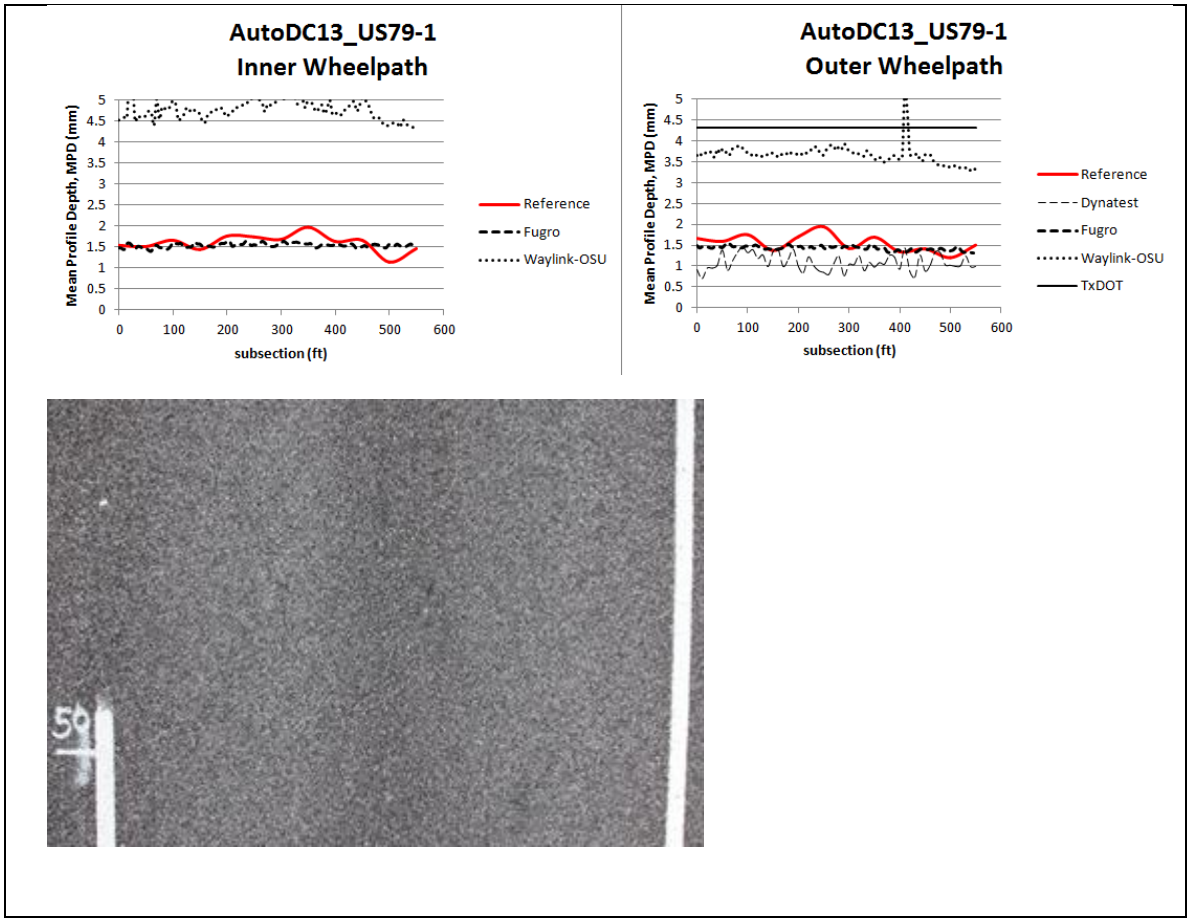

Figure A13: Inner and outer wheelpath texture graphs for AutoDC13_US79-1 with image close-up of the pavement section

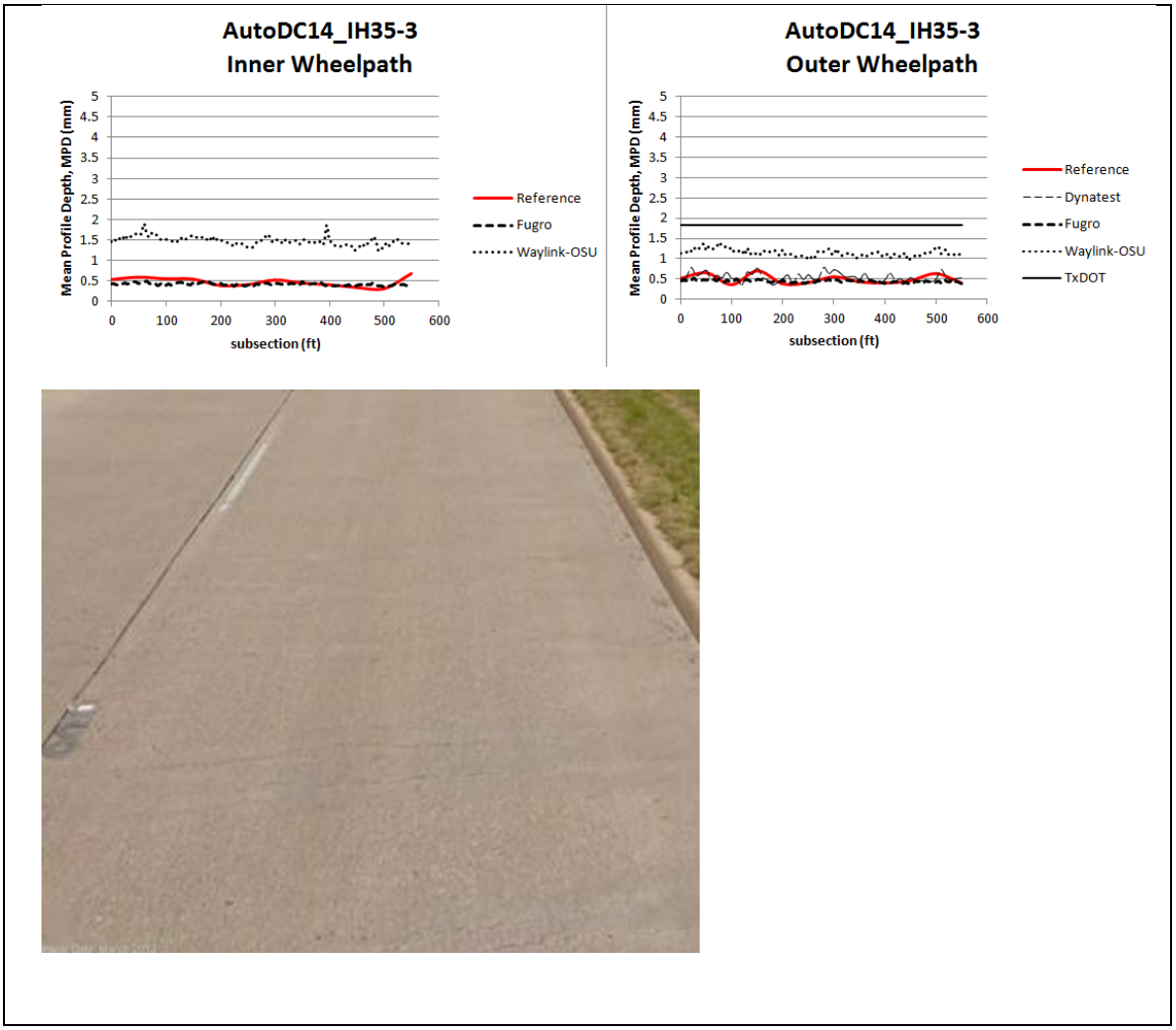

Figure A14: Inner and outer wheelpath texture graphs for AutoDC14_IH35-3 with image close-up of the pavement section

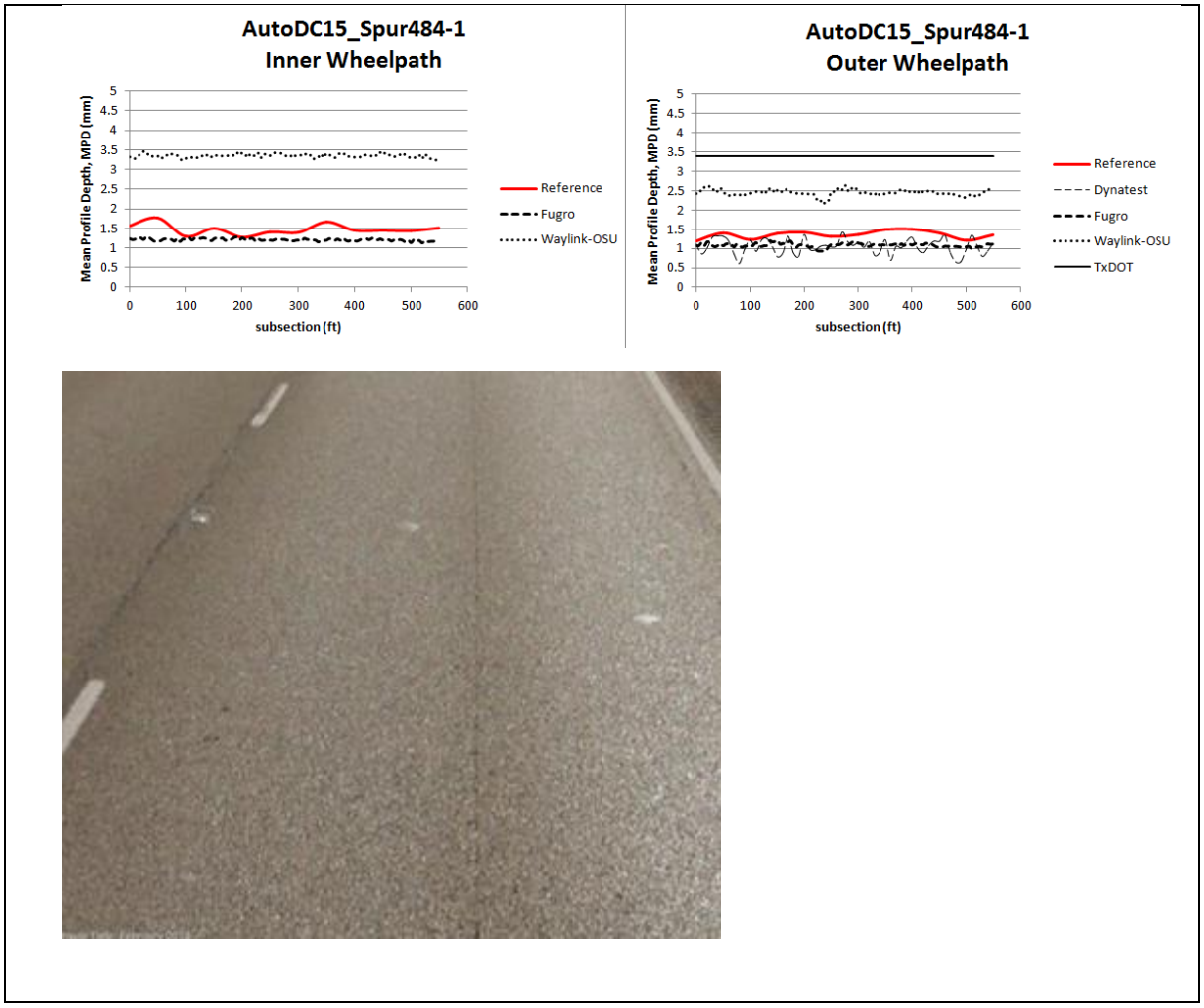

Figure A15: Inner and outer wheelpath texture graphs for AutoDC15_Spur484-1 with image close-up of the pavement section

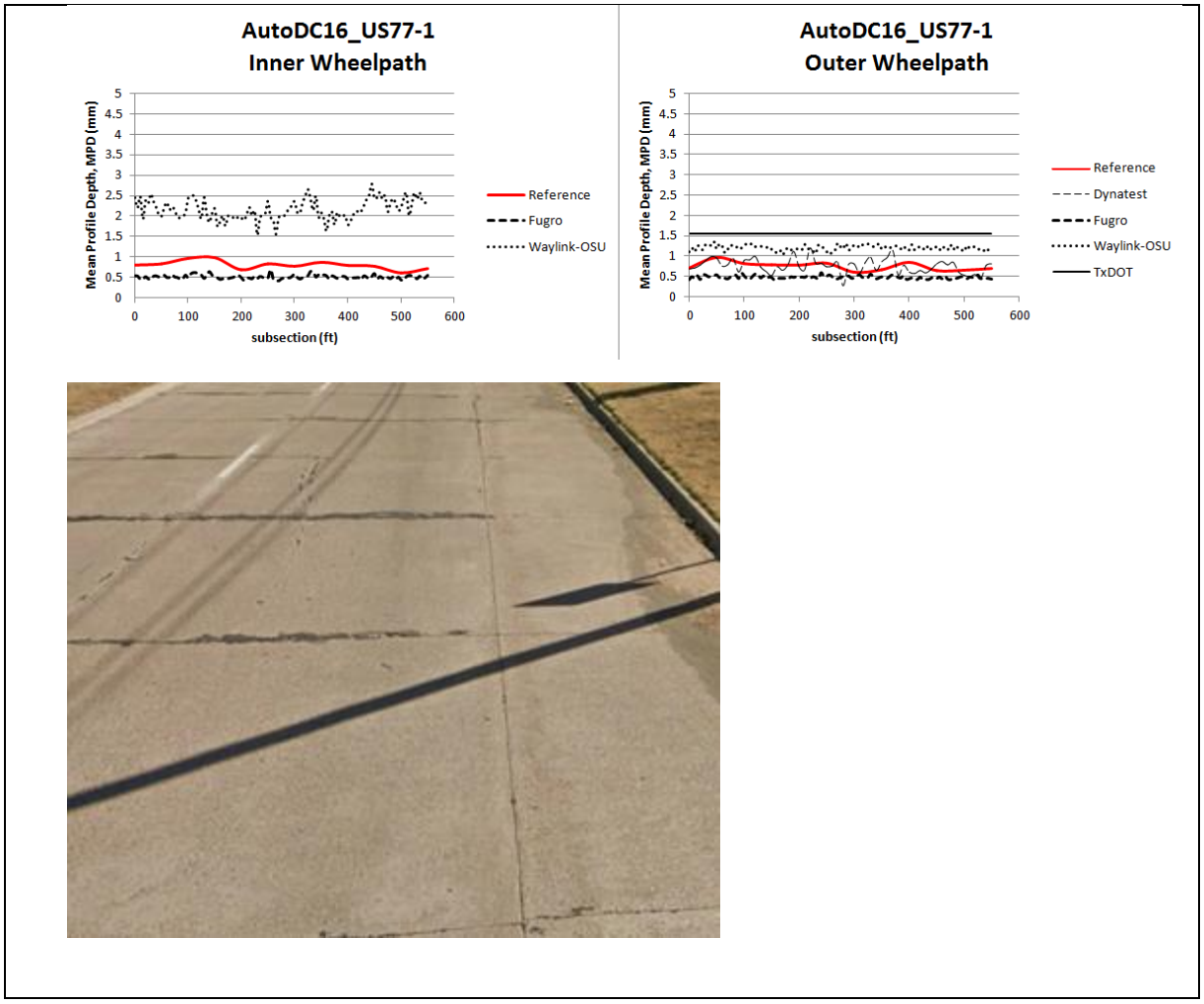

Figure A16: Inner and outer wheelpath texture graphs for AutoDC16_US77-1 with image close-up of the pavement section

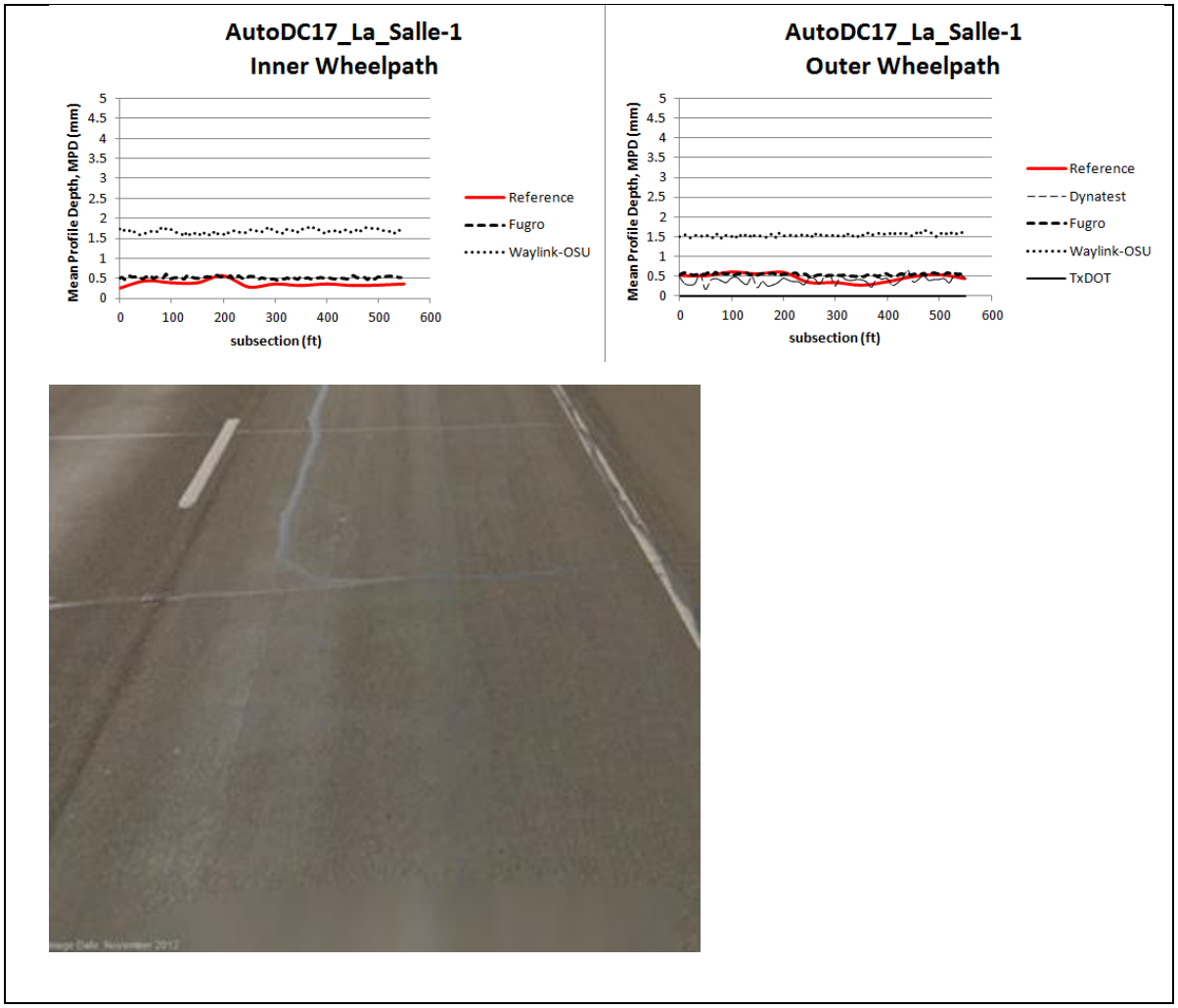

Figure A17: Inner and outer wheelpath texture graphs for AutoDC17_La_Salle-1 with image close-up of the pavement section

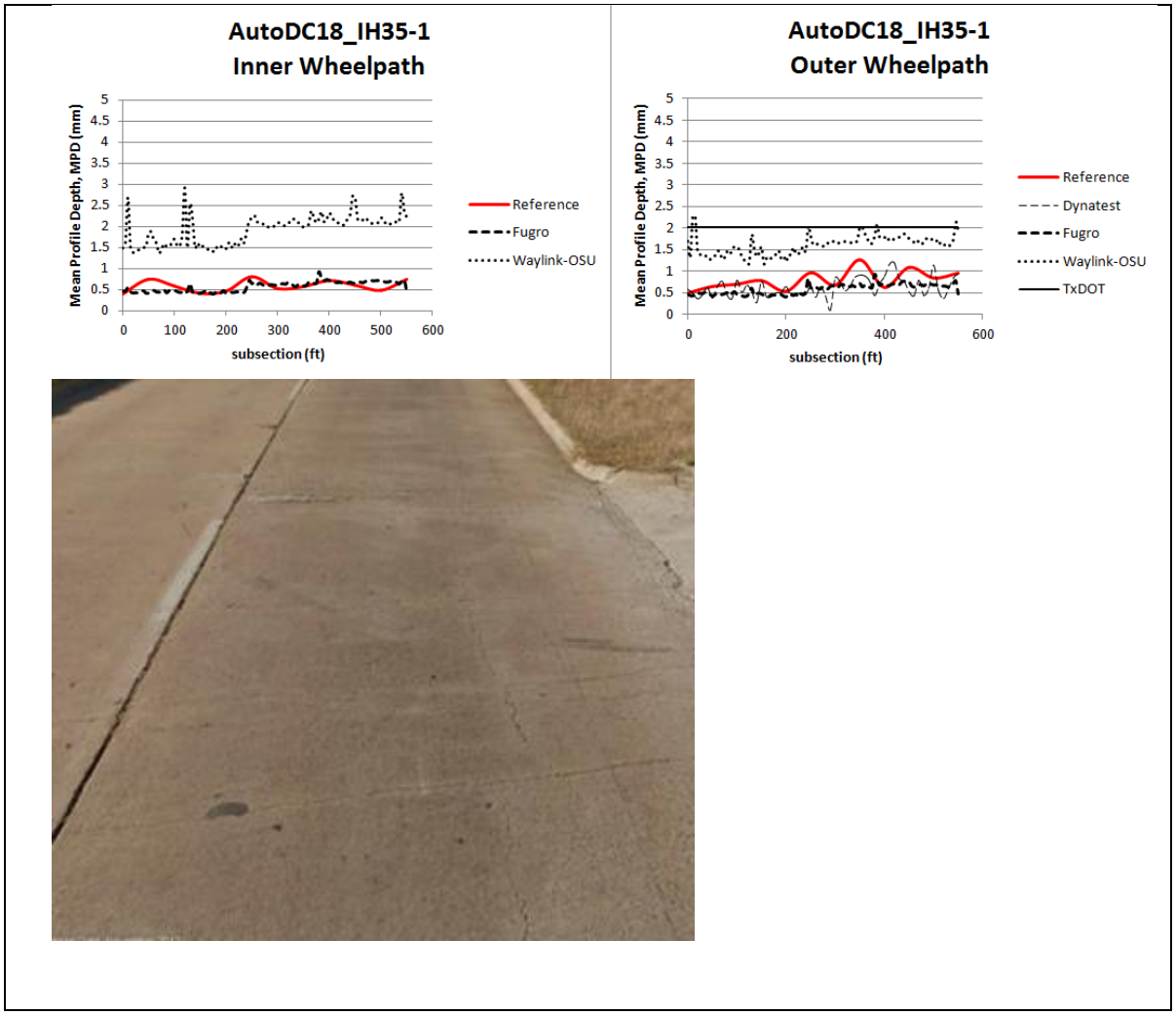

Figure A18: Inner and outer wheelpath texture graphs for AutoDC18_IH35-1 with image close-up of the pavement section

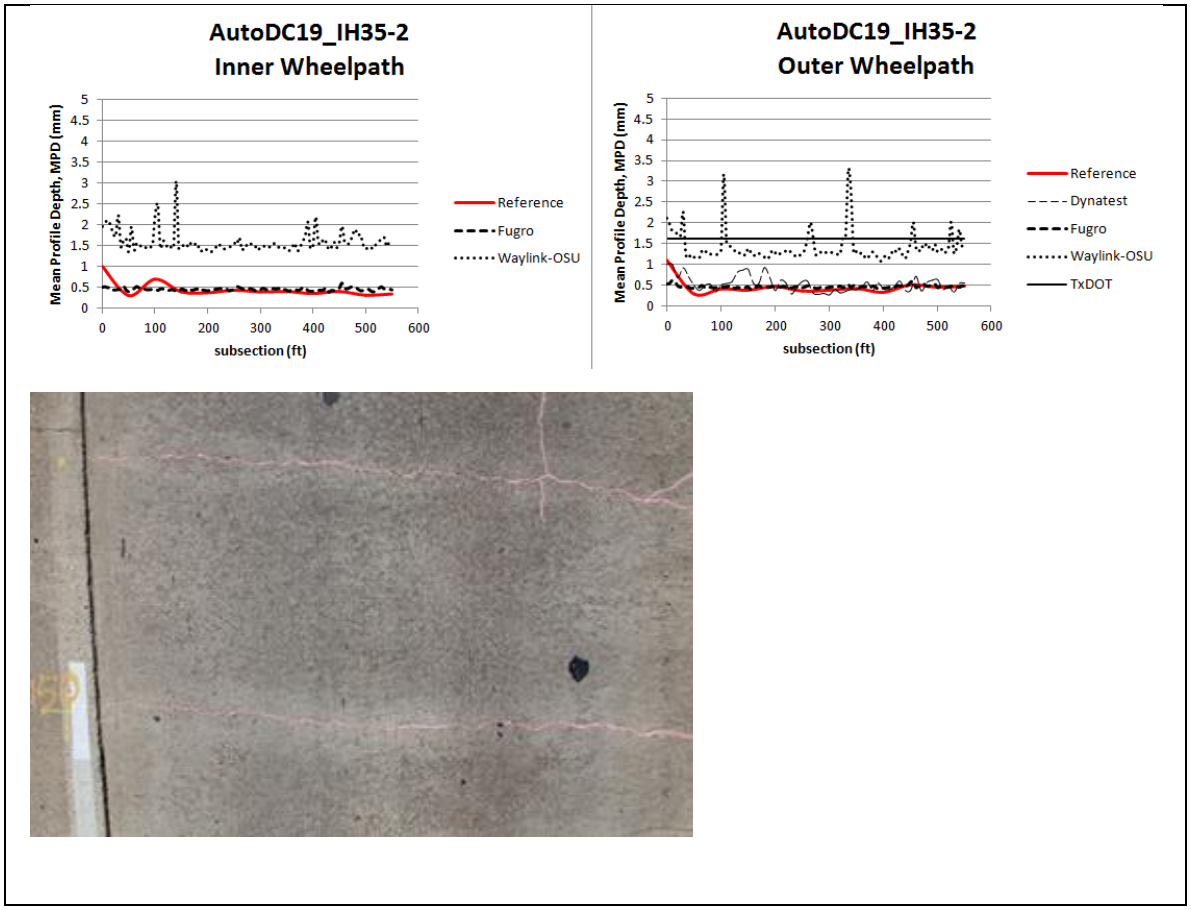

Figure A19: Inner and outer wheelpath texture graphs for AutoDC19_IH35-2 with image close-up of the pavement section

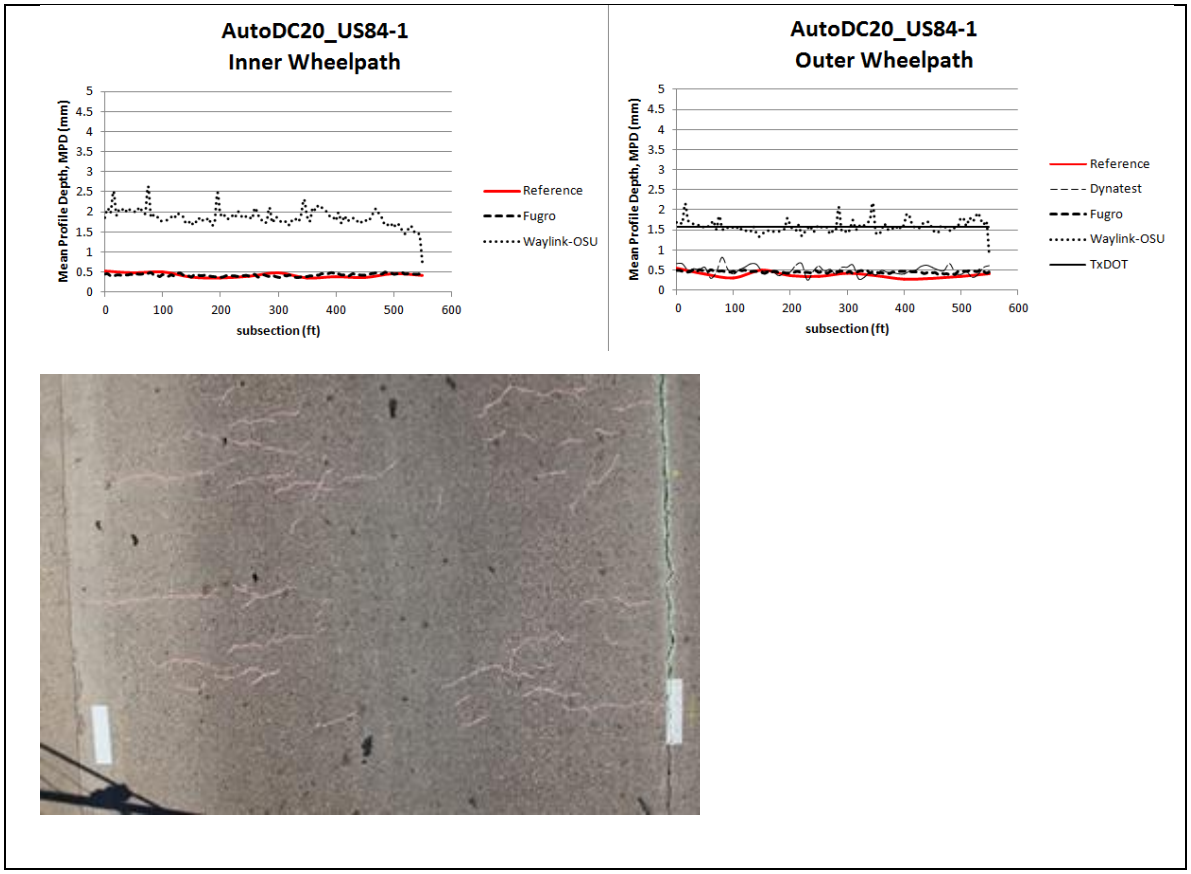

Figure A20: Inner and outer wheelpath texture graphs for AutoDC20_US84-1 with image close-up of the pavement section

Appendix B. Average Texture Every Subsection (Inner Wheelpath)

Table B1: Average inner wheelpath texture every subsection for AutoDC1_FM973-1

***Inner* wheelpath (IWP) - Mean Profile Depth, MPD (mm)**

		Vendors			
subsection	Reference	Dynatest	Fugro	Waylink-OSU	TxDOT
0'	0.66	-	-	2.061	-
50'	0.44	-	0.51	2.047	-
100'	0.48	-	0.53	2.036	-
150'	0.55	-	0.57	2.038	-
200'	0.51	-	0.57	2.152	-
250'	0.53	-	0.56	2.174	-
300'	0.41	-	0.53	2.05	-
350'	0.65	-	0.52	2.224	-
400'	0.47	-	0.57	2.075	-
450'	0.65	-	0.52	1.958	-
500'	0.63	-	0.54	2.167	-
550'	0.57	-	0.57	2.138	-
Average	0.55	-	0.54	2.09	-

***Inner* wheelpath (IWP) - MPD Error (mm)**

	Vendors			
subsection	Dynatest	Fugro	Waylink-OSU	TxDOT
0'	-	-	-1.40	-
50'	-	-0.07	-1.61	-
100'	-	-0.05	-1.56	-
150'	-	-0.02	-1.49	-
200'	-	-0.06	-1.64	-
250'	-	-0.03	-1.64	-
300'	-	-0.12	-1.64	-
350'	-	0.13	-1.57	-
400'	-	-0.10	-1.61	-
450'	-	0.13	-1.31	-
500'	-	0.09	-1.54	-
550'	-	0.00	-1.57	-
Total		-0.10	-18.57	
Average	-	0.00	-1.55	-
Std. Dev.		0.09	0.10	

Table B2: Average inner wheelpath texture every subsection for AutoDC2_FM3177-1

***Inner* wheelpath (IWP) - Mean Profile Depth, MPD (mm)**

		Vendors			
subsection	Reference	Dynatest	Fugro	Waylink-OSU	TxDOT
0'	0.47	-	0.53	1.703	-
50'	0.88	-	0.50	1.795	-
100'	1.02	-	0.66	1.903	-
150'	1.06	-	0.63	1.856	-
200'	0.72	-	0.64	1.934	-
250'	0.42	-	0.50	1.826	-
300'	0.4	-	0.46	1.888	-
350'	0.37	-	0.44	1.897	-
400'	0.44	-	0.51	1.922	-
450'	0.99	-	0.69	1.859	-
500'	0.94	-	0.78	1.788	-
550'	1	-	0.79	1.895	-
Average	0.73	-	0.59	1.86	-

***Inner* wheelpath (IWP) - MPD Error (mm)**

	Vendors			
subsection	Dynatest	Fugro	Waylink-OSU	TxDOT
0'	-	-0.06	-1.23	-
50'	-	0.38	-0.92	-
100'	-	0.36	-0.88	-
150'	-	0.43	-0.80	-
200'	-	0.08	-1.21	-
250'	-	-0.08	-1.41	-
300'	-	-0.06	-1.49	-
350'	-	-0.07	-1.53	-
400'	-	-0.07	-1.48	-
450'	-	0.30	-0.87	-
500'	-	0.16	-0.85	-
550'	-	0.21	-0.90	-
Total		1.57	-13.56	
Average	-	0.13	-1.13	-
Std. Dev.		0.20	0.29	

Table B3: Average inner wheelpath texture every subsection for AutoDC3_FM696-1

***Inner* wheelpath (IWP) - Mean Profile Depth, MPD (mm)**

		Vendors			
subsection	Reference	Dynatest	Fugro	Waylink-OSU	TxDOT
0'	0.72	-	0.48	2.128	-
50'	0.59	-	0.49	2.719	-
100'	0.65	-	0.55	2.34	-
150'	0.63	-	0.57	2.232	-
200'	1.14	-	0.73	2.218	-
250'	1.4	-	0.86	2.18	-
300'	0.83	-	0.75	2.315	-
350'	0.69	-	0.54	2.101	-
400'	0.94	-	0.70	2.201	-
450'	0.72	-	0.55	2.316	-
500'	0.7	-	0.49	2.133	-
550'	0.82	-	0.62	2.401	-
Average	0.82	-	0.61	2.27	-

***Inner* wheelpath (IWP) - MPD Error (mm)**

	Vendors			
subsection	Dynatest	Fugro	Waylink-OSU	TxDOT
0'	-	0.24	-1.41	-
50'	-	0.10	-2.13	-
100'	-	0.10	-1.69	-
150'	-	0.06	-1.60	-
200'	-	0.41	-1.08	-
250'	-	0.54	-0.78	-
300'	-	0.08	-1.49	-
350'	-	0.15	-1.41	-
400'	-	0.24	-1.26	-
450'	-	0.17	-1.60	-
500'	-	0.21	-1.43	-
550'	-	0.20	-1.58	-
Total		2.50	-17.45	
Average	-	0.21	-1.45	-
Std. Dev.		0.14	0.33	

Table B4: Average inner wheelpath texture every subsection for AutoDC4_FM696-3

***Inner* wheelpath (IWP) - Mean Profile Depth, MPD (mm)**

		Vendors			
subsection	Reference	Dynatest	Fugro	Waylink-OSU	TxDOT
0'	0.58	-	0.54	1.849	-
50'	0.43	-	0.47	1.673	-
100'	0.57	-	0.51	1.651	-
150'	0.59	-	0.51	1.699	-
200'	0.44	-	0.47	1.672	-
250'	0.43	-	0.48	1.685	-
300'	0.54	-	0.48	1.747	-
350'	0.57	-	0.55	1.634	-
400'	0.48	-	0.52	1.647	-
450'	0.49	-	0.52	1.707	-
500'	0.5	-	0.57	1.755	-
550'	0.59	-	0.47	1.648	-
Average	0.52	-	0.51	1.70	-

***Inner* wheelpath (IWP) - MPD Error (mm)**

	Vendors			
subsection	Dynatest	Fugro	Waylink-OSU	TxDOT
0'	-	0.04	-1.27	-
50'	-	-0.04	-1.24	-
100'	-	0.06	-1.08	-
150'	-	0.08	-1.11	-
200'	-	-0.03	-1.23	-
250'	-	-0.05	-1.26	-
300'	-	0.06	-1.21	-
350'	-	0.02	-1.06	-
400'	-	-0.04	-1.17	-
450'	-	-0.03	-1.22	-
500'	-	-0.07	-1.26	-
550'	-	0.12	-1.06	-
Total		0.10	-14.16	
Average	-	0.01	-1.18	-
Std. Dev.		0.06	0.08	

Table B5: Average inner wheelpath texture every subsection for AutoDC5_FM696-4

***Inner* wheelpath (IWP) - Mean Profile Depth, MPD (mm)**

		Vendors			
subsection	Reference	Dynatest	Fugro	Waylink-OSU	TxDOT
0'	0.56	-	0.49	1.783	-
50'	0.55	-	0.52	1.954	-
100'	0.53	-	0.51	1.901	-
150'	0.48	-	0.51	1.889	-
200'	0.44	-	0.53	1.966	-
250'	0.49	-	0.52	2.075	-
300'	0.61	-	0.56	3.015	-
350'	0.47	-	0.57	1.912	-
400'	0.58	-	0.54	2.04	-
450'	0.51	-	0.51	2.051	-
500'	0.52	-	0.59	2.067	-
550'	0.52	-	-	2.032	-
Average	0.52	-	0.53	2.06	-

***Inner* wheelpath (IWP) - MPD Error (mm)**

	Vendors			
subsection	Dynatest	Fugro	Waylink-OSU	TxDOT
0'	-	0.07	-1.22	-
50'	-	0.03	-1.40	-
100'	-	0.02	-1.37	-
150'	-	-0.03	-1.41	-
200'	-	-0.09	-1.53	-
250'	-	-0.03	-1.59	-
300'	-	0.05	-2.41	-
350'	-	-0.10	-1.44	-
400'	-	0.04	-1.46	-
450'	-	0.00	-1.54	-
500'	-	-0.07	-1.55	-
550'	-	-	-1.51	-
Total		-0.11	-18.43	
Average	-	-0.01	-1.54	-
Std. Dev.		0.06	0.29	

Table B6: Average inner wheelpath texture every subsection for AutoDC6_FM696-2

***Inner* wheelpath (IWP) - Mean Profile Depth, MPD (mm)**

		Vendors			
subsection	Reference	Dynatest	Fugro	Waylink-OSU	TxDOT
0'	1.04	-	-	2.438	-
50'	0.65	-	0.68	2.482	-
100'	0.84	-	0.86	2.431	-
150'	0.81	-	0.67	2.758	-
200'	0.78	-	0.74	2.381	-
250'	0.82	-	0.80	2.528	-
300'	0.9	-	0.72	2.361	-
350'	0.79	-	0.75	2.539	-
400'	0.72	-	0.84	2.554	-
450'	0.78	-	0.88	2.467	-
500'	1.35	-	1.18	2.961	-
550'	0.75	-	0.86	2.35	-
Average	0.85	-	0.82	2.52	-

***Inner* wheelpath (IWP) - MPD Error (mm)**

	Vendors			
subsection	Dynatest	Fugro	Waylink-OSU	TxDOT
0'	-	-	-1.40	-
50'	-	-0.03	-1.83	-
100'	-	-0.02	-1.59	-
150'	-	0.14	-1.95	-
200'	-	0.04	-1.60	-
250'	-	0.02	-1.71	-
300'	-	0.18	-1.46	-
350'	-	0.04	-1.75	-
400'	-	-0.12	-1.83	-
450'	-	-0.10	-1.69	-
500'	-	0.17	-1.61	-
550'	-	-0.11	-1.60	-
Total		0.19	-20.02	
Average	-	0.03	-1.67	-
Std. Dev.		0.11	0.16	

Table B7: Average inner wheelpath texture every subsection for AutoDC7_FM696-5

***Inner* wheelpath (IWP) - Mean Profile Depth, MPD (mm)**

		Vendors			
subsection	Reference	Dynatest	Fugro	Waylink-OSU	TxDOT
0'	0.97	-	0.67	2.101	-
50'	1.2	-	0.62	2.025	-
100'	0.94	-	0.86	2.108	-
150'	0.96	-	0.72	1.916	-
200'	0.67	-	0.60	1.861	-
250'	0.78	-	0.58	1.923	-
300'	0.81	-	0.72	2.01	-
350'	0.75	-	0.52	1.882	-
400'	1.1	-	0.66	1.706	-
450'	1.3	-	0.67	2.053	-
500'	1.33	-	0.92	2.111	-
550'	1.45	-	0.93	2.325	-
Average	1.02	-	0.70	2.00	-

***Inner* wheelpath (IWP) - MPD Error (mm)**

	Vendors			
subsection	Dynatest	Fugro	Waylink-OSU	TxDOT
0'	-	0.30	-1.13	-
50'	-	0.58	-0.83	-
100'	-	0.08	-1.17	-
150'	-	0.24	-0.96	-
200'	-	0.07	-1.19	-
250'	-	0.20	-1.14	-
300'	-	0.09	-1.20	-
350'	-	0.23	-1.13	-
400'	-	0.44	-0.61	-
450'	-	0.63	-0.75	-
500'	-	0.41	-0.78	-
550'	-	0.52	-0.88	-
Total		3.80	-11.76	
Average	-	0.32	-0.98	-
Std. Dev.		0.20	0.21	

Table B8: Average inner wheelpath texture every subsection for AutoDC8_FM619-1

***Inner* wheelpath (IWP) - Mean Profile Depth, MPD (mm)**

		Vendors			
subsection	Reference	Dynatest	Fugro	Waylink-OSU	TxDOT
0'	2.14	-	1.34	3.048	-
50'	2.13	-	1.30	3.275	-
100'	1.57	-	0.65	2.064	-
150'	1.4	-	0.71	2.488	-
200'	1.18	-	0.54	1.549	-
250'	1.57	-	1.42	2.52	-
300'	0.89	-	0.67	1.83	-
350'	1.06	-	0.69	1.75	-
400'	0.64	-	0.67	1.807	-
450'	1.19	-	0.80	2.214	-
500'	0.86	-	0.81	3.07	-
550'	2.34	-	1.08	3.163	-
Average	1.41	-	0.89	2.40	-

***Inner* wheelpath (IWP) - MPD Error (mm)**

	Vendors			
subsection	Dynatest	Fugro	Waylink-OSU	TxDOT
0'	-	0.80	-0.91	-
50'	-	0.83	-1.15	-
100'	-	0.92	-0.49	-
150'	-	0.69	-1.09	-
200'	-	0.64	-0.37	-
250'	-	0.15	-0.95	-
300'	-	0.22	-0.94	-
350'	-	0.37	-0.69	-
400'	-	-0.03	-1.17	-
450'	-	0.39	-1.02	-
500'	-	0.05	-2.21	-
550'	-	1.26	-0.82	-
Total		6.27	-11.81	
Average	-	0.52	-0.98	-
Std. Dev.		0.40	0.46	

Table B9: Average inner wheelpath texture every subsection for AutoDC9_FM112-1

***Inner* wheelpath (IWP) - Mean Profile Depth, MPD (mm)**

		Vendors			
subsection	Reference	Dynatest	Fugro	Waylink-OSU	TxDOT
0'	1.05	-	0.66	2.218	-
50'	1.8	-	0.57	1.894	-
100'	0.98	-	0.78	2.01	-
150'	1.03	-	0.70	2.147	-
200'	1	-	0.78	2.365	-
250'	0.93	-	0.72	2.004	-
300'	1.27	-	0.70	1.981	-
350'	1.57	-	0.84	1.991	-
400'	0.97	-	0.69	1.67	-
450'	0.5	-	0.61	1.862	-
500'	1.06	-	0.85	1.908	-
550'	0.51	-	0.62	1.989	-
Average	1.06	-	0.71	2.00	-

***Inner* wheelpath (IWP) - MPD Error (mm)**

	Vendors			
subsection	Dynatest	Fugro	Waylink-OSU	TxDOT
0'	-	0.39	-1.17	-
50'	-	1.23	-0.09	-
100'	-	0.20	-1.03	-
150'	-	0.33	-1.12	-
200'	-	0.22	-1.37	-
250'	-	0.21	-1.07	-
300'	-	0.57	-0.71	-
350'	-	0.73	-0.42	-
400'	-	0.28	-0.70	-
450'	-	-0.11	-1.36	-
500'	-	0.21	-0.85	-
550'	-	-0.11	-1.48	-
Total		4.16	-11.37	
Average	-	0.35	-0.95	-
Std. Dev.		0.37	0.41	

Table B10: Average inner wheelpath texture every subsection for AutoDC10_FM1331-1

***Inner* wheelpath (IWP) - Mean Profile Depth, MPD (mm)**

		Vendors			
subsection	Reference	Dynatest	Fugro	Waylink-OSU	TxDOT
0'	1.35	-	1.17	3.587	-
50'	1.78	-	1.30	3.29	-
100'	1.59	-	1.20	3.717	-
150'	1.41	-	1.14	4.113	-
200'	1.54	-	1.22	4.177	-
250'	1.88	-	1.23	3.548	-
300'	1.5	-	1.03	4.299	-
350'	1.51	-	1.09	4.146	-
400'	1.52	-	1.21	4.056	-
450'	1.35	-	1.37	4.177	-
500'	1.51	-	1.14	3.736	-
550'	1.28	-	-	3.937	-
Average	1.52	-	1.19	3.90	-

***Inner* wheelpath (IWP) - MPD Error (mm)**

	Vendors			
subsection	Dynatest	Fugro	Waylink-OSU	TxDOT
0'	-	0.18	-2.24	-
50'	-	0.48	-1.51	-
100'	-	0.39	-2.13	-
150'	-	0.27	-2.70	-
200'	-	0.32	-2.64	-
250'	-	0.65	-1.67	-
300'	-	0.47	-2.80	-
350'	-	0.42	-2.64	-
400'	-	0.31	-2.54	-
450'	-	-0.02	-2.83	-
500'	-	0.37	-2.23	-
550'	-	-	-2.66	-
Total		3.86	-28.56	
Average	-	0.33	-2.38	-
Std. Dev.		0.17	0.44	

Table B11: Average inner wheelpath texture every subsection for AutoDC11_FM1331-2

***Inner* wheelpath (IWP) - Mean Profile Depth, MPD (mm)**

		Vendors			
subsection	Reference	Dynatest	Fugro	Waylink-OSU	TxDOT
0'	1.51	-	0.96	2.309	-
50'	1.28	-	0.72	2.581	-
100'	1.51	-	0.78	2.341	-
150'	1.41	-	0.72	2.536	-
200'	1.26	-	0.87	2.916	-
250'	0.93	-	0.64	2.754	-
300'	1.17	-	0.67	2.937	-
350'	1.46	-	0.97	2.762	-
400'	1.42	-	0.75	2.956	-
450'	1.07	-	0.81	2.627	-
500'	1.68	-	0.85	2.664	-
550'	1.39	-	-	2.558	-
Average	1.34	-	0.79	2.66	-

***Inner* wheelpath (IWP) - MPD Error (mm)**

	Vendors			
subsection	Dynatest	Fugro	Waylink-OSU	TxDOT
0'	-	0.55	-0.80	-
50'	-	0.56	-1.30	-
100'	-	0.73	-0.83	-
150'	-	0.69	-1.13	-
200'	-	0.39	-1.66	-
250'	-	0.29	-1.82	-
300'	-	0.50	-1.77	-
350'	-	0.49	-1.30	-
400'	-	0.67	-1.54	-
450'	-	0.26	-1.56	-
500'	-	0.83	-0.98	-
550'	-	-	-1.17	-
Total		5.96	-15.85	
Average	-	0.55	-1.32	-
Std. Dev.		0.18	0.35	

Table B12: Average inner wheelpath texture every subsection for AutoDC12_FM1063-1

***Inner* wheelpath (IWP) - Mean Profile Depth, MPD (mm)**

		Vendors			
subsection	Reference	Dynatest	Fugro	Waylink-OSU	TxDOT
0'	1.55	-	0.93	3.228	-
50'	1.58	-	1.20	3.166	-
100'	1.9	-	1.11	3.389	-
150'	2.42	-	1.54	3.789	-
200'	2.56	-	1.36	3.459	-
250'	1.91	-	1.27	3.07	-
300'	1.71	-	1.18	2.98	-
350'	1.79	-	1.21	3.014	-
400'	1.66	-	1.15	3.015	-
450'	1.72	-	1.12	3.141	-
500'	1.59	-	1.14	2.732	-
550'	1.39	-	1.08	2.441	-
Average	1.82	-	1.19	3.12	-

***Inner* wheelpath (IWP) - MPD Error (mm)**

	Vendors			
subsection	Dynatest	Fugro	Waylink-OSU	TxDOT
0'	-	0.62	-1.68	-
50'	-	0.38	-1.59	-
100'	-	0.79	-1.49	-
150'	-	0.88	-1.37	-
200'	-	1.20	-0.90	-
250'	-	0.64	-1.16	-
300'	-	0.53	-1.27	-
350'	-	0.58	-1.22	-
400'	-	0.51	-1.36	-
450'	-	0.60	-1.42	-
500'	-	0.45	-1.14	-
550'	-	0.31	-1.05	-
Total		7.50	-15.64	
Average	-	0.62	-1.30	-
Std. Dev.		0.24	0.22	

Table B13: Average inner wheelpath texture every subsection for AutoDC13_US79-1

***Inner* wheelpath (IWP) - Mean Profile Depth, MPD (mm)**

		Vendors			
subsection	Reference	Dynatest	Fugro	Waylink-OSU	TxDOT
0'	1.54	-	1.49	4.529	-
50'	1.51	-	1.48	4.627	-
100'	1.66	-	1.60	4.998	-
150'	1.44	-	1.57	4.658	-
200'	1.76	-	1.62	4.609	-
250'	1.74	-	1.56	5.002	-
300'	1.68	-	1.58	5.103	-
350'	1.97	-	1.57	5.06	-
400'	1.63	-	1.57	4.675	-
450'	1.66	-	1.51	5.069	-
500'	1.14	-	1.56	4.439	-
550'	1.46	-	-	4.333	-
Average	1.60	-	1.56	4.76	-

***Inner* wheelpath (IWP) - MPD Error (mm)**

	Vendors			
subsection	Dynatest	Fugro	Waylink-OSU	TxDOT
0'	-	0.05	-2.99	-
50'	-	0.03	-3.12	-
100'	-	0.06	-3.34	-
150'	-	-0.13	-3.22	-
200'	-	0.14	-2.85	-
250'	-	0.18	-3.26	-
300'	-	0.10	-3.42	-
350'	-	0.40	-3.09	-
400'	-	0.06	-3.05	-
450'	-	0.15	-3.41	-
500'	-	-0.42	-3.30	-
550'	-	-	-2.87	-
Total		0.61	-37.91	
Average	-	0.04	-3.16	-
Std. Dev.		0.20	0.20	

Table B14: Average inner wheelpath texture every subsection for AutoDC14_IH35-3

***Inner* wheelpath (IWP) - Mean Profile Depth, MPD (mm)**

		Vendors			
subsection	Reference	Dynatest	Fugro	Waylink-OSU	TxDOT
0'	0.54	-	0.43	1.464	-
50'	0.6	-	0.45	1.612	-
100'	0.56	-	0.40	1.522	-
150'	0.55	-	0.46	1.62	-
200'	0.39	-	0.45	1.512	-
250'	0.41	-	0.41	1.326	-
300'	0.53	-	0.44	1.451	-
350'	0.45	-	0.50	1.487	-
400'	0.41	-	0.39	1.486	-
450'	0.34	-	0.40	1.305	-
500'	0.31	-	0.36	1.317	-
550'	0.69	-	0.39	1.493	-
Average	0.48	-	0.42	1.47	-

***Inner* wheelpath (IWP) - MPD Error (mm)**

	Vendors			
subsection	Dynatest	Fugro	Waylink-OSU	TxDOT
0'	-	0.11	-0.92	-
50'	-	0.15	-1.01	-
100'	-	0.16	-0.96	-
150'	-	0.09	-1.07	-
200'	-	-0.06	-1.12	-
250'	-	0.00	-0.92	-
300'	-	0.09	-0.92	-
350'	-	-0.05	-1.04	-
400'	-	0.02	-1.08	-
450'	-	-0.06	-0.97	-
500'	-	-0.05	-1.01	-
550'	-	0.30	-0.80	-
Total		0.71	-11.82	
Average	-	0.06	-0.98	-
Std. Dev.		0.11	0.09	

Table B15: Average inner wheelpath texture every subsection for AutoDC15_Spur484-1

***Inner* wheelpath (IWP) - Mean Profile Depth, MPD (mm)**

		Vendors			
subsection	Reference	Dynatest	Fugro	Waylink-OSU	TxDOT
0'	1.56	-	1.24	3.312	-
50'	1.76	-	1.19	3.342	-
100'	1.3	-	1.23	3.265	-
150'	1.5	-	1.24	3.374	-
200'	1.28	-	1.26	3.423	-
250'	1.41	-	1.20	3.349	-
300'	1.4	-	1.20	3.364	-
350'	1.66	-	1.20	3.332	-
400'	1.45	-	1.19	3.306	-
450'	1.45	-	1.20	3.468	-
500'	1.44	-	1.14	3.285	-
550'	1.51	-	1.16	3.237	-
Average	1.48	-	1.20	3.34	-

***Inner* wheelpath (IWP) - MPD Error (mm)**

	Vendors			
subsection	Dynatest	Fugro	Waylink-OSU	TxDOT
0'	-	0.32	-1.75	-
50'	-	0.57	-1.58	-
100'	-	0.07	-1.97	-
150'	-	0.26	-1.87	-
200'	-	0.02	-2.14	-
250'	-	0.21	-1.94	-
300'	-	0.20	-1.96	-
350'	-	0.46	-1.67	-
400'	-	0.26	-1.86	-
450'	-	0.25	-2.02	-
500'	-	0.30	-1.85	-
550'	-	0.35	-1.73	-
Total		3.27	-22.34	
Average	-	0.27	-1.86	-
Std. Dev.		0.15	0.16	

Table B16: Average inner wheelpath texture every subsection for AutoDC16_US77-1

***Inner* wheelpath (IWP) - Mean Profile Depth, MPD (mm)**

		Vendors			
subsection	Reference	Dynatest	Fugro	Waylink-OSU	TxDOT
0'	0.8	-	0.54	2.451	-
50'	0.83	-	0.53	2.003	-
100'	0.97	-	0.49	2.436	-
150'	0.99	-	0.52	2.182	-
200'	0.68	-	0.49	1.958	-
250'	0.83	-	0.49	2.368	-
300'	0.77	-	0.58	2.356	-
350'	0.87	-	0.52	2.088	-
400'	0.79	-	0.46	1.796	-
450'	0.77	-	0.59	2.431	-
500'	0.6	-	0.44	2.217	-
550'	0.71	-	0.55	2.24	-
Average	0.80	-	0.52	2.21	-

***Inner* wheelpath (IWP) - MPD Error (mm)**

	Vendors			
subsection	Dynatest	Fugro	Waylink-OSU	TxDOT
0'	-	0.26	-1.65	-
50'	-	0.30	-1.17	-
100'	-	0.48	-1.47	-
150'	-	0.47	-1.19	-
200'	-	0.19	-1.28	-
250'	-	0.34	-1.54	-
300'	-	0.19	-1.59	-
350'	-	0.35	-1.22	-
400'	-	0.33	-1.01	-
450'	-	0.18	-1.66	-
500'	-	0.16	-1.62	-
550'	-	0.16	-1.53	-
Total		3.40	-16.92	
Average	-	0.28	-1.41	-
Std. Dev.		0.11	0.22	

Table B17: Average inner wheelpath texture every subsection for AutoDC17_La_Salle-1

***Inner* wheelpath (IWP) - Mean Profile Depth, MPD (mm)**

		Vendors			
subsection	Reference	Dynatest	Fugro	Waylink-OSU	TxDOT
0'	0.24	-	0.51	1.727	-
50'	0.43	-	0.54	1.622	-
100'	0.38	-	0.50	1.71	-
150'	0.38	-	0.51	1.565	-
200'	0.56	-	0.55	1.608	-
250'	0.27	-	0.55	1.681	-
300'	0.35	-	0.49	1.683	-
350'	0.31	-	0.53	1.728	-
400'	0.35	-	0.52	1.692	-
450'	0.31	-	0.57	1.656	-
500'	0.32	-	0.54	1.735	-
550'	0.35	-	-	1.706	-
Average	0.35	-	0.53	1.68	-

***Inner* wheelpath (IWP) - MPD Error (mm)**

	Vendors			
subsection	Dynatest	Fugro	Waylink-OSU	TxDOT
0'	-	-0.27	-1.49	-
50'	-	-0.11	-1.19	-
100'	-	-0.12	-1.33	-
150'	-	-0.13	-1.19	-
200'	-	0.01	-1.05	-
250'	-	-0.28	-1.41	-
300'	-	-0.14	-1.33	-
350'	-	-0.22	-1.42	-
400'	-	-0.17	-1.34	-
450'	-	-0.26	-1.35	-
500'	-	-0.22	-1.42	-
550'	-	-	-1.36	-
Total		-1.91	-15.86	
Average	-	-0.17	-1.32	-
Std. Dev.		0.09	0.12	

Table B18: Average inner wheelpath texture every subsection for AutoDC18_IH35-1

***Inner* wheelpath (IWP) - Mean Profile Depth, MPD (mm)**

		Vendors			
subsection	Reference	Dynatest	Fugro	Waylink-OSU	TxDOT
0'	0.4	-	0.46	1.494	-
50'	0.75	-	0.41	1.85	-
100'	0.59	-	0.48	1.706	-
150'	0.42	-	0.41	1.5	-
200'	0.47	-	0.41	1.478	-
250'	0.81	-	0.64	2.185	-
300'	0.53	-	0.60	2.091	-
350'	0.58	-	0.59	1.988	-
400'	0.72	-	0.72	2.316	-
450'	0.61	-	0.66	2.654	-
500'	0.49	-	0.69	2.202	-
550'	0.75	-	0.44	2.219	-
Average	0.59	-	0.54	1.97	-

***Inner* wheelpath (IWP) - MPD Error (mm)**

	Vendors			
subsection	Dynatest	Fugro	Waylink-OSU	TxDOT
0'	-	-0.06	-1.09	-
50'	-	0.34	-1.10	-
100'	-	0.11	-1.12	-
150'	-	0.01	-1.08	-
200'	-	0.06	-1.01	-
250'	-	0.17	-1.38	-
300'	-	-0.07	-1.56	-
350'	-	-0.01	-1.41	-
400'	-	0.00	-1.60	-
450'	-	-0.05	-2.04	-
500'	-	-0.20	-1.71	-
550'	-	0.31	-1.47	-
Total		0.61	-16.56	
Average	-	0.05	-1.38	-
Std. Dev.		0.16	0.32	

Table B19: Average inner wheelpath texture every subsection for AutoDC19_IH35-2

***Inner* wheelpath (IWP) - Mean Profile Depth, MPD (mm)**

		Vendors			
subsection	Reference	Dynatest	Fugro	Waylink-OSU	TxDOT
0'	1.01	-	0.50	1.958	-
50'	0.3	-	0.39	1.35	-
100'	0.7	-	0.45	2.227	-
150'	0.39	-	0.46	1.48	-
200'	0.37	-	0.41	1.366	-
250'	0.43	-	0.45	1.564	-
300'	0.39	-	0.44	1.468	-
350'	0.4	-	0.43	1.385	-
400'	0.35	-	0.41	1.488	-
450'	0.4	-	0.48	1.58	-
500'	0.31	-	0.45	1.415	-
550'	0.34	-	0.44	1.641	-
Average	0.45	-	0.44	1.58	-

***Inner* wheelpath (IWP) - MPD Error (mm)**

	Vendors			
subsection	Dynatest	Fugro	Waylink-OSU	TxDOT
0'	-	0.51	-0.95	-
50'	-	-0.09	-1.05	-
100'	-	0.25	-1.53	-
150'	-	-0.07	-1.09	-
200'	-	-0.04	-1.00	-
250'	-	-0.02	-1.13	-
300'	-	-0.05	-1.08	-
350'	-	-0.03	-0.99	-
400'	-	-0.06	-1.14	-
450'	-	-0.08	-1.18	-
500'	-	-0.14	-1.11	-
550'	-	-0.10	-1.30	-
Total		0.09	-13.53	
Average	-	0.01	-1.13	-
Std. Dev.		0.18	0.16	

Table B20: Average inner wheelpath texture every subsection for AutoDC20_US84-1

***Inner* wheelpath (IWP) - Mean Profile Depth, MPD (mm)**

		Vendors			
subsection	Reference	Dynatest	Fugro	Waylink-OSU	TxDOT
0'	0.52	-	0.46	1.852	-
50'	0.48	-	0.43	2.012	-
100'	0.5	-	0.44	1.777	-
150'	0.38	-	0.38	1.662	-
200'	0.36	-	0.37	1.929	-
250'	0.4	-	0.41	1.89	-
300'	0.48	-	0.38	1.831	-
350'	0.36	-	0.39	1.908	-
400'	0.39	-	0.44	1.779	-
450'	0.37	-	0.43	1.803	-
500'	0.46	-	0.46	1.607	-
550'	0.42	-	0.48	0.742	-
Average	0.43	-	0.42	1.73	-

***Inner* wheelpath (IWP) - MPD Error (mm)**

	Vendors			
subsection	Dynatest	Fugro	Waylink-OSU	TxDOT
0'	-	0.06	-1.33	-
50'	-	0.05	-1.53	-
100'	-	0.06	-1.28	-
150'	-	0.00	-1.28	-
200'	-	-0.01	-1.57	-
250'	-	-0.01	-1.49	-
300'	-	0.10	-1.35	-
350'	-	-0.03	-1.55	-
400'	-	-0.05	-1.39	-
450'	-	-0.06	-1.43	-
500'	-	0.00	-1.15	-
550'	-	-0.06	-0.32	-
Total		0.07	-15.67	
Average	-	0.01	-1.31	-
Std. Dev.		0.05	0.33	

Appendix C. Average Texture Every Subsection (Outer Wheelpath)

Table C1: Average outer wheelpath texture every subsection for AutoDC1_FM973-1

***Outer* wheelpath (OWP) - Mean Profile Depth, MPD (mm)**

		Vendors			
subsection	Reference	Dynatest	Fugro	Waylink-OSU	TxDOT
0'	0.48	0.61	-	2.545	1.745
50'	0.47	0.38	0.64	3.615	-
100'	0.4	0.39	0.59	2.322	-
150'	0.44	0.57	0.63	2.102	-
200'	0.47	0.21	0.66	1.81	-
250'	0.4	0.40	0.57	1.798	-
300'	0.53	0.40	0.62	1.87	-
350'	0.5	0.56	0.67	1.746	-
400'	0.59	0.65	0.61	1.868	-
450'	0.54	0.36	0.61	2.831	-
500'	0.48	0.57	0.67	2.36	-
550'	0.53	0.45	0.61	1.78	-
Average	0.49	0.46	0.62	2.22	1.745

***Outer* wheelpath (OWP) - MPD Error (mm)**

	Vendors			
subsection	Dynatest	Fugro	Waylink-OSU	TxDOT
0'	-0.13	-	-2.07	-1.27
50'	0.09	-0.17	-3.15	-
100'	0.01	-0.19	-1.92	-
150'	-0.13	-0.19	-1.66	-
200'	0.26	-0.19	-1.34	-
250'	0.00	-0.17	-1.40	-
300'	0.13	-0.09	-1.34	-
350'	-0.06	-0.17	-1.25	-
400'	-0.06	-0.02	-1.28	-
450'	0.18	-0.07	-2.29	-
500'	-0.09	-0.19	-1.88	-
550'	0.08	-0.08	-1.25	-
Total	0.29	-1.52	-20.82	-1.27
Average	0.02	-0.14	-1.73	-1.26
Std. Dev.	0.13	0.06	0.57	

Table C2: Average outer wheelpath texture every subsection for AutoDC2_FM3177-1

***Outer* wheelpath (OWP) - Mean Profile Depth, MPD (mm)**

		Vendors			
subsection	Reference	Dynatest	Fugro	Waylink-OSU	TxDOT
0'	1.06	0.65	0.68	1.727	1.788
50'	1.43	0.71	0.73	1.796	-
100'	1.29	0.81	0.70	1.762	-
150'	0.87	0.55	0.56	1.628	-
200'	1.37	0.64	0.64	1.711	-
250'	0.66	0.23	0.54	1.763	-
300'	0.62	0.48	0.50	1.755	-
350'	0.66	0.36	0.55	1.822	-
400'	0.54	0.52	0.54	1.795	-
450'	0.75	0.46	0.47	1.549	-
500'	1.29	0.37	0.63	1.845	-
550'	1.45	0.54	0.85	2.109	-
Average	1.00	0.53	0.62	1.77	1.788

***Outer* wheelpath (OWP) - MPD Error (mm)**

	Vendors			
subsection	Dynatest	Fugro	Waylink-OSU	TxDOT
0'	0.41	0.38	-0.67	-0.73
50'	0.72	0.70	-0.37	-
100'	0.48	0.59	-0.47	-
150'	0.32	0.31	-0.76	-
200'	0.73	0.73	-0.34	-
250'	0.43	0.12	-1.10	-
300'	0.14	0.12	-1.14	-
350'	0.30	0.11	-1.16	-
400'	0.02	0.00	-1.26	-
450'	0.29	0.28	-0.80	-
500'	0.92	0.66	-0.56	-
550'	0.91	0.60	-0.66	-
Total	5.66	4.59	-9.27	-0.73
Average	0.47	0.38	-0.77	-0.79
Std. Dev.	0.29	0.26	0.32	

Table C3: Average outer wheelpath texture every subsection for AutoDC3_FM696-1

***Outer* wheelpath (OWP) - Mean Profile Depth, MPD (mm)**

		Vendors			
subsection	Reference	Dynatest	Fugro	Waylink-OSU	TxDOT
0'	0.95	0.64	0.67	2.21	4.513
50'	1.23	0.92	0.64	2.756	-
100'	1.49	1.00	0.63	1.963	-
150'	1.23	0.52	0.69	2.284	-
200'	1.67	0.51	0.79	1.981	-
250'	1.44	0.90	0.74	1.979	-
300'	0.97	0.58	0.82	2.131	-
350'	0.93	0.42	0.62	2.381	-
400'	0.69	0.69	0.90	2.42	-
450'	1.29	1.14	0.86	2.29	-
500'	1.11	0.74	0.68	1.909	-
550'	1.41	0.92	0.70	1.887	-
Average	1.20	0.75	0.73	2.18	4.513

***Outer* wheelpath (OWP) - MPD Error (mm)**

	Vendors			
subsection	Dynatest	Fugro	Waylink-OSU	TxDOT
0'	0.31	0.28	-1.26	-3.56
50'	0.31	0.59	-1.53	-
100'	0.49	0.86	-0.47	-
150'	0.71	0.54	-1.05	-
200'	1.16	0.88	-0.31	-
250'	0.54	0.70	-0.54	-
300'	0.39	0.15	-1.16	-
350'	0.51	0.31	-1.45	-
400'	0.00	-0.21	-1.73	-
450'	0.15	0.43	-1.00	-
500'	0.37	0.43	-0.80	-
550'	0.49	0.71	-0.48	-
Total	5.44	5.67	-11.78	-3.56
Average	0.45	0.47	-0.98	-3.31
Std. Dev.	0.29	0.31	0.47	

Table C4: Average outer wheelpath texture every subsection for AutoDC4_FM696-3

***Outer* wheelpath (OWP) - Mean Profile Depth, MPD (mm)**

		Vendors			
subsection	Reference	Dynatest	Fugro	Waylink-OSU	TxDOT
0'	0.59	0.65	0.54	1.56	3.122
50'	0.56	0.53	0.51	1.511	-
100'	0.57	0.47	0.49	1.555	-
150'	0.7	0.67	0.53	1.55	-
200'	0.6	0.34	0.46	1.527	-
250'	0.54	0.41	0.45	1.526	-
300'	0.57	0.52	0.53	1.514	-
350'	0.63	0.46	0.51	1.563	-
400'	0.48	0.56	0.49	1.493	-
450'	0.56	0.47	0.52	1.404	-
500'	0.49	0.57	0.50	1.447	-
550'	0.45	0.60	0.50	1.487	-
Average	0.56	0.52	0.50	1.51	3.122

***Outer* wheelpath (OWP) - MPD Error (mm)**

	Vendors			
subsection	Dynatest	Fugro	Waylink-OSU	TxDOT
0'	-0.06	0.05	-0.97	-2.53
50'	0.03	0.05	-0.95	-
100'	0.10	0.08	-0.99	-
150'	0.03	0.17	-0.85	-
200'	0.26	0.14	-0.93	-
250'	0.13	0.09	-0.99	-
300'	0.05	0.04	-0.94	-
350'	0.17	0.12	-0.93	-
400'	-0.08	-0.01	-1.01	-
450'	0.09	0.04	-0.84	-
500'	-0.08	-0.01	-0.96	-
550'	-0.15	-0.05	-1.04	-
Total	0.47	0.71	-11.40	-2.53
Average	0.04	0.06	-0.95	-2.56
Std. Dev.	0.12	0.06	0.06	

Table C5: Average outer wheelpath texture every subsection for AutoDC5_FM696-4

***Outer* wheelpath (OWP) - Mean Profile Depth, MPD (mm)**

		Vendors			
subsection	Reference	Dynatest	Fugro	Waylink-OSU	TxDOT
0'	0.5	0.59	0.49	1.44	2.049
50'	0.48	0.50	0.50	1.545	-
100'	0.5	0.33	0.50	1.627	-
150'	0.5	0.48	0.52	1.593	-
200'	0.43	0.53	0.52	1.708	-
250'	0.53	0.60	0.53	1.603	-
300'	0.48	0.42	0.52	1.664	-
350'	0.41	0.42	0.56	1.658	-
400'	0.55	0.50	0.56	1.683	-
450'	0.58	0.46	0.53	1.618	-
500'	0.54	0.53	0.56	1.706	-
550'	0.57	0.60	-	1.63	-
Average	0.51	0.50	0.53	1.62	2.049

***Outer* wheelpath (OWP) - MPD Error (mm)**

	Vendors			
subsection	Dynatest	Fugro	Waylink-OSU	TxDOT
0'	-0.09	0.01	-0.94	-1.55
50'	-0.02	-0.02	-1.07	-
100'	0.17	0.00	-1.13	-
150'	0.02	-0.02	-1.09	-
200'	-0.10	-0.09	-1.28	-
250'	-0.07	0.00	-1.07	-
300'	0.06	-0.04	-1.18	-
350'	-0.01	-0.15	-1.25	-
400'	0.05	-0.01	-1.13	-
450'	0.12	0.05	-1.04	-
500'	0.01	-0.02	-1.17	-
550'	-0.03	-	-1.06	-
Total	0.11	-0.30	-13.41	-1.55
Average	0.01	-0.02	-1.12	-1.54
Std. Dev.	0.08	0.05	0.09	

Table C6: Average outer wheelpath texture every subsection for AutoDC6_FM696-2

***Outer* wheelpath (OWP) - Mean Profile Depth, MPD (mm)**

		Vendors			
subsection	Reference	Dynatest	Fugro	Waylink-OSU	TxDOT
0'	1.35	0.97	-	2.484	1.427
50'	0.65	0.60	0.82	2.123	-
100'	1.27	0.94	0.82	2.447	-
150'	1.09	1.13	0.85	2.264	-
200'	1.07	0.95	0.82	2.215	-
250'	0.91	0.92	0.94	2.596	-
300'	0.97	0.93	0.85	2.123	-
350'	0.87	0.62	0.78	3.131	-
400'	0.77	0.71	0.77	2.102	-
450'	0.81	1.18	0.97	2.367	-
500'	0.84	0.92	0.94	3.454	-
550'	0.76	0.97	0.89	2.471	-
Average	0.95	0.90	0.86	2.48	1.427

***Outer* wheelpath (OWP) - MPD Error (mm)**

	Vendors			
subsection	Dynatest	Fugro	Waylink-OSU	TxDOT
0'	0.38	-	-1.13	-0.08
50'	0.05	-0.17	-1.47	-
100'	0.33	0.45	-1.18	-
150'	-0.04	0.24	-1.17	-
200'	0.12	0.25	-1.15	-
250'	-0.01	-0.03	-1.69	-
300'	0.04	0.12	-1.15	-
350'	0.25	0.09	-2.26	-
400'	0.06	0.00	-1.33	-
450'	-0.37	-0.16	-1.56	-
500'	-0.08	-0.10	-2.61	-
550'	-0.21	-0.13	-1.71	-
Total	0.53	0.57	-18.42	-0.08
Average	0.04	0.09	-1.53	-0.48
Std. Dev.	0.21	0.20	0.48	

Table C7: Average outer wheelpath texture every subsection for AutoDC7_FM696-5

***Outer* wheelpath (OWP) - Mean Profile Depth, MPD (mm)**

		Vendors			
subsection	Reference	Dynatest	Fugro	Waylink-OSU	TxDOT
0'	1.08	0.67	0.68	1.938	2.978
50'	1.07	0.60	0.56	1.794	-
100'	1.29	1.16	0.86	2.358	-
150'	0.99	0.73	0.68	1.73	-
200'	0.95	0.69	0.55	1.769	-
250'	1.11	0.62	0.67	1.782	-
300'	1.11	0.59	0.63	1.768	-
350'	0.93	0.85	0.64	1.714	-
400'	1.49	1.15	1.28	2.626	-
450'	1.48	1.29	1.24	2.501	-
500'	1.42	1.06	1.13	2.273	-
550'	1.64	0.77	1.17	2.14	-
Average	1.21	0.85	0.84	2.03	2.978

***Outer* wheelpath (OWP) - MPD Error (mm)**

	Vendors			
subsection	Dynatest	Fugro	Waylink-OSU	TxDOT
0'	0.41	0.40	-0.86	-1.90
50'	0.47	0.51	-0.72	-
100'	0.13	0.43	-1.07	-
150'	0.26	0.31	-0.74	-
200'	0.26	0.40	-0.82	-
250'	0.49	0.44	-0.67	-
300'	0.52	0.48	-0.66	-
350'	0.08	0.29	-0.78	-
400'	0.34	0.21	-1.14	-
450'	0.19	0.24	-1.02	-
500'	0.36	0.29	-0.85	-
550'	0.87	0.47	-0.50	-
Total	4.37	4.48	-9.83	-1.90
Average	0.36	0.37	-0.82	-1.76
Std. Dev.	0.21	0.10	0.18	

Table C8: Average outer wheelpath texture every subsection for AutoDC8_FM619-1

***Outer* wheelpath (OWP) - Mean Profile Depth, MPD (mm)**

		Vendors			
subsection	Reference	Dynatest	Fugro	Waylink-OSU	TxDOT
0'	2.33	1.13	1.31	3.13	4.101
50'	2.5	1.12	1.47	3.057	-
100'	1.66	0.97	0.85	2.277	-
150'	1.2	0.90	0.87	2.123	-
200'	0.92	0.98	0.75	1.985	-
250'	2.23	1.28	1.25	3.064	-
300'	1.24	0.87	0.83	3.016	-
350'	1.65	1.10	0.84	2.824	-
400'	1.81	0.70	0.91	4.187	-
450'	1.64	0.99	0.83	2.891	-
500'	1.7	0.93	0.72	2.457	-
550'	1.79	0.96	1.04	3.291	-
Average	1.72	0.99	0.97	2.86	4.101

***Outer* wheelpath (OWP) - MPD Error (mm)**

	Vendors			
subsection	Dynatest	Fugro	Waylink-OSU	TxDOT
0'	1.20	1.02	-0.80	-1.77
50'	1.38	1.03	-0.56	-
100'	0.69	0.81	-0.62	-
150'	0.30	0.33	-0.92	-
200'	-0.06	0.17	-1.07	-
250'	0.95	0.98	-0.83	-
300'	0.37	0.41	-1.78	-
350'	0.55	0.81	-1.17	-
400'	1.11	0.90	-2.38	-
450'	0.65	0.81	-1.25	-
500'	0.77	0.98	-0.76	-
550'	0.83	0.75	-1.50	-
Total	8.75	9.00	-13.63	-1.77
Average	0.73	0.75	-1.14	-2.38
Std. Dev.	0.41	0.29	0.53	

Table C9: Average outer wheelpath texture every subsection for AutoDC9_FM112-1

***Outer* wheelpath (OWP) - Mean Profile Depth, MPD (mm)**

		Vendors			
subsection	Reference	Dynatest	Fugro	Waylink-OSU	TxDOT
0'	1.19	1.08	0.80	1.654	3.3
50'	0.79	0.59	0.73	2.021	-
100'	1.71	0.84	0.78	1.723	-
150'	1.02	1.05	0.79	1.706	-
200'	0.98	1.33	1.02	2.012	-
250'	1.74	0.92	0.85	1.954	-
300'	0.76	0.72	0.65	1.236	-
350'	0.94	1.12	0.65	1.865	-
400'	1.29	1.34	0.82	2.05	-
450'	1.55	0.95	0.90	2.494	-
500'	1.39	1.28	0.96	2.117	-
550'	1.13	0.99	1.06	1.467	-
Average	1.21	1.02	0.83	1.86	3.3

***Outer* wheelpath (OWP) - MPD Error (mm)**

	Vendors			
subsection	Dynatest	Fugro	Waylink-OSU	TxDOT
0'	0.11	0.39	-0.46	-2.11
50'	0.20	0.06	-1.23	-
100'	0.87	0.93	-0.01	-
150'	-0.03	0.23	-0.69	-
200'	-0.35	-0.04	-1.03	-
250'	0.82	0.89	-0.21	-
300'	0.04	0.11	-0.48	-
350'	-0.18	0.29	-0.93	-
400'	-0.05	0.47	-0.76	-
450'	0.60	0.65	-0.94	-
500'	0.11	0.43	-0.73	-
550'	0.14	0.07	-0.34	-
Total	2.27	4.49	-7.81	-2.11
Average	0.19	0.37	-0.65	-2.09
Std. Dev.	0.38	0.32	0.36	

Table C10: Average outer wheelpath texture every subsection for AutoDC10_FM1331-1

***Outer* wheelpath (OWP) - Mean Profile Depth, MPD (mm)**

		Vendors			
subsection	Reference	Dynatest	Fugro	Waylink-OSU	TxDOT
0'	1.47	0.77	0.87	3.291	3.481
50'	1.34	0.92	0.88	4.757	-
100'	1.32	0.52	0.80	86.9	-
150'	1.7	0.75	0.83	3.518	-
200'	1.29	0.54	0.84	3.206	-
250'	1.52	0.94	1.08	2.907	-
300'	1.6	1.02	0.98	2.995	-
350'	1.36	0.61	0.97	2.872	-
400'	1.39	0.87	1.00	4.451	-
450'	1.48	1.00	1.08	3.739	-
500'	1.6	1.24	1.01	4.446	-
550'	1.65	0.99	-	8.744	-
Average	1.48	0.85	0.94	10.99	3.481

***Outer* wheelpath (OWP) - MPD Error (mm)**

	Vendors			
subsection	Dynatest	Fugro	Waylink-OSU	TxDOT
0'	0.70	0.60	-1.82	-2.01
50'	0.42	0.46	-3.42	-
100'	0.80	0.52	-85.58	-
150'	0.95	0.87	-1.82	-
200'	0.75	0.45	-1.92	-
250'	0.58	0.44	-1.39	-
300'	0.58	0.62	-1.40	-
350'	0.75	0.39	-1.51	-
400'	0.52	0.39	-3.06	-
450'	0.48	0.40	-2.26	-
500'	0.36	0.59	-2.85	-
550'	0.66	-	-7.09	-
Total	7.53	5.76	-114.11	-2.01
Average	0.63	0.54	-9.51	-2.00
Std. Dev.	0.17	0.14	24.01	

Table C11: Average outer wheelpath texture every subsection for AutoDC11_FM1331-2

***Outer* wheelpath (OWP) - Mean Profile Depth, MPD (mm)**

		Vendors			
subsection	Reference	Dynatest	Fugro	Waylink-OSU	TxDOT
0'	1.17	0.88	0.74	2.357	3.254
50'	0.89	0.60	0.81	2.484	-
100'	1.01	0.82	0.76	2.342	-
150'	1.03	0.83	0.69	2.776	-
200'	2.2	1.20	0.81	2.313	-
250'	1.15	0.69	0.67	2.32	-
300'	1.59	1.05	0.86	12.12	-
350'	1.75	0.87	0.87	2.667	-
400'	1.55	0.90	0.70	2.586	-
450'	0.9	0.44	0.68	2.41	-
500'	0.96	0.90	0.70	2.555	-
550'	1.54	1.11	-	2.618	-
Average	1.31	0.86	0.75	3.30	3.254

***Outer* wheelpath (OWP) - MPD Error (mm)**

	Vendors			
subsection	Dynatest	Fugro	Waylink-OSU	TxDOT
0'	0.29	0.43	-1.19	-2.08
50'	0.29	0.08	-1.59	-
100'	0.19	0.25	-1.33	-
150'	0.20	0.34	-1.75	-
200'	1.00	1.39	-0.11	-
250'	0.46	0.48	-1.17	-
300'	0.54	0.73	-10.53	-
350'	0.88	0.88	-0.92	-
400'	0.65	0.85	-1.04	-
450'	0.46	0.22	-1.51	-
500'	0.06	0.26	-1.60	-
550'	0.43	-	-1.08	-
Total	5.45	5.91	-23.81	-2.08
Average	0.45	0.56	-1.98	-1.94
Std. Dev.	0.28	0.39	2.73	

Table C12: Average outer wheelpath texture every subsection for AutoDC12_FM1063-1

***Outer* wheelpath (OWP) - Mean Profile Depth, MPD (mm)**

		Vendors			
subsection	Reference	Dynatest	Fugro	Waylink-OSU	TxDOT
0'	1.18	0.51	0.72	1.882	2.863
50'	1.2	0.43	0.84	2.332	-
100'	0.95	0.78	0.73	3.497	-
150'	2.21	1.29	1.42	3.668	-
200'	2.01	1.01	0.89	2.409	-
250'	1.24	1.12	0.61	1.84	-
300'	1.11	0.85	0.63	2.015	-
350'	1.15	0.59	0.66	1.843	-
400'	1.08	0.83	0.65	3.18	-
450'	0.84	0.45	0.56	1.764	-
500'	1.22	0.47	0.65	1.992	-
550'	1.14	0.74	0.60	1.855	-
Average	1.28	0.76	0.75	2.36	2.863

***Outer* wheelpath (OWP) - MPD Error (mm)**

	Vendors			
subsection	Dynatest	Fugro	Waylink-OSU	TxDOT
0'	0.67	0.46	-0.70	-1.68
50'	0.77	0.36	-1.13	-
100'	0.17	0.22	-2.55	-
150'	0.92	0.79	-1.46	-
200'	1.00	1.12	-0.40	-
250'	0.12	0.63	-0.60	-
300'	0.26	0.48	-0.91	-
350'	0.56	0.49	-0.69	-
400'	0.25	0.43	-2.10	-
450'	0.39	0.28	-0.92	-
500'	0.75	0.57	-0.77	-
550'	0.40	0.54	-0.72	-
Total	6.25	6.37	-12.95	-1.68
Average	0.52	0.53	-1.08	-1.59
Std. Dev.	0.30	0.24	0.65	

Table C13: Average outer wheelpath texture every subsection for AutoDC13_US79-1

***Outer* wheelpath (OWP) - Mean Profile Depth, MPD (mm)**

		Vendors			
subsection	Reference	Dynatest	Fugro	Waylink-OSU	TxDOT
0'	1.67	0.92	1.49	3.662	4.308
50'	1.6	1.38	1.44	3.803	-
100'	1.76	1.32	1.47	3.71	-
150'	1.38	1.34	1.41	3.705	-
200'	1.71	1.00	1.47	3.651	-
250'	1.95	0.86	1.43	3.672	-
300'	1.43	1.04	1.45	3.76	-
350'	1.7	0.98	1.48	3.583	-
400'	1.35	0.93	1.36	3.568	-
450'	1.42	0.89	1.41	3.674	-
500'	1.21	1.02	1.36	3.38	-
550'	1.51	1.00	-	3.311	-
Average	1.56	1.06	1.43	3.62	4.308

***Outer* wheelpath (OWP) - MPD Error (mm)**

	Vendors			
subsection	Dynatest	Fugro	Waylink-OSU	TxDOT
0'	0.75	0.18	-1.99	-2.64
50'	0.22	0.16	-2.20	-
100'	0.44	0.29	-1.95	-
150'	0.04	-0.03	-2.33	-
200'	0.71	0.24	-1.94	-
250'	1.09	0.52	-1.72	-
300'	0.39	-0.02	-2.33	-
350'	0.72	0.22	-1.88	-
400'	0.42	-0.01	-2.22	-
450'	0.53	0.01	-2.25	-
500'	0.19	-0.15	-2.17	-
550'	0.51	-	-1.80	-
Total	6.00	1.41	-24.79	-2.64
Average	0.50	0.12	-2.07	-2.75
Std. Dev.	0.29	0.19	0.21	

Table C14: Average outer wheelpath texture every subsection for AutoDC14_IH35-3

***Outer* wheelpath (OWP) - Mean Profile Depth, MPD (mm)**

		Vendors			
subsection	Reference	Dynatest	Fugro	Waylink-OSU	TxDOT
0'	0.52	0.52	0.46	1.125	1.82
50'	0.66	0.71	0.48	1.194	-
100'	0.37	0.51	0.43	1.157	-
150'	0.71	0.77	0.50	1.151	-
200'	0.39	0.51	0.48	1.211	-
250'	0.42	0.60	0.44	0.968	-
300'	0.56	0.73	0.46	1.093	-
350'	0.44	0.48	0.47	1.054	-
400'	0.41	0.47	0.40	1.05	-
450'	0.47	0.53	0.41	1.004	-
500'	0.64	0.50	0.43	1.255	-
550'	0.41	0.52	0.39	1.083	-
Average	0.50	0.57	0.45	1.11	1.82

***Outer* wheelpath (OWP) - MPD Error (mm)**

	Vendors			
subsection	Dynatest	Fugro	Waylink-OSU	TxDOT
0'	0.00	0.06	-0.61	-1.30
50'	-0.05	0.18	-0.53	-
100'	-0.14	-0.06	-0.79	-
150'	-0.06	0.21	-0.44	-
200'	-0.12	-0.09	-0.82	-
250'	-0.18	-0.02	-0.55	-
300'	-0.17	0.10	-0.53	-
350'	-0.04	-0.03	-0.61	-
400'	-0.06	0.01	-0.64	-
450'	-0.06	0.06	-0.53	-
500'	0.14	0.21	-0.62	-
550'	-0.11	0.02	-0.67	-
Total	-0.86	0.66	-7.35	-1.30
Average	-0.07	0.05	-0.61	-1.32
Std. Dev.	0.09	0.10	0.11	

Table C15: Average outer wheelpath texture every subsection for AutoDC15_Spur484-1

***Outer* wheelpath (OWP) - Mean Profile Depth, MPD (mm)**

		Vendors			
subsection	Reference	Dynatest	Fugro	Waylink-OSU	TxDOT
0'	1.2	1.11	1.07	2.437	3.385
50'	1.41	1.31	1.06	2.494	-
100'	1.24	1.20	1.03	2.446	-
150'	1.4	0.77	1.20	2.53	-
200'	1.43	1.35	1.07	2.435	-
250'	1.32	1.03	1.10	2.478	-
300'	1.37	1.15	1.13	2.483	-
350'	1.5	1.22	1.08	2.435	-
400'	1.51	1.28	1.08	2.448	-
450'	1.41	1.17	1.03	2.454	-
500'	1.22	0.98	1.04	2.347	-
550'	1.36	1.13	1.11	2.519	-
Average	1.36	1.14	1.08	2.46	3.385

***Outer* wheelpath (OWP) - MPD Error (mm)**

	Vendors			
subsection	Dynatest	Fugro	Waylink-OSU	TxDOT
0'	0.09	0.13	-1.24	-2.19
50'	0.10	0.35	-1.08	-
100'	0.04	0.21	-1.21	-
150'	0.63	0.20	-1.13	-
200'	0.08	0.36	-1.01	-
250'	0.29	0.22	-1.16	-
300'	0.22	0.24	-1.11	-
350'	0.28	0.42	-0.94	-
400'	0.23	0.43	-0.94	-
450'	0.24	0.38	-1.04	-
500'	0.24	0.18	-1.13	-
550'	0.23	0.25	-1.16	-
Total	2.68	3.35	-13.14	-2.19
Average	0.22	0.28	-1.09	-2.02
Std. Dev.	0.15	0.10	0.10	

Table C16: Average outer wheelpath texture every subsection for AutoDC16_US77-1

***Outer* wheelpath (OWP) - Mean Profile Depth, MPD (mm)**

		Vendors			
subsection	Reference	Dynatest	Fugro	Waylink-OSU	TxDOT
0'	0.7	0.68	0.43	1.112	1.555
50'	0.96	0.94	0.54	1.183	-
100'	0.81	0.88	0.52	1.254	-
150'	0.78	0.51	0.48	1.17	-
200'	0.77	0.72	0.48	1.186	-
250'	0.82	0.73	0.51	1.119	-
300'	0.6	0.80	0.47	1.27	-
350'	0.66	0.85	0.50	1.182	-
400'	0.84	0.60	0.45	1.157	-
450'	0.64	0.80	0.45	1.23	-
500'	0.65	0.52	0.48	1.123	-
550'	0.69	0.80	0.44	1.052	-
Average	0.74	0.74	0.48	1.17	1.555

***Outer* wheelpath (OWP) - MPD Error (mm)**

	Vendors			
subsection	Dynatest	Fugro	Waylink-OSU	TxDOT
0'	0.02	0.27	-0.41	-0.86
50'	0.02	0.42	-0.22	-
100'	-0.07	0.29	-0.44	-
150'	0.27	0.30	-0.39	-
200'	0.05	0.29	-0.42	-
250'	0.09	0.31	-0.30	-
300'	-0.20	0.13	-0.67	-
350'	-0.19	0.16	-0.52	-
400'	0.24	0.39	-0.32	-
450'	-0.16	0.19	-0.59	-
500'	0.13	0.17	-0.47	-
550'	-0.11	0.25	-0.36	-
Total	0.07	3.18	-5.12	-0.86
Average	0.01	0.27	-0.43	-0.81
Std. Dev.	0.16	0.09	0.13	

Table C17: Average outer wheelpath texture every subsection for AutoDC17_La_Salle-1

***Outer* wheelpath (OWP) - Mean Profile Depth, MPD (mm)**

		Vendors			
subsection	Reference	Dynatest	Fugro	Waylink-OSU	TxDOT
0'	0.53	0.47	0.53	1.49	0
50'	0.52	0.17	0.55	1.488	-
100'	0.62	0.45	0.57	1.509	-
150'	0.57	0.21	0.53	1.507	-
200'	0.61	0.44	0.56	1.513	-
250'	0.35	0.45	0.49	1.553	-
300'	0.35	0.25	0.50	1.485	-
350'	0.28	0.41	0.51	1.565	-
400'	0.37	0.44	0.55	1.591	-
450'	0.5	0.36	0.55	1.513	-
500'	0.55	0.41	0.56	1.52	-
550'	0.45	0.43	-	1.565	-
Average	0.48	0.37	0.54	1.52	0

***Outer* wheelpath (OWP) - MPD Error (mm)**

	Vendors			
subsection	Dynatest	Fugro	Waylink-OSU	TxDOT
0'	0.06	0.00	-0.96	0.53
50'	0.35	-0.03	-0.97	-
100'	0.17	0.05	-0.89	-
150'	0.36	0.04	-0.94	-
200'	0.17	0.05	-0.90	-
250'	-0.10	-0.14	-1.20	-
300'	0.10	-0.15	-1.14	-
350'	-0.13	-0.23	-1.29	-
400'	-0.07	-0.18	-1.22	-
450'	0.14	-0.05	-1.01	-
500'	0.14	-0.01	-0.97	-
550'	0.02	-	-1.12	-
Total	1.21	-0.65	-12.60	0.53
Average	0.10	-0.06	-1.05	0.48
Std. Dev.	0.16	0.10	0.14	

Table C18: Average outer wheelpath texture every subsection for AutoDC18_IH35-1

***Outer* wheelpath (OWP) - Mean Profile Depth, MPD (mm)**

		Vendors			
subsection	Reference	Dynatest	Fugro	Waylink-OSU	TxDOT
0'	0.5	0.59	0.47	1.691	2.015
50'	0.65	0.38	0.43	1.28	-
100'	0.7	0.79	0.47	1.562	-
150'	0.78	0.77	0.47	1.555	-
200'	0.54	0.65	0.41	1.219	-
250'	0.96	0.65	0.62	1.804	-
300'	0.68	0.85	0.65	1.644	-
350'	1.25	0.91	0.72	2.021	-
400'	0.63	0.87	0.70	1.775	-
450'	1.08	0.53	0.75	1.754	-
500'	0.84	1.14	0.68	1.709	-
550'	0.95	0.94	0.48	1.955	-
Average	0.80	0.75	0.57	1.66	2.015

***Outer* wheelpath (OWP) - MPD Error (mm)**

	Vendors			
subsection	Dynatest	Fugro	Waylink-OSU	TxDOT
0'	-0.09	0.03	-1.19	-1.52
50'	0.27	0.22	-0.63	-
100'	-0.09	0.23	-0.86	-
150'	0.01	0.31	-0.78	-
200'	-0.11	0.13	-0.68	-
250'	0.31	0.34	-0.84	-
300'	-0.17	0.03	-0.96	-
350'	0.34	0.53	-0.77	-
400'	-0.24	-0.07	-1.15	-
450'	0.55	0.33	-0.67	-
500'	-0.30	0.16	-0.87	-
550'	0.01	0.47	-1.01	-
Total	0.50	2.72	-10.41	-1.52
Average	0.04	0.23	-0.87	-1.22
Std. Dev.	0.27	0.18	0.18	

Table C19: Average outer wheelpath texture every subsection for AutoDC19_IH35-2

***Outer* wheelpath (OWP) - Mean Profile Depth, MPD (mm)**

		Vendors			
subsection	Reference	Dynatest	Fugro	Waylink-OSU	TxDOT
0'	1.09	0.99	0.53	2.114	1.609
50'	0.28	0.50	0.43	1.176	-
100'	0.4	0.50	0.46	1.341	-
150'	0.37	0.87	0.46	1.391	-
200'	0.46	0.37	0.45	1.287	-
250'	0.35	0.58	0.43	1.26	-
300'	0.37	0.27	0.45	1.273	-
350'	0.41	0.39	0.46	1.317	-
400'	0.32	0.41	0.43	1.157	-
450'	0.5	0.37	0.57	1.549	-
500'	0.44	0.63	0.43	1.302	-
550'	0.47	0.55	0.48	1.468	-
Average	0.46	0.54	0.46	1.39	1.609

***Outer* wheelpath (OWP) - MPD Error (mm)**

	Vendors			
subsection	Dynatest	Fugro	Waylink-OSU	TxDOT
0'	0.10	0.56	-1.02	-0.52
50'	-0.22	-0.15	-0.90	-
100'	-0.10	-0.06	-0.94	-
150'	-0.50	-0.09	-1.02	-
200'	0.09	0.01	-0.83	-
250'	-0.23	-0.08	-0.91	-
300'	0.10	-0.08	-0.90	-
350'	0.02	-0.05	-0.91	-
400'	-0.09	-0.11	-0.84	-
450'	0.13	-0.07	-1.05	-
500'	-0.19	0.01	-0.86	-
550'	-0.08	-0.01	-1.00	-
Total	-0.97	-0.12	-11.18	-0.52
Average	-0.08	-0.01	-0.93	-1.15
Std. Dev.	0.19	0.19	0.08	

Table C20: Average outer wheelpath texture every subsection for AutoDC20_US84-1

***Outer* wheelpath (OWP) - Mean Profile Depth, MPD (mm)**

		Vendors			
subsection	Reference	Dynatest	Fugro	Waylink-OSU	TxDOT
0'	0.55	0.66	0.49	1.696	1.581
50'	0.4	0.56	0.49	1.612	-
100'	0.3	0.39	0.46	1.581	-
150'	0.5	0.47	0.43	1.403	-
200'	0.36	0.45	0.42	1.608	-
250'	0.34	0.59	0.43	1.63	-
300'	0.42	0.56	0.44	1.425	-
350'	0.36	0.37	0.45	1.455	-
400'	0.27	0.39	0.46	1.65	-
450'	0.29	0.56	0.43	1.516	-
500'	0.34	0.38	0.45	1.809	-
550'	0.41	0.61	0.45	0.833	-
Average	0.38	0.50	0.45	1.52	1.581

***Outer* wheelpath (OWP) - MPD Error (mm)**

	Vendors			
subsection	Dynatest	Fugro	Waylink-OSU	TxDOT
0'	-0.11	0.06	-1.15	-1.03
50'	-0.16	-0.09	-1.21	-
100'	-0.09	-0.16	-1.28	-
150'	0.03	0.07	-0.90	-
200'	-0.09	-0.06	-1.25	-
250'	-0.25	-0.09	-1.29	-
300'	-0.14	-0.02	-1.01	-
350'	-0.01	-0.09	-1.10	-
400'	-0.12	-0.19	-1.38	-
450'	-0.27	-0.14	-1.23	-
500'	-0.04	-0.11	-1.47	-
550'	-0.20	-0.04	-0.42	-
Total	-1.45	-0.87	-13.68	-1.03
Average	-0.12	-0.07	-1.14	-1.20
Std. Dev.	0.09	0.08	0.27	

Appendix D. Cross Slope For Each 50-Ft Subsection

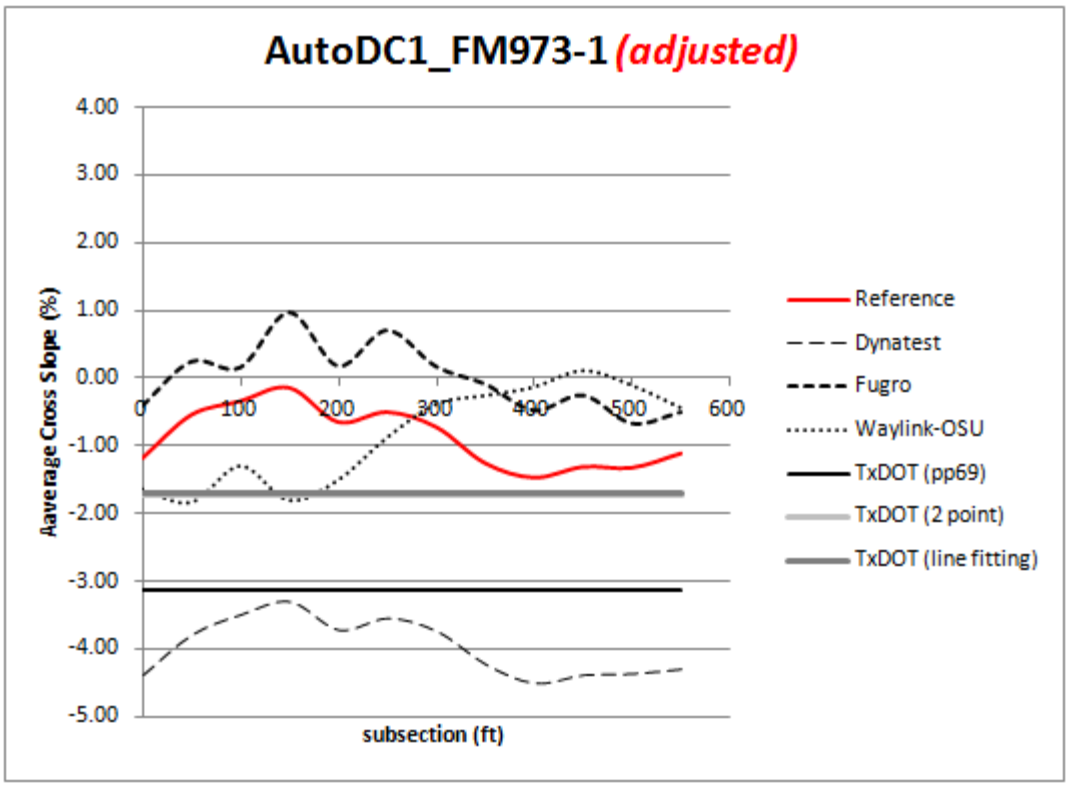

Figure D1: Cross slope for each 50-ft. subsection for AutoDC1_FM973-1

Table D1: Cross slope error for each 50-ft. subsection for AutoDC1_FM973-1

	Vendor - ***Error after adjusted (percent)***					
	Dynatest	**Fugro**	**Waylink-OSU**	**TxDOT**		
subsection (ft)	(percent)	for entire lane width (percent)	(percent) average	using AASHTO pp69 algorithm (percent)	using 2 point algorithm (percent)	using line fitting algorithm (percent)
0	3.19	-0.78	0.44			
50	3.24	-0.79	1.28			
100	3.15	-0.51	0.94			
150	3.15	-1.13	1.65			
200	3.06	-0.84	0.84			
250	3.04	-1.22	0.36			
300	3.01	-0.90	-0.35			
350	2.96	-1.17	-1.01			
400	3.03	-1.00	-1.35			
450	3.07	-1.06	-1.44			
500	3.04	-0.66	-1.23			
550	3.18	-0.61	-0.69			
average	**3.09**	**-0.89**	**-0.05**	**2.25**	**0.85**	**0.80**
std. dev.	0.09	0.23	1.10			

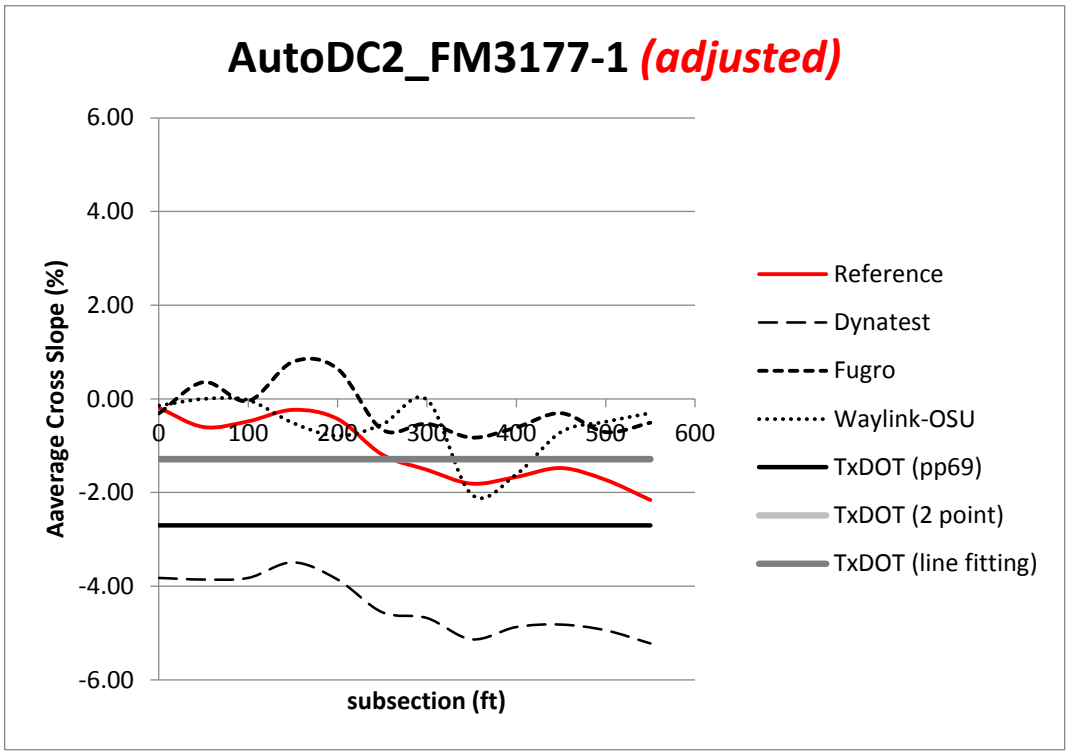

Figure D2: Cross slope for each 50-ft. subsection for AutoDC2_FM3177-1

Table D2: Cross slope error for each 50-ft. subsection for AutoDC2_FM3177-1

subsection (ft)	Vendor - *Error after adjusted (percent)*			TxDOT		
	Dynatest	**Fugro**	**Waylink-OSU**			
	(percent)	for entire lane width (percent)	(percent) average	using AASHTO pp69 algorithm (percent)	using 2 point algorithm (percent)	using line fitting algorithm (percent)
0	3.63	0.12	-0.05			
50	3.26	-0.96	-0.60			
100	3.34	-0.43	-0.45			
150	3.26	-1.03	0.28			
200	3.43	-1.07	0.36			
250	3.37	-0.53	-0.64			
300	3.17	-0.98	-1.50			
350	3.32	-0.98	0.23			
400	3.21	-1.06	-0.05			
450	3.34	-1.17	-0.77			
500	3.21	-1.02	-1.24			
550	3.06	-1.65	-1.86			
average	**3.30**	**-0.90**	**-0.52**	**1.58**	**0.17**	**0.16**
std. dev.	0.14	0.44	0.72			

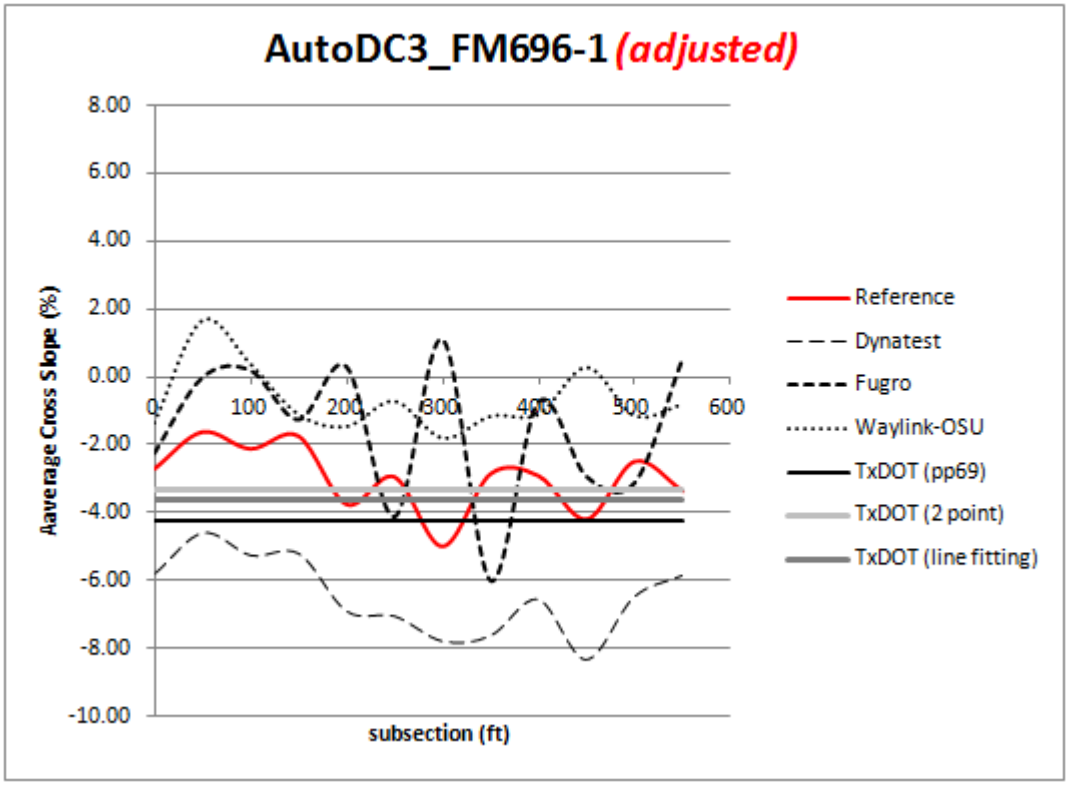

Figure D3: Cross slope for each 50-ft. subsection for AutoDC3_FM696-1

Table D3: Cross slope error for each 50-ft. subsection for AutoDC3_FM696-1

	Vendor - ***Error after adjusted (percent)***					
	Dynatest	**Fugro**	**Waylink-OSU**	**TxDOT**		
subsection (ft)	(percent)	for entire lane width (percent)	(percent) average	using AASHTO pp69 algorithm (percent)	using 2 point algorithm (percent)	using line fitting algorithm (percent)
0	3.03	-0.49	-1.38			
50	2.93	-1.64	-3.31			
100	3.10	-2.35	-2.53			
150	3.42	-0.52	-0.66			
200	3.11	-4.09	-2.30			
250	4.06	1.15	-2.25			
300	2.75	-6.13	-3.19			
350	4.73	3.13	-1.71			
400	3.60	-2.22	-1.83			
450	4.10	-1.28	-4.49			
500	3.95	0.60	-1.36			
550	2.46	-3.95	-2.57			
average	**3.44**	**-1.48**	**-2.30**	**1.24**	**0.34**	**0.64**
std. dev.	0.66	2.53	1.03			

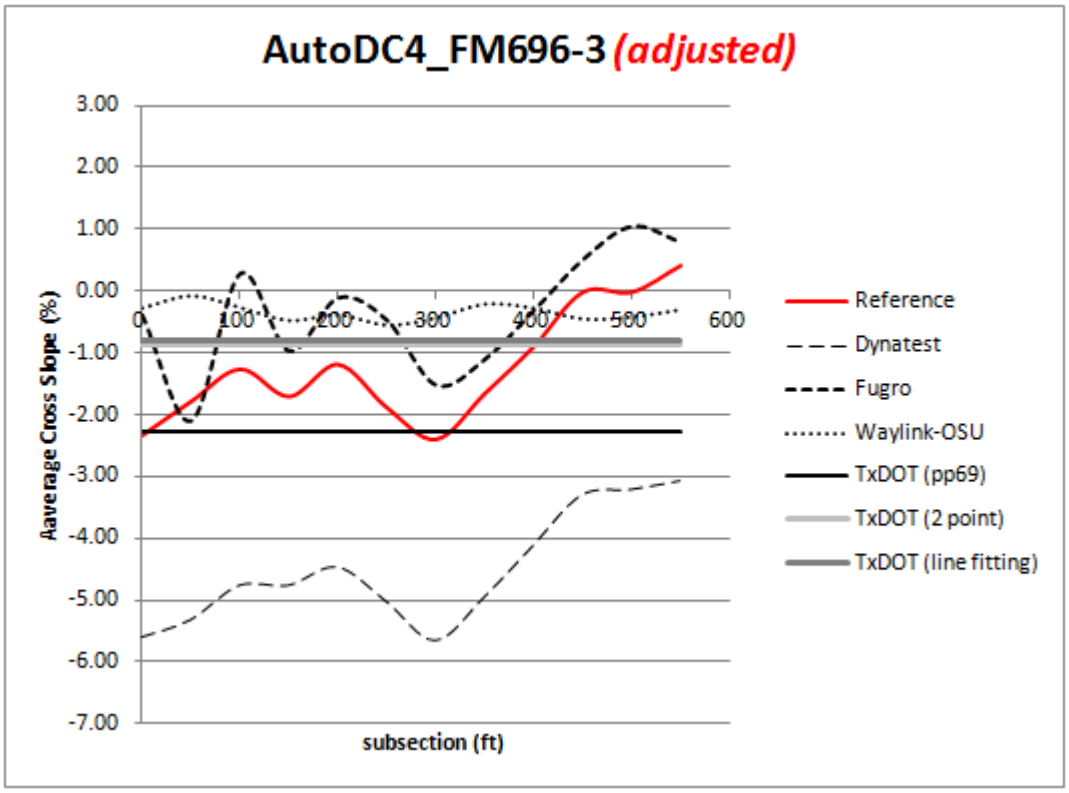

Figure D4: Cross slope for each 50-ft. subsection for AutoDC4_FM696-3

Table D4: Cross slope error for each 50-ft. subsection for AutoDC4_FM696-3

	Vendor - ***Error after adjusted (percent)***			**TxDOT**		
	Dynatest	**Fugro**	**Waylink-OSU**			
subsection (ft)	(percent)	for entire lane width (percent)	(percent) average	using AASHTO pp69 algorithm (percent)	using 2 point algorithm (percent)	using line fitting algorithm (percent)
0	3.27	-1.95	-2.05			
50	3.54	0.32	-1.70			
100	3.50	-1.55	-0.99			
150	3.06	-0.74	-1.22			
200	3.28	-1.08	-0.79			
250	3.14	-1.42	-1.33			
300	3.25	-0.88	-1.96			
350	3.30	-0.55	-1.44			
400	3.23	-0.58	-0.61			
450	3.29	-0.52	0.45			
500	3.20	-1.06	0.42			
550	3.49	-0.38	0.73			
average	**3.29**	**-0.87**	**-0.88**	**1.03**	**-0.37**	**-0.43**
std. dev.	0.15	0.60	0.95			

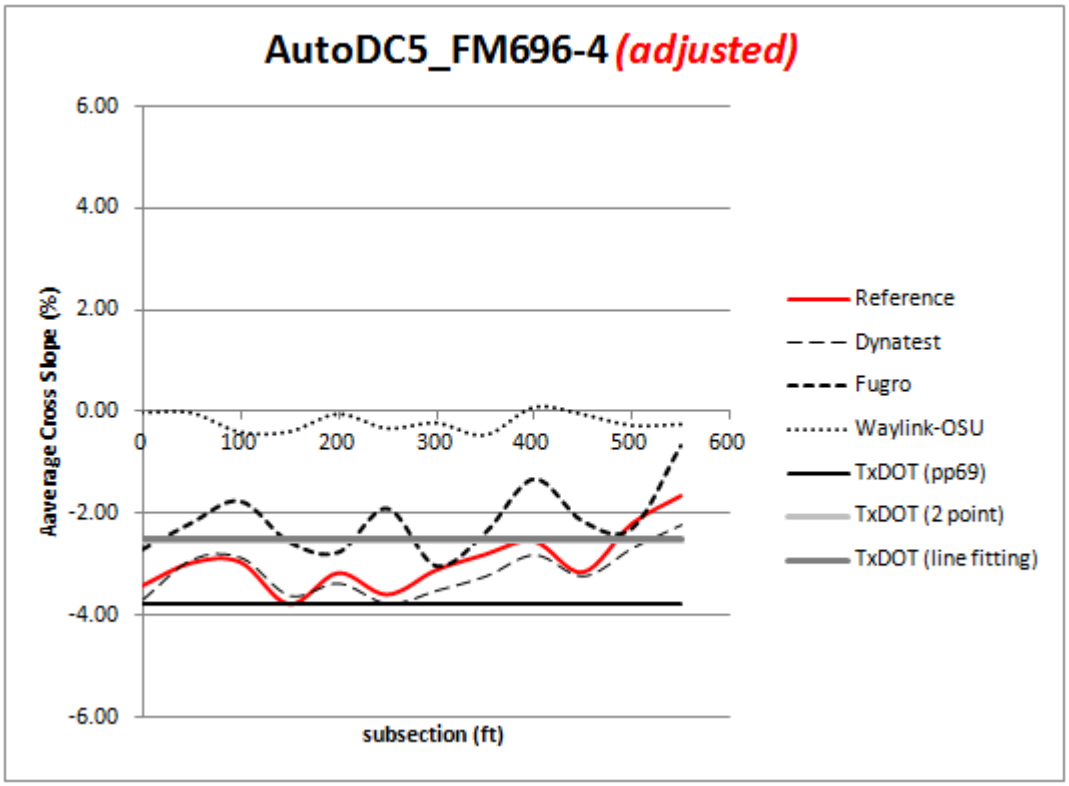

Figure D5: Cross slope for each 50-ft. subsection for AutoDC5_FM696-4

Table D5: Cross slope error for each 50-ft. subsection for AutoDC5_FM696-4

	Vendor - ***Error after adjusted (percent)***			**TxDOT**		
	Dynatest	**Fugro**	**Waylink-OSU**			
subsection (ft)	(percent)	for entire lane width (percent)	(percent) average	using AASHTO pp69 algorithm (percent)	using 2 point algorithm (percent)	using line fitting algorithm (percent)
0	0.28	-0.69	-3.40			
50	-0.06	-0.77	-2.96			
100	-0.08	-1.18	-2.55			
150	-0.15	-1.20	-3.39			
200	0.21	-0.39	-3.13			
250	0.19	-1.68	-3.27			
300	0.41	-0.06	-2.90			
350	0.44	-0.41	-2.35			
400	0.27	-1.22	-2.64			
450	0.09	-0.99	-3.11			
500	0.48	0.11	-1.94			
550	0.57	-0.98	-1.42			
average	**0.22**	**-0.79**	**-2.75**	**0.84**	**-0.41**	**-0.45**
std. dev.	0.23	0.52	0.61			

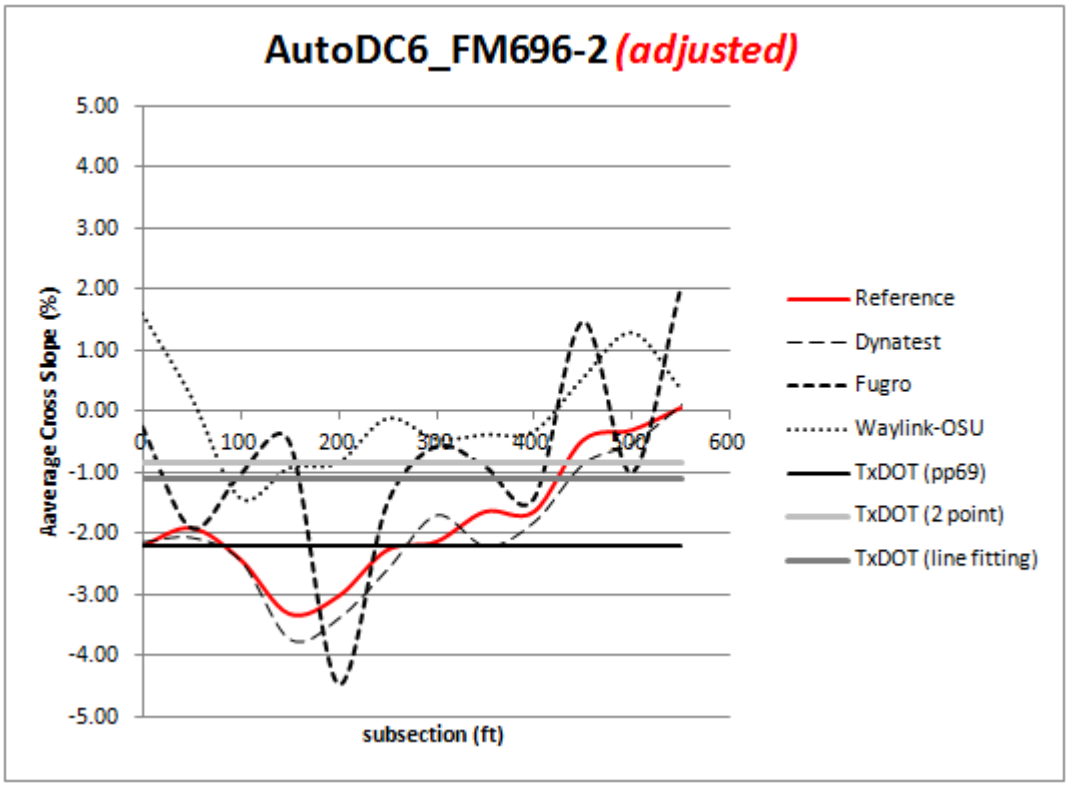

Figure D6: Cross slope for each 50-ft. subsection for AutoDC6_FM696-2

Table D6: Cross slope error for each 50-ft. subsection for AutoDC6_FM696-2

	Vendor - ***Error after adjusted (percent)***			**TxDOT**		
	Dynatest	**Fugro**	**Waylink-OSU**			
subsection (ft)	(percent)	for entire lane width (percent)	(percent) average	using AASHTO pp69 algorithm (percent)	using 2 point algorithm (percent)	using line fitting algorithm (percent)
0	-0.06	-1.94	-3.80			
50	0.16	0.01	-2.14			
100	0.03	-1.38	-0.99			
150	0.41	-2.81	-2.37			
200	0.35	1.44	-2.18			
250	0.31	-0.75	-2.15			
300	-0.43	-1.55	-1.68			
350	0.57	-0.73	-1.25			
400	0.17	-0.21	-1.31			
450	0.39	-1.93	-1.01			
500	0.23	0.71	-1.59			
550	-0.03	-1.95	-0.30			
average	**0.17**	**-0.92**	**-1.73**	**0.43**	**-0.92**	**-0.67**
std. dev.	0.27	1.24	0.89			

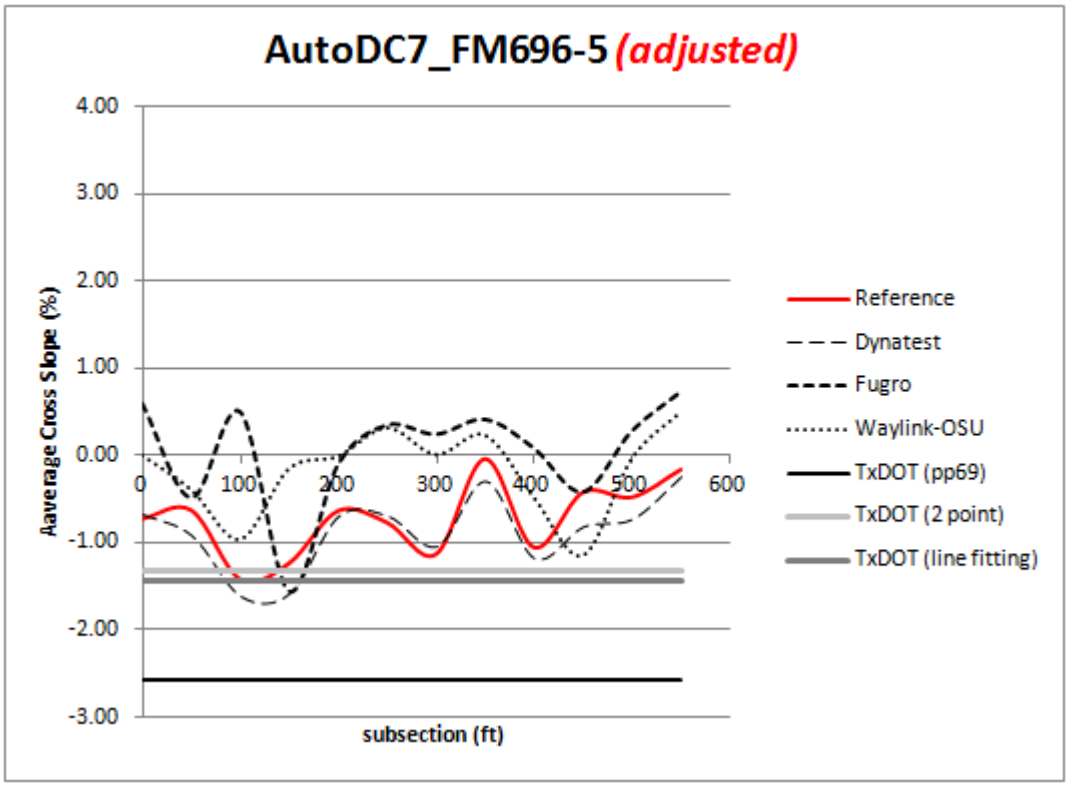

Figure D7: Cross slope for each 50-ft. subsection for AutoDC7_FM696-5

Table D7: Cross slope error for each 50-ft. subsection for AutoDC7_FM696-5

	Vendor - ***Error after adjusted (percent)***			**TxDOT**		
	Dynatest	**Fugro**	**Waylink-OSU**			
subsection (ft)	(percent)	for entire lane width (percent)	(percent) average	using AASHTO pp69 algorithm (percent)	using 2 point algorithm (percent)	using line fitting algorithm (percent)
0	-0.05	-1.33	-0.72			
50	0.29	-0.15	-0.23			
100	0.21	-1.92	-0.44			
150	0.36	0.33	-1.08			
200	0.06	-0.54	-0.63			
250	-0.07	-1.13	-1.09			
300	-0.08	-1.38	-1.14			
350	0.24	-0.47	-0.28			
400	0.13	-1.14	-0.56			
450	0.39	-0.01	0.72			
500	0.25	-0.77	-0.45			
550	0.07	-0.91	-0.67			
average	**0.15**	**-0.78**	**-0.55**	**1.85**	**0.60**	**0.72**
std. dev.	0.17	0.65	0.50			

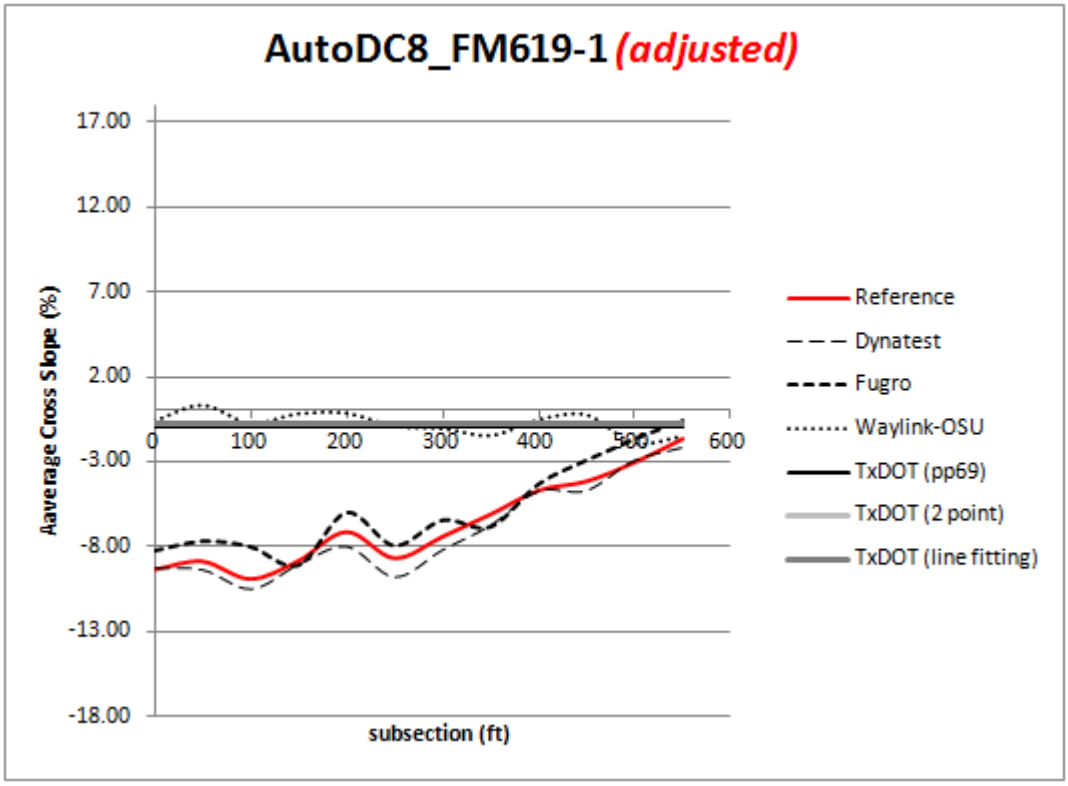

Figure D8: Cross slope for each 50-ft. subsection for AutoDC8_FM619-1

Table D8: Cross slope error for each 50-ft. subsection for AutoDC8_FM619-1

subsection (ft)	Vendor - *Error after adjusted (percent)*			TxDOT		
	Dynatest	**Fugro**	**Waylink-OSU**			
	(percent)	for entire lane width (percent)	(percent) average	using AASHTO pp69 algorithm (percent)	using 2 point algorithm (percent)	using line fitting algorithm (percent)
0	-0.14	-1.10	-8.77			
50	0.45	-1.17	-9.22			
100	0.52	-1.88	-9.19			
150	0.15	0.28	-8.69			
200	0.84	-1.11	-6.99			
250	1.06	-0.71	-7.80			
300	0.75	-0.95	-6.39			
350	0.63	0.77	-4.66			
400	0.06	-0.34	-4.14			
450	0.57	-1.22	-3.89			
500	-0.07	-1.36	-1.11			
550	0.58	-1.03	-0.13			
average	**0.45**	**-0.82**	**-5.91**	**-5.74**	**-5.87**	**-5.93**
std. dev.	0.37	0.73	3.13			

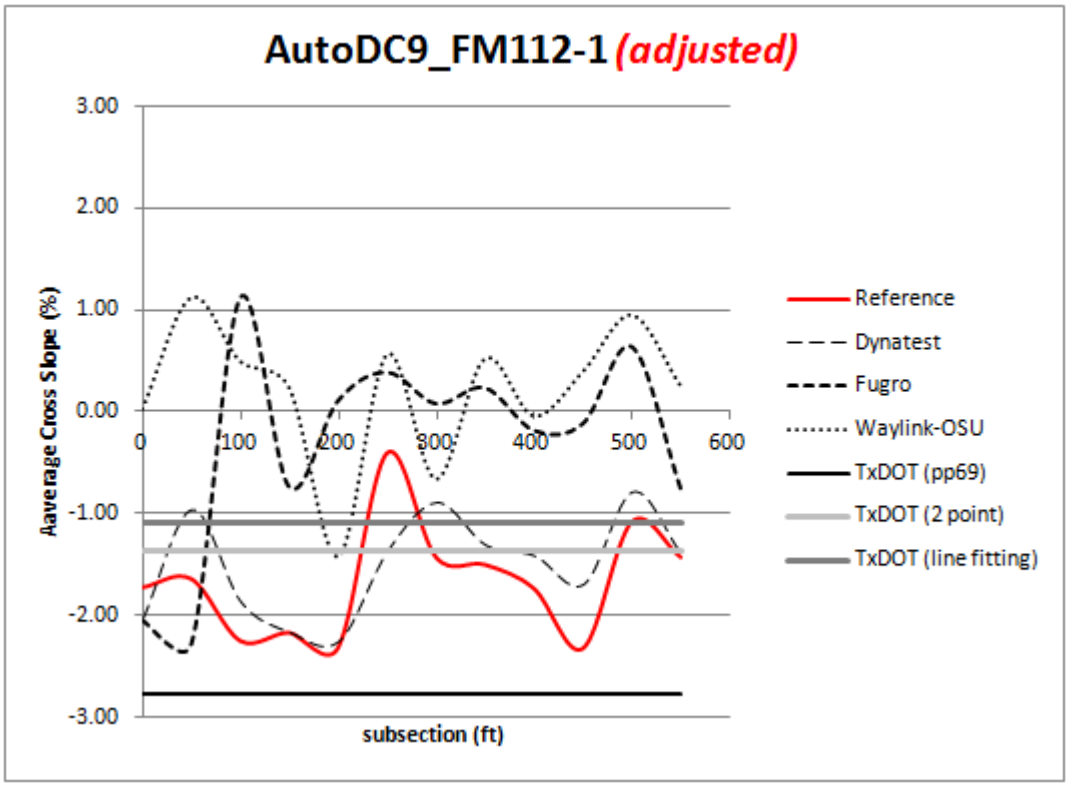

Figure D9: Cross slope for each 50-ft. subsection for AutoDC9_FM112-1

Table D9: Cross slope error for each 50-ft. subsection for AutoDC9_FM112-1

	Vendor - ***Error after adjusted (percent)***			**TxDOT**		
	Dynatest	**Fugro**	**Waylink-OSU**			
subsection (ft)	(percent)	for entire lane width (percent)	(percent) average	using AASHTO pp69 algorithm (percent)	using 2 point algorithm (percent)	using line fitting algorithm (percent)
0	0.29	0.31	-1.76			
50	-0.69	0.63	-2.77			
100	-0.39	-3.37	-2.75			
150	-0.01	-1.44	-2.41			
200	-0.07	-2.43	-0.90			
250	0.95	-0.80	-0.97			
300	-0.55	-1.51	-0.77			
350	-0.20	-1.74	-2.03			
400	-0.33	-1.56	-1.70			
450	-0.64	-2.21	-2.72			
500	-0.30	-1.72	-2.03			
550	-0.04	-0.67	-1.68			
average	**-0.16**	**-1.38**	**-1.87**	**1.10**	**-0.30**	**-0.58**
std. dev.	0.45	1.12	0.72			

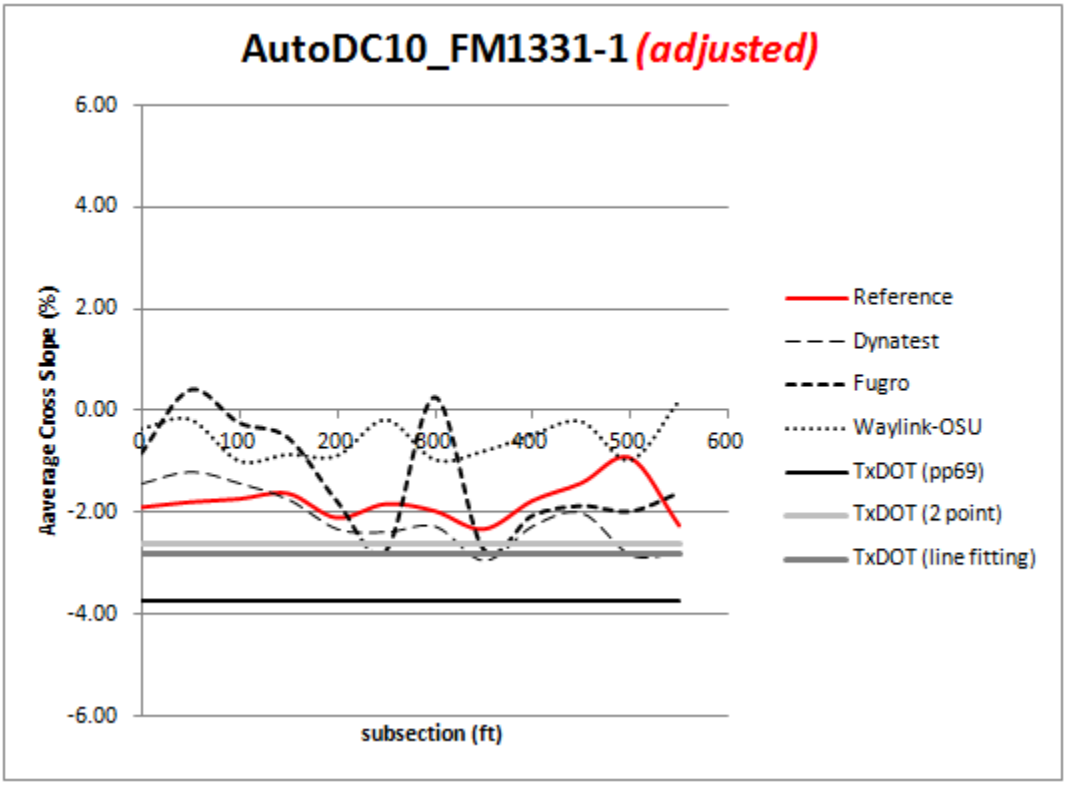

Figure D10: Cross slope for each 50-ft. subsection for AutoDC10_FM1331-1

Table D10: Cross slope error for each 50-ft. subsection for AutoDC10_FM1331-1

	Vendor - ***Error after adjusted (percent)***			**TxDOT**		
	Dynatest	**Fugro**	**Waylink-OSU**			
subsection (ft)	(percent)	for entire lane width (percent)	(percent) average	using AASHTO pp69 algorithm (percent)	using 2 point algorithm (percent)	using line fitting algorithm (percent)
0	-0.46	-1.06	-1.54			
50	-0.58	-2.21	-1.62			
100	-0.29	-1.50	-0.74			
150	0.13	-1.09	-0.75			
200	0.23	-0.32	-1.21			
250	0.55	0.95	-1.65			
300	0.31	-2.24	-1.00			
350	0.62	0.41	-1.52			
400	0.50	0.31	-1.29			
450	0.60	0.46	-1.20			
500	1.92	1.07	0.06			
550	0.53	-0.63	-2.45			
average	**0.34**	**-0.49**	**-1.24**	**1.96**	**0.83**	**1.00**
std. dev.	0.65	1.15	0.62			

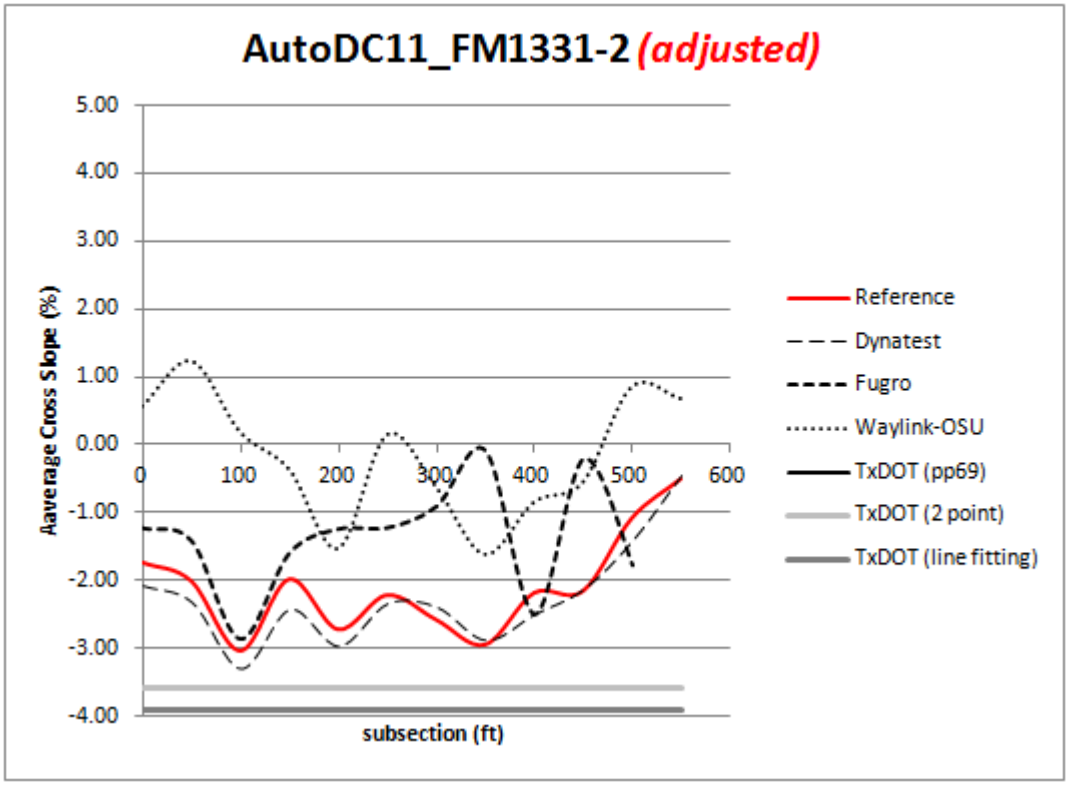

Figure D11: Cross slope for each 50-ft. subsection for AutoDC11_FM1331-2

Table D11: Cross slope error for each 50-ft. subsection for AutoDC11_FM1331-2

	Vendor - ***Error after adjusted (percent)***			**TxDOT**		
	Dynatest	**Fugro**	**Waylink-OSU**			
subsection (ft)	(percent)	for entire lane width (percent)	(percent) average	using AASHTO pp69 algorithm (percent)	using 2 point algorithm (percent)	using line fitting algorithm (percent)
0	0.36	-0.52	-2.31			
50	0.33	-0.60	-3.25			
100	0.28	-0.18	-3.23			
150	0.46	-0.39	-1.63			
200	0.26	-1.49	-1.19			
250	0.14	-1.00	-2.37			
300	-0.17	-1.68	-1.96			
350	-0.05	-2.86	-1.33			
400	0.33	0.31	-1.34			
450	-0.01	-1.95	-1.61			
500	0.35	0.69	-1.94			
550	-0.03	-0.51	-1.19			
average	**0.19**	**-0.73**	**-1.95**	**2.18**	**1.49**	**1.81**
std. dev.	0.20	1.00	0.72			

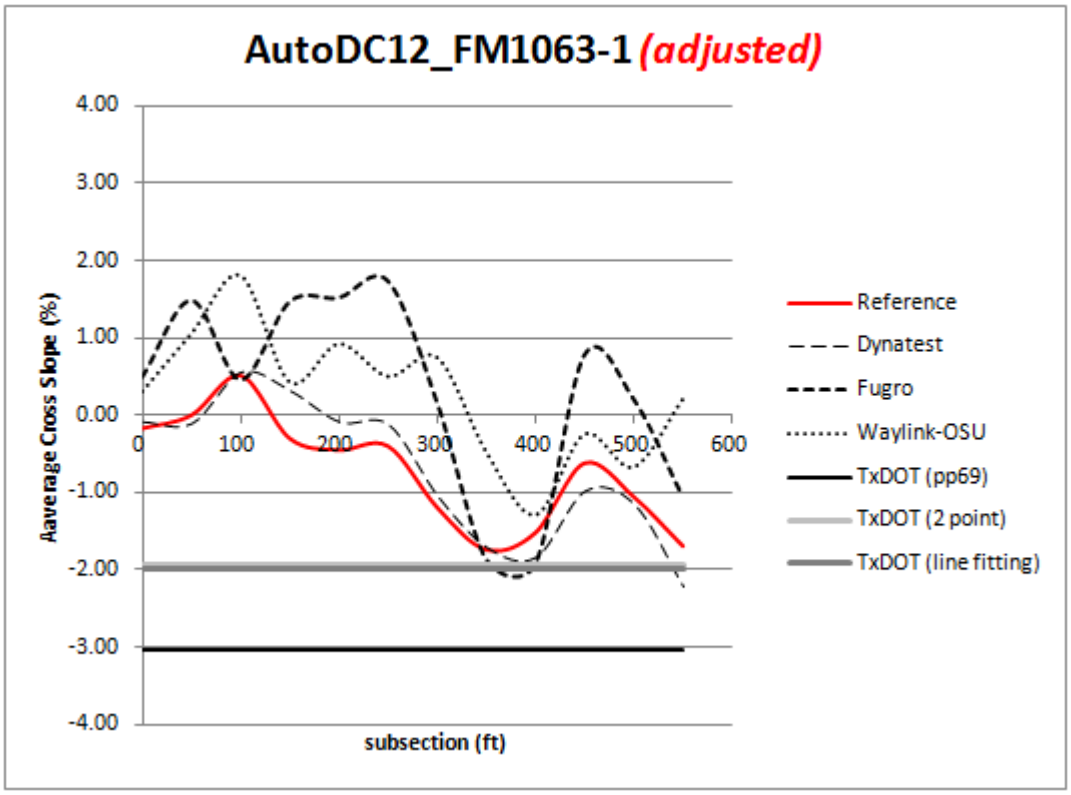

Figure D12: Cross slope for each 50-ft. subsection for AutoDC12_FM1063-1

Table D12: Cross slope error for each 50-ft. subsection for AutoDC12_FM1063-1

	Vendor - ***Error after adjusted (percent)***			**TxDOT**		
	Dynatest	**Fugro**	**Waylink-OSU**			
subsection (ft)	(percent)	for entire lane width (percent)	(percent) average	using AASHTO pp69 algorithm (percent)	using 2 point algorithm (percent)	using line fitting algorithm (percent)
0	-0.09	-0.67	-0.50			
50	0.10	-1.49	-1.08			
100	-0.06	0.04	-1.31			
150	-0.62	-1.78	-0.75			
200	-0.37	-1.98	-1.39			
250	-0.28	-2.14	-0.92			
300	-0.15	-1.35	-1.95			
350	-0.03	0.13	-1.27			
400	0.31	0.40	-0.24			
450	0.35	-1.41	-0.39			
500	0.09	-1.26	-0.40			
550	0.53	-0.63	-1.91			
average	**-0.02**	**-1.01**	**-1.01**	**2.32**	**1.22**	**1.27**
std. dev.	0.32	0.85	0.58			

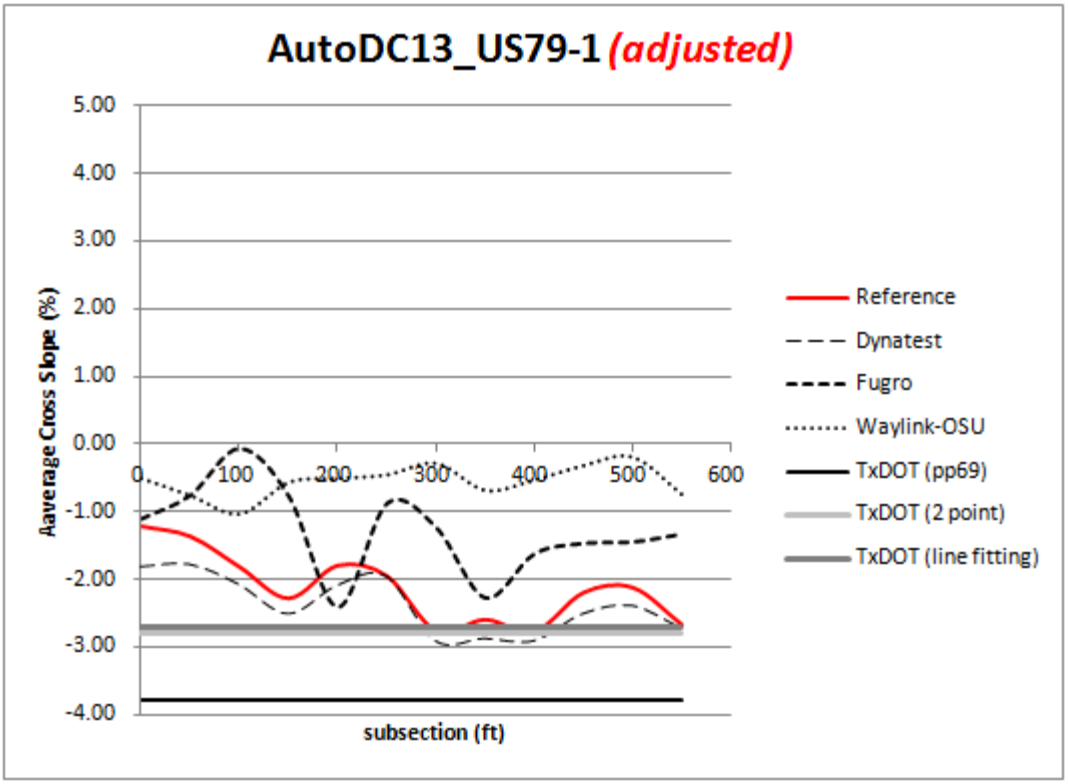

Figure D13: Cross slope for each 50-ft. subsection for AutoDC13_US79-1

Table D13: Cross slope error for each 50-ft. subsection for AutoDC13_US79-1

	Vendor - ***Error after adjusted (percent)***			**TxDOT**		
	Dynatest	**Fugro**	**Waylink-OSU**			
subsection (ft)	(percent)	for entire lane width (percent)	(percent) average	using AASHTO pp69 algorithm (percent)	using 2 point algorithm (percent)	using line fitting algorithm (percent)
0	0.60	-0.11	-0.70			
50	0.42	-0.61	-0.60			
100	0.26	-1.76	-0.78			
150	0.23	-1.52	-1.71			
200	0.30	0.60	-1.28			
250	0.00	-1.08	-1.49			
300	0.14	-1.55	-2.48			
350	0.28	-0.34	-1.91			
400	0.13	-1.17	-2.25			
450	0.31	-0.74	-1.87			
500	0.26	-0.69	-1.92			
550	0.04	-1.35	-1.93			
average	**0.25**	**-0.86**	**-1.58**	**1.67**	**0.67**	**0.58**
std. dev.	0.16	0.69	0.62			

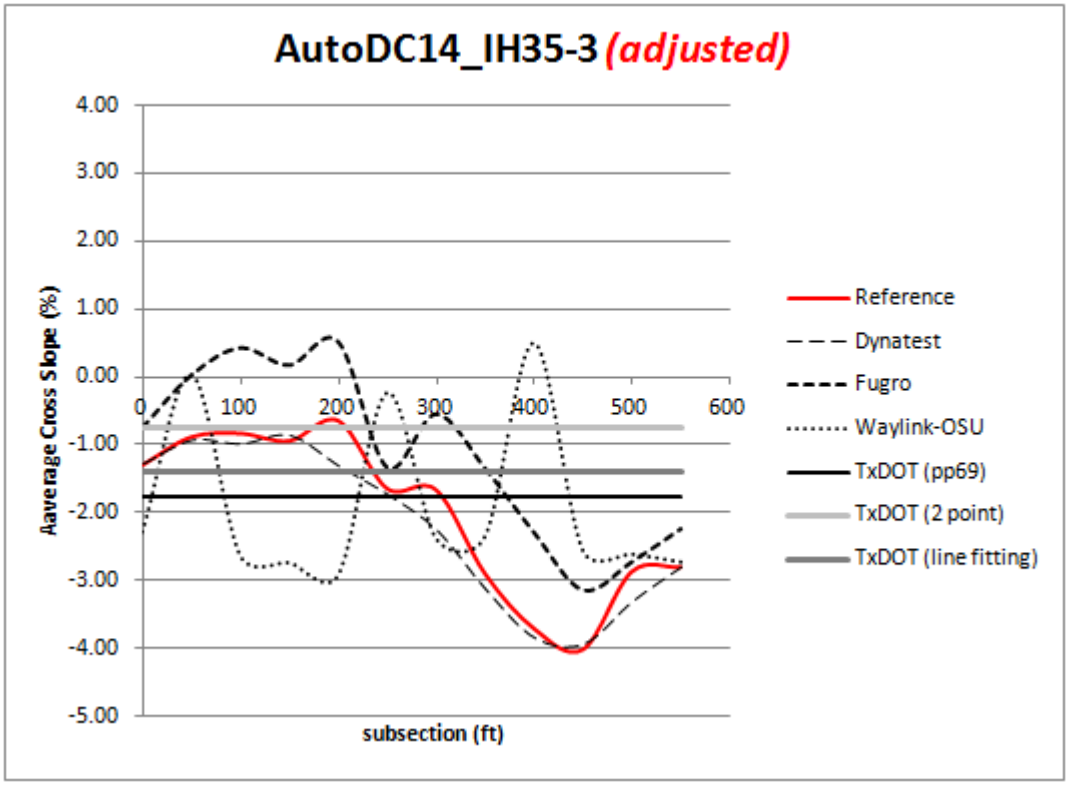

Figure D14: Cross slope for each 50-ft. subsection for AutoDC14_IH35-3

Table D14: Cross slope error for each 50-ft. subsection for AutoDC14_IH35-3

	Vendor - ***Error after adjusted (percent)***					
	Dynatest	**Fugro**	**Waylink-OSU**	**TxDOT**		
subsection (ft)	(percent)	for entire lane width (percent)	(percent) average	using AASHTO pp69 algorithm (percent)	using 2 point algorithm (percent)	using line fitting algorithm (percent)
0	-0.03	-0.55	0.97			
50	0.03	-0.91	-0.93			
100	0.14	-1.25	1.79			
150	-0.10	-1.11	1.78			
200	0.66	-1.16	2.27			
250	0.08	-0.31	-1.42			
300	0.58	-1.11	0.71			
350	0.21	-1.56	-0.56			
400	0.12	-1.42	-4.22			
450	-0.10	-0.89	-1.47			
500	0.42	-0.15	-0.27			
550	-0.02	-0.57	-0.09			
average	**0.17**	**-0.92**	**-0.12**	**-0.24**	**-1.27**	**-0.63**
std. dev.	0.26	0.44	1.81			

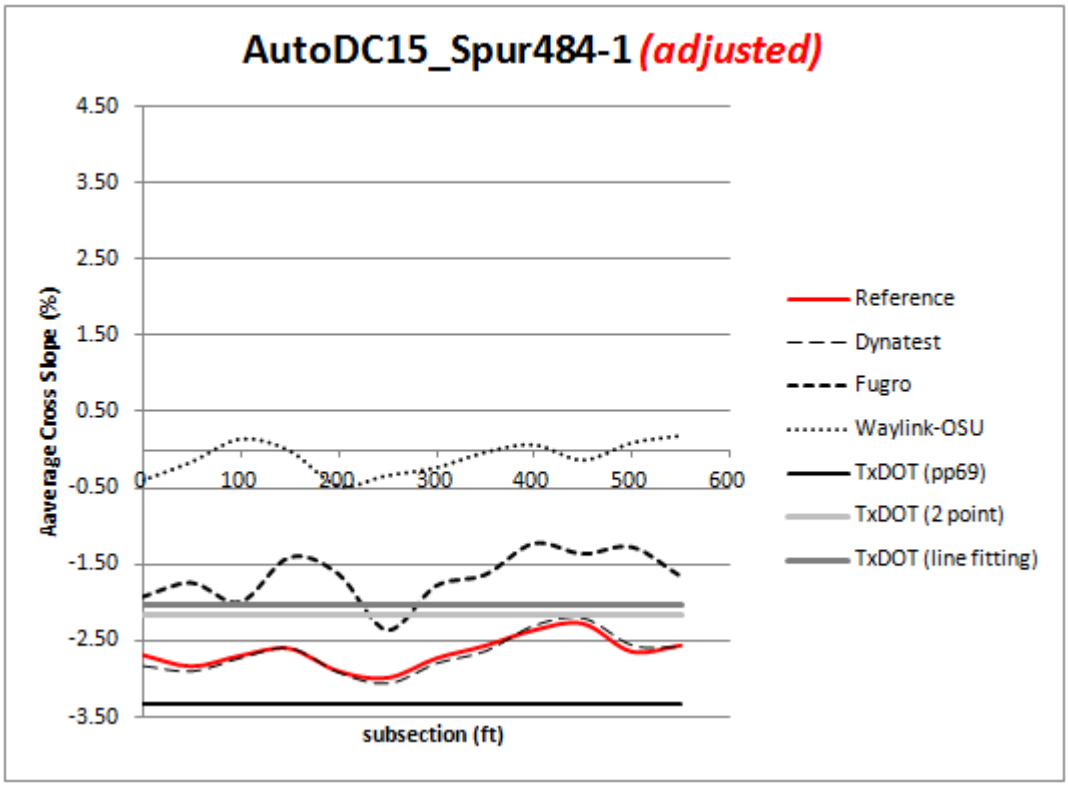

Figure D15: Cross slope for each 50-ft. subsection for AutoDC15_Spur484-1

Table D15: Cross slope error for each 50-ft. subsection for AutoDC15_Spur484-1

	Vendor - ***Error after adjusted (percent)***					
	Dynatest	**Fugro**	**Waylink-OSU**	**TxDOT**		
subsection (ft)	(percent)	for entire lane width (percent)	(percent) average	using AASHTO pp69 algorithm (percent)	using 2 point algorithm (percent)	using line fitting algorithm (percent)
0	0.14	-0.76	-2.28			
50	0.06	-1.09	-2.67			
100	0.03	-0.70	-2.83			
150	0.00	-1.20	-2.59			
200	0.02	-1.28	-2.43			
250	0.07	-0.62	-2.65			
300	0.06	-0.95	-2.49			
350	0.07	-0.93	-2.53			
400	-0.05	-1.14	-2.42			
450	-0.06	-0.91	-2.14			
500	-0.07	-1.38	-2.73			
550	0.02	-0.90	-2.74			
average	**0.02**	**-0.99**	**-2.54**	**0.67**	**-0.50**	**-0.62**
std. dev.	0.06	0.23	0.20			

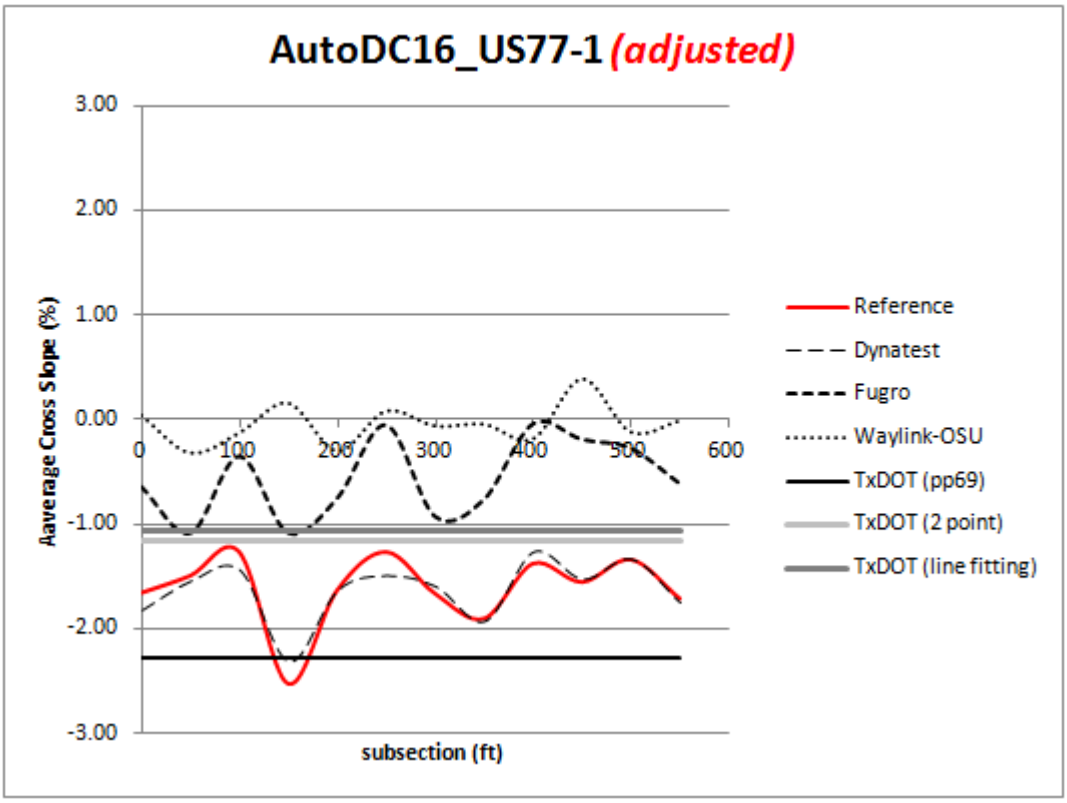

Figure D16: Cross slope for each 50-ft. subsection for AutoDC16_US77-1

Table D16: Cross slope error for each 50-ft. subsection for AutoDC16_US77-1

	Vendor - ***Error after adjusted (percent)***			**TxDOT**		
	Dynatest	**Fugro**	**Waylink-OSU**			
subsection (ft)	(percent)	for entire lane width (percent)	(percent) average	using AASHTO pp69 algorithm (percent)	using 2 point algorithm (percent)	using line fitting algorithm (percent)
0	0.18	-1.01	-1.70			
50	0.06	-0.40	-1.17			
100	0.19	-0.91	-1.14			
150	-0.21	-1.45	-2.70			
200	0.01	-0.88	-1.33			
250	0.24	-1.20	-1.35			
300	-0.06	-0.74	-1.61			
350	0.03	-1.14	-1.86			
400	-0.10	-1.33	-1.19			
450	-0.01	-1.36	-1.95			
500	0.01	-1.06	-1.22			
550	0.05	-1.10	-1.70			
average	**0.03**	**-1.05**	**-1.58**	**0.67**	**-0.45**	**-0.54**
std. dev.	0.13	0.29	0.45			

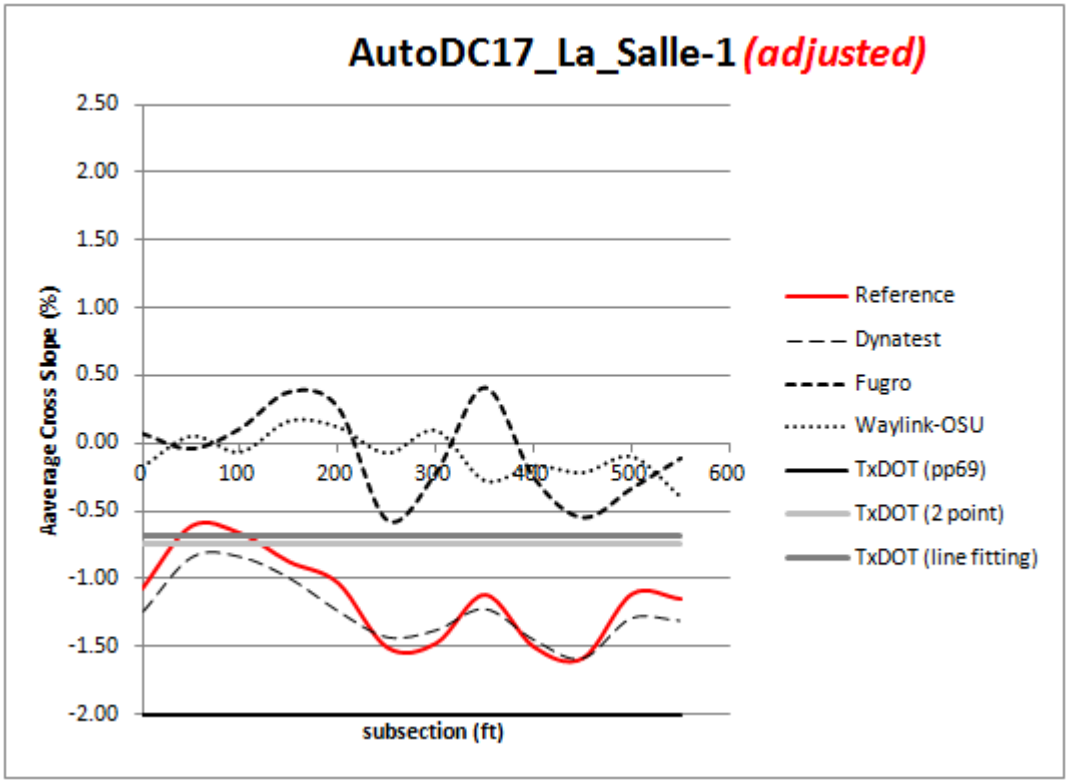

Figure D17: Cross slope for each 50-ft. subsection for AutoDC17_La_Salle-1

Table D17: Cross slope error for each 50-ft. subsection for AutoDC17_La_Salle-1

	Vendor - ***Error after adjusted (percent)***					
	Dynatest	**Fugro**	**Waylink-OSU**	**TxDOT**		
subsection (ft)	(percent)	for entire lane width (percent)	(percent) average	using AASHTO pp69 algorithm (percent)	using 2 point algorithm (percent)	using line fitting algorithm (percent)
0	0.16	-1.15	-0.90			
50	0.23	-0.58	-0.66			
100	0.17	-0.78	-0.59			
150	0.12	-1.26	-1.03			
200	0.20	-1.31	-1.15			
250	-0.08	-0.95	-1.44			
300	-0.10	-1.27	-1.57			
350	0.10	-1.54	-0.84			
400	-0.06	-1.26	-1.34			
450	-0.01	-1.05	-1.37			
500	0.17	-0.79	-1.01			
550	0.16	-1.05	-0.76			
average	**0.09**	**-1.08**	**-1.06**	**0.86**	**-0.40**	**-0.46**
std. dev.	0.12	0.27	0.32			

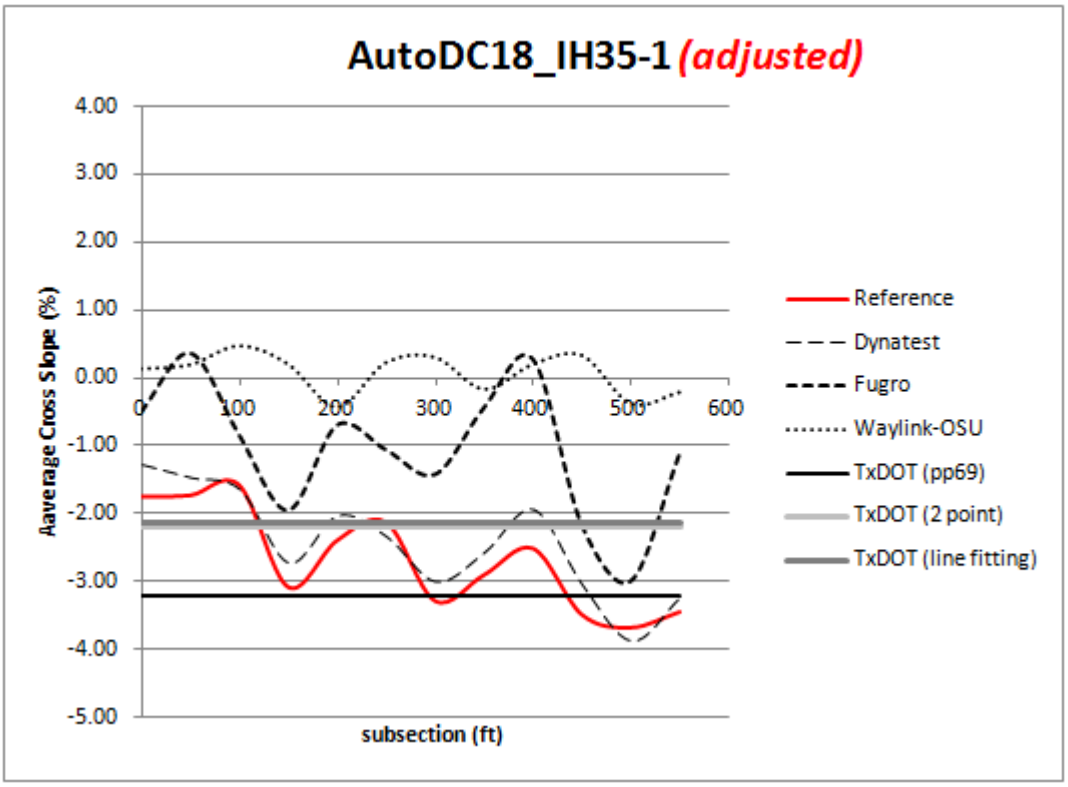

Figure D18: Cross slope for each 50-ft. subsection for AutoDC18_IH35-1

Table D18: Cross slope error for each 50-ft. subsection for AutoDC18_IH35-1

	Vendor - ***Error after adjusted (percent)***			**TxDOT**		
	Dynatest	**Fugro**	**Waylink-OSU**			
subsection (ft)	(percent)	for entire lane width (percent)	(percent) average	using AASHTO pp69 algorithm (percent)	using 2 point algorithm (percent)	using line fitting algorithm (percent)
0	-0.45	-1.24	-1.89			
50	-0.24	-2.08	-1.93			
100	0.08	-0.72	-2.06			
150	-0.34	-1.12	-3.29			
200	-0.35	-1.68	-1.97			
250	0.23	-1.05	-2.36			
300	-0.26	-1.85	-3.60			
350	-0.32	-2.45	-2.74			
400	-0.55	-2.77	-2.72			
450	-0.41	-1.30	-3.83			
500	0.22	-0.67	-3.31			
550	-0.20	-2.33	-3.25			
average	**-0.22**	**-1.60**	**-2.75**	**0.54**	**-0.47**	**-0.53**
std. dev.	0.26	0.70	0.70			

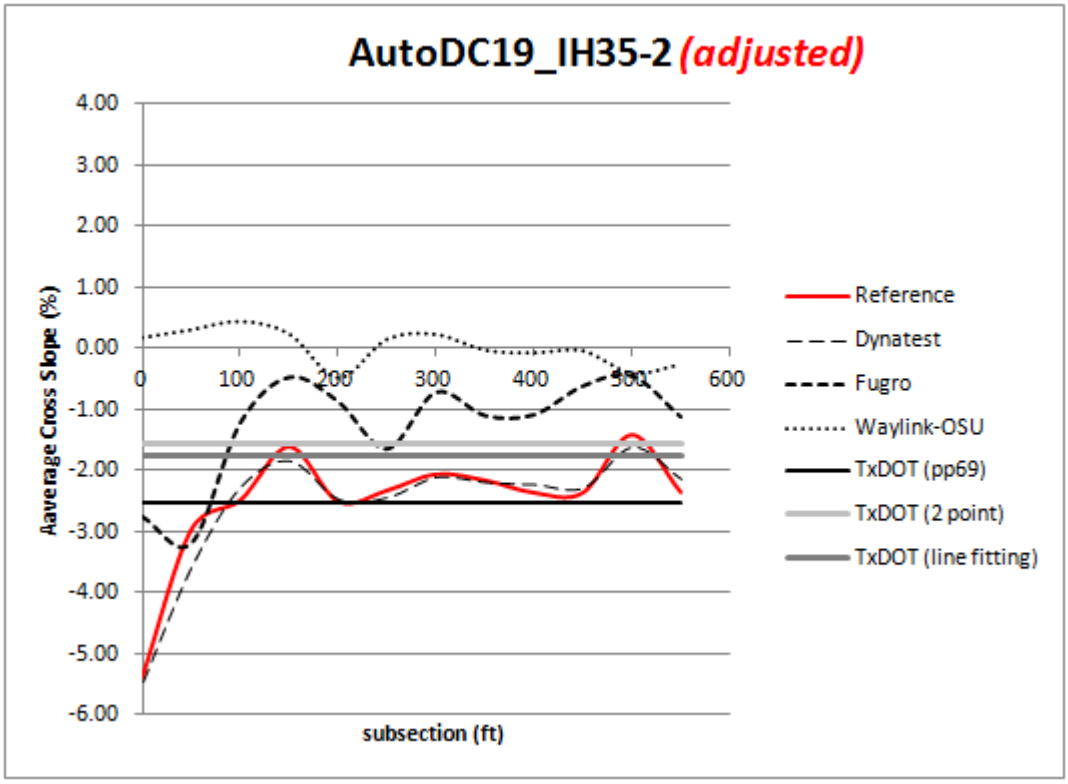

Figure D19: Cross slope for each 50-ft. subsection for AutoDC19_IH35-2

Table D19: Cross slope error for each 50-ft. subsection for AutoDC19_IH35-2

	Vendor - ***Error after adjusted (percent)***					
	Dynatest	**Fugro**	**Waylink-OSU**	**TxDOT**		
subsection (ft)	(percent)	for entire lane width (percent)	(percent) average	using AASHTO pp69 algorithm (percent)	using 2 point algorithm (percent)	using line fitting algorithm (percent)
0	0.06	-2.65	-5.57			
50	0.60	0.21	-3.27			
100	-0.21	-1.26	-2.92			
150	0.25	-1.12	-1.84			
200	-0.02	-1.63	-2.04			
250	0.12	-0.68	-2.47			
300	0.06	-1.33	-2.28			
350	0.05	-1.05	-2.13			
400	-0.12	-1.27	-2.29			
450	-0.07	-1.74	-2.33			
500	0.22	-0.95	-1.01			
550	-0.20	-1.23	-2.10			
average	**0.06**	**-1.23**	**-2.52**	**0.04**	**-0.94**	**-0.75**
std. dev.	0.22	0.67	1.11			

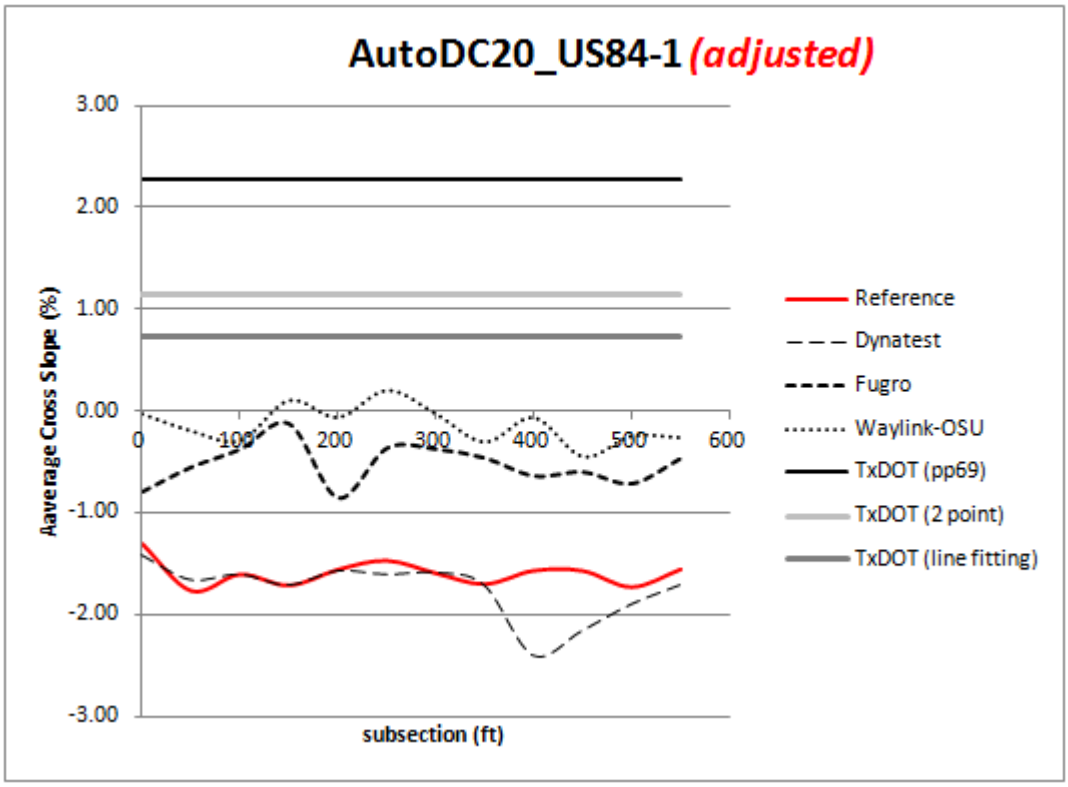

Figure D20: Cross slope for each 50-ft. subsection for AutoDC20_US84-1

Table D20: Cross slope error for each 50-ft. subsection for AutoDC20_US84-1

	Vendor - ***Error after adjusted (percent)***					
	Dynatest	**Fugro**	**Waylink-OSU**	**TxDOT**		
subsection (ft)	(percent)	for entire lane width (percent)	(percent) average	using AASHTO pp69 algorithm (percent)	using 2 point algorithm (percent)	using line fitting algorithm (percent)
0	0.10	-0.52	-1.29			
50	-0.10	-1.21	-1.57			
100	0.00	-1.23	-1.32			
150	0.00	-1.59	-1.82			
200	0.01	-0.71	-1.50			
250	0.13	-1.11	-1.68			
300	0.00	-1.22	-1.57			
350	0.01	-1.24	-1.40			
400	0.84	-0.93	-1.51			
450	0.59	-0.98	-1.13			
500	0.18	-1.02	-1.48			
550	0.16	-1.09	-1.30			
average	**0.16**	**-1.07**	**-1.46**	**0.68**	**-0.46**	**-0.87**
std. dev.	0.28	0.27	0.19			

Appendix E. Cross Slope For Every Transverse Foot Of Every 50-Ft Subsection

(with the height in feet in the vertical axis and the transverse feet in the horizontal axis)

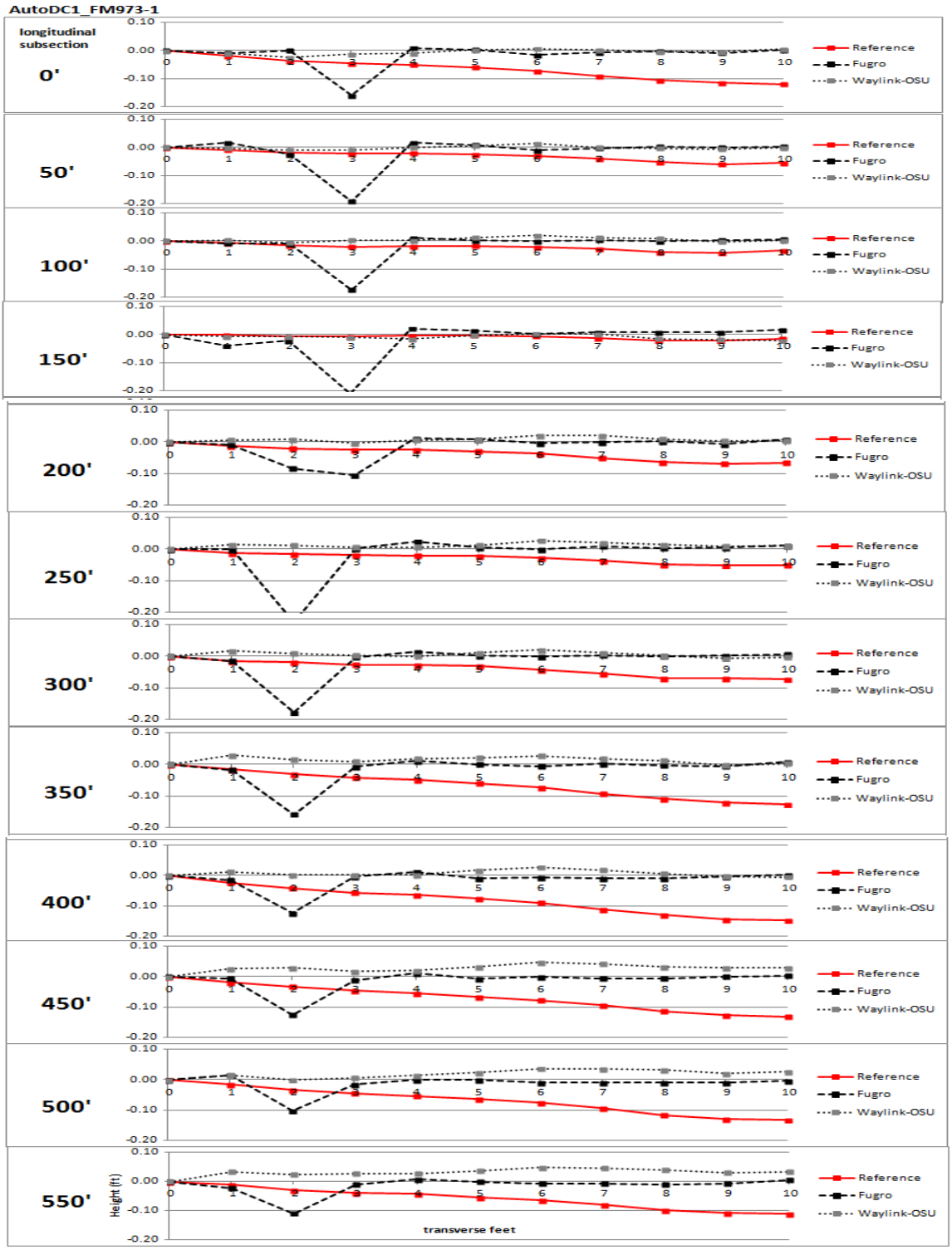

Figure E1: Cross slope for every transverse foot of every 50-ft. subsection for AutoDC1_FM973-1

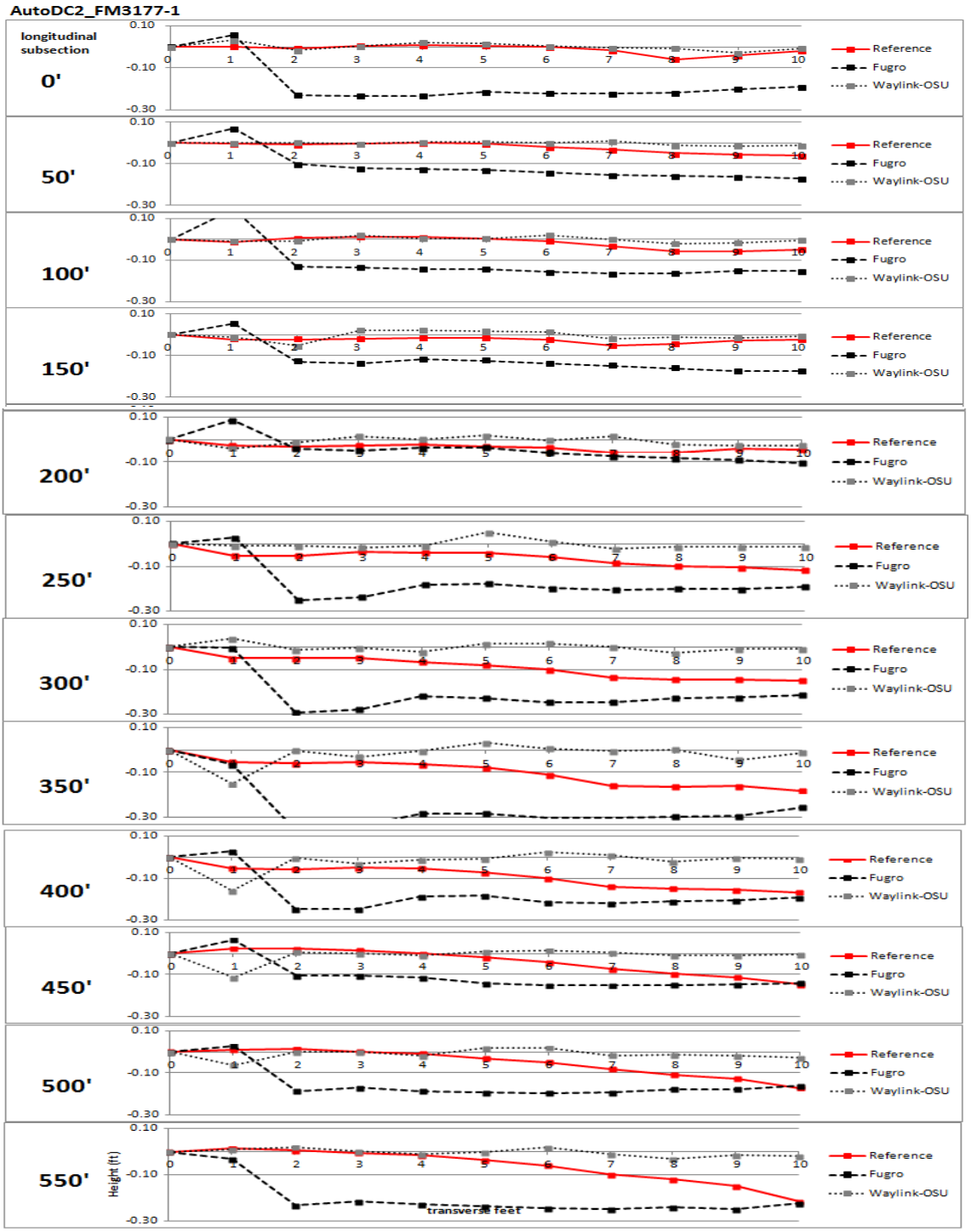

Figure E2: Cross slope for every transverse foot of every 50-ft. subsection for AutoDC2_FM3177-1

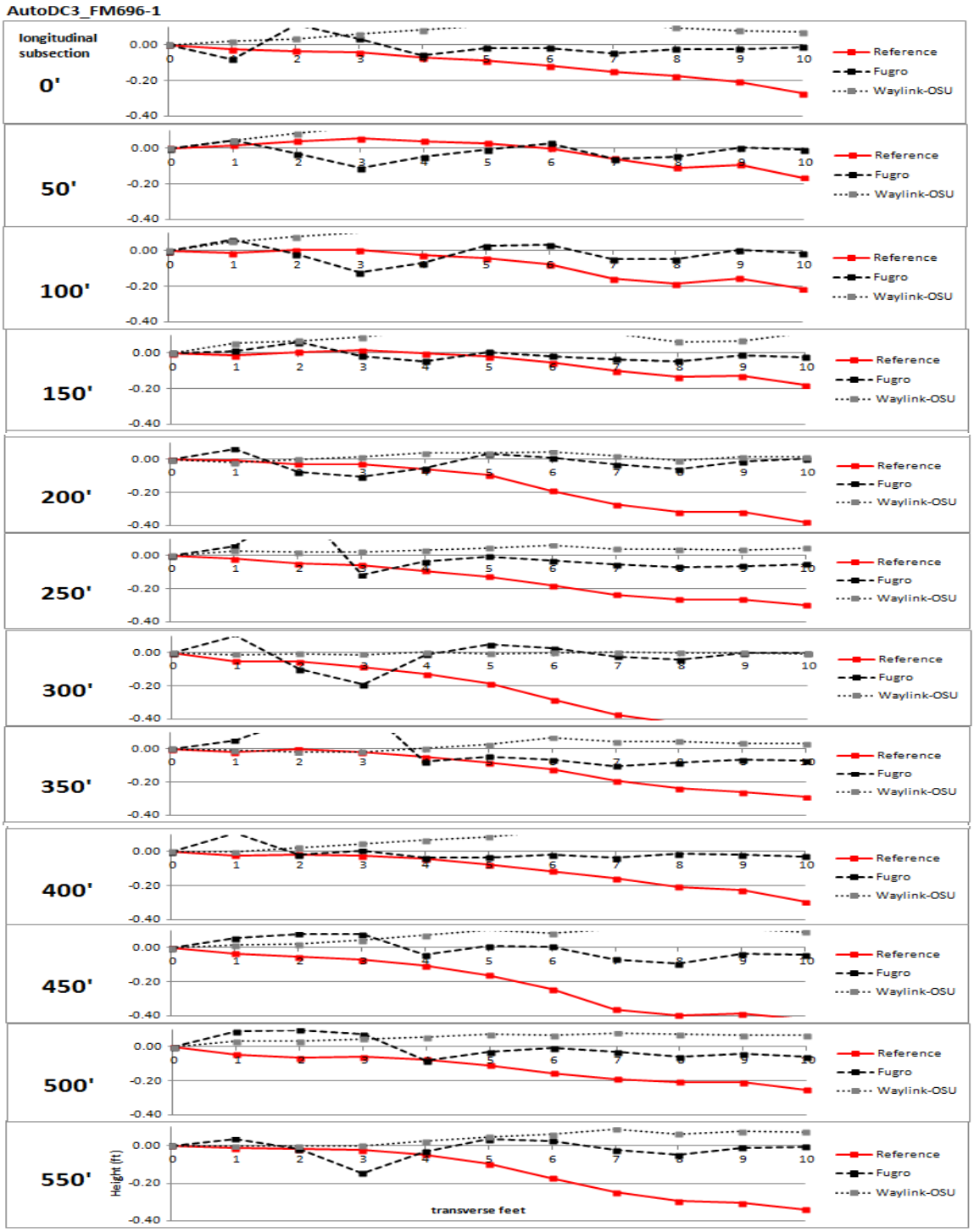

Figure E3: Cross slope for every transverse foot of every 50-ft. subsection for AutoDC3_FM696-1

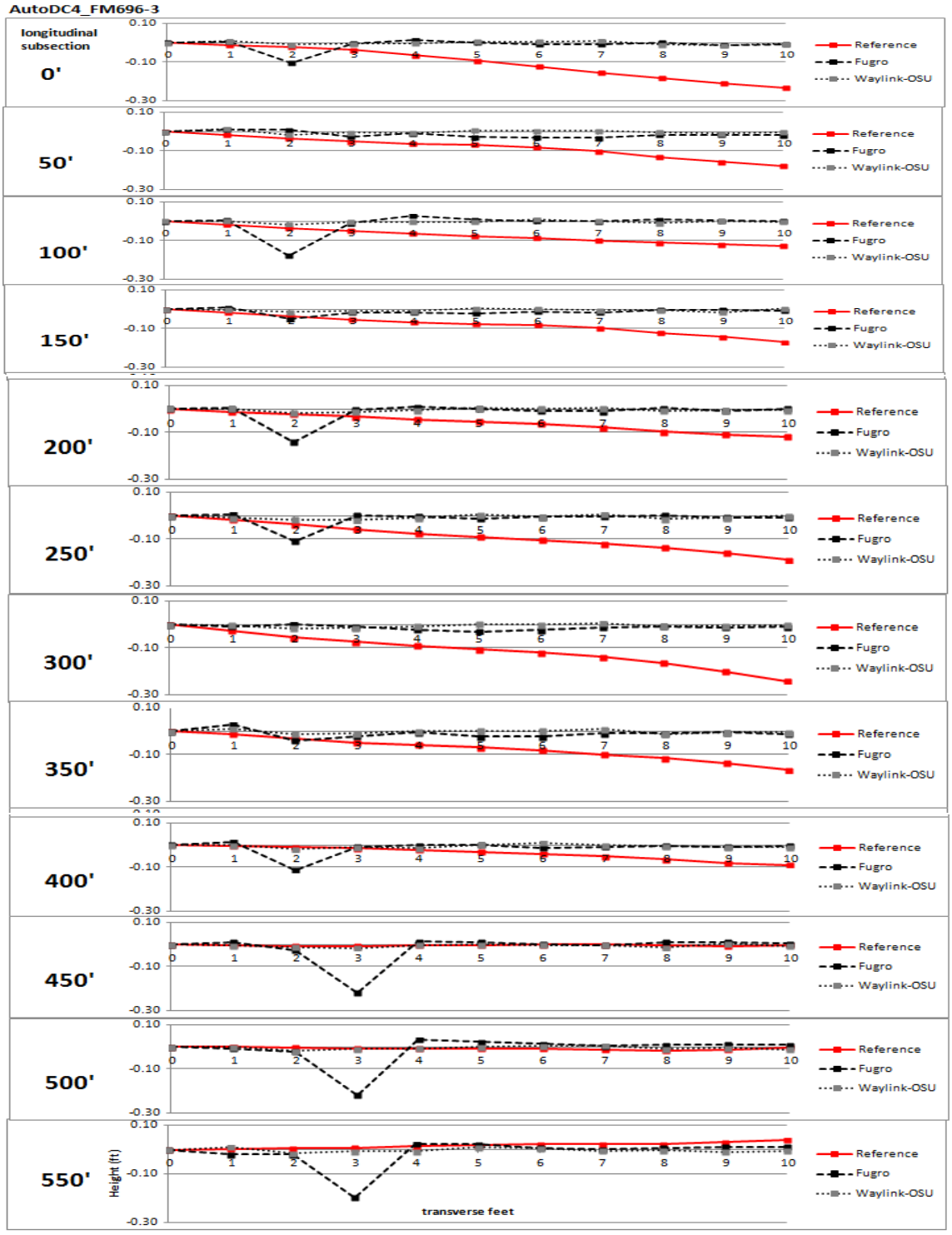

Figure E4: Cross slope for every transverse foot of every 50-ft. subsection for AutoDC4_FM696-3

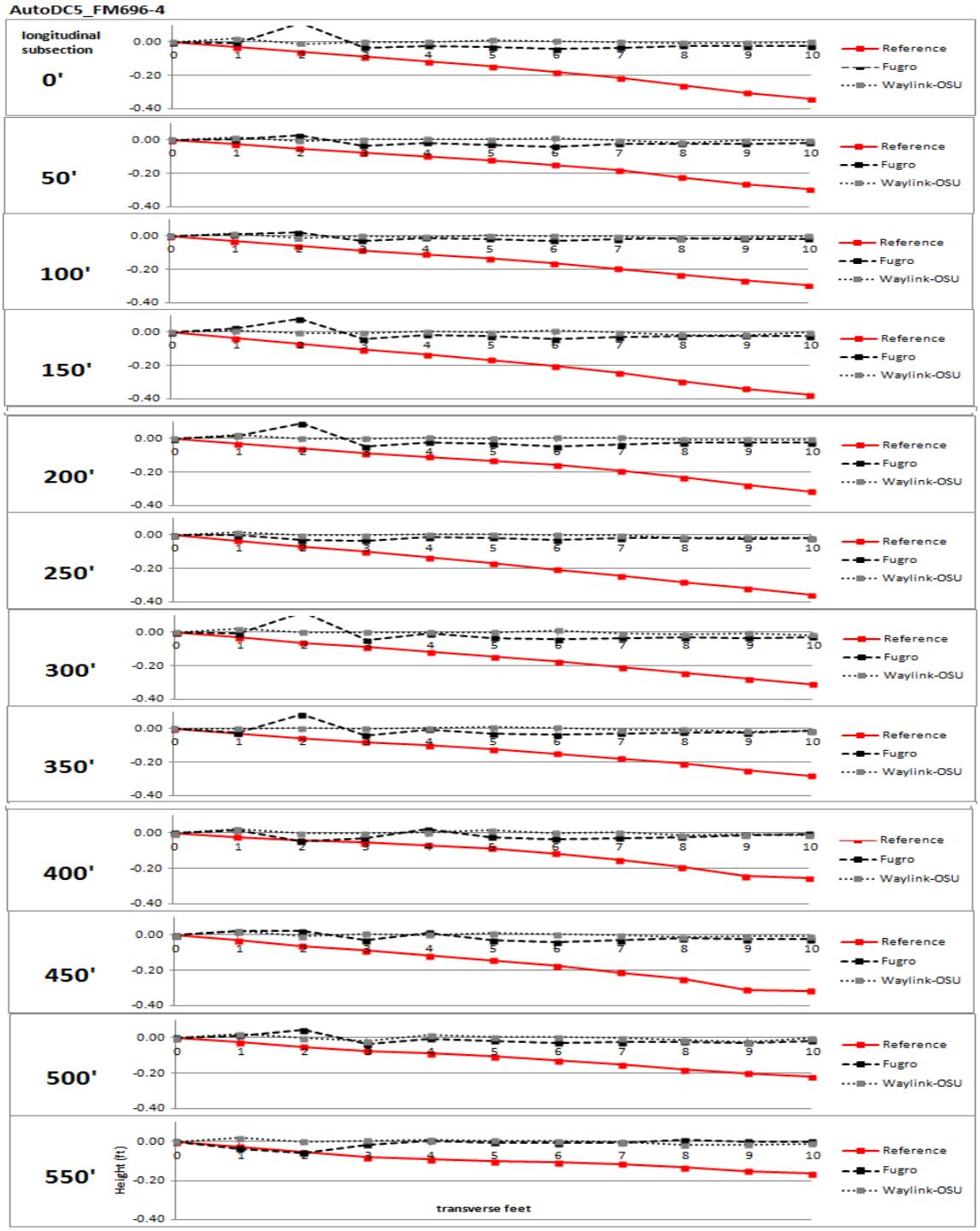

Figure E5: Cross slope for every transverse foot of every 50-ft. subsection for AutoDC5_FM696-4

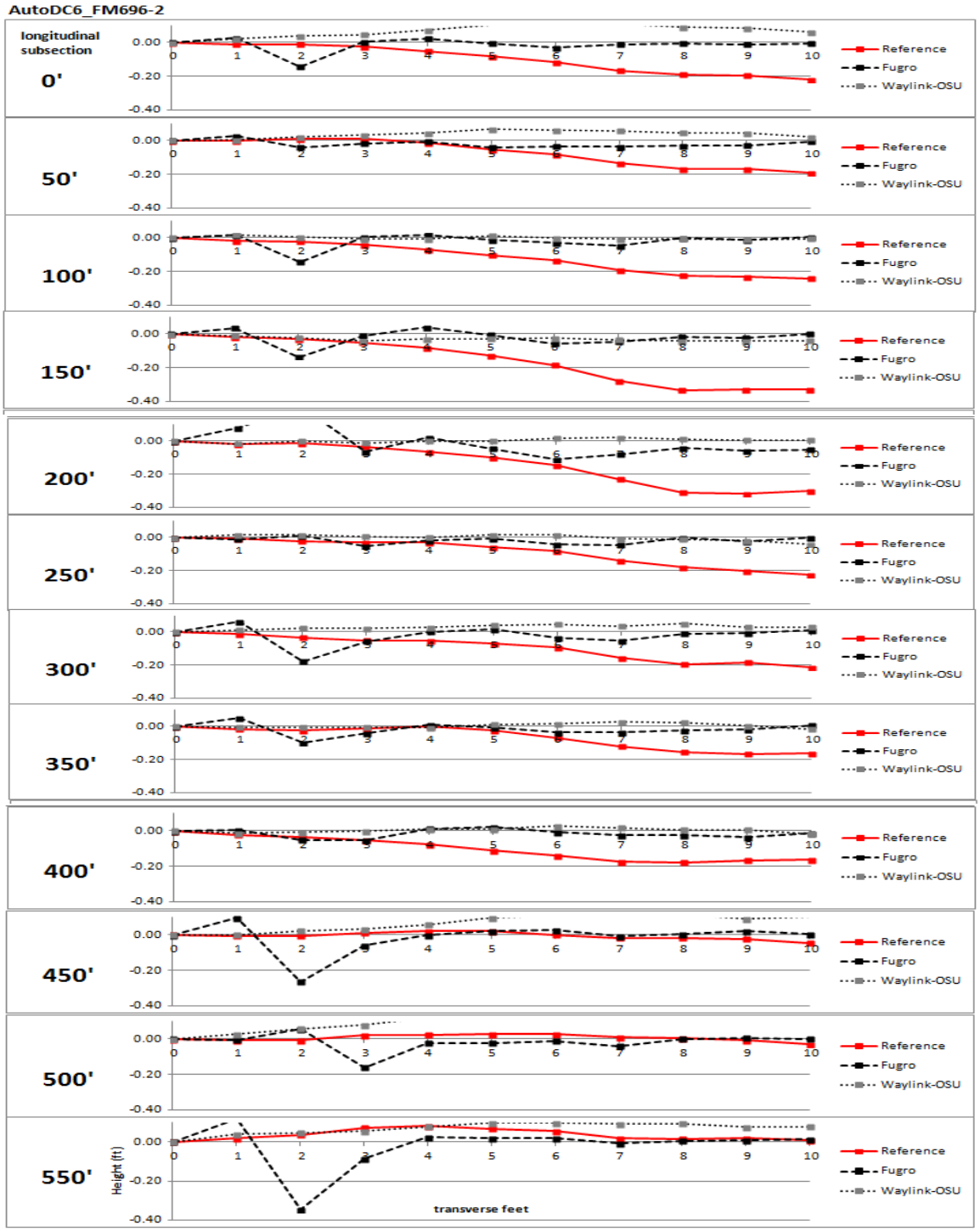

Figure E6: Cross slope for every transverse foot of every 50-ft. subsection for AutoDC6_FM696-2

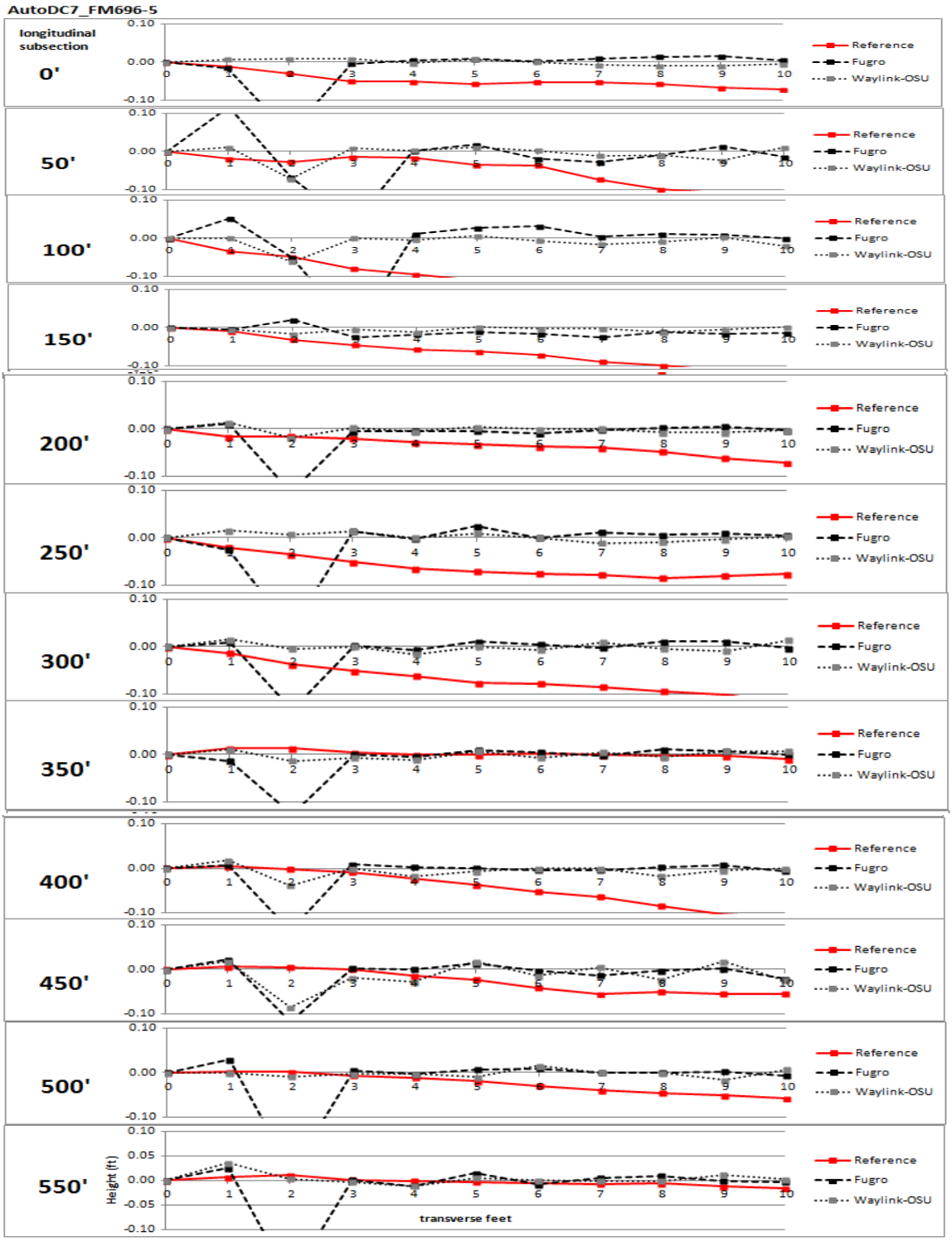

Figure E7: Cross slope for every transverse foot of every 50-ft. subsection for AutoDC7_FM696-5

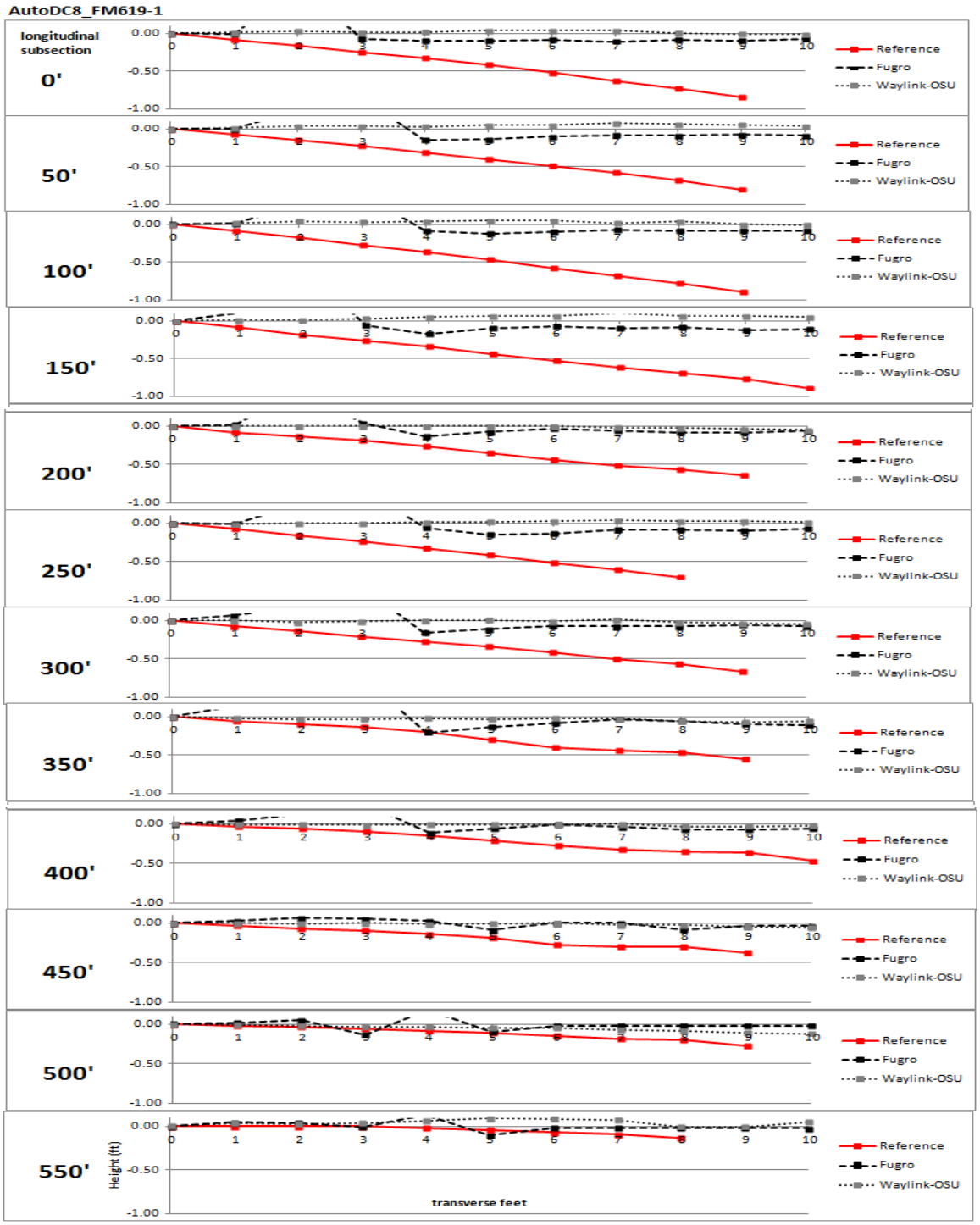

Figure E8: Cross slope for every transverse foot of every 50-ft. subsection for AutoDC8_FM619-1

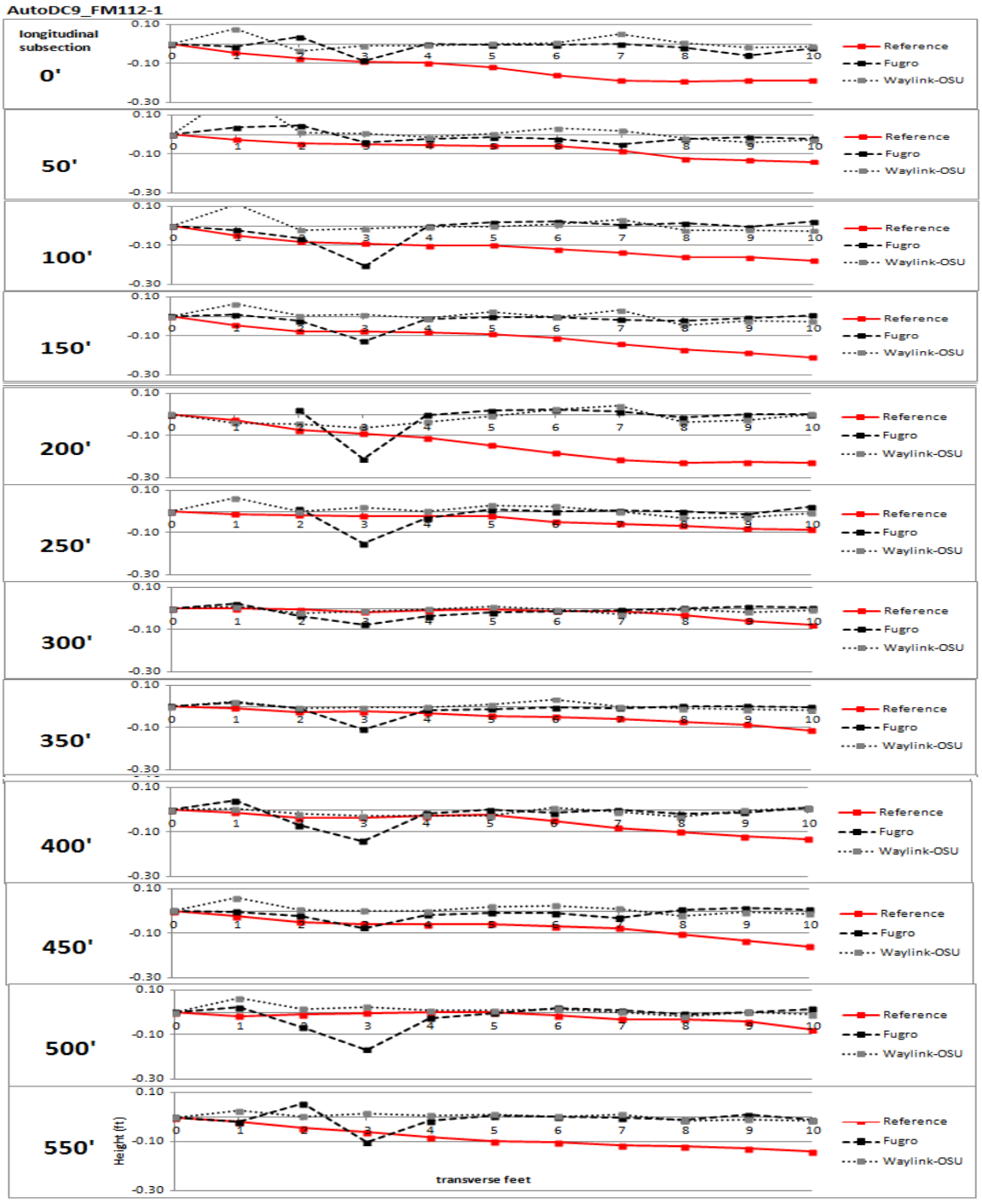

Figure E9: Cross slope for every transverse foot of every 50-ft. subsection for AutoDC9_FM112-1

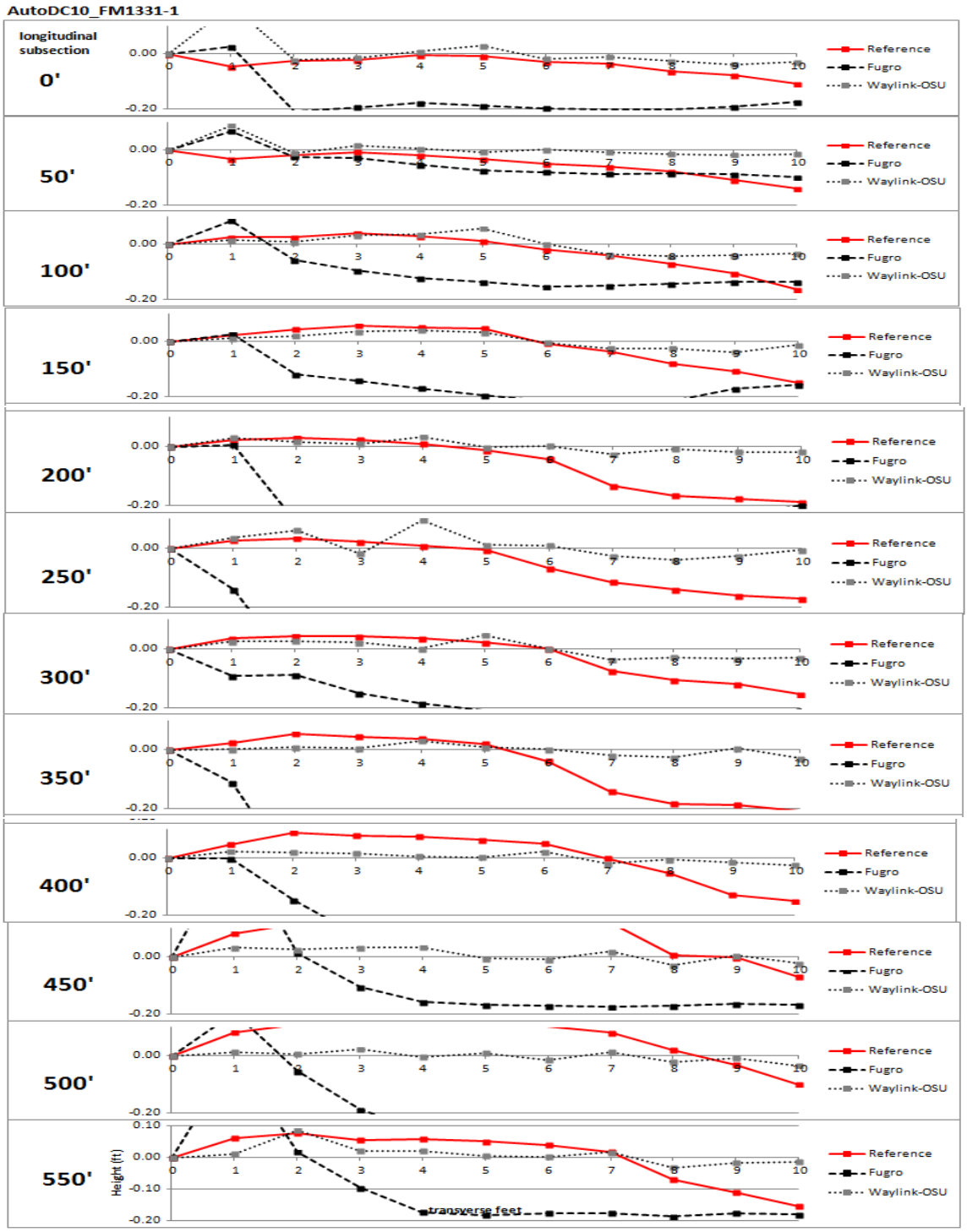

Figure E10: Cross slope for every transverse foot of every 50-ft. subsection for AutoDC10_FM1331-1

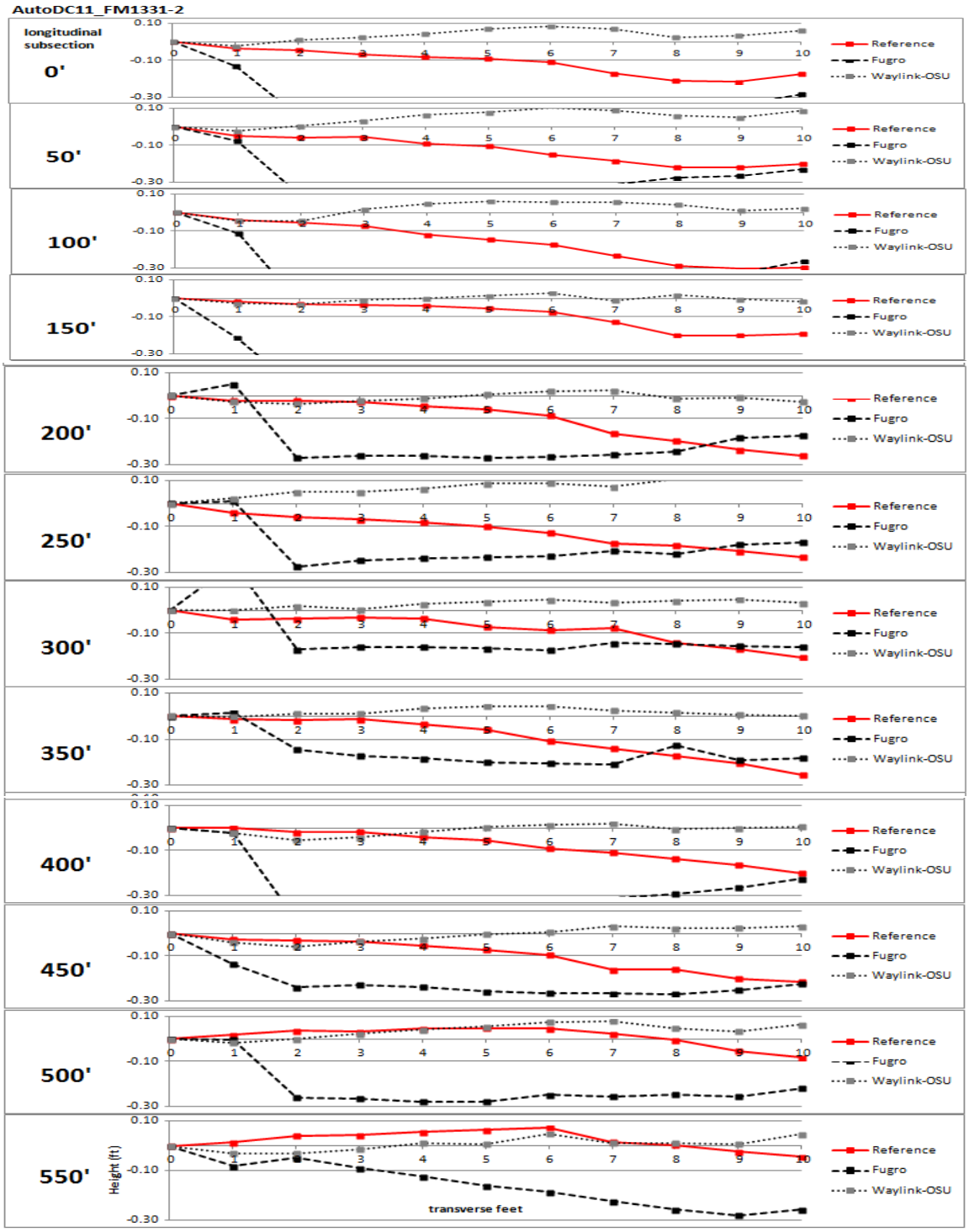

Figure E11: Cross slope for every transverse foot of every 50-ft. subsection for AutoDC11_FM1331-2

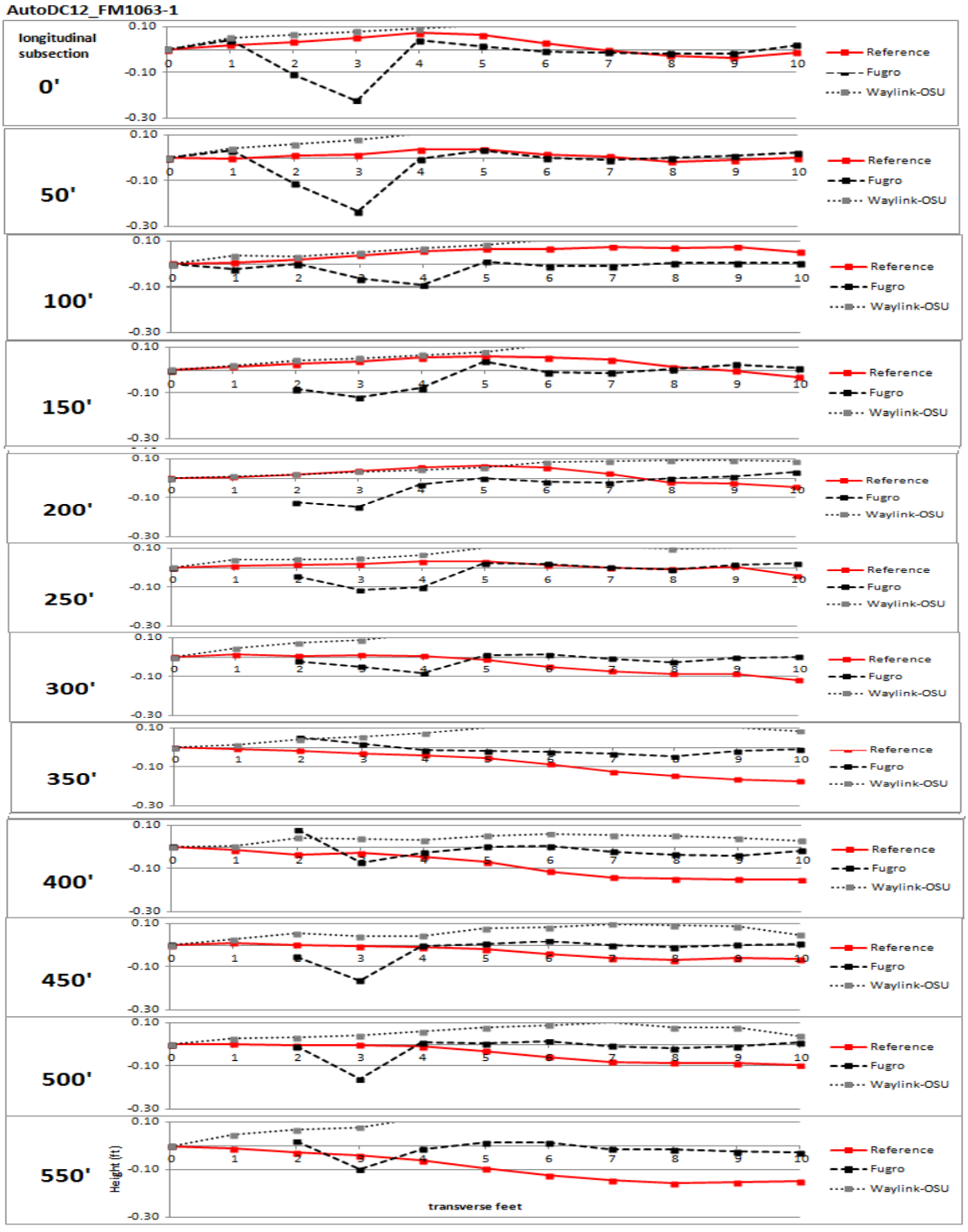

Figure E12: Cross slope for every transverse foot of every 50-ft. subsection for AutoDC12_FM1063-1

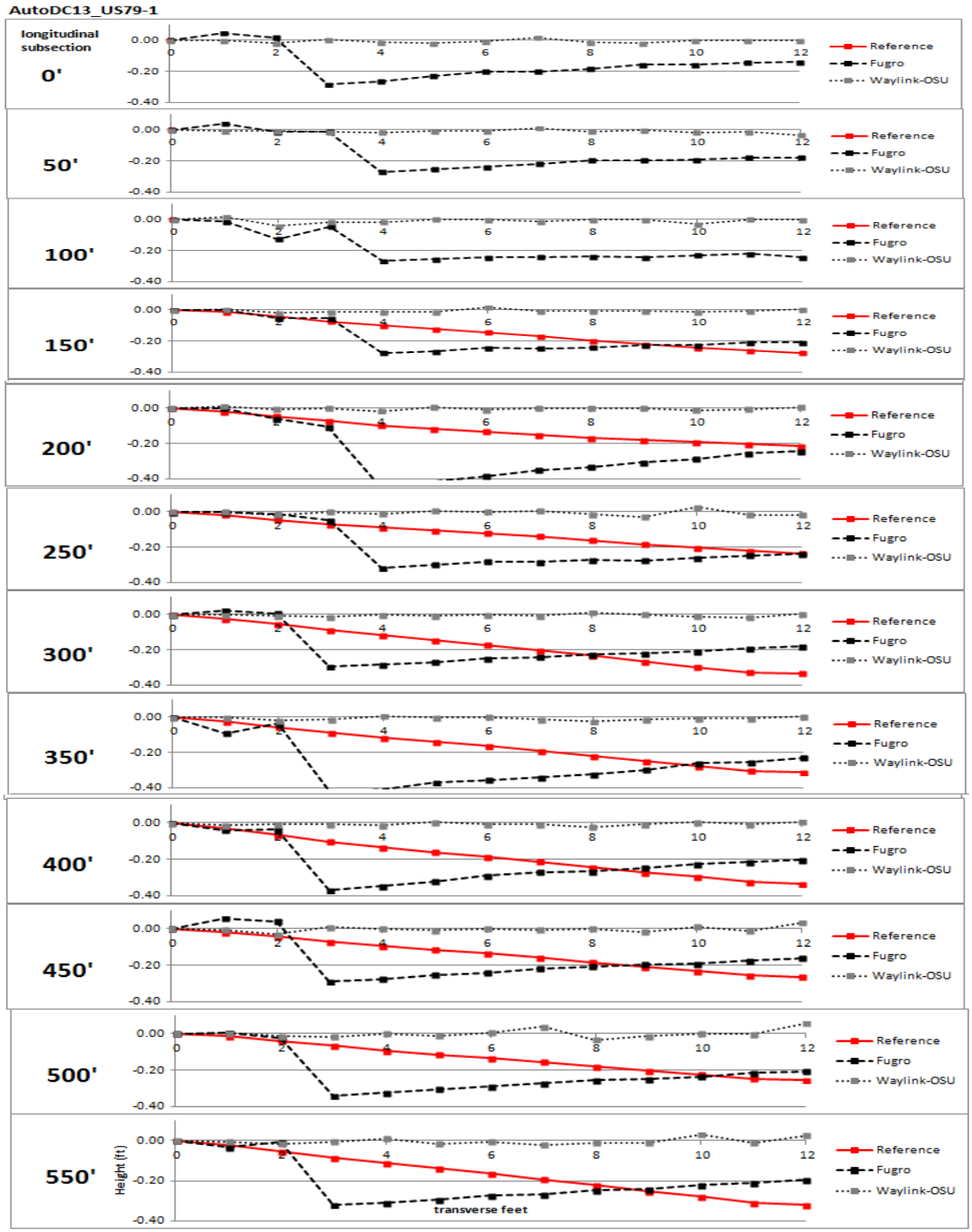

Figure E13: Cross slope for every transverse foot of every 50-ft. subsection for AutoDC13_US79-1

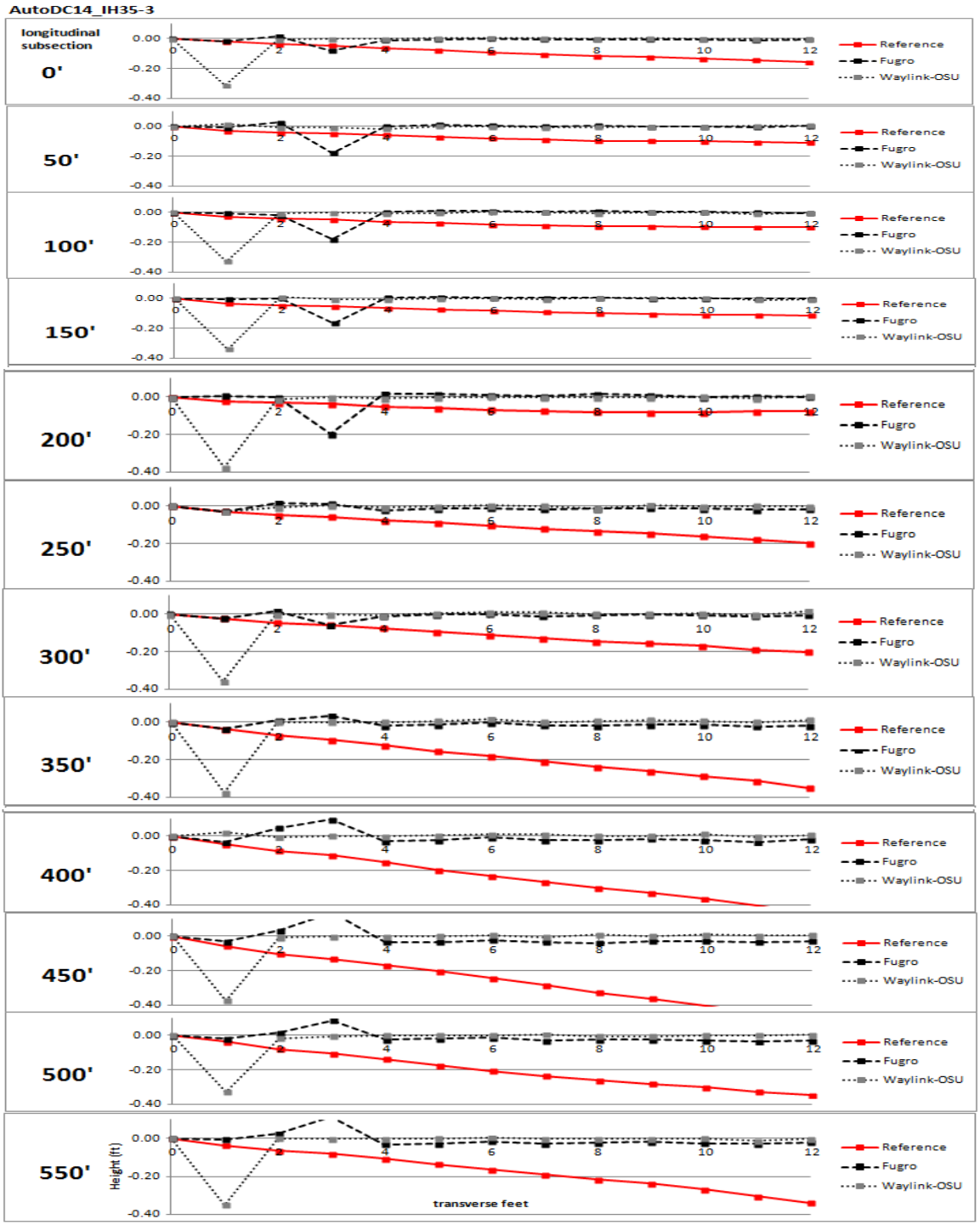

Figure E14: Cross slope for every transverse foot of every 50-ft. subsection for AutoDC14_IH35-3

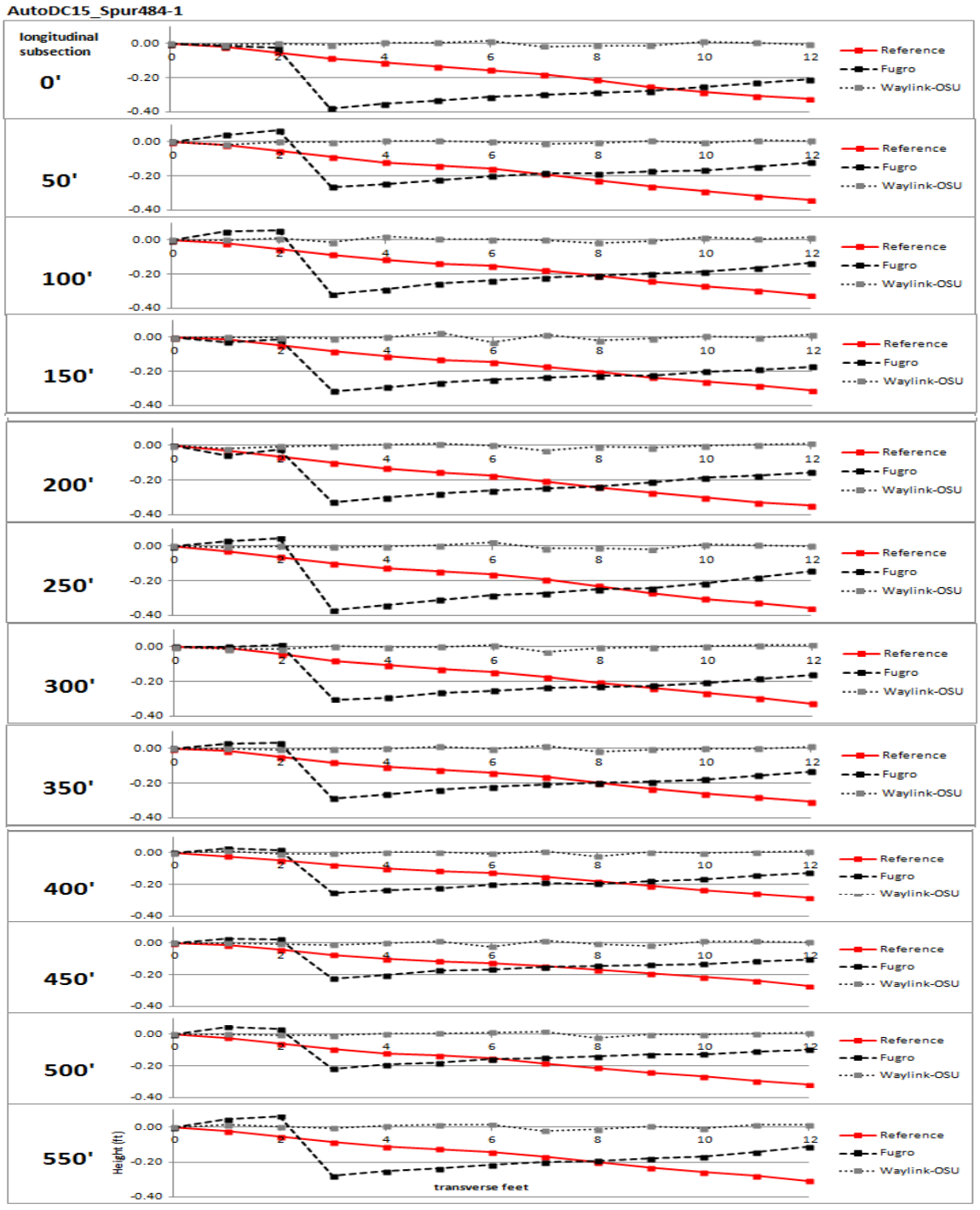

Figure E15: Cross slope for every transverse foot of every 50-ft. subsection for AutoDC15_Spur484-1

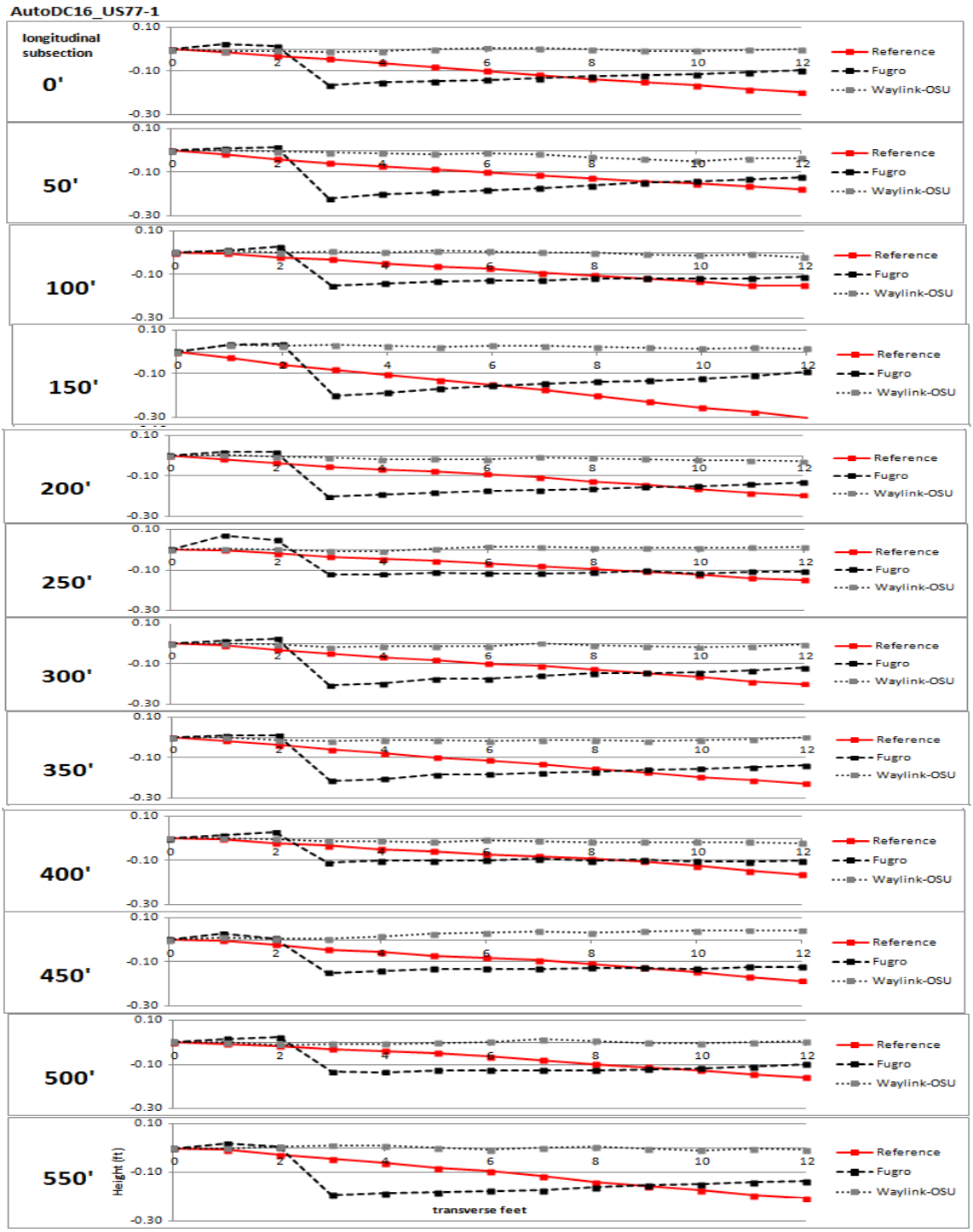

Figure E16: Cross slope for every transverse foot of every 50-ft. subsection for AutoDC16_US77-1

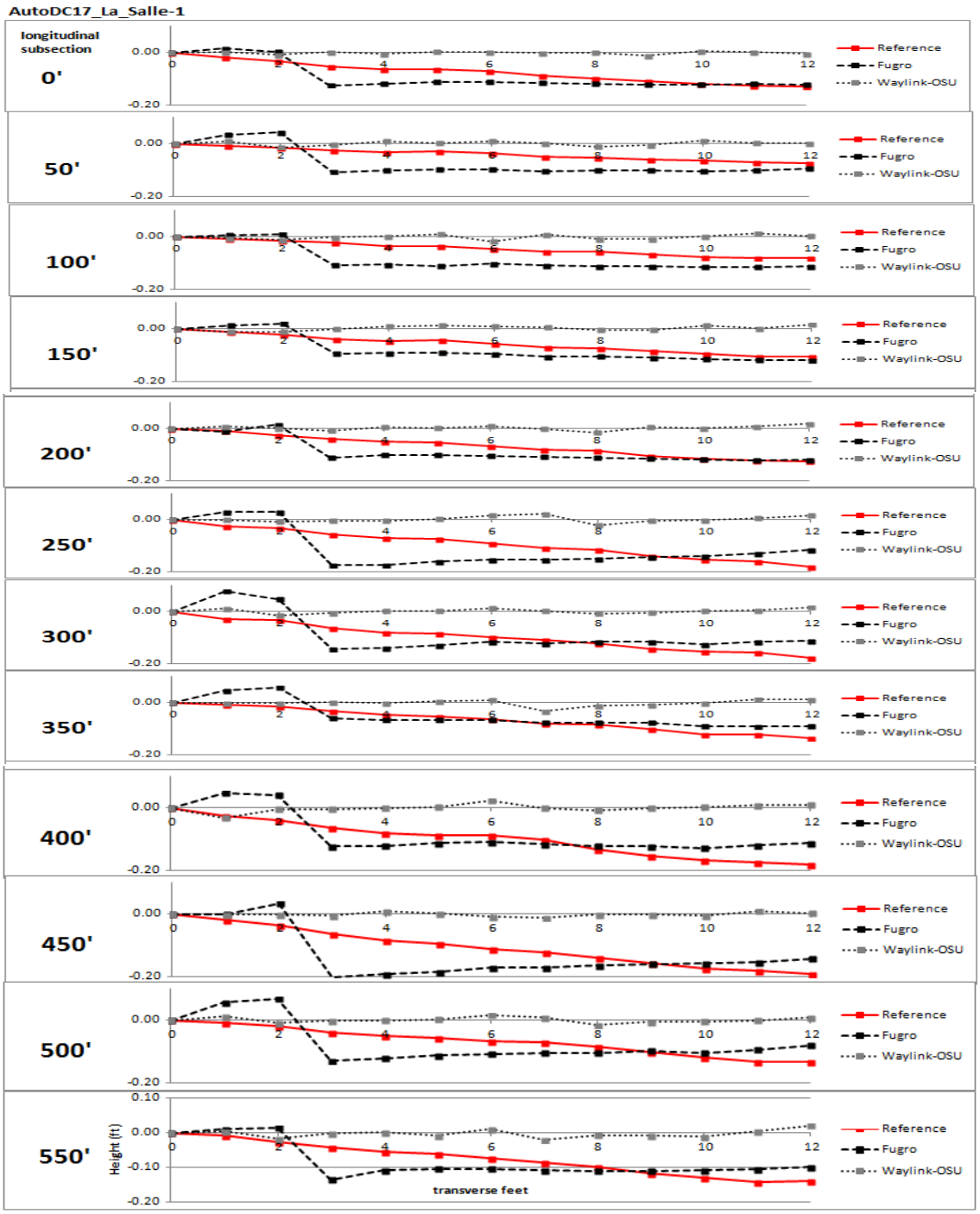

Figure E17: Cross slope for every transverse foot of every 50-ft. subsection for AutoDC17_La_Salle-1

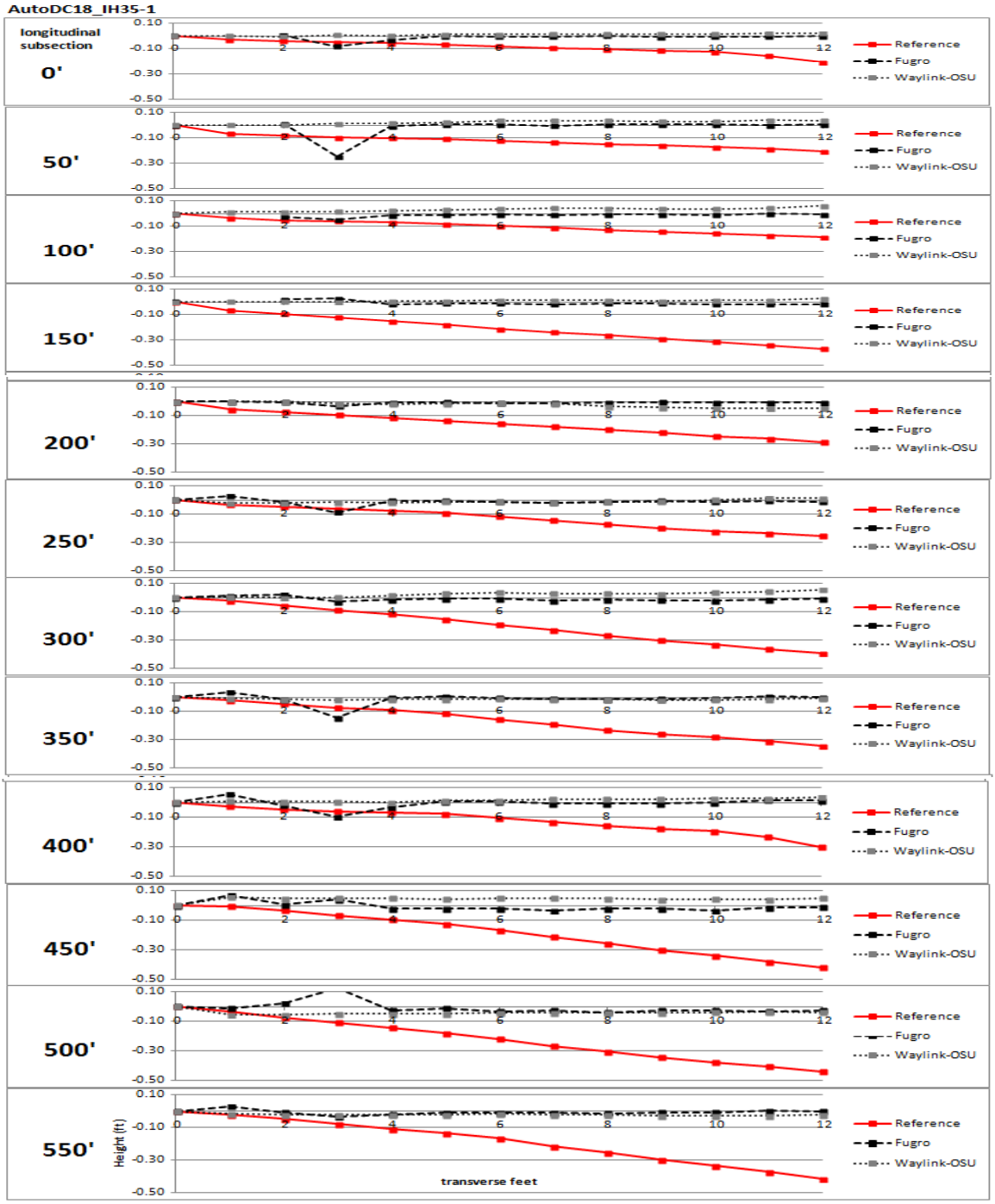

Figure E18: Cross slope for every transverse foot of every 50-ft. subsection for AutoDC18_IH35-1

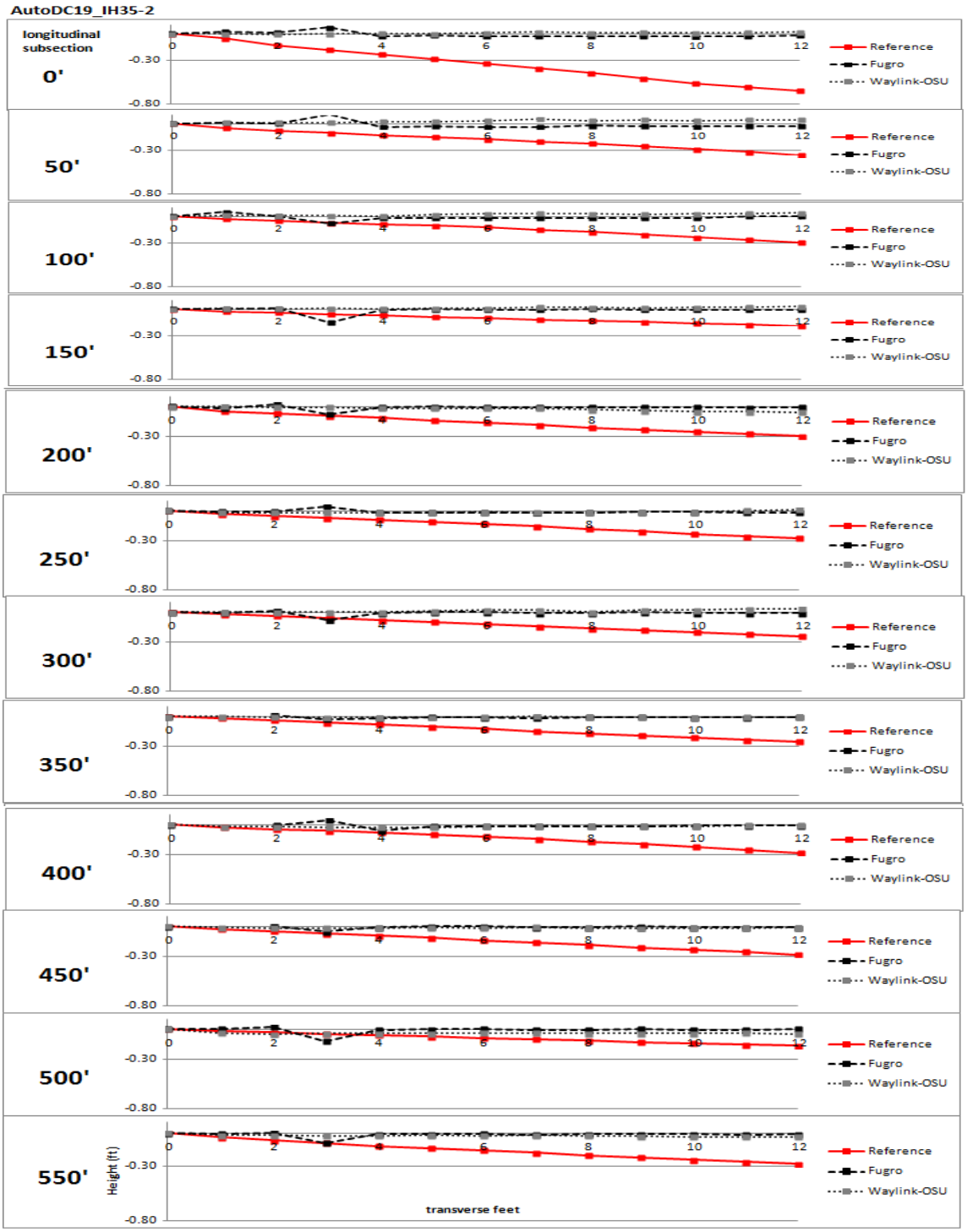

Figure E19: Cross slope for every transverse foot of every 50-ft. subsection for AutoDC19_IH35-2

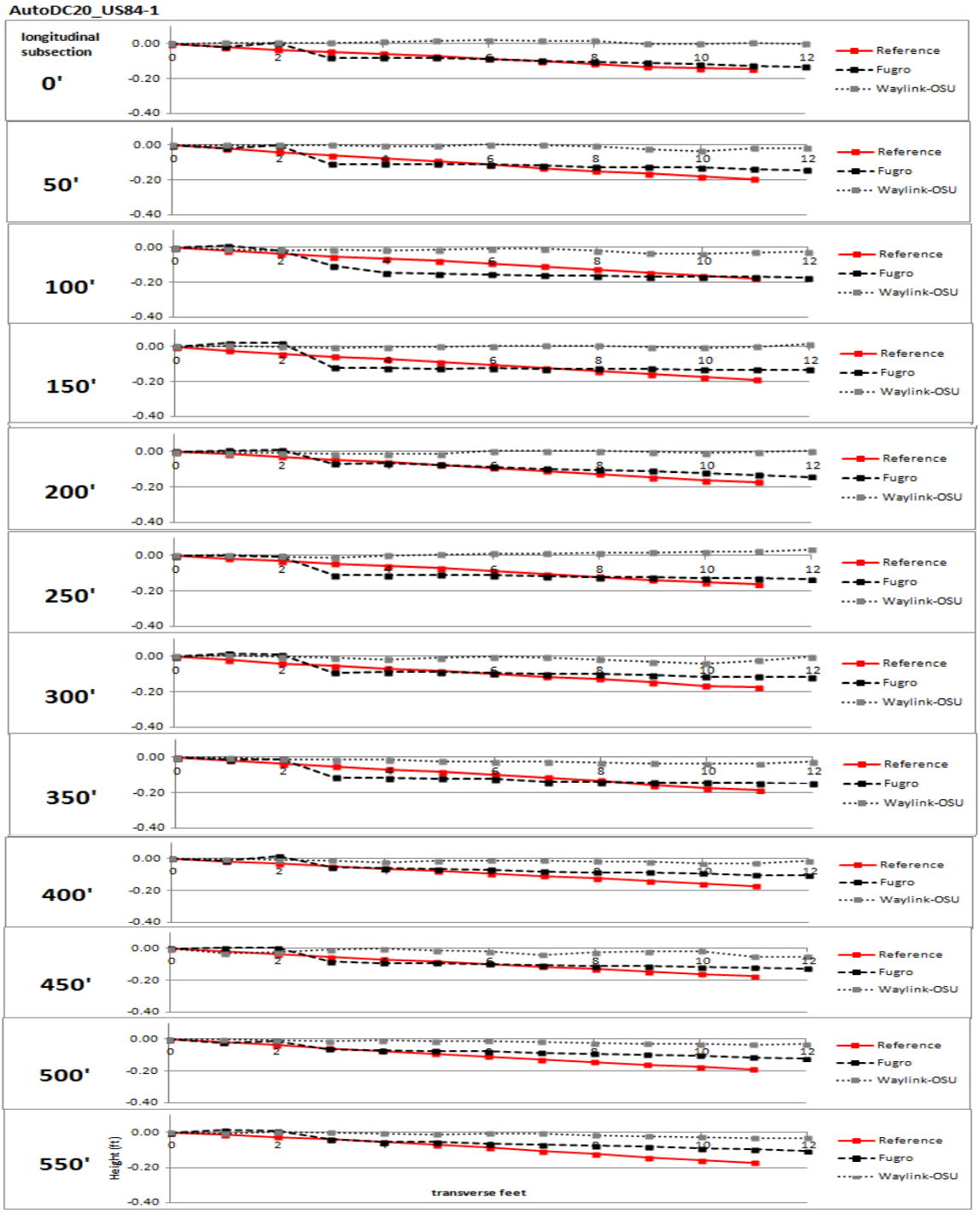

Figure E20: Cross slope for every transverse foot of every 50-ft. subsection for AutoDC20_US84-1

Appendix F. Summary Data From Reference Of Potential Water In Surface Depressions (Ruts) For Each Cross Slope Profile

Table F1: Summary data from reference of potential water in surface depressions (ruts) for each cross slope profile for AutoDC1_FM973-1

				if more than one with max. value, takes first in sequence from left to right (starting with left peaks, then right peaks)		if more than one with max. value, takes first in sequence from left to right (starting with left peaks, then right peaks)
Subsection (ft)	**Total Number of Puddles/Ruts**	**Cumulative Area of All Water**	**Maximum Depth**	**Corresponding Width to Max. Depth**	**Maximum Width**	**Corresponding Depth to Max. Width**
0	0	0.0000	0.0000		0.0000	
50	2	0.0051	0.0046	1.7000	1.7000	0.0046
100	2	0.0136	0.0075	2.4058	2.5600	0.0023
150	2	0.0220	0.0074	2.9000	3.6061	0.0046
200	1	0.0023	0.0030	1.5625	1.5625	0.0030
250	1	0.0002	0.0003	1.1333	1.1333	0.0003
300	0	0.0000	0.0000		0.0000	
350	0	0.0000	0.0000		0.0000	
400	0	0.0000	0.0000		0.0000	
450	0	0.0000	0.0000		0.0000	
500	0	0.0000	0.0000		0.0000	
550	0	0.0000	0.0000		0.0000	

Table F2: Summary data from reference of potential water in surface depressions (ruts) for each cross slope profile for AutoDC2_FM3177-1

				if more than one with max. value, takes first in sequence from left to right (starting with left peaks, then right peaks)		if more than one with max. value, takes first in sequence from left to right (starting with left peaks, then right peaks)
Subsection (ft)	**Total Number of Puddles/Ruts**	**Cumulative Area of All Water**	**Maximum Depth**	**Corresponding Width to Max. Depth**	**Maximum Width**	**Corresponding Depth to Max. Width**
0	2	0.0676	0.0394	2.9600	2.9600	0.0394
50	1	0.0137	0.0080	3.6667	3.6667	0.0080
100	2	0.0251	0.0118	1.6667	2.3551	0.0098
150	2	0.0712	0.0287	4.1452	4.3182	0.0074
200	2	0.0553	0.0205	2.8243	3.1905	0.0108
250	1	0.0308	0.0184	2.3500	2.3500	0.0184
300	1	0.0055	0.0036	2.0705	2.0705	0.0036
350	2	0.0098	0.0075	2.0091	2.0091	0.0075
400	1	0.0102	0.0082	2.0693	2.0693	0.0082
450	0	0.0000	0.0000		0.0000	
500	0	0.0000	0.0000		0.0000	
550	0	0.0000	0.0000		0.0000	

Table F3: Summary data from reference of potential water in surface depressions (ruts) for each cross slope profile for AutoDC3_FM696-1

				if more than one with max. value, takes first in sequence from left to right (starting with left peaks, then right peaks)		if more than one with max. value, takes first in sequence from left to right (starting with left peaks, then right peaks)
Subsection (ft)	**Total Number of Puddles/Ruts**	**Cumulative Area of All Water**	**Maximum Depth**	**Corresponding Width to Max. Depth**	**Maximum Width**	**Corresponding Depth to Max. Width**
0	0	0.0000	0.0000		0.0000	
50	1	0.0118	0.0177	1.3303	1.3303	0.0177
100	2	0.0408	0.0303	2.0301	2.0301	0.0303
150	2	0.0107	0.0105	1.5766	1.5766	0.0105
200	1	0.0002	0.0003	1.0070	1.0070	0.0003
250	1	0.0005	0.0010	1.0326	1.0326	0.0010
300	0	0.0000	0.0000		0.0000	
350	1	0.0159	0.0164	1.9346	1.9346	0.0164
400	1	0.0048	0.0072	1.3212	1.3212	0.0072
450	1	0.0056	0.0089	1.2596	1.2596	0.0089
500	1	0.0030	0.0049	1.2308	1.2308	0.0049
550	0	0.0000	0.0000		0.0000	

Table F4: Summary data from reference of potential water in surface depressions (ruts) for each cross slope profile for AutoDC4_FM696-3

				if more than one with max. value, takes first in sequence from left to right (starting with left peaks, then right peaks)		if more than one with max. value, takes first in sequence from left to right (starting with left peaks, then right peaks)
Subsection (ft)	**Total Number of Puddles/Ruts**	**Cumulative Area of All Water**	**Maximum Depth**	**Corresponding Width to Max. Depth**	**Maximum Width**	**Corresponding Depth to Max. Width**
0	0	0.0000	0.0000		0.0000	
50	0	0.0000	0.0000		0.0000	
100	0	0.0000	0.0000		0.0000	
150	0	0.0000	0.0000		0.0000	
200	0	0.0000	0.0000		0.0000	
250	0	0.0000	0.0000		0.0000	
300	0	0.0000	0.0000		0.0000	
350	0	0.0000	0.0000		0.0000	
400	0	0.0000	0.0000		0.0000	
450	2	0.0288	0.0062	5.6667	5.6667	0.0062
500	1	0.0629	0.0164	8.2667	8.2667	0.0164
550	1	0.0002	0.0003	1.0435	1.0435	0.0003

Table F5: Summary data from reference of potential water in surface depressions (ruts) for each cross slope profile for AutoDC5_FM696-4

				if more than one with max. value, takes first in sequence from left to right (starting with left peaks, then right peaks)		if more than one with max. value, takes first in sequence from left to right (starting with left peaks, then right peaks)
Subsection (ft)	**Total Number of Puddles/Ruts**	**Cumulative Area of All Water**	**Maximum Depth**	**Corresponding Width to Max. Depth**	**Maximum Width**	**Corresponding Depth to Max. Width**
0	0	0.0000	0.0000		0.0000	
50	0	0.0000	0.0000		0.0000	
100	0	0.0000	0.0000		0.0000	
150	0	0.0000	0.0000		0.0000	
200	0	0.0000	0.0000		0.0000	
250	0	0.0000	0.0000		0.0000	
300	0	0.0000	0.0000		0.0000	
350	0	0.0000	0.0000		0.0000	
400	0	0.0000	0.0000		0.0000	
450	0	0.0000	0.0000		0.0000	
500	0	0.0000	0.0000		0.0000	
550	0	0.0000	0.0000		0.0000	

Table F6: Summary data from reference of potential water in surface depressions (ruts) for each cross slope profile for AutoDC6_FM696-2

				if more than one with max. value, takes first in sequence from left to right (starting with left peaks, then right peaks)		if more than one with max. value, takes first in sequence from left to right (starting with left peaks, then right peaks)
Subsection (ft)	**Total Number of Puddles/Ruts**	**Cumulative Area of All Water**	**Maximum Depth**	**Corresponding Width to Max. Depth**	**Maximum Width**	**Corresponding Depth to Max. Width**
0	0	0.0000	0.0000		0.0000	
50	1	0.0006	0.0011	1.0972	1.0972	0.0011
100	0	0.0000	0.0000		0.0000	
150	1	0.0018	0.0028	2.0489	2.0489	0.0028
200	2	0.0226	0.0164	2.0777	2.0777	0.0164
250	1	0.0003	0.0005	1.0612	1.0612	0.0005
300	1	0.0061	0.0097	1.2670	1.2670	0.0097
350	2	0.0450	0.0218	3.8043	3.8043	0.0218
400	1	0.0239	0.0149	3.3202	3.3202	0.0149
450	2	0.0127	0.0062	2.3846	2.3846	0.0062
500	1	0.0097	0.0062	2.2035	2.2035	0.0062
550	1	0.0029	0.0028	2.0045	2.0045	0.0028

Table F7: Summary data from reference of potential water in surface depressions (ruts) for each cross slope profile for AutoDC7_FM696-5

				if more than one with max. value, takes first in sequence from left to right (starting with left peaks, then right peaks)		if more than one with max. value, takes first in sequence from left to right (starting with left peaks, then right peaks)
Subsection (ft)	**Total Number of Puddles/Ruts**	**Cumulative Area of All Water**	**Maximum Depth**	**Corresponding Width to Max. Depth**	**Maximum Width**	**Corresponding Depth to Max. Width**
0	1	0.0041	0.0048	1.7250	1.7250	0.0048
50	2	0.1248	0.0394	4.0969	4.0969	0.0394
100	0	0.0000	0.0000		0.0000	
150	0	0.0000	0.0000		0.0000	
200	2	0.0016	0.0020	1.1818	1.1818	0.0020
250	1	0.0128	0.0080	3.5333	3.5333	0.0080
300	0	0.0000	0.0000		0.0000	
350	2	0.0061	0.0046	1.5957	2.2424	0.0016
400	0	0.0000	0.0000		0.0000	
450	1	0.0259	0.0090	4.5851	4.5851	0.0090
500	1	0.0045	0.0052	1.7111	1.7111	0.0052
550	1	0.0009	0.0013	1.4444	1.4444	0.0013

Table F8: Summary data from reference of potential water in surface depressions (ruts) for each cross slope profile for AutoDC8_FM619-1

				if more than one with max. value, takes first in sequence from left to right (starting with left peaks, then right peaks)		if more than one with max. value, takes first in sequence from left to right (starting with left peaks, then right peaks)
Subsection (ft)	**Total Number of Puddles/Ruts**	**Cumulative Area of All Water**	**Maximum Depth**	**Corresponding Width to Max. Depth**	**Maximum Width**	**Corresponding Depth to Max. Width**
0	0	0.0000	0.0000		0.0000	
50	0	0.0000	0.0000		0.0000	
100	0	0.0000	0.0000		0.0000	
150	0	0.0000	0.0000		0.0000	
200	0	0.0000	0.0000		0.0000	
250	0	0.0000	0.0000		0.0000	
300	0	0.0000	0.0000		0.0000	
350	0	0.0000	0.0000		0.0000	
400	0	0.0000	0.0000		0.0000	
450	1	0.0010	0.0020	1.0591	1.0591	0.0020
500	0	0.0000	0.0000		0.0000	
550	0	0.0000	0.0000		0.0000	

Table F9: Summary data from reference of potential water in surface depressions (ruts) for each cross slope profile for AutoDC9_FM112-1

				if more than one with max. value, takes first in sequence from left to right (starting with left peaks, then right peaks)		if more than one with max. value, takes first in sequence from left to right (starting with left peaks, then right peaks)
Subsection (ft)	**Total Number of Puddles/Ruts**	**Cumulative Area of All Water**	**Maximum Depth**	**Corresponding Width to Max. Depth**	**Maximum Width**	**Corresponding Depth to Max. Width**
0	1	0.0044	0.0046	1.9032	1.9032	0.0046
50	0	0.0000	0.0000		0.0000	
100	1	0.0003	0.0007	1.0635	1.0635	0.0007
150	0	0.0000	0.0000		0.0000	
200	1	0.0004	0.0008	1.0714	1.0714	0.0008
250	2	0.1628	0.0682	6.0000	6.0000	0.0682
300	1	0.0160	0.0118	2.9863	2.9863	0.0118
350	1	0.0008	0.0015	1.0783	1.0783	0.0015
400	1	0.0296	0.0144	3.5333	3.5333	0.0144
450	1	0.0010	0.0010	2.0000	2.0000	0.0010
500	1	0.0295	0.0164	3.8696	3.8696	0.0164
550	0	0.0000	0.0000		0.0000	

Table F10: Summary data from reference of potential water in surface depressions (ruts) for each cross slope profile for AutoDC10_FM1331-1

				if more than one with max. value, takes first in sequence from left to right (starting with left peaks, then right peaks)		if more than one with max. value, takes first in sequence from left to right (starting with left peaks, then right peaks)
Subsection (ft)	**Total Number of Puddles/Ruts**	**Cumulative Area of All Water**	**Maximum Depth**	**Corresponding Width to Max. Depth**	**Maximum Width**	**Corresponding Depth to Max. Width**
0	1	0.0751	0.0423	3.8836	3.8836	0.0423
50	1	0.0373	0.0276	2.8000	2.8000	0.0276
100	0	0.0000	0.0000		0.0000	
150	0	0.0000	0.0000		0.0000	
200	0	0.0000	0.0000		0.0000	
250	0	0.0000	0.0000		0.0000	
300	0	0.0000	0.0000		0.0000	
350	0	0.0000	0.0000		0.0000	
400	0	0.0000	0.0000		0.0000	
450	0	0.0000	0.0000		0.0000	
500	0	0.0000	0.0000		0.0000	
550	1	0.0014	0.0025	1.1163	1.1163	0.0025

Table F11: Summary data from reference of potential water in surface depressions (ruts) for each cross slope profile for AutoDC11_FM1331-2

				if more than one with max. value, takes first in sequence from left to right (starting with left peaks, then right peaks)		if more than one with max. value, takes first in sequence from left to right (starting with left peaks, then right peaks)
Subsection (ft)	**Total Number of Puddles/Ruts**	**Cumulative Area of All Water**	**Maximum Depth**	**Corresponding Width to Max. Depth**	**Maximum Width**	**Corresponding Depth to Max. Width**
0	1	0.0805	0.0448	2.9530	2.9530	0.0448
50	2	0.0293	0.0167	2.4657	2.4657	0.0167
100	1	0.0043	0.0061	1.4066	1.4066	0.0061
150	1	0.0120	0.0077	2.1056	2.1056	0.0077
200	0	0.0000	0.0000		0.0000	
250	0	0.0000	0.0000		0.0000	
300	2	0.0199	0.0103	1.6632	2.2213	0.0089
350	1	0.0040	0.0039	2.0111	2.0111	0.0039
400	1	0.0003	0.0007	1.0345	1.0345	0.0007
450	1	0.0004	0.0008	1.0120	1.0120	0.0008
500	1	0.0044	0.0061	1.4458	1.4458	0.0061
550	0	0.0000	0.0000		0.0000	

Table F12: Summary data from reference of potential water in surface depressions (ruts) for each cross slope profile for AutoDC12_FM1063-1

				if more than one with max. value, takes first in sequence from left to right (starting with left peaks, then right peaks)		if more than one with max. value, takes first in sequence from left to right (starting with left peaks, then right peaks)
Subsection (ft)	**Total Number of Puddles/Ruts**	**Cumulative Area of All Water**	**Maximum Depth**	**Corresponding Width to Max. Depth**	**Maximum Width**	**Corresponding Depth to Max. Width**
0	1	0.0362	0.0238	2.6327	2.6327	0.0238
50	2	0.0239	0.0153	2.6691	2.6691	0.0153
100	2	0.0031	0.0030	2.0000	2.0000	0.0030
150	0	0.0000	0.0000		0.0000	
200	0	0.0000	0.0000		0.0000	
250	1	0.0222	0.0153	2.5625	2.5625	0.0153
300	2	0.0040	0.0041	1.5435	1.5435	0.0041
350	0	0.0000	0.0000		0.0000	
400	1	0.0032	0.0051	1.2627	1.2627	0.0051
450	1	0.0102	0.0098	2.0315	2.0315	0.0098
500	1	0.0023	0.0030	1.5294	1.5294	0.0030
550	1	0.0062	0.0064	2.4699	2.4699	0.0064

Table F13: Summary data from reference of potential water in surface depressions (ruts) for each cross slope profile for AutoDC13_US79-1

				if more than one with max. value, takes first in sequence from left to right (starting with left peaks, then right peaks)		if more than one with max. value, takes first in sequence from left to right (starting with left peaks, then right peaks)
Subsection (ft)	**Total Number of Puddles/Ruts**	**Cumulative Area of All Water**	**Maximum Depth**	**Corresponding Width to Max. Depth**	**Maximum Width**	**Corresponding Depth to Max. Width**
0	0	0.0000	0.0000		0.0000	
50	0	0.0000	0.0000		0.0000	
100	0	0.0000	0.0000		0.0000	
150	0	0.0000	0.0000		0.0000	
200	0	0.0000	0.0000		0.0000	
250	0	0.0000	0.0000		0.0000	
300	0	0.0000	0.0000		0.0000	
350	0	0.0000	0.0000		0.0000	
400	0	0.0000	0.0000		0.0000	
450	0	0.0000	0.0000		0.0000	
500	0	0.0000	0.0000		0.0000	
550	0	0.0000	0.0000		0.0000	

Table F14: Summary data from reference of potential water in surface depressions (ruts) for each cross slope profile for AutoDC14_IH35-3

				if more than one with max. value, takes first in sequence from left to right (starting with left peaks, then right peaks)		if more than one with max. value, takes first in sequence from left to right (starting with left peaks, then right peaks)
Subsection (ft)	**Total Number of Puddles/Ruts**	**Cumulative Area of All Water**	**Maximum Depth**	**Corresponding Width to Max. Depth**	**Maximum Width**	**Corresponding Depth to Max. Width**
0	0	0.0000	0.0000		0.0000	
50	0	0.0000	0.0000		0.0000	
100	0	0.0000	0.0000		0.0000	
150	0	0.0000	0.0000		0.0000	
200	1	0.0092	0.0057	3.1053	3.1053	0.0057
250	0	0.0000	0.0000		0.0000	
300	0	0.0000	0.0000		0.0000	
350	0	0.0000	0.0000		0.0000	
400	0	0.0000	0.0000		0.0000	
450	0	0.0000	0.0000		0.0000	
500	0	0.0000	0.0000		0.0000	
550	0	0.0000	0.0000		0.0000	

Table F15: Summary data from reference of potential water in surface depressions (ruts) for each cross slope profile for AutoDC15_Spur484-1

				if more than one with max. value, takes first in sequence from left to right (starting with left peaks, then right peaks)		if more than one with max. value, takes first in sequence from left to right (starting with left peaks, then right peaks)
Subsection (ft)	**Total Number of Puddles/Ruts**	**Cumulative Area of All Water**	**Maximum Depth**	**Corresponding Width to Max. Depth**	**Maximum Width**	**Corresponding Depth to Max. Width**
0	0	0.0000	0.0000		0.0000	
50	0	0.0000	0.0000		0.0000	
100	0	0.0000	0.0000		0.0000	
150	0	0.0000	0.0000		0.0000	
200	0	0.0000	0.0000		0.0000	
250	0	0.0000	0.0000		0.0000	
300	0	0.0000	0.0000		0.0000	
350	0	0.0000	0.0000		0.0000	
400	0	0.0000	0.0000		0.0000	
450	0	0.0000	0.0000		0.0000	
500	0	0.0000	0.0000		0.0000	
550	0	0.0000	0.0000		0.0000	

Table F16: Summary data from reference of potential water in surface depressions (ruts) for each cross slope profile for AutoDC16_US77-1

				if more than one with max. value, takes first in sequence from left to right (starting with left peaks, then right peaks)		if more than one with max. value, takes first in sequence from left to right (starting with left peaks, then right peaks)
Subsection (ft)	**Total Number of Puddles/Ruts**	**Cumulative Area of All Water**	**Maximum Depth**	**Corresponding Width to Max. Depth**	**Maximum Width**	**Corresponding Depth to Max. Width**
0	0	0.0000	0.0000		0.0000	
50	0	0.0000	0.0000		0.0000	
100	0	0.0000	0.0000		0.0000	
150	0	0.0000	0.0000		0.0000	
200	0	0.0000	0.0000		0.0000	
250	0	0.0000	0.0000		0.0000	
300	0	0.0000	0.0000		0.0000	
350	0	0.0000	0.0000		0.0000	
400	0	0.0000	0.0000		0.0000	
450	0	0.0000	0.0000		0.0000	
500	0	0.0000	0.0000		0.0000	
550	0	0.0000	0.0000		0.0000	

Table F17: Summary data from reference of potential water in surface depressions (ruts) for each cross slope profile for AutoDC17_La_Salle-1

				if more than one with max. value, takes first in sequence from left to right (starting with left peaks, then right peaks)		if more than one with max. value, takes first in sequence from left to right (starting with left peaks, then right peaks)
Subsection (ft)	**Total Number of Puddles/Ruts**	**Cumulative Area of All Water**	**Maximum Depth**	**Corresponding Width to Max. Depth**	**Maximum Width**	**Corresponding Depth to Max. Width**
0	0	0.0000	0.0000		0.0000	
50	1	0.0036	0.0044	1.6136	1.6136	0.0044
100	2	0.0014	0.0016	1.1010	1.1786	0.0008
150	1	0.0014	0.0021	1.3171	1.3171	0.0021
200	0	0.0000	0.0000		0.0000	
250	0	0.0000	0.0000		0.0000	
300	0	0.0000	0.0000		0.0000	
350	0	0.0000	0.0000		0.0000	
400	0	0.0000	0.0000		0.0000	
450	0	0.0000	0.0000		0.0000	
500	0	0.0000	0.0000		0.0000	
550	1	0.0033	0.0048	1.3718	1.3718	0.0048

Table F18: Summary data from reference of potential water in surface depressions (ruts) for each cross slope profile for AutoDC18_IH35-1

				if more than one with max. value, takes first in sequence from left to right (starting with left peaks, then right peaks)		if more than one with max. value, takes first in sequence from left to right (starting with left peaks, then right peaks)
Subsection (ft)	**Total Number of Puddles/Ruts**	**Cumulative Area of All Water**	**Maximum Depth**	**Corresponding Width to Max. Depth**	**Maximum Width**	**Corresponding Depth to Max. Width**
0	0	0.0000	0.0000		0.0000	
50	0	0.0000	0.0000		0.0000	
100	0	0.0000	0.0000		0.0000	
150	0	0.0000	0.0000		0.0000	
200	0	0.0000	0.0000		0.0000	
250	0	0.0000	0.0000		0.0000	
300	0	0.0000	0.0000		0.0000	
350	0	0.0000	0.0000		0.0000	
400	0	0.0000	0.0000		0.0000	
450	0	0.0000	0.0000		0.0000	
500	0	0.0000	0.0000		0.0000	
550	0	0.0000	0.0000		0.0000	

Table F19: Summary data from reference of potential water in surface depressions (ruts) for each cross slope profile for AutoDC19_IH35-2

				if more than one with max. value, takes first in sequence from left to right (starting with left peaks, then right peaks)		if more than one with max. value, takes first in sequence from left to right (starting with left peaks, then right peaks)
Subsection (ft)	**Total Number of Puddles/Ruts**	**Cumulative Area of All Water**	**Maximum Depth**	**Corresponding Width to Max. Depth**	**Maximum Width**	**Corresponding Depth to Max. Width**
0	0	0.0000	0.0000		0.0000	
50	0	0.0000	0.0000		0.0000	
100	0	0.0000	0.0000		0.0000	
150	0	0.0000	0.0000		0.0000	
200	0	0.0000	0.0000		0.0000	
250	0	0.0000	0.0000		0.0000	
300	0	0.0000	0.0000		0.0000	
350	0	0.0000	0.0000		0.0000	
400	0	0.0000	0.0000		0.0000	
450	0	0.0000	0.0000		0.0000	
500	0	0.0000	0.0000		0.0000	
550	0	0.0000	0.0000		0.0000	

Table F20: Summary data from reference of potential water in surface depressions (ruts) for each cross slope profile for AutoDC20_US84-1

				if more than one with max. value, takes first in sequence from left to right (starting with left peaks, then right peaks)		if more than one with max. value, takes first in sequence from left to right (starting with left peaks, then right peaks)
Subsection (ft)	**Total Number of Puddles/Ruts**	**Cumulative Area of All Water**	**Maximum Depth**	**Corresponding Width to Max. Depth**	**Maximum Width**	**Corresponding Depth to Max. Width**
0	0	0.0000	0.0000		0.0000	
50	0	0.0000	0.0000		0.0000	
100	0	0.0000	0.0000		0.0000	
150	0	0.0000	0.0000		0.0000	
200	0	0.0000	0.0000		0.0000	
250	0	0.0000	0.0000		0.0000	
300	0	0.0000	0.0000		0.0000	
350	0	0.0000	0.0000		0.0000	
400	0	0.0000	0.0000		0.0000	
450	0	0.0000	0.0000		0.0000	
500	0	0.0000	0.0000		0.0000	
550	0	0.0000	0.0000		0.0000	

Appendix G. Drainage Path Lengths Using Reference Data

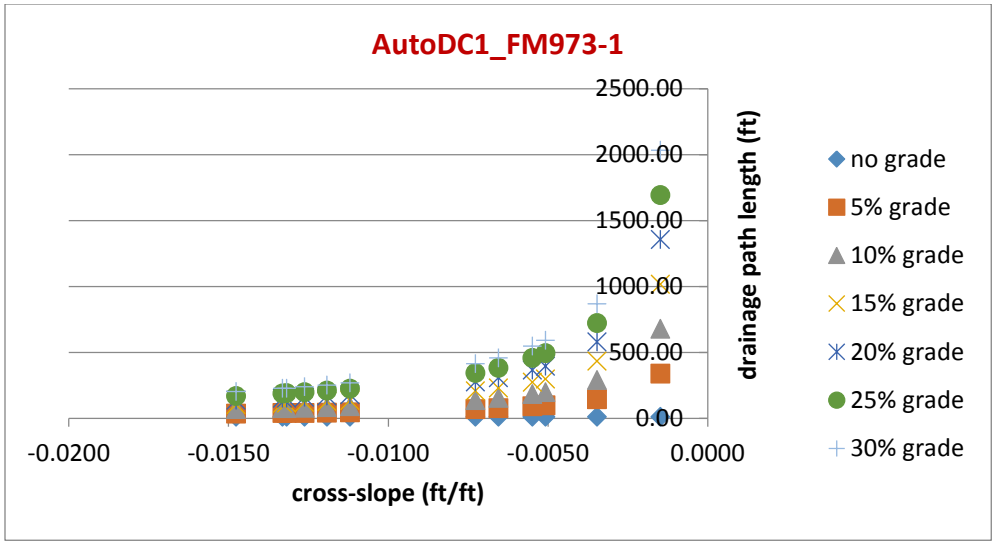

Figure G1: Drainage path lengths using reference data for AutoDC1_FM973-1

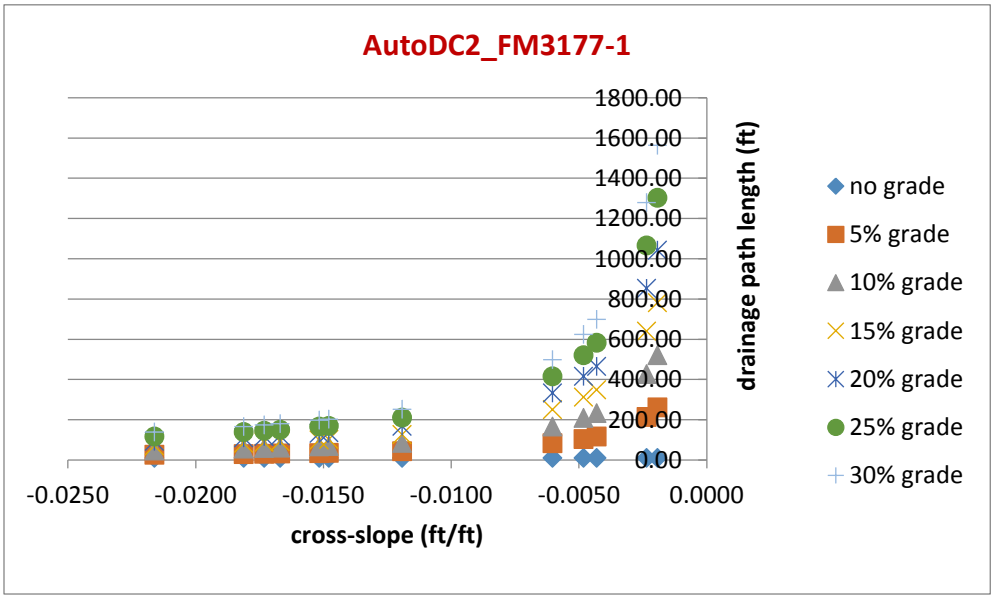

Figure G2: Drainage path lengths using reference data for AutoDC2_FM3177-1

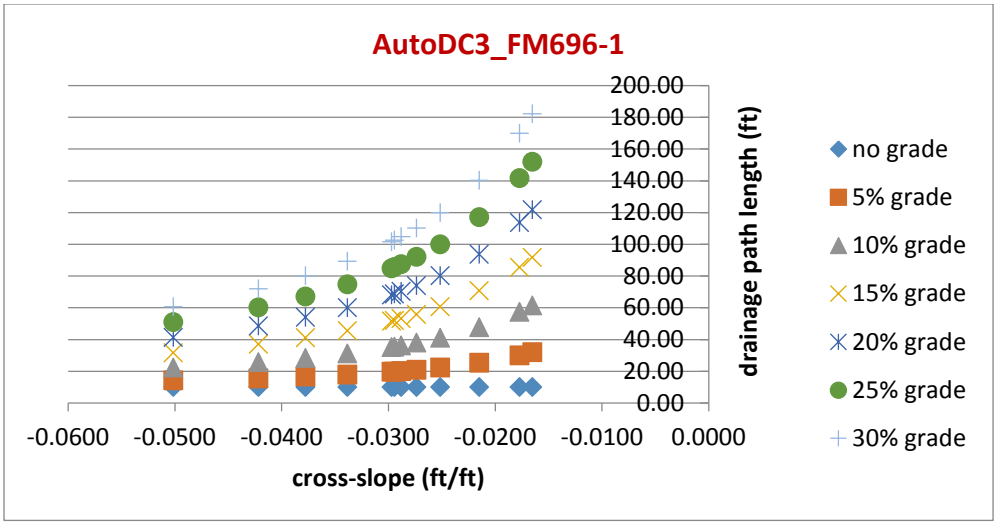

Figure G3: Drainage path lengths using reference data for AutoDC3_FM696-1

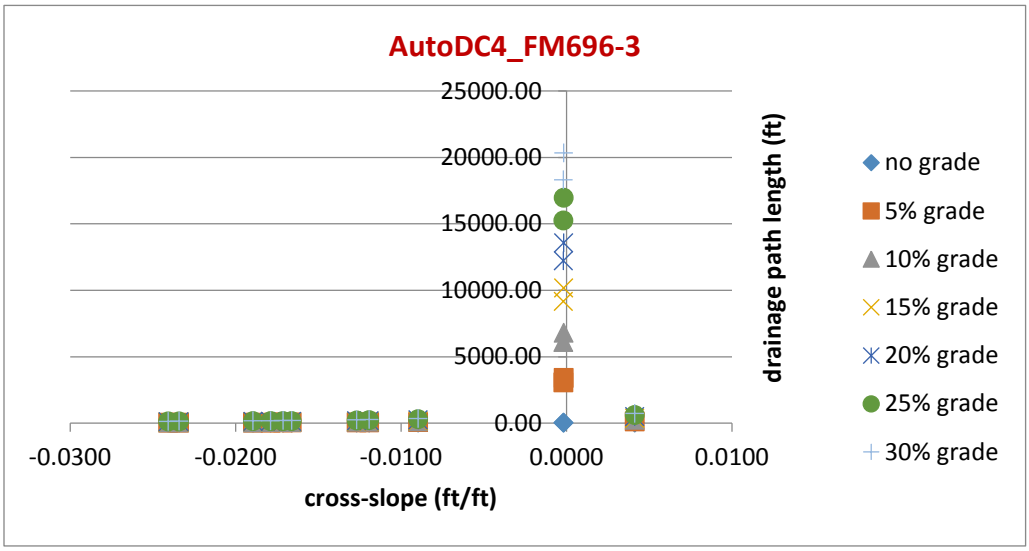

Figure G4: Drainage path lengths using reference data for AutoDC4_FM696-3

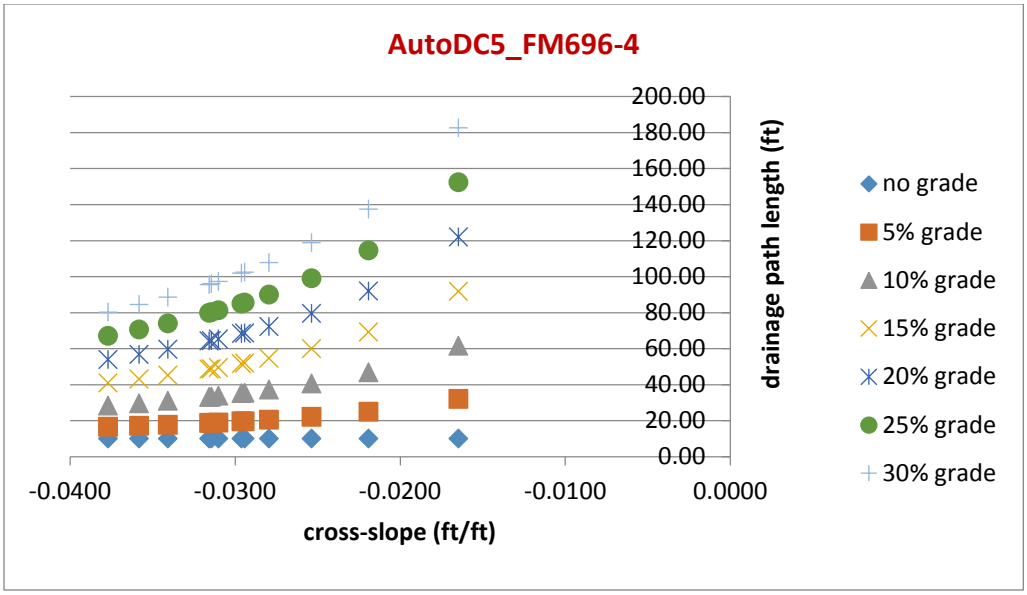

Figure G5: Drainage path lengths using reference data for AutoDC5_FM696-4

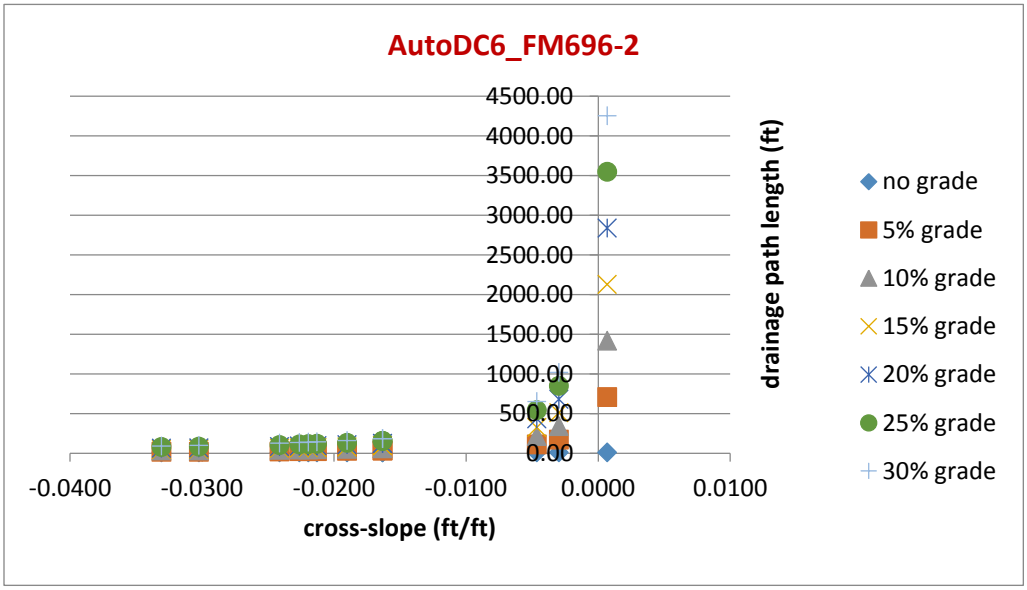

Figure G6: Drainage path lengths using reference data for AutoDC6_FM696-2

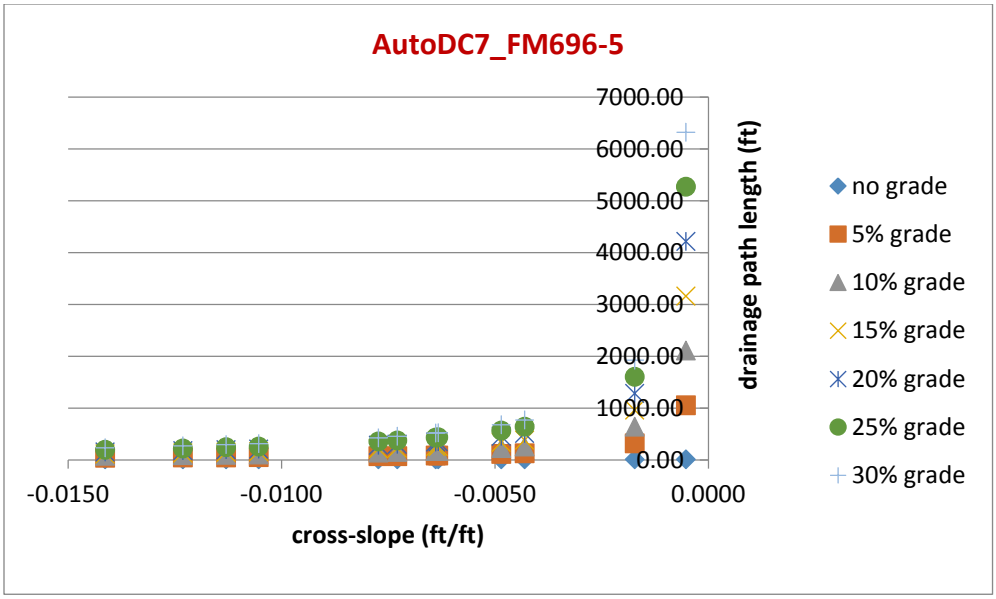

Figure G7: Drainage path lengths using reference data for AutoDC7_FM696-5

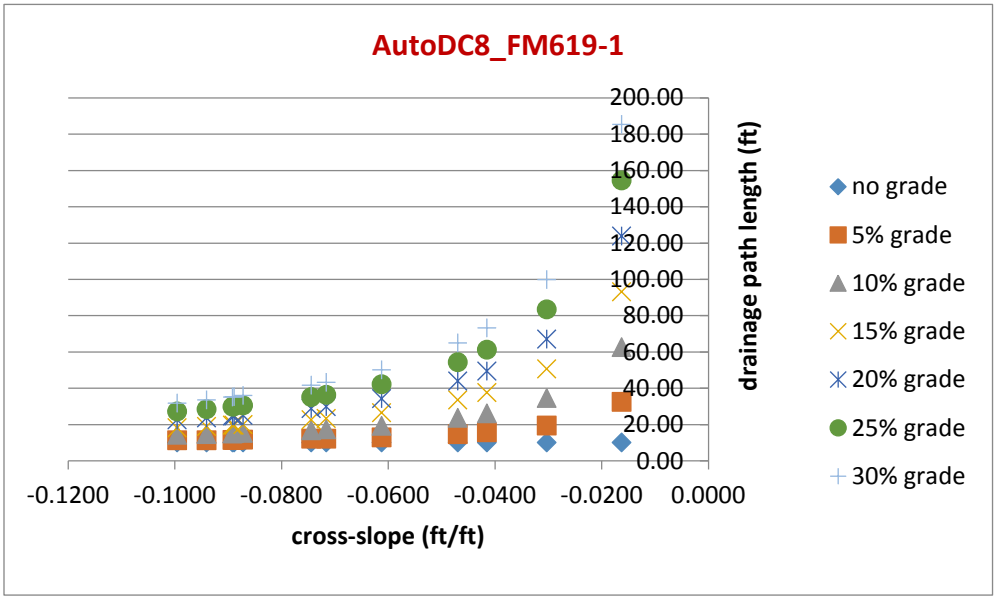

Figure G8: Drainage path lengths using reference data for AutoDC8_FM619-1

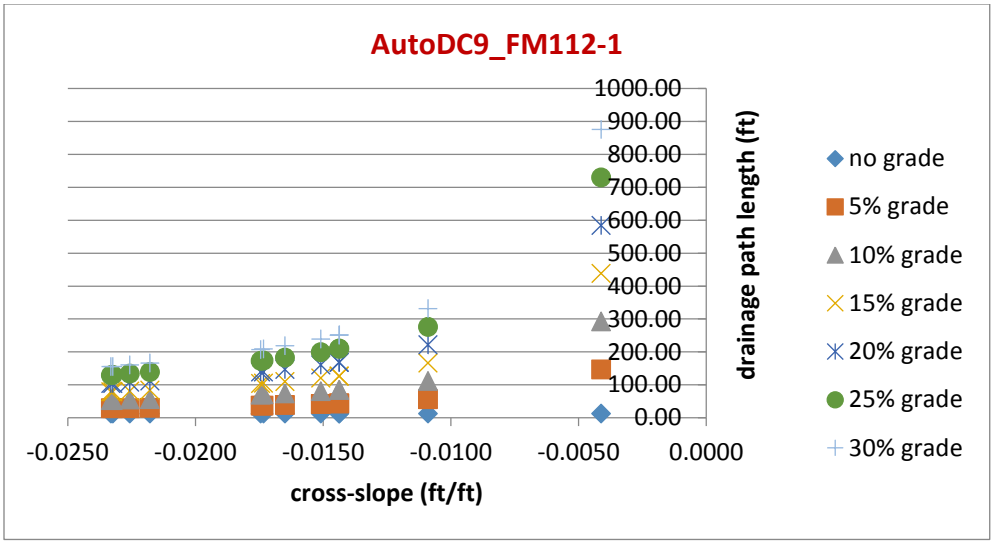

Figure G9: Drainage path lengths using reference data for AutoDC9_FM112-1

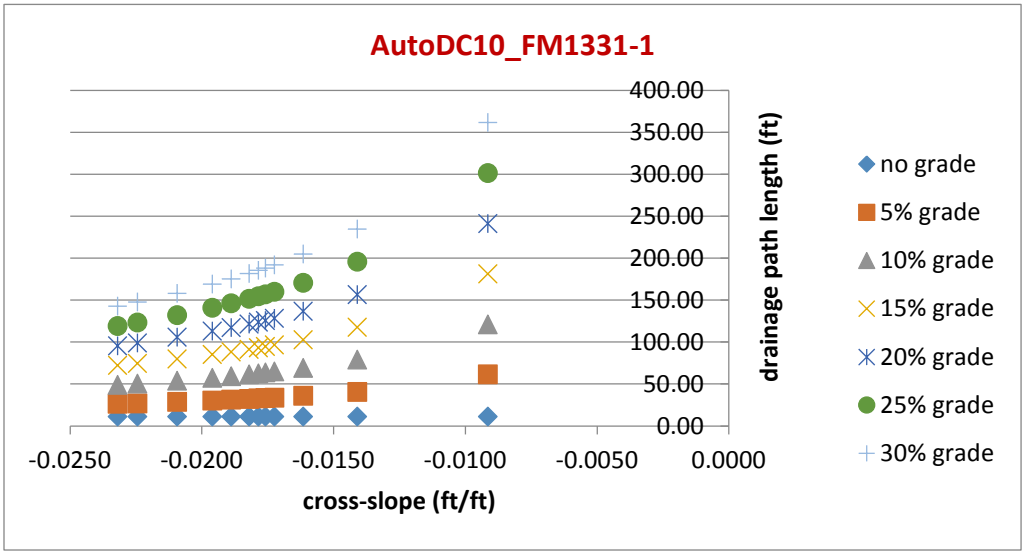

Figure G10: Drainage path lengths using reference data for AutoDC10_FM1331-1

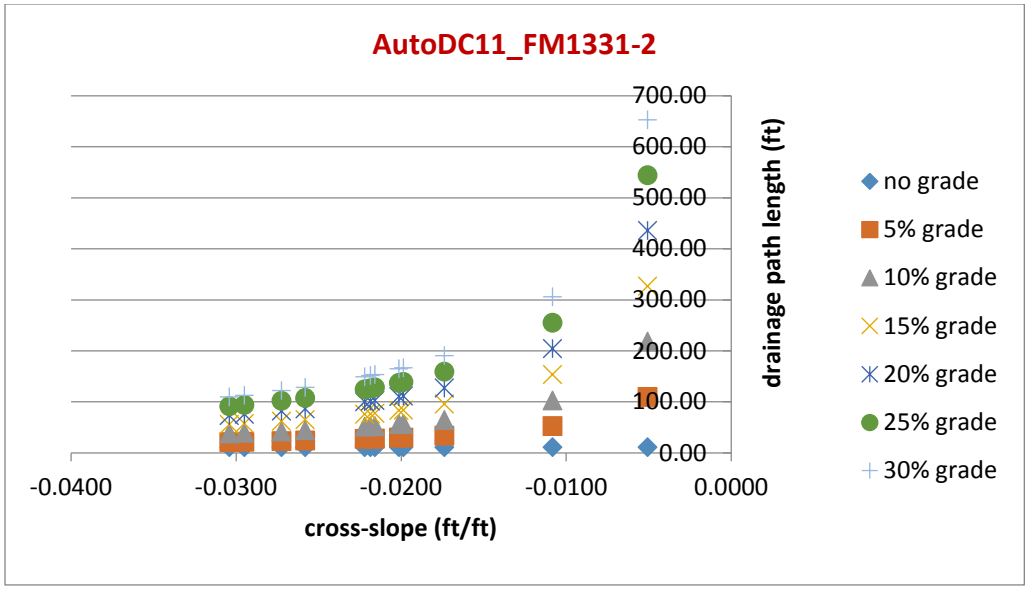

Figure G11: Drainage path lengths using reference data for AutoDC11_FM1331-2

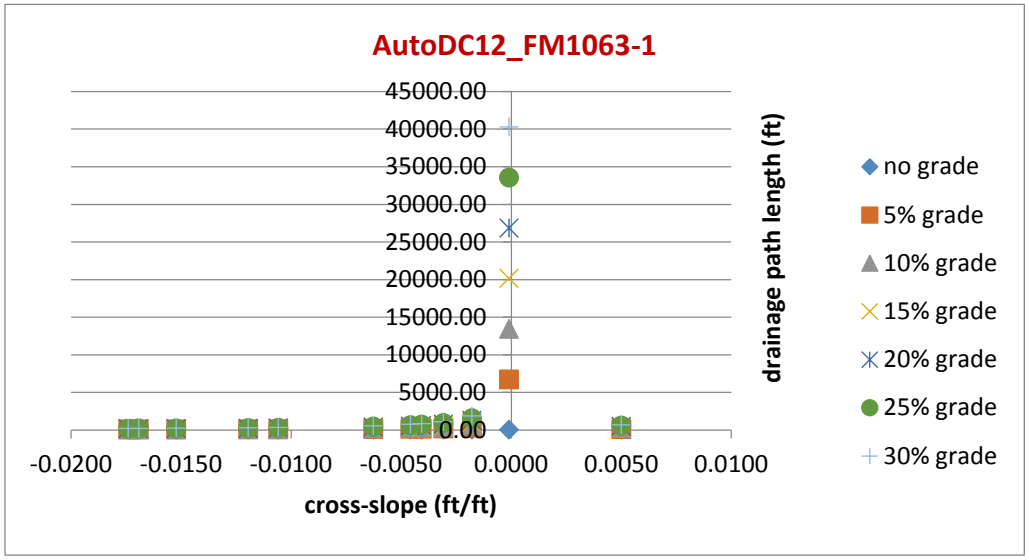

Figure G12: Drainage path lengths using reference data for AutoDC12_FM1063-1

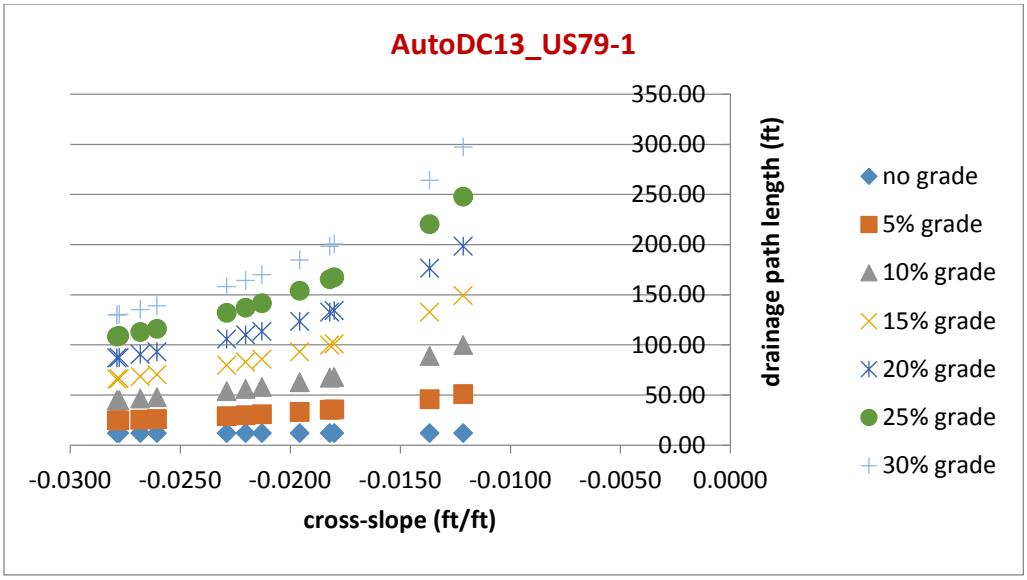

Figure G13: Drainage path lengths using reference data for AutoDC13_US79-1

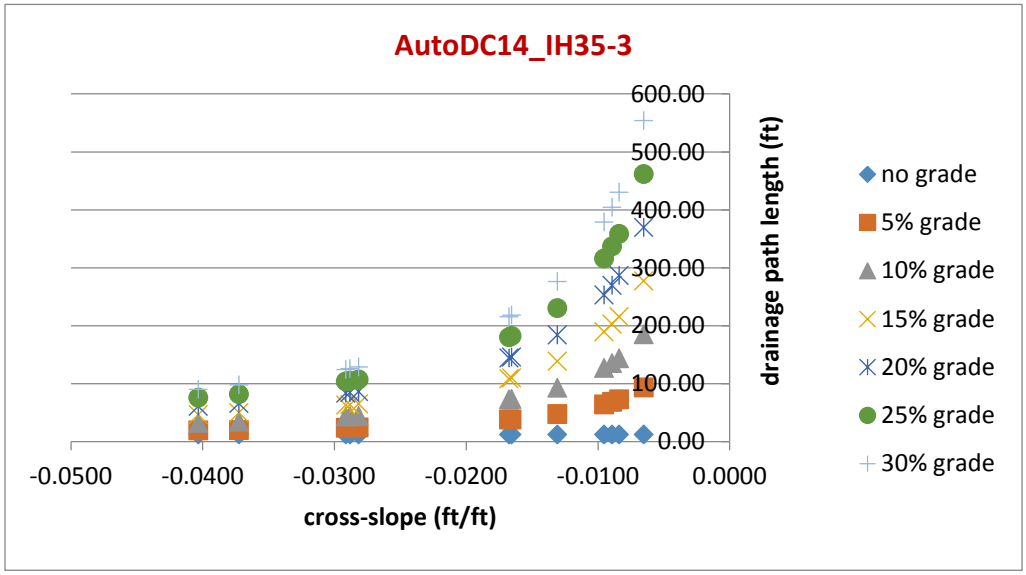

Figure G14: Drainage path lengths using reference data for AutoDC14_IH35-3

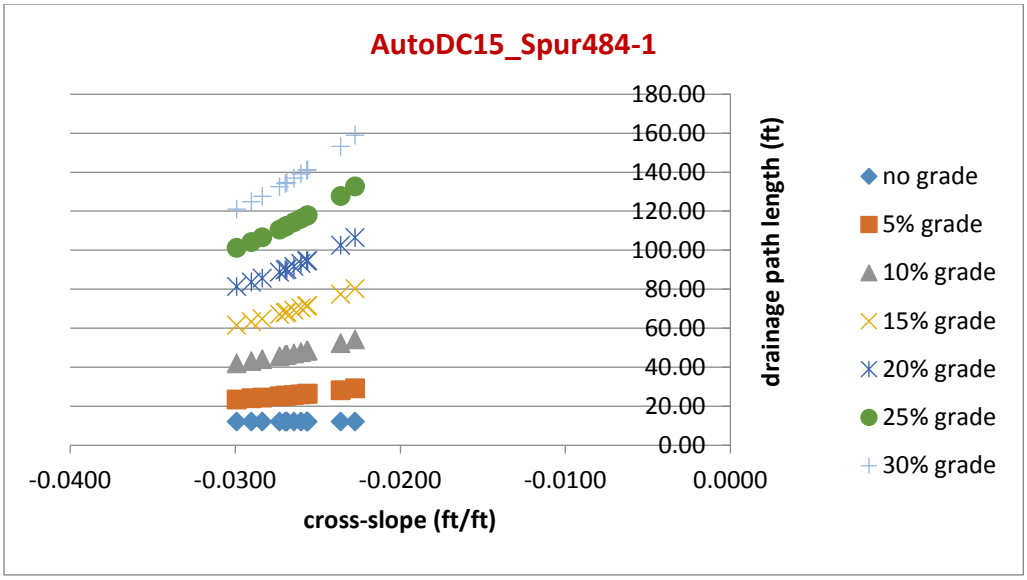

Figure G15: Drainage path lengths using reference data for AutoDC15_Spur484-1

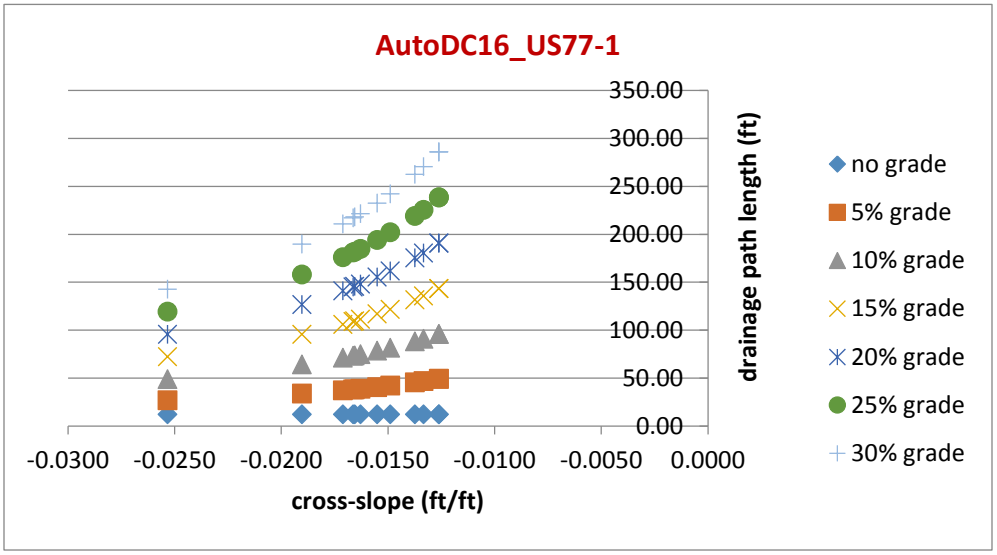

Figure G16: Drainage path lengths using reference data for AutoDC16_US77-1

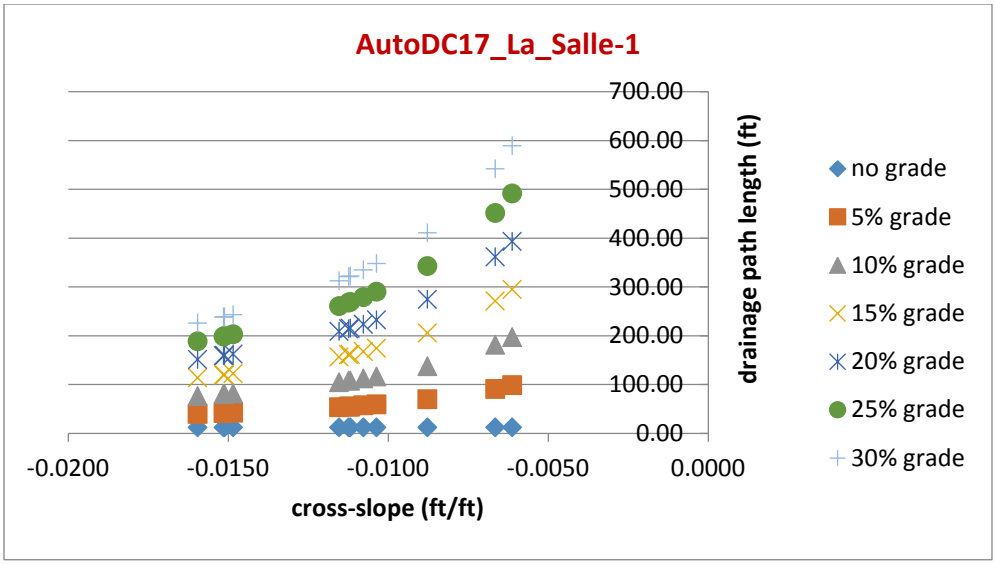

Figure G17: Drainage path lengths using reference data for AutoDC17_La_Salle-1

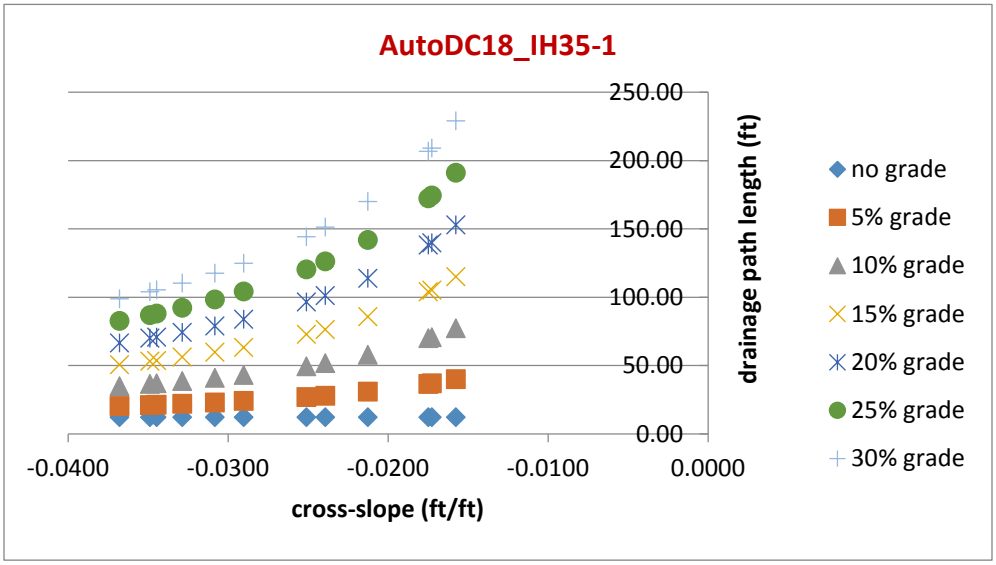

Figure G18: Drainage path lengths using reference data for AutoDC18_IH35-1

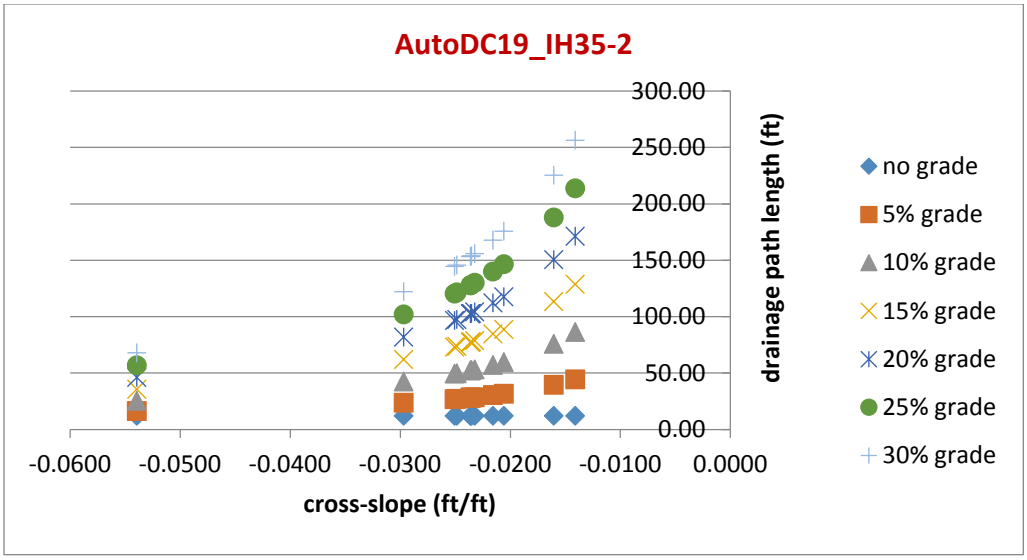

Figure G19: Drainage path lengths using reference data for AutoDC19_IH35-2

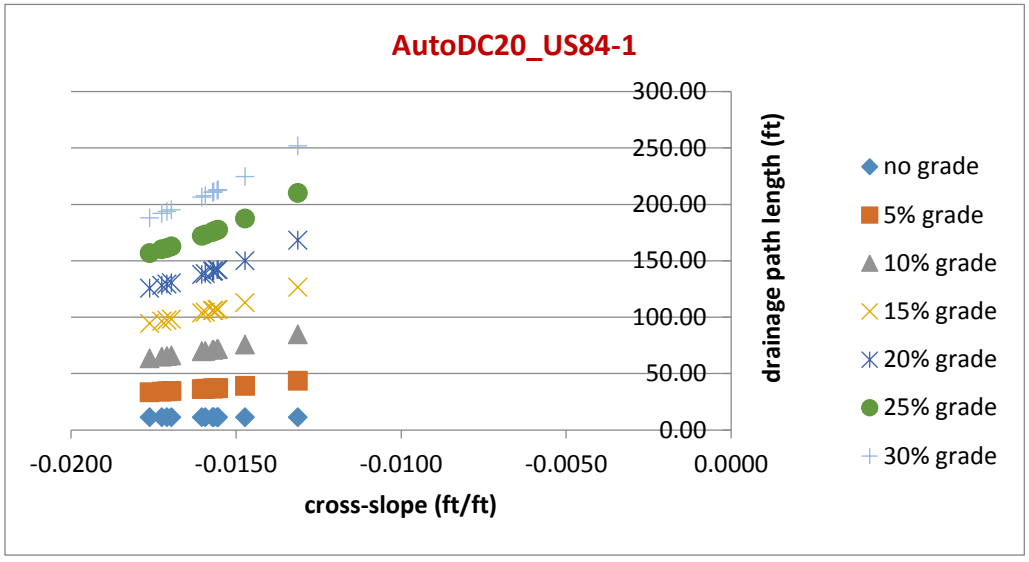

Figure G20: Drainage path lengths using reference data for AutoDC20_US84-1

Appendix H. Distress - PMIS Vs. TxDOT

Flexible Pavement Sections

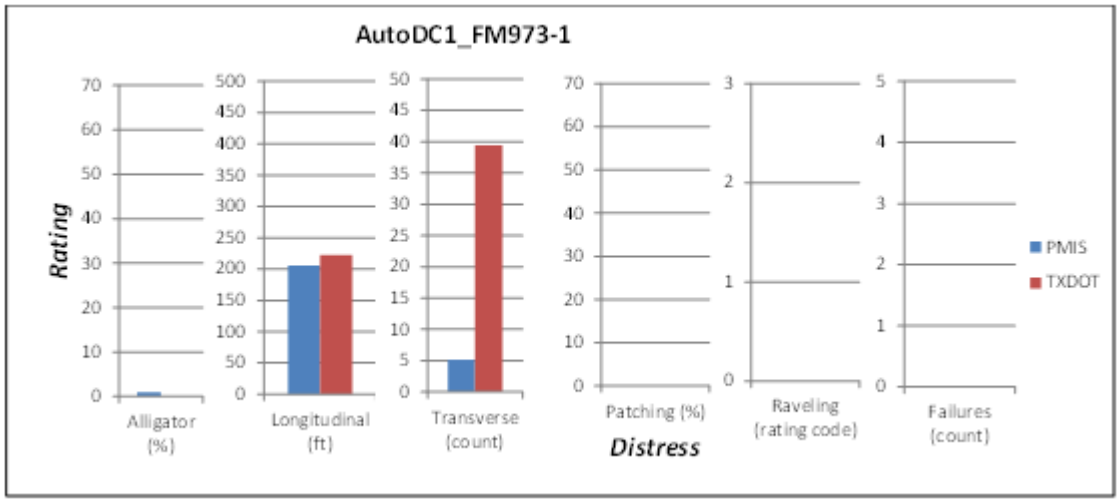

Figure H1: Distress results for PMIS (blue) and TxDOT (red) for AutoDC1_FM973-1

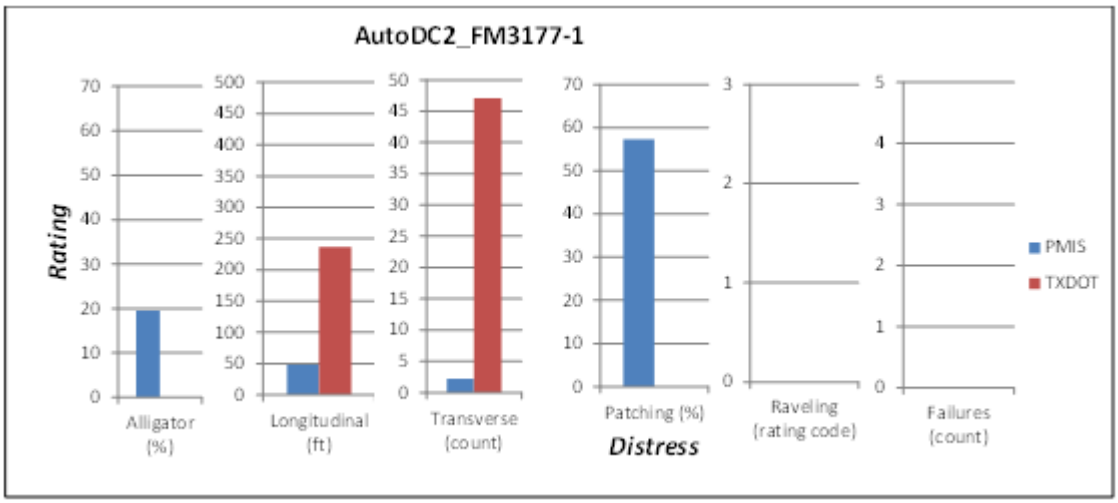

Figure H2: Distress results for PMIS (blue) and TxDOT (red) for AutoDC2_FM3177-1

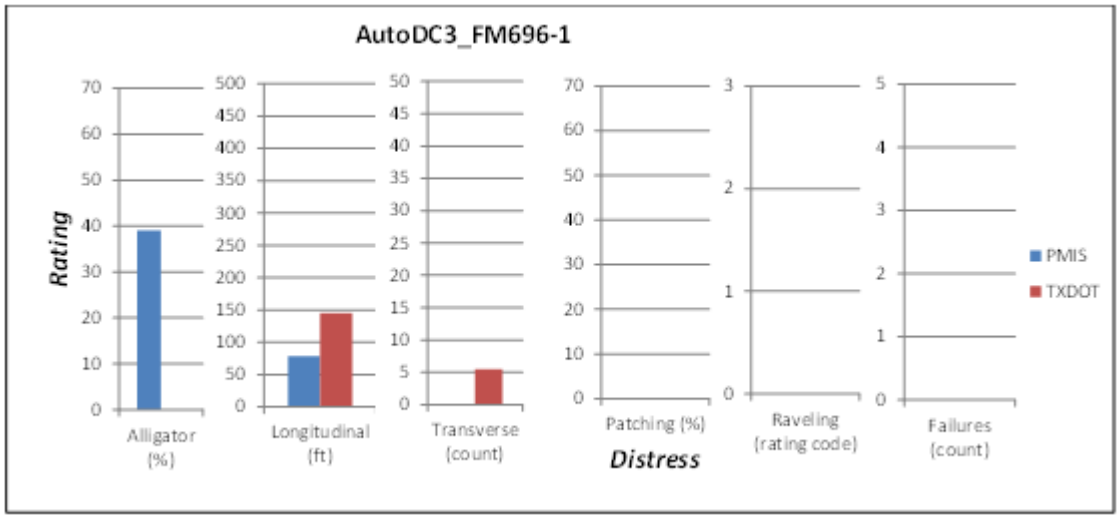

Figure H3: Distress results for PMIS (blue) and TxDOT (red) for AutoDC3_FM696-1

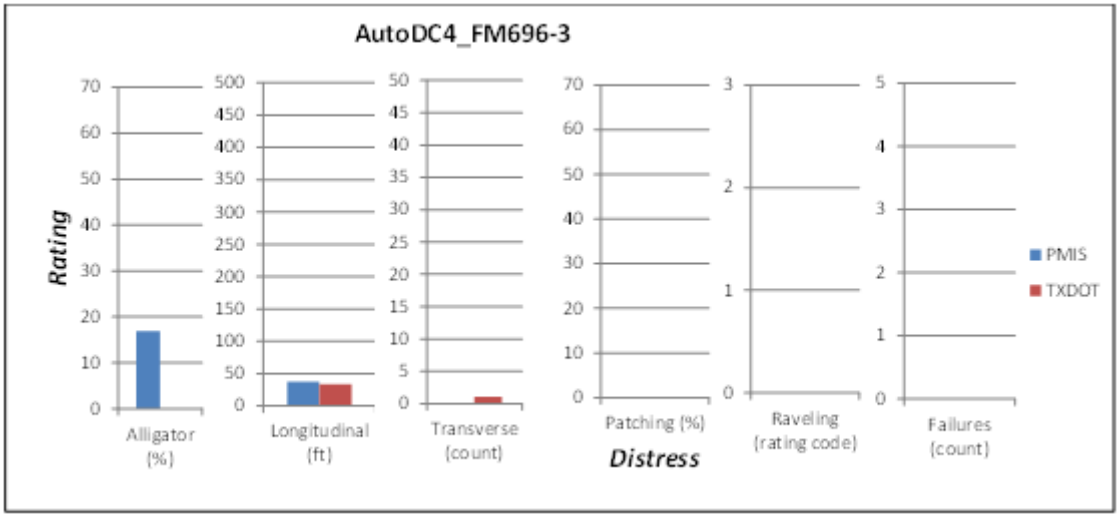

Figure H4: Distress results for PMIS (blue) and TxDOT (red) for AutoDC4_FM696-3

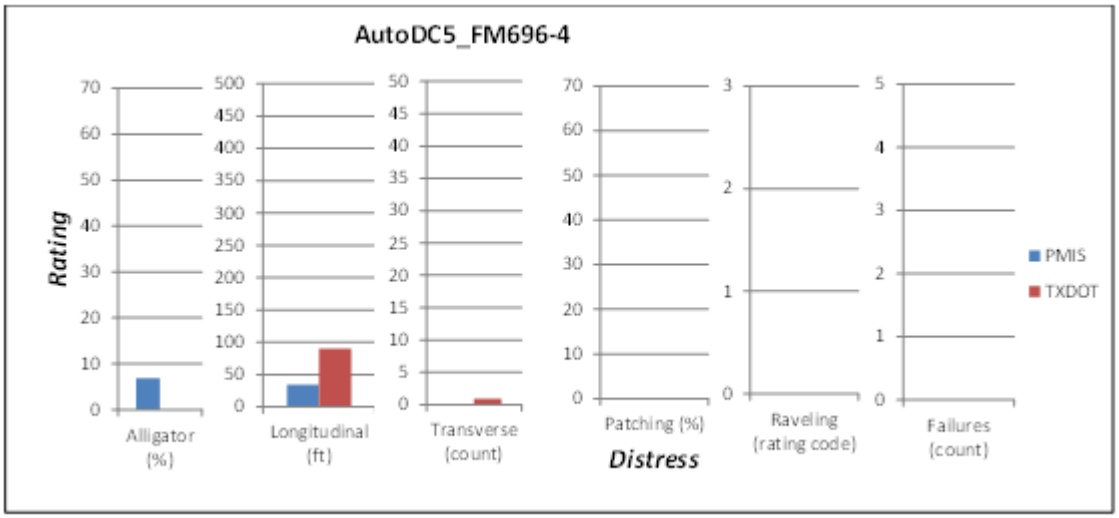

Figure H5: Distress results for PMIS (blue) and TxDOT (red) for AutoDC5_FM696-4

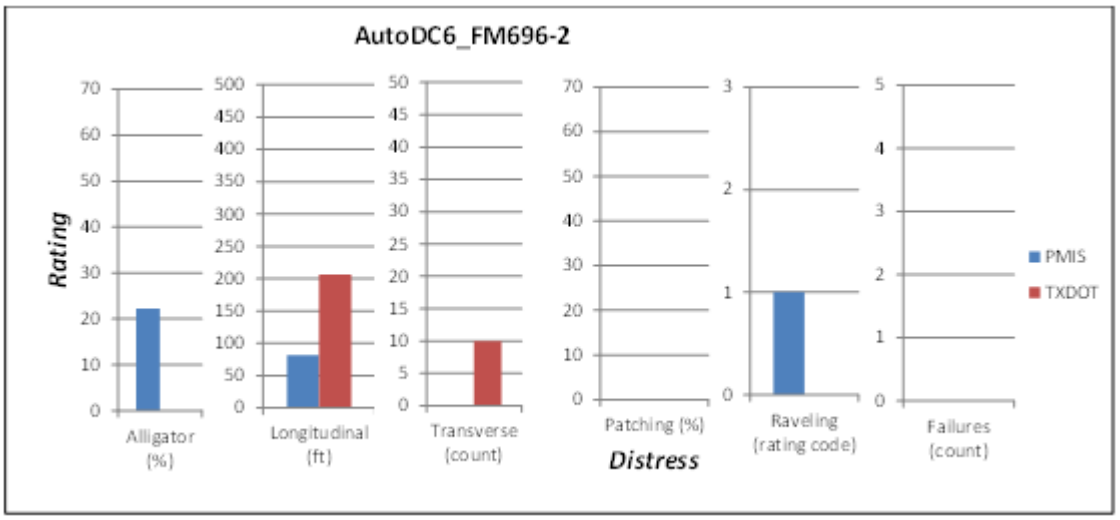

Figure H6: Distress results for PMIS (blue) and TxDOT (red) for AutoDC6_FM696-2

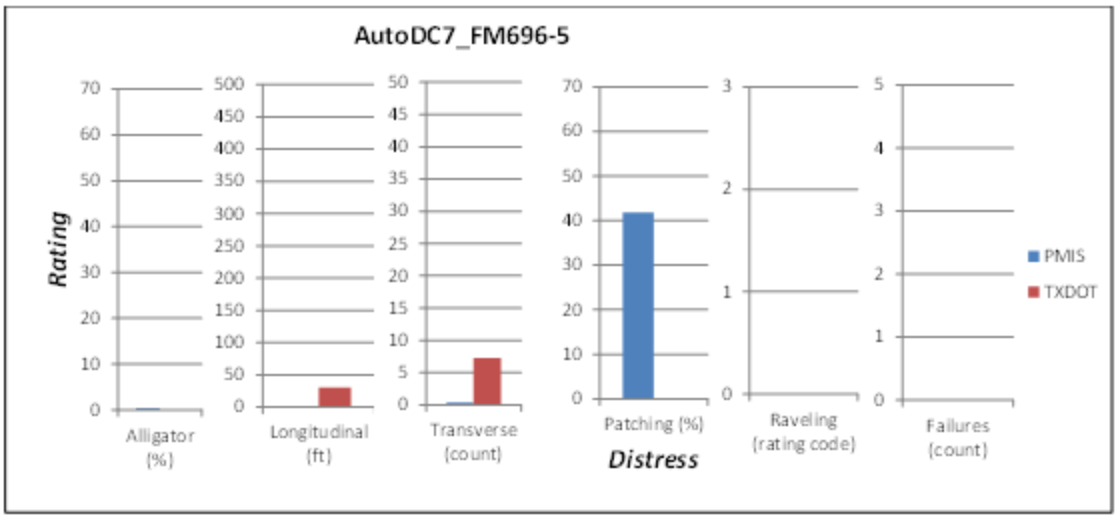

Figure H7: Distress results for PMIS (blue) and TxDOT (red) for AutoDC7_FM696-5

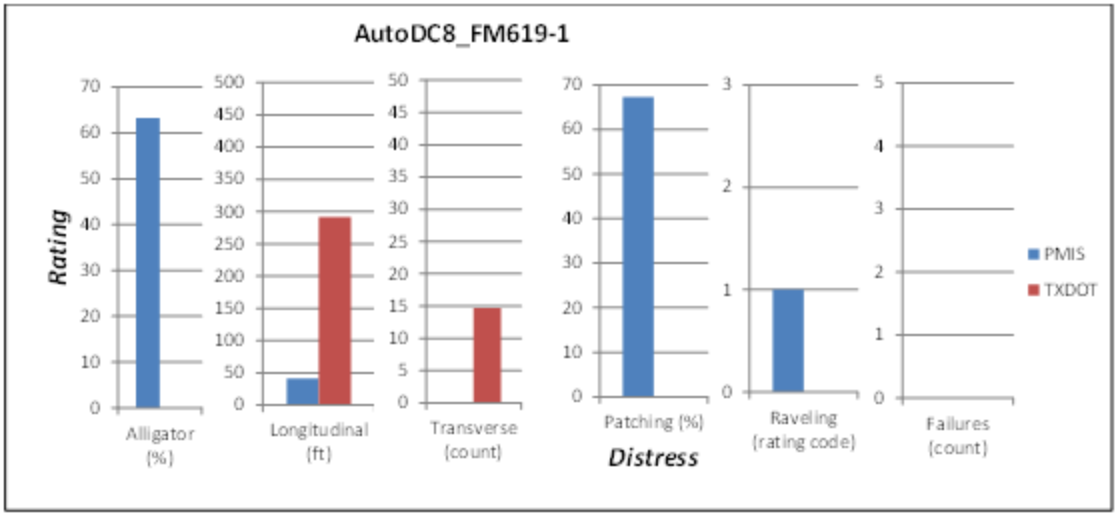

Figure H8: Distress results for PMIS (blue) and TxDOT (red) for AutoDC8_FM619-1

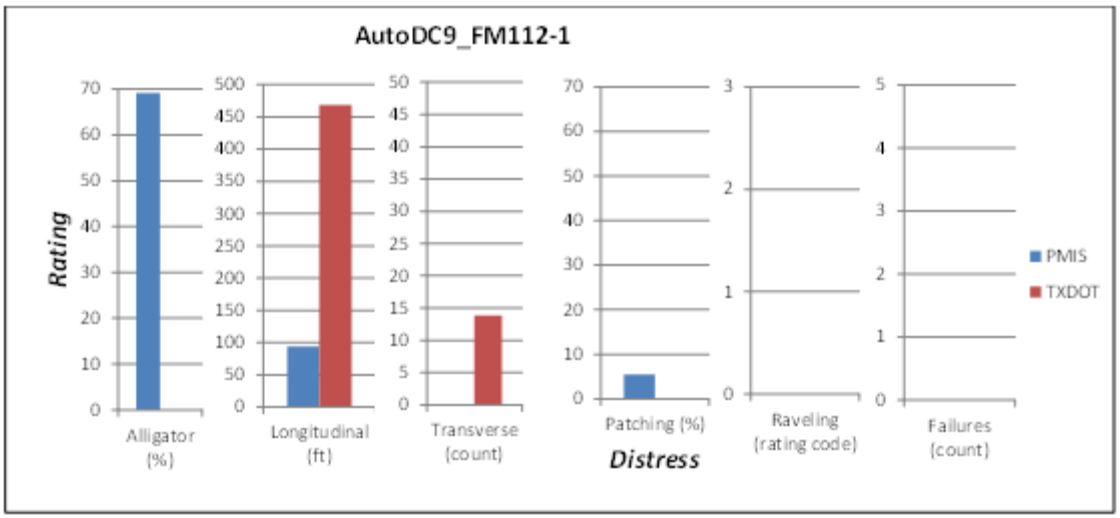

Figure H9: Distress results for PMIS (blue) and TxDOT (red) for AutoDC9_FM112-1

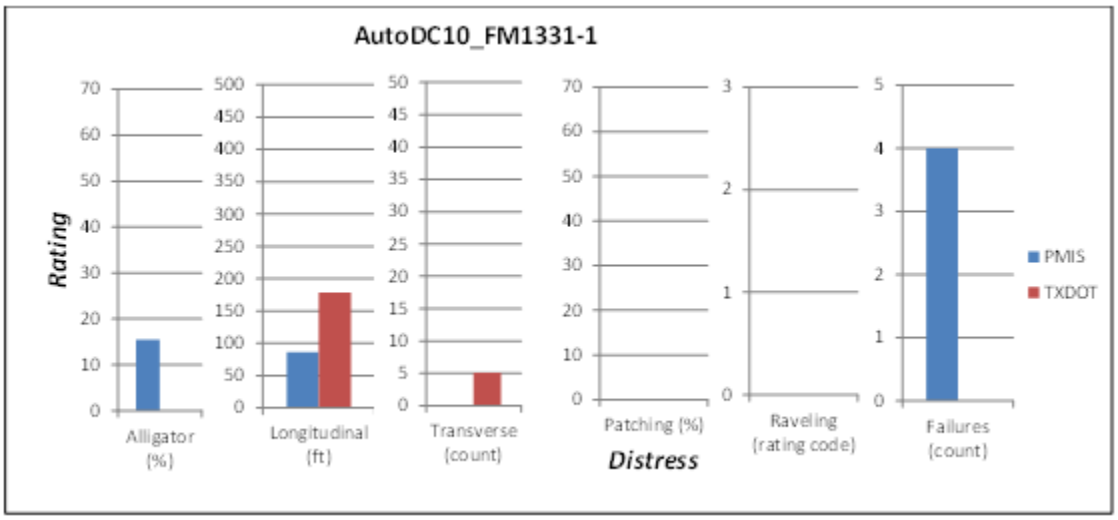

Figure H10: Distress results for PMIS (blue) and TxDOT (red) for AutoDC10_FM1331-1

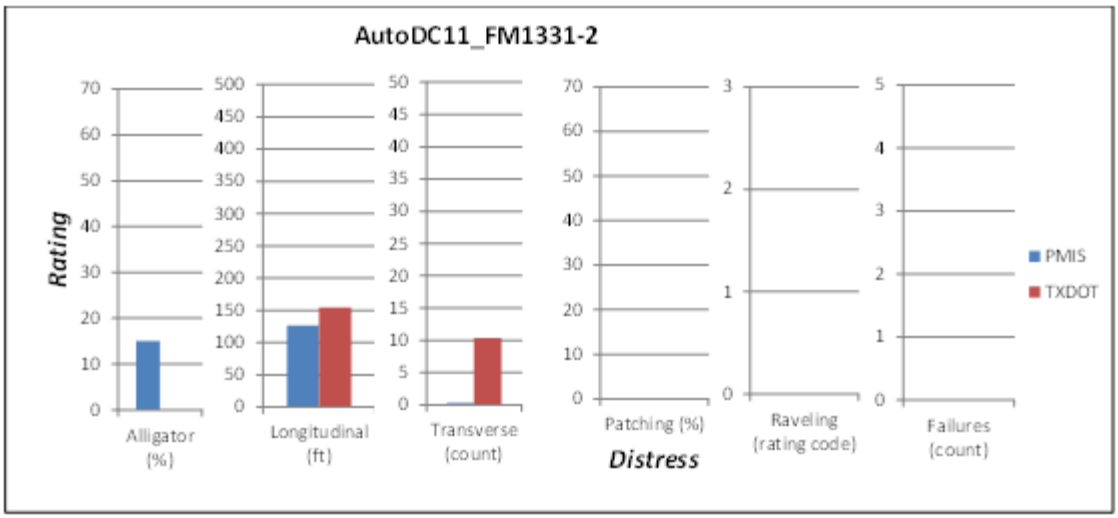

Figure H11: Distress results for PMIS (blue) and TxDOT (red) for AutoDC11_FM1331-2

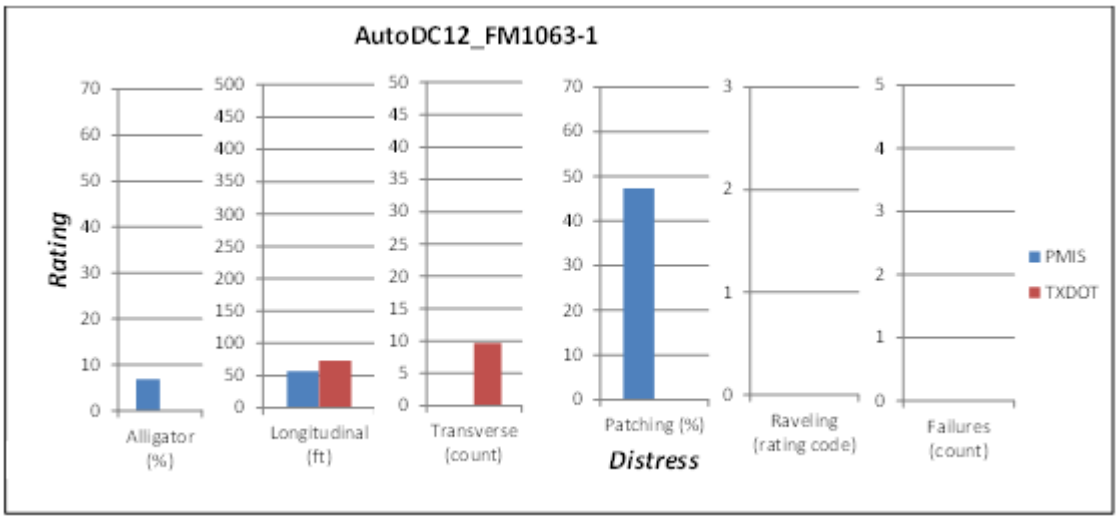

Figure H12: Distress results for PMIS (blue) and TxDOT (red) for AutoDC12_FM1063-1

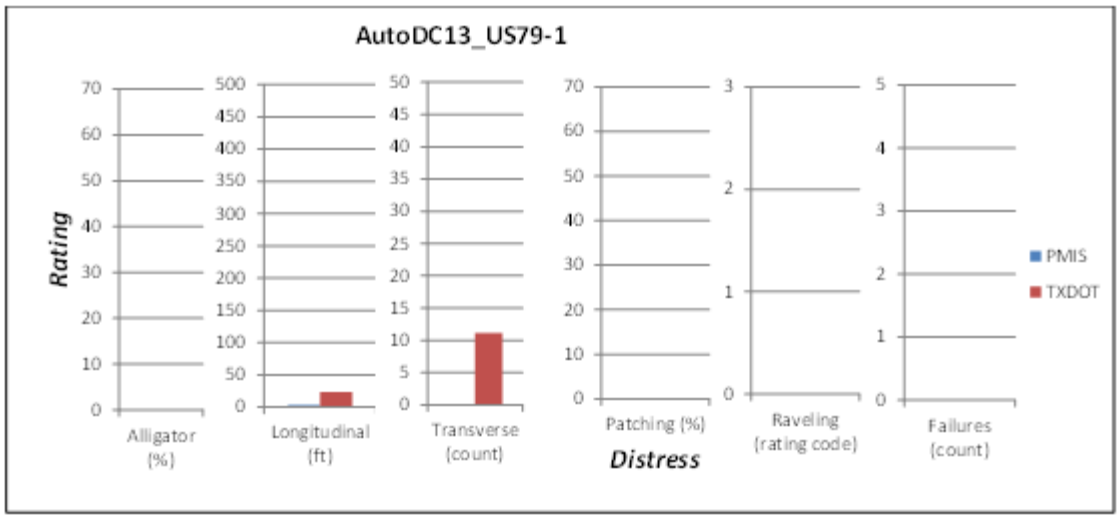

Figure H13: Distress results for PMIS (blue) and TxDOT (red) for AutoDC13_US79-1

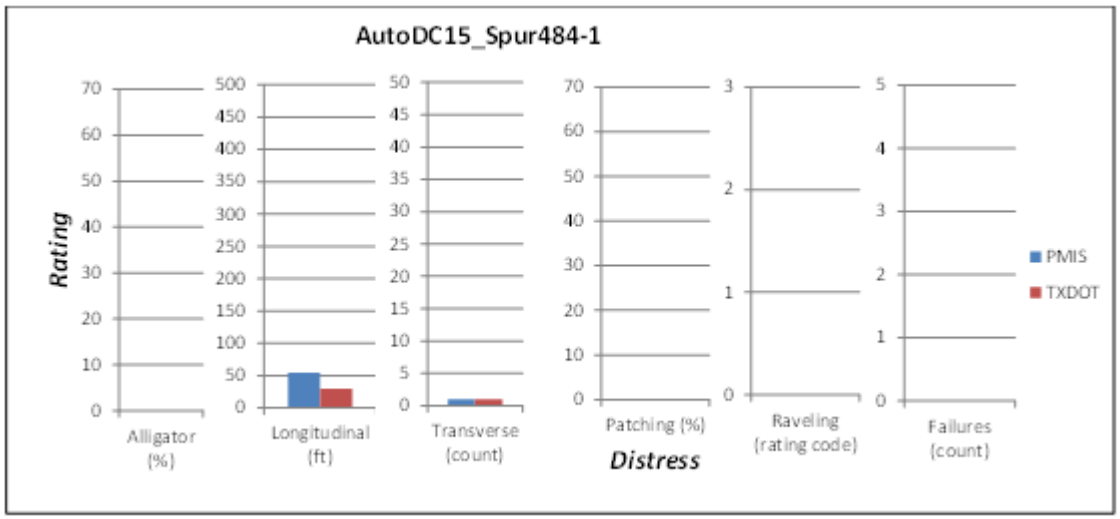

Figure H14: Distress results for PMIS (blue) and TxDOT (red) for AutoDC15_Spur484-1

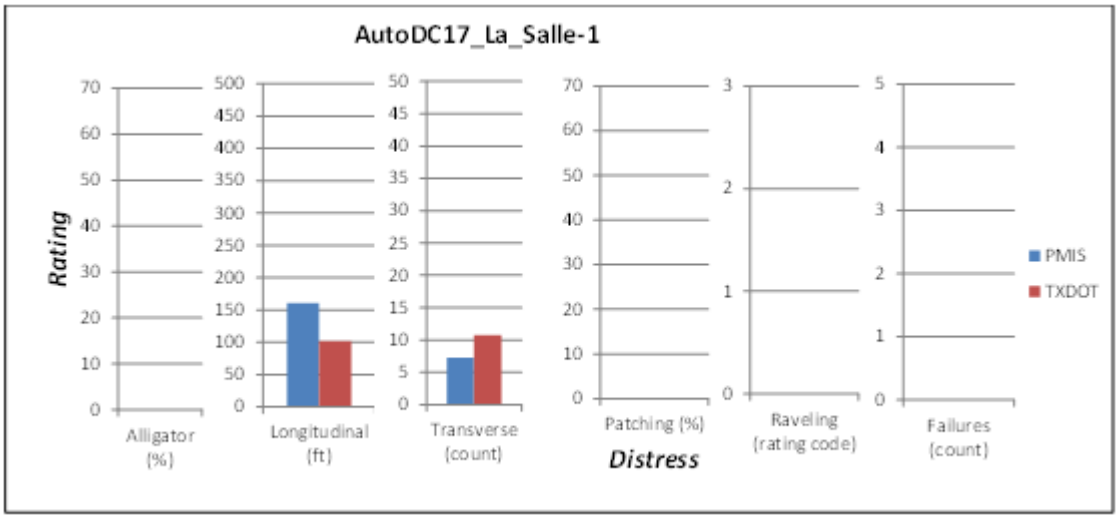

Figure H15: Distress results for PMIS (blue) and TxDOT (red) for AutoDC17_La_Salle-1

JCP Sections

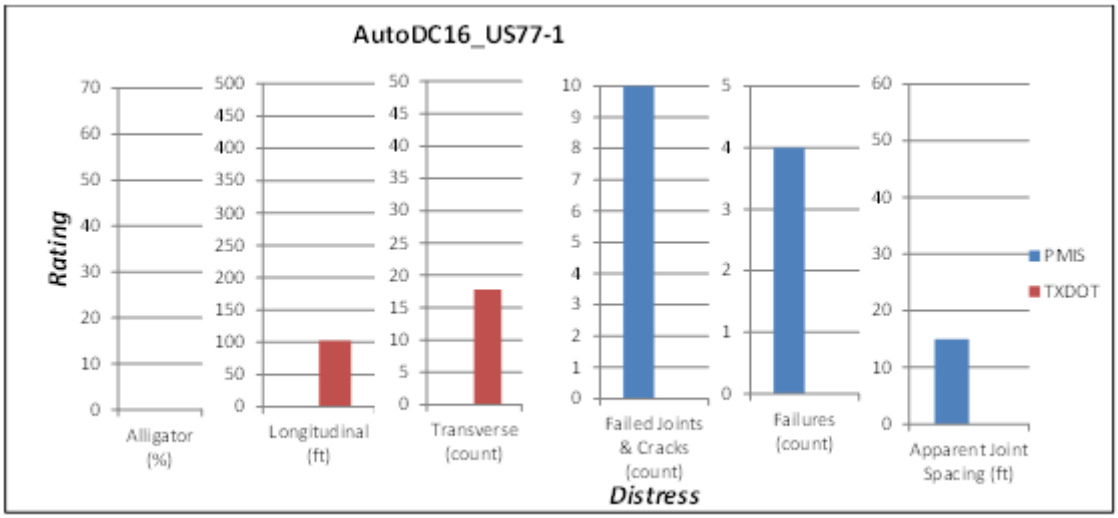

Figure H16: Distress results for PMIS (blue) and TxDOT (red) for AutoDC16_US77-1

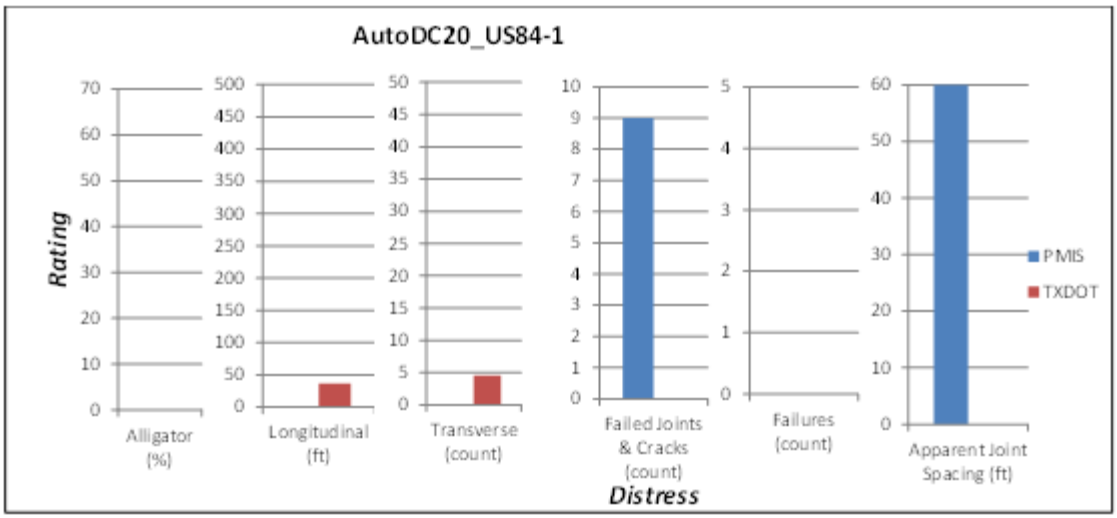

Figure H17: Distress results for PMIS (blue) and TxDOT (red) for AutoDC20_US84-1

CRCP Sections

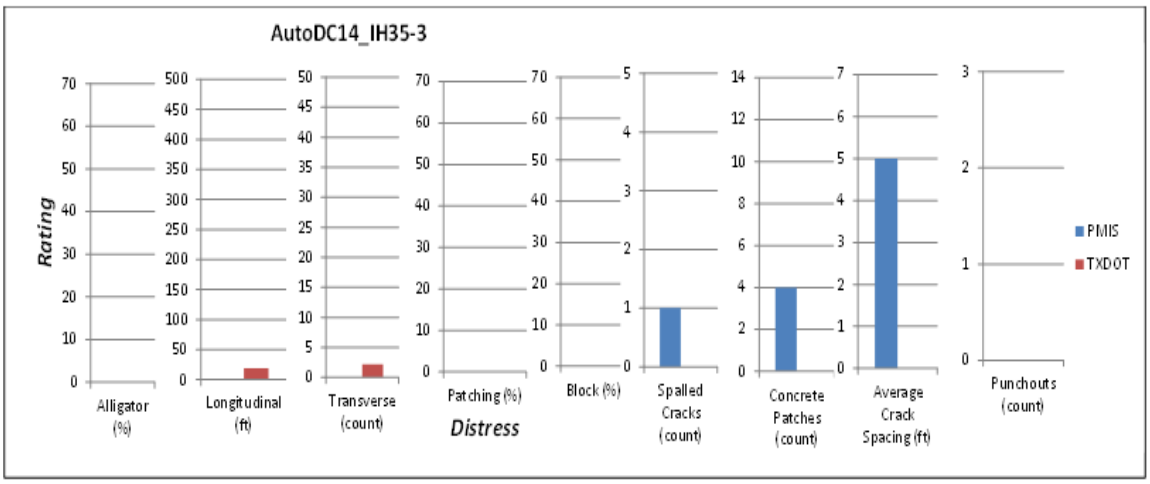

Figure H18: Distress results for PMIS (blue) and TxDOT (red) for AutoDC14_IH35-3

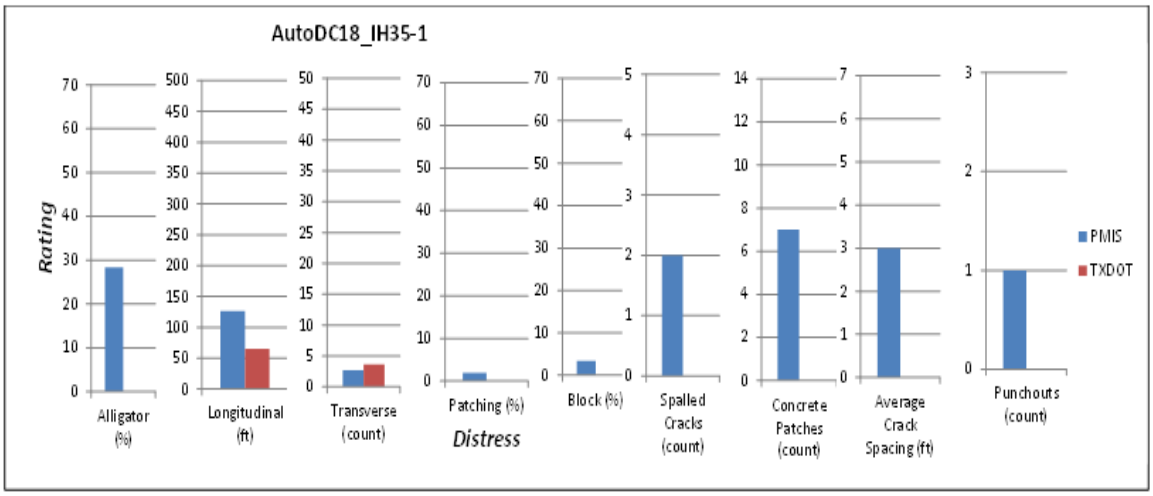

Figure H19: Distress results for PMIS (blue) and TxDOT (red) for AutoDC18_IH35-1

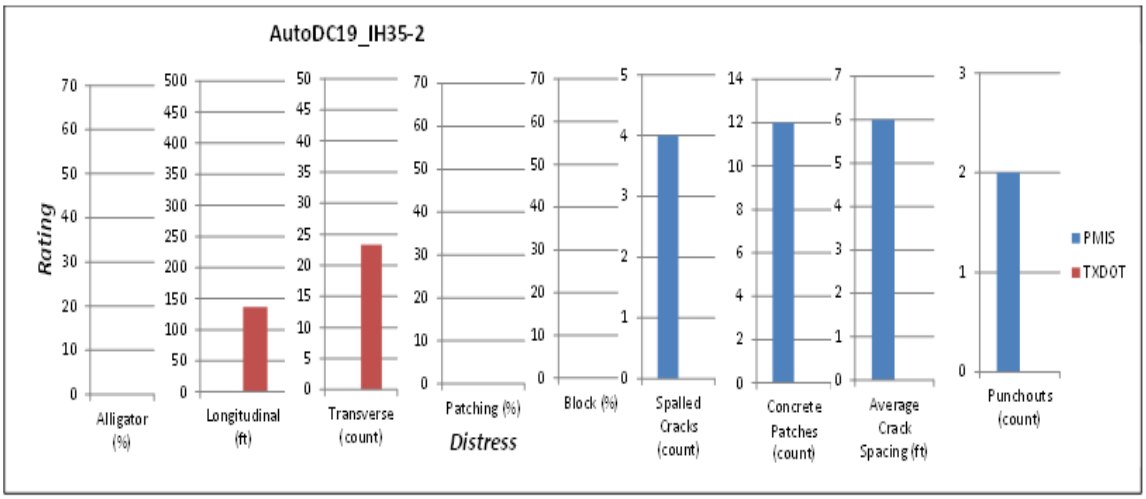

Figure H20: Distress results for PMIS (blue) and TxDOT (red) for AutoDC19_IH35-2

References

AASHTO - Geometric Design of Highways and Streets. (2001). *Chapter 4 – Cross Section Elements*. Retrieved April 14, 2014 from http://www.ahm531.com/My%20courses/AASHTOO/Chapter%2004%20-%20Cross%20Section%20Elements.pdf

Alyami, Z., Farashah, M. K., & Tighe, S. L. (2012). Selection of Automated Data Collection Technologies Using Multi Criteria Decision Making Approach for Pavement Management Systems. *Transportation Research Board 91st Annual Meeting.* Washington D.C.

Balmer, G. G., & Gallaway, B. M. (1983). Pavement Design And Controls For Minimizing Automotive Hydroplaning And Increasing Traction. *Frictional Interaction of Tire and Pavement, ASTM STP 793*, W. E. Meyer and J. D. Walter, Eds., American Society for Testing and Materials, 167-190.

Bolzon, G., Caroti, G., & Piemonte, A. (2007). Accuracy Check Of Road's Cross Slope Evaluation Using MMS Vehicle. *The 5th International Symposium on Mobile Mapping Technology*. Padua, Italy.

Buddhavarapu, P., Smit, A. D. F., Trevino, M., Banerjee, A., & Prozzi, J. A. (2013). Evaluation of the Benefits of Diamond Grinding of a CRCP. *Transportation Research Board 92nd Annual Meeting*. Washington D.C.

Byram, D., Xiao, D. X., Wang, K. C.P., Hall, K. D., & Li, Q. J. (2013). Comparing MEPDG Distress Predictions to Automated and Manual Interpretations. *Transportation Research Board 92nd Annual Meeting.* Washington D.C.

Chang-Albitres, C. M., Smith, R. E., & Pendleton, O. J. (2007). Comparison of Automated Pavement Distress Data Collection Procedures for Local Agencies in San Francisco Bay Area, California. *Transportation Research Record: Journal of the Transportation Research Board*, 1990, 119-126.

Dean, C. M., & Baladi, G. Y. (2013). The Impacts of Continuous Data Collection on the Accuracy of Pavement Management Decisions. *Transportation Research Board 92nd Annual Meeting*. Washington D.C.

Dennis, E. P., Hong, Q., Wallace, R., Tansil, W., & Smith, M. (2014). Pavement Condition Monitoring with Crowdsourced Connected Vehicle Data. *Transportation Research Board 93rd Annual Meeting*. Washington D.C.

Freitas, E., Pereira, P., Antunes, M. L., & Domingos, P. (2008). Analysis of Test Methods for Texture Depth Evaluation Applied in Portugal. *Seminário Avaliação das Características de Superfície dos pavimentos*.Guimarães, Portugal.

Fwa, T. F., Pasindu, H. R., & Ong, G. P. (2012). Critical Rut Depth for Pavement Maintenance Based on Vehicle Skidding and Hydroplaning Consideration. *Journal of Transportation Engineering*, 138(4), 423-429.

Gallaway, B. M., Benson, F. C., Mounce, J. M., Bissell, H. H., & Rosenbaum, M. J. (1982). Pavement Surface. Chapter 2 of *Synthesis of Safety Related to Traffic Control and Roadway Elements*, Volume 1. FHWA-TS-82-232. FHWA, U.S. Department of Transportation.

Gallaway, B. M., et. al. (1979). *Pavement and Geometric Design Criteria for Minimizing Hydroplaning*. Federal Highway Administration, Report No. FHWA-RD-79-31.

Gallaway, B. M., Schiller, R. E., & Rose, J. G. (1971). *The Effects of Rainfall Intensity, Pavement Cross Slope, Surface Texture, and Drainage Length on Pavement Water Depths*. Texas Transportation Institute. Research Report 138-5.

Glennon, J. C. (2006). *Hydroplaning - The Trouble With Highway Cross Slope*. Retrieved March 5, 2014, from http://www.crashforensics.com/papers.cfm?PaperID=8

Granlund, J. (2008). A new approach to prevent skid accidents on bumpy roads. *Internatinoal Safer Roads Conference, May 2008.*Cheltenham, UK.

Haas, C., Shen, H., Phang, W. A., & Haas, R. (1985). An Expert System for Automation of Pavement Condition Inventory Data. *1st North American Pavement Management Conference*.

Haas, R., Hudson, W. R., Zaniewski, J. (1994). *Modern Pavement Management*. Krieger Publishing Co.

Huber, R., Kingston, T., Laflamme, C., & Larouche, C. (2008). Automation and Mobile Mapping for Safe and Accurate Pavement Analysis. *7th International Conference on Managing Pavement Assets*. Retrieved January 29, 2014, from http://www.pavementmanagement.org/ICMPfiles/2008055.pdf

ISO 13473-1. (1997). *Characterization of Pavement Texture by Use of Surface Profiles – Part I: Determination of Mean Profile Depth.*

Lea, J. D., Harvey, J. T., & Tseng, E. (2014). Aggregating and Modeling Automated Pavement Condition Survey Data of Jointed Concrete And Sensor Data for Use in Pavement Management. *Transportation Research Board 93rd Annual Meeting*.

Washington D.C. Retrieved January 15, 2014, from http://amonline.trb.org/2014-1.405766/14-5553-1.416322?qr=1

Losa, M., Leandri, P., & Bacci, R. (2007). Measurements of Pavement Macrotexture with Stationary and Mobile Profilometers. *Fifth International Conference on Maintenance and Rehabilitation of Pavements and Technological Control (MAIREPAV5).* Park City, Utah.

Miller, J. S., & Bellinger, W. Y. (2003). *Distress Identification Manual for the Long-Term Pavement Performance Program*. Publication No. FHWA-RD-03-031. U.S. Department of Transportation. Federal Highway Administration. McLean, VA.

Mounce, J. M., & Bartoskewitz, R. T. (1993). Hydroplaning and Roadway Tort Liability. *Transportation Research Record*, 1401, 117-124.

Mraz, A., & Nazef, A. (2007). *Innovative Techniques with Multi-Purpose Survey Vehicle for Automated Analysis of Cross-Slope Data*. Applied Research Associates, Inc., Transportation Sector, Florida Department of Transportation.

Mullis, C., Shippen, N., Brooks, E., & Reid, J. (2005). *AUTOMATED DATA COLLECTION EQUIPMENT FOR MONITORING HIGHWAY CONDITION*. Oregon Department of Transportation and Federal Highway Administration. Report No. FHWA-OR-RD-05-10.

National Cooperative Highway Research Program. (2004). *Automated Pavement Distress Collection Techniques*. NCHRP Synthesis 334.

Ong, G. P. R., Noureldin, S., & Sinha, K. C. (2010). *Automated Pavement Condition Data Collection Quality Control, Quality Assurance, and Reliability.* Joint Transportation Research Program Technical Report FHWA/IN/JTRP-2009/17.

Pierce, L. M., McGovern, G., & Zimmerman, K. A. (2013). *Practical Guide for Quality Management of Pavement Condition Data Collection*. U.S. Department of Transportation Federal Highwa Administration. Contract DTFH61-07-D-00028.

Serigos, P. A., Burton, M., Smit, A., Prozzi, J. A., & Murphy, M. R. (2014). *Field Evaluation of Automated Rutting Measuring Equipment*. Technical Report No. FHWA/TX-12/0-6663-2. Center for Transportation Research. Texas Department of Transportation. Austin, TX.

Sergios, P. A., Murphy, M., & Prozzi, J. A. (2013). Evaluation of Rut-Depth Accuracy and Precision Using Different Automated Systems for Texas Conditions. *Transportation Research Board 92nd Annual Meeting*. Washington D.C.

Smith, R. E., & Chang-Albitres, C. M. (2007). *The Impact of Semi-Automated Pavement Distress Collection Methods on Pavement Management Network-Level Analysis Using The Mtc Streetsaver.* Metropolitan Transportation Commission (MTC), Texas Transportation Institute. Project 476290.

Smith, R. E., Freeman, T. J., & Pendleton, O. J. (1998). Evaluation of Automated Pavement Distress Data Collection Procedures for Local Agency Pavement Management. *4th International Conference on Managing Pavements*.

Souleyrette, R., Hallmark, S., Pattnaik, S., O'Brien, M., and Veneziano, D. (2003). *Grade and Cross Slope Estimation from LIDAR-based Surface Models*. U.S. Department of Transportation, Iowa Department of Transportation. MTC-2001-02.

Teede Tehnokeskus. (n. d.). *Rut Depth Measurements.*Retrieved March 5, 2014, from http://www.teed.ee/eng/services/testing-and-measurement/measurements/rut-depth-measurements

Texas Department of Transportation. (2004). *Standard Specifications for Construction and Maintenance of Highways, Streets, and Bridges*.

Timm, D. H., & McQueen, J. M. (2004). *A Study of Manual vs. Automated Pavement Condition Surveys*. Highway Research Center, Auburn University. Alabama Department of Transportation Report IR-04-01.

Tsai, Y., Wang, Z., Li, F. (2011). Assessment of Rut Depth Measurement Using Emerging 3D Continuous Laser Profiling Technology. *Transportation Research Board 90th Annual Meeting.* Washington D.C.

TxDOT Hydraulic Design Manual. (2011). *Chapter 10: Storm Drains, Section 4: Pavement Drainage.* Retrieved March 20, 2014, from http://onlinemanuals.txdot.gov/txdotmanuals/hyd/pavement_drainage.htm

TxDOT Pavement Design Guide – Online Manual. (2011). *Chapter 4: Pavement Evaluation, Section 2: Visual Pavement Condition Surveys*. Retrieved March 10, 2014, from http://onlinemanuals.txdot.gov/txdotmanuals/pdm/visual_pavement_condition_surveys.htm

TxDOT. *Pavement Management Information System – Rater's Manual For Fiscal Year 2010*. (2009). Texas Department of Transportation.

TxDOT Wet Weather Accident Reduction Program (WWARP). (2006). Retrieved March 10, 2014, from http://ftp.dot.state.tx.us/pub/txdot-

info/tta/ih635/FINAL%20REQUEST%20FOR%20PROPOSALS_9-18-07/6%20-%20REFERENCE%20INFORMATION%20DOCUMENTS/11%20-%20STUDIES%20AND%20REPORTS/Technical%20Resources/070530wwarp.pdf

Wang, K. (2011). *Automated Survey of Pavement Distress based on 2D and 3D Laser Images*. Mack-Blackwell Rural Transportation Center, University of Arkansas. MBTC DOT 3023.

Yeager, R. W. (1974). Tire Hydroplaning: Testing, Analysis, and Design. *The Physics of Tire Traction: Theory and Experiment*, D. F. Hays and A. L. Browne, Eds. Plenum Press, New York.